The future of short-term electricity balancing in Europe : Impact of common balancing energy markets and decarbonization

Florent Cogen

PSL
UNIVERSITÉ PARIS

THÈSE DE DOCTORAT
DE L'UNIVERSITÉ PSL

Préparée à l'Université Paris-Dauphine

The future of short-term electricity balancing in Europe: impact of common balancing energy markets and decarbonization

Soutenue par
Florent COGEN
Le 03 juillet 2024

Ecole doctorale n° ED 543
Ecole doctorale SDOSE

Spécialité
Sciences économiques

Composition du jury :

Jan-Horst, KEPPLER Professeur des universités, Université Paris Dauphine – PSL	*Président*
Anke, WEIDLICH Full professor, Albert-Ludwigs-Universität Freiburg	*Rapporteur*
Olivier, MASSOL Professeur des universités, CentraleSupélec	*Rapporteur*
Marie, PETITET Research lead, KAPSARC	*Examinateur*
Erik, DELARUE Associate professor, KU Leuven	*Examinateur*
Fabien, ROQUES Professeur associé, Université Paris Dauphine – PSL	*Directeur de thèse*

Dauphine | PSL
UNIVERSITÉ PARIS

Acknowledgements

I want to start by thanking the various members of my thesis jury, Jan-Horst Keppler, Anke Weidlich, Olivier Massol, Marie Petitet and Erik Delarue, for taking the time to read this manuscript in detail and contributing their respective points of view. Their comments were valuable, leading to an enriching discussion during the defense.

Mes remerciements s'adressent également à mon directeur de thèse Fabien Roques, qui m'a suivi tout au long de la thèse et apporté sa connaissance poussée de la recherche académique, toujours avec une approche pertinente et constructive. Son adaptation et sa flexibilité vis-à-vis des enjeux particuliers d'une thèse CIFRE ont notamment permis à cette thèse d'aboutir.

Je souhaite remercier chaleureusement RTE, et surtout mes encadrants au sein de l'entreprise. Frédéric, j'ai eu beaucoup de chance de pouvoir travailler avec toi durant toute la première partie de thèse. Ton expertise et ton enthousiasme pour les sujets d'EOD m'ont guidé et motivé pendant ces 4 années. Ton aide lors de la prise en main, pas forcément évidente, de Prometheus et d'ATLAS, et lors de toutes les phases de développement a été déterminante. Un grand merci à Virginie pour ton encadrement essentiel lors de la fin de thèse. Ta capacité à comprendre tous les enjeux d'un sujet évoqué en une phrase m'impressionnera toujours, et a été cruciale lors de la production des résultats. Emily, merci beaucoup pour ta disponibilité de tous les instants et ton soutien pendant cette dernière année. Tu m'as aidé à gérer les moments difficiles et les deadlines. Et merci énormément à toutes les deux pour vos relectures détaillées, notamment celles de mes premiers jets hasardeux : sans elles, la rédaction du manuscrit n'aurait probablement pas pu aboutir. Merci également à tous ceux qui ont suivi ma thèse d'un peu plus loin, en particulier Jean-Yves pour tes avis et apports très enrichissants.

J'aimerai aussi beaucoup remercier la feuille de route EOD, et tous les (ex-) doctorants de la R&D avec qui j'ai partagé ces années de thèse : Arnauld, Emily, Gabriel, Marie, Marie-Alix, Marion, Maxime, Rémi, Thomas et Thomas. J'ai beaucoup progressé à votre contact, professionnellement mais aussi humainement.

Finalement, merci beaucoup à mes amis d'enfance Guillaume, Louis, Matthias et Raphaël, et à ma famille, Maman, Papa et Romain, pour leurs soutiens et encouragements constants. Même sans être experts des sujets techniques, vous avez tous été très importants pour moi lors de cette thèse. Je pense très fort à mon Papy, qui nous a quitté l'année dernière, et à Mamy qui reste toujours forte et positive.

Table of Contents

List of Figures

List of Tables

List of Abbreviations

aFRR	automatic Frequency Restoration Reserve
ATC	Available Transmission Capacity
ATLAS	Agent-based short-Term eLectricity mArkets Simulation
BRP	Balancing Responsible Party
BSP	Balancing Services Provider
CCGT	Combined Cycle Gas Turbine
CMOL	Common Merit Order List
ENTSO-E	European Network of Transmission System Operators
EU	European Union
EUPHEMIA	pan-EUroPean Hybrid Electricity Market Integration Algorithm
FAT	Full Activation Time
FCR	Frequency Containment Reserve
FrBM	French Balancing Mechanism
GCT	Gate Closure Time
GHG	Greenhouse Gas
ISP	Imbalance Settlement Price
MARI	Manually Activated Reserves Initiative
mFRR	manual Frequency Restoration Reserve
OCGT	Open Cycle Gas Turbine
P2G	Power to Gas
PHS	Pumped Hydro Storage
PICASSO	Platform for the International Coordination of Automated Frequency Restoration and Stable System Operation
RR	Replacement Reserve
RTE	Réseau de Transport d'Electricité
TERRE	Trans European Replacement Reserves Exchange
TSO	Transmission System Operator
vRES	variable Renewable Energy Sources

Chapter 1

General Introduction

Contents

Power systems are a cornerstone of modern societies, as they power vital infrastructures and services and provide instant energy access to end-consumers. Their importance is set to intensify, as the share of electricity in worldwide energy consumption that currently accounts for more than 20% is expected to rise up to 50% by 2050[1]. The management of power systems is notoriously complex. Indeed, electricity stands out amongst other types of energy vectors since it is the only one that needs conversion into another type of energy to be stored. This implies that an exact balance between generation and consumption must be reached at all times. Managing this supply-demand balance is rendered even more challenging if we factor in the variable aspect of both supply and demand, the profound diversity of technologies and actors involved

[1] See https://www.iea.org/energy-system/electricity

in a modern power system, and its interconnected and cross-border aspects. To achieve balance in real time, generation and load programs are defined through a sequential process, in which adjustments are made at different lead times. Five stages are usually considered in supply-demand balance management: long-term, day-ahead, intraday, balancing and imbalance settlement. Figure 1.1 illustrates them for a fixed delivery date t_d.

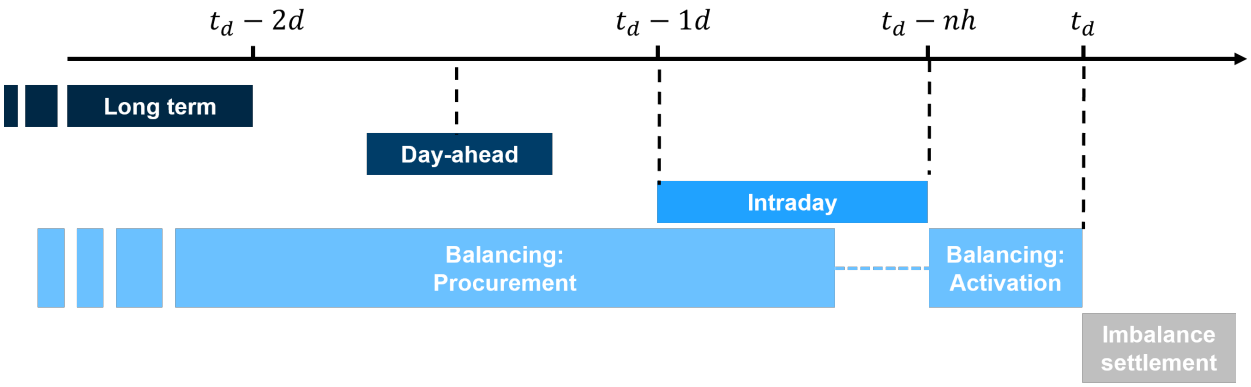

Figure 1.1: Usual stages of supply-demand balance management

The overall shape of generation and load programs is defined during the long-term and day-ahead stages. Intraday processes aim to make successive adjustments to the previously defined overall shape, accounting for new information likely to affect the level of both supply and demand sides. Finally, the role of the balancing stage is to make the final corrections to ensure that supply meets demand in real time, by activating "balancing reserves". To do so, this stage is generally comprised of two distinct steps: the procurement of these reserves, and their activation. The objective of the procurement step is to secure power capacities in advance, to ensure that the amount of capacity available during real-time balancing processes is always sufficient. Depending on the area, it can be executed hours, days or even months ahead of the delivery date. In contrast, the activation step takes place right before the delivery date, usually within the last hour, and it aims to activate balancing energy to compensate for observed or forecasted imbalances. Finally, the imbalance settlement stage–performed ex-post–allocates the balancing costs between the entities responsible for imbalances.

Two major transformations have been reshaping power systems for the last few decades, and will likely continue to do so for the foreseeable future: liberalization and decarbonization. As the last resort guaranteeing an adequate energy delivery, the balancing stage plays a crucial role in the power system management and is at the forefront of these evolutions. Indeed, its organization is currently transitioning from local processes to common European markets, and the power system evolution tied with decarbonization will deeply modify the characteristics of short-term balancing processes. Following these observations, the main motivation of this thesis is to answer the following general question:

What are the impacts of the ongoing liberalization and decarbonization on the short-term management of the supply-demand balance?

The scope of this thesis is consequently set on the balancing stage. More specifically, it focuses on the activation step, and does not analyze the procurement step. Therefore, any subsequent mention of balancing markets or balancing processes will only refer to energy activation, unless otherwise specified. In addition, we

only consider high-level network aspects of power systems, and focus on challenges associated with supply-demand adequacy.

The rest of this introduction develops the implicit challenges behind the general question. First, Section 1.1 details the two main evolutions previously evoked. To understand the scale of the balancing stage transformation, an overview of the historical balancing processes in Europe is then provided in Section 1.2, followed by a description of the future balancing energy markets in Section 1.3. Section 1.4 highlights the main research fields on balancing markets covered in the literature, and finally Section 1.5 details the main research questions, the contributions of this thesis and the manuscript organization.

1.1 Ongoing evolutions of the European power system

1.1.1 The ongoing liberalization

Small-scale and local implementations of power systems started throughout the world at the beginning of the 20^{th} century. In Europe, the development of nationwide power networks began between 1900 and 1937, but faced a significant setback during World War II. The subsequent rebuilding process was mostly conducted by states or state-owned vertically integrated companies. These entities controlled the different aspects of their local power system, i.e. the power generation, its transmission across large areas, and finally its distribution to end-consumers. At the time, this type of organization was required given the intricacies of both implementing and managing power systems: offering a reliable and stable supply to all consumers in a large area not only involves building and operating a large-scale network, but also necessitates a high degree of coordination between all the aspects previously mentioned.

Since the 1980s, the complete vertical integration of power systems has been challenged, notably by (Joskow and Schmalensee, 1983). The main objectives of the discussed liberalization were to ensure security of supply while providing a competitive price for all actors involved in power systems. The proposed solution revolved around electricity markets, and was based on key works focused on market design, such as the marginal pricing developed by (Boiteux, 1951) or the spot pricing theory published by (Caramanis et al., 1982). In the United States, these concepts were put into practice through the National Energy Policy Act of 1992. Europe followed closely, formalizing its objectives in the First and Second Energy Packages, respectively approved in 1996 and 2003. These directives focused on the creation of common electricity markets, advocating for a decentralized system using self-dispatch processes conducted by portfolios gathering diverse assets.

Following these directives, local implementations of day-ahead markets began during the 1990s and the beginning of the 2000s (Meeus, 2020). Norway led the way with the creation of the day-ahead market Statnett Marked in 1993, which became known as Nordpool after the integration of Sweden 3 years later. In Western Europe, similar markets were created at the beginning of the 21^{st} century (in 2000 in Germany, and 2001 in France for example). Intraday markets were next in line, and their local implementation within the different areas followed that of day-ahead markets by a few years. We can cite as examples the intraday creation dates in Nordpool (1999), France (2003) and Germany (2004).

These markets remained local for several years, mostly operated at the scale of a single country (or a few

countries in the case of Nordpool). Meanwhile, energy was already exchanged between areas, thanks to the well-interconnected state of Europe. Improving these exchanges then became the next important step of the liberalization process, through the cross-border integration of existing markets. For day-ahead markets, this process occurred in three separate waves, in 2008, 2010 and eventually 2014. This last milestone resulted in the creation of the so-called Single Day-Ahead Coupling that initially regrouped 17 European countries in a common market. Since then, additional countries have progressively been integrated, effectively creating a common and harmonized design for the day-ahead market in Europe. The cross-border integration of intraday markets began in 2018, and was successfully conducted over 4 different waves until 2022.

During the last two decades, the liberalization focus was mainly set on the day-ahead and intraday stages. In contrast, the balancing stage was mostly left out of the scope of common and harmonized markets, for both procurement and activation steps. Until recently, it was still managed locally by the different Transmission System Operators (TSOs) in Europe, each one using specific and tailor-made processes. This resulted in a collection of diverse and heterogeneous designs in Europe (see Rebours et al., 2007a, Rebours et al., 2007b, Ocker et al., 2016 or Håberg and Doorman, 2016). A detailed look at this historical status is proposed in Section 1.2.

The organization of the balancing stage is now changing as well, following the integration process experienced for day-ahead and intraday lead times. Indeed, the economic efficiency of historical processes has been questioned by both institutional and academic European actors on the following points:

- The local aspect effectively means a reduction in the overall pool of available balancing offers. Each area only has access to a smaller pool, which would result in activating less optimal reserves.
- Local processes could lack transparency, which would create barriers for new actors seeking to participate in the balancing stage.
- The incomplete market design convergence could also be detrimental to already harmonized markets. Incentives carried out by local balancing processes have the potential to influence actor behavior on day-ahead and intraday markets, possibly leading to distortions.

To tackle these limitations, the creation of common balancing energy markets was endorsed in 2017 with the European Balancing Guideline (Commission, 2017). Their design is described in Section 1.3.

To summarize, the European power system liberalization and the market design convergence process are still incomplete: well advanced for day-ahead and intraday markets, but ongoing for balancing processes.

1.1.2 The ever-needed decarbonization

The various reports published by the Intergovernmental Panel on Climate Change continue to confirm that climate change could have dramatic consequences in the future, putting at risk the equilibrium of our entire world. Their 6^{th} report (Core Writing Team and (eds.), 2023) identifies humanity as a clear source in the increase of greenhouse gas (GHG) emissions, in which the energy sector plays a significant role. Indeed, this report estimated that it has been accounting for approximately 75% of European GHG emissions each year. Hence, reducing the environmental impact of the energy sector is crucial, and can be more difficult to achieve for some energy vectors compared to others. Electricity stands out as its decarbonization is easier to fulfill

than that of fuel or gas vectors. European countries are therefore projecting a high level of electrification in the coming decades, and consequently an increase in electricity consumption.

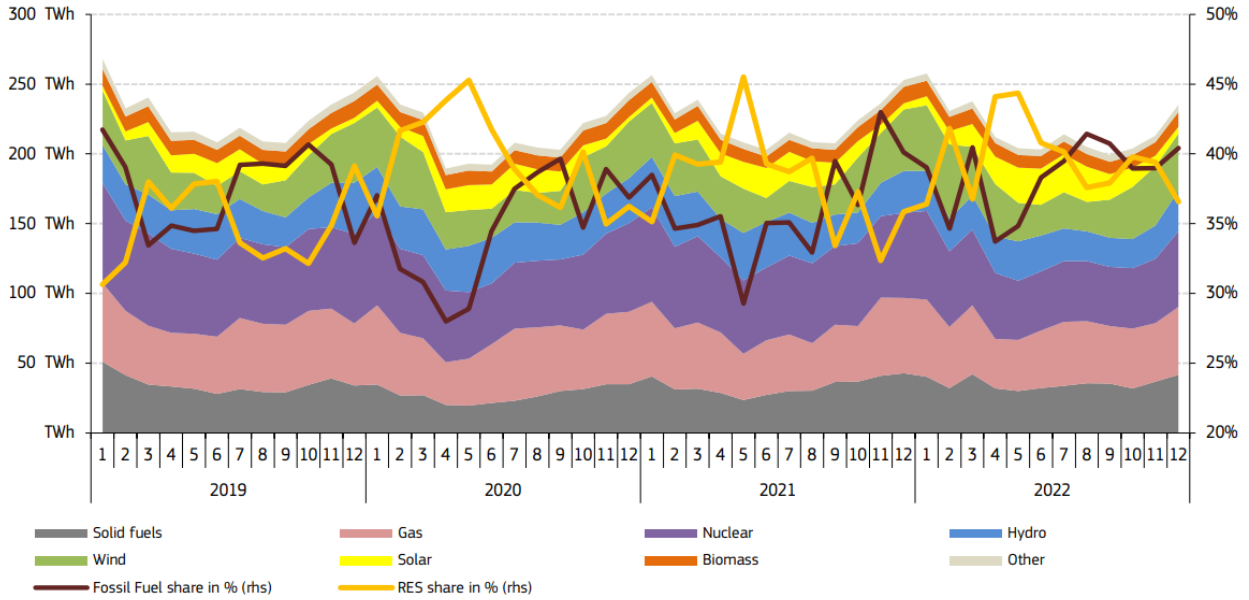

Figure 1.2: Monthly power generation in EU per type of technology (*European Commission, Quarterly report on European electricity markets*, 2023)

While significant decarbonization of power systems is achievable, considerable changes to their core composition are still required. One of the main evolution concerns the generation mix, which still relies on a large share of GHG emitting generators as of today (accounting for around 35% to 40 % of the electricity produced in the EU, Figure 1.2[2]). Most European countries are planning to phase out of these technologies, and focus instead on variable Renewable Energy Sources (vRES)–wind and solar units–which offer carbon-free generation once installed. Several national projections aim to cover over 80% of their electricity generation using renewable sources by 2050[3]. Because of the intermittent aspect of vRES, these shares of final energy generation require massive installed capacities, which brings new challenges upon power system management. Indeed, the uncertainty on their power output is expected to increase balancing needs (see (Doherty et al., 2009), (Holttinen et al., 2011), (Goodarzi et al., 2019) or (Heggarty et al., 2019) for instance). Meanwhile, the aforementioned massive electrification will not only lead to a significant increase in energy consumption, but also create opportunities for new types of flexibilities through more adaptable and controllable demand assets (notably demand response, power-to-gas and electric vehicles). Storage technologies will also play a crucial role as local flexibility options in future power systems (IEA, 2021).

The new European balancing energy markets were designed with these modifications of generation and consumption sides in mind. They should provide the tools to compensate for the increase of balancing needs linked with vRES assets by (i) enhancing the pool of available reserves in all areas, (ii) improving the access to balancing processes for new actors of the energy transition–vRES themselves, but also storage or demand

[2]The fossil fuel share is a good indicator here, as it only counts GHG emitting fuels and notably not nuclear.

[3]According to the Long Term Strategies of the European Commission, available at https://commission.europa.eu/energy-climate-change-environment/implementation-eu-countries/energy-and-climate-governance-and-reporting/national-long-term-strategies_en

response–, and (iii) providing actors with new close-to-real-time opportunities to balance themselves.

1.2 Overview of historical balancing processes in Europe

To grasp the challenges and opportunities associated with common balancing markets, it is essential to gain a comprehensive understanding of the historical processes they aim to replace. As previously noted, the different TSOs in Europe historically managed the balancing stage locally, employing diverse and heterogeneous processes. Setting a common balancing system requires complete harmonization, while the differences between historical balancing processes were numerous (for instance, the type of balancing reserves used, the TSO strategy or the remuneration scheme). Systemic differences can be linked to the composition of the local power system. Section 1.2.1 details some of these links, concluding with a brief comparison of the German and French power systems and their impact on balancing processes. Other types of disparity between balancing processes are overview in Section 1.2.2. Finally, a practical example is proposed in Section 1.2.3 through a more detailed description of the French balancing process.

1.2.1 Detailed description of specific differences that can be linked to the local power system composition

Historical types of balancing reserves: diverse nomenclature and heterogeneous local usage

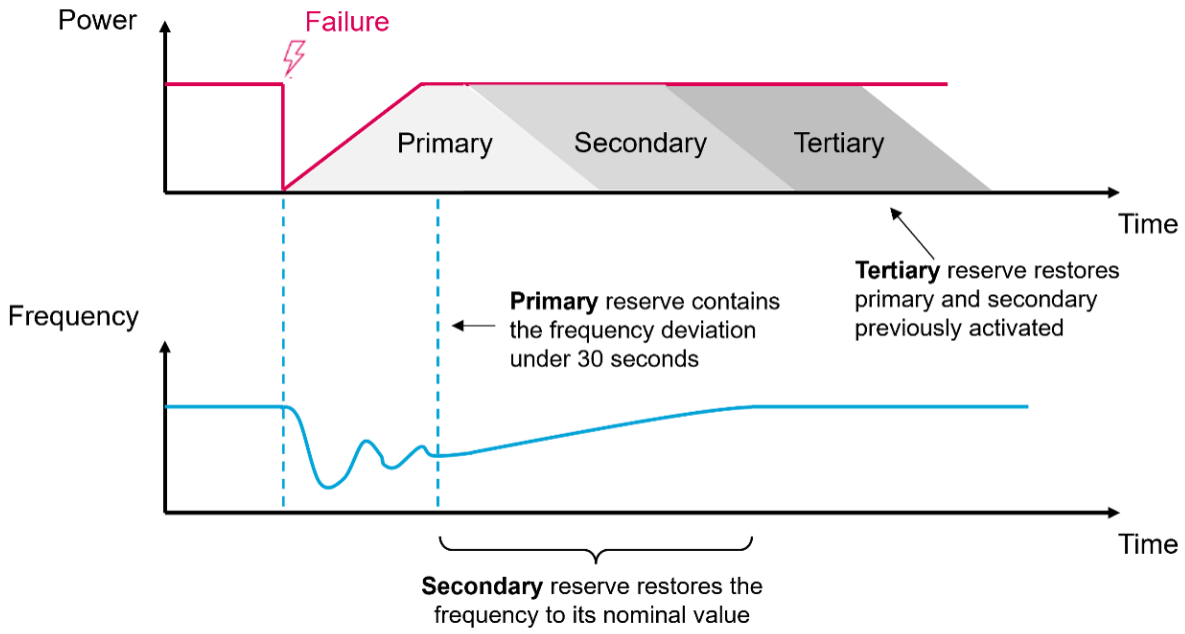

Figure 1.3: Historical reserve types and roles, based on https://www.services-rte.com/en/learn-more-about-our-services/providing-frequency-ancillary-services.html

The term “balancing reserves" does not represent a single type of product, but instead, a series of products

with different characteristics, response times and objectives. Historically, there has been little harmonization between European areas on both the types of reserves used and their nomenclature. It is still possible to classify them into three main categories (Rebours et al., 2007a), while highlighting key usage differences on the basis of the ENTSO-E report (ENTSO-E, 2021):

- *Primary* reserves correspond to the fastest type of reserves, linked with the inertia of the power system. These reserves are automatically activated within a few seconds to stop any frequency deviation around its nominal value of 50 Hz[4]. This automatic activation has already been performed at the cross-border scale for several decades, in synchronous areas (the larger one covers most of continental Europe, with another synchronous area gathering Finland, Norway and Sweden). Primary reserves are used in almost all areas, with the exception of Baltic States which are supplied by the Russian TSO (Ocker et al., 2016).

- *Secondary* reserves are also activated automatically, in the range of a few seconds to a few minutes. As opposed to primary reserves, their activation is performed locally, within the control area of a given TSO. The main objectives of this type of reserve are to restore exchanges with other control areas (which were modified by the primary reserves activation), and to bring the frequency back to its nominal value. Secondary reserves are employed in all areas, except the Baltic States, Ireland and the United Kingdom.

- *Tertiary* reserves are manually activated reserves, with an activation time typically within 15 to 30 minutes. Their main purpose is to replace previously activated primary and secondary reserves, to enable them to respond again to future imbalances. Because of their manual aspect, they can also be activated preemptively, in anticipation of future imbalances. Depending on the area, tertiary reserves can be further subdivided into two categories: *fast tertiary* reserves that can be activated within 15 minutes, and *slow tertiary* activated within 30 minutes. Fast tertiary reserves are used in all areas, except Ireland, Italy, Hungary and Poland. Meanwhile, slow tertiary reserves are only used in a subset of European states: France, Greece, Hungary, Italy, Lithuania, Poland, Portugal, Romania, Spain, Switzerland, and the United Kingdom.

As a first example of links between reserve usage and power system characteristics, the lack of secondary reserves in the United Kingdom and Ireland can be explained by their island aspect. As described before, one of the main roles of this type of reserve is to restore exchanges with other areas. Since these countries are connected to the rest of Europe by HVDC links, they are not part of the European synchronous zone: imbalances in their area only affect their local frequency, and do not change exchanges with other areas. To extend this analysis to the characteristics of German and French power systems, additional design differences must be detailed, which is the objective of the rest of this section.

It is important to note that the set of physical constraints associated with automatic reserves (primary and secondary) differs significantly from that of manual reserves (tertiary). Consequently, their modeling practices diverge as well, and it is difficult to encompass both categories in the same model or study. The scope of this thesis is then further narrowed to manual reserves, and automatic reserves will only be mentioned sporadically.

[4]Frequency is the image of the supply-demand balance, and is supposed to be at 50 Hz at equilibrium in the European synchronous area. A lack of generation results in a frequency decrease, while the opposite induces a frequency increase.

Proactive or reactive: two different strategies for European TSOs

To resolve their local imbalances, two main approaches are used by the different TSOs in Europe: the *reactive* strategy, and the *proactive* strategy. Reactive TSOs only carry out balancing actions when imbalances are observed. Consequently, they usually procure and activate large quantities of balancing reserves of fast to mid types (secondary and fast tertiary reserves). Conversely, proactive TSOs seek to forecast their imbalance ahead of real time, and to activate balancing energy in advance. This activation is performed using manual reserves (i.e. tertiary), and notably includes slow tertiary reserves. Similar to reactive TSOs, proactive TSOs also perform balancing activations for observed imbalances, but usually in lower volumes thanks to proactive measures. This diminution of reactive activation would, in turn, result in lower procurement volumes.

Each strategy has its advantages and disadvantages. Being reactive lowers the requirement in forecast and computation processes, as there is no need to estimate future imbalances. However, it usually results in higher volumes of observed imbalances, which are then absorbed by fast reserves (notably by secondary and fast tertiary types). To ensure the sufficient availability of these reserves, they should be procured in large quantities, which leads to significant procurement costs. Meanwhile, the proactive strategy is more complex and requires upfront investments in forecast processes, but results in lower balancing costs because of two aspects: the lower procurement requirements, and the activation of slower–hence usually cheaper–tertiary reserves. In addition, this strategy can also be used to cover the lack of specific reserve types. This is for instance the case in the United Kingdom, which compensates its absence of secondary reserves by proactively activating tertiary reserve (Håberg and Doorman, 2016).

(Håberg and Doorman, 2016) classified European TSOs according to their chosen strategy. Germany, Austria, Belgium and the Netherlands tend to gravitate more towards the reactive strategy. Meanwhile, the United Kingdom, France, Switzerland, Nordic countries, and to a lesser extent Denmark used the proactive strategy.

Dispatch systems in Europe

As a last detailed example of design difference, the type of dispatch system employed for balancing processes varies in the different European countries. We note that, within a given country, it can even differ from the dispatch system used for day-ahead or intraday processes.

Three main dispatch types can be distinguished in Europe, according to (ENTSO-E, 2021). With a *central dispatch* system, the TSO directly determines the power output of most generation units in its area, which includes any balancing activation. In a *unit-based self-dispatch* system, each unit sets its own schedule. Balancing energy activations are consequently performed at the unit scale. Finally, the *portfolio-based self-dispatch* system is similar to the unit-based system, in that TSOs do not control the program of units. With this system, however, balancing activations are performed at the scale of a portfolio, meaning an aggregation of several units.

Dispatch system	Central dispatch	Unit-based self-dispatch	Portfolio-based self-dispatch
Areas	Bosnia, Greece, Ireland, Italy, Poland, Romania, Serbia	Belgium, Czech Republic, Estonia, France, Lithuania, Norway, Spain, United Kingdom	Austria, Croatia, Denmark, Finland, Germany, Hungary, Latvia, Netherlands, Portugal, Slovakia, Slovenia, Sweden, Switzerland

Table 1.1: Dispatch systems used by European countries for balancing processes

The differences between central dispatch and self-dispatch systems are analyzed in (Ahlqvist et al., 2018). While the central system should theoretically be more effective (with a more precisely model of the power system), but is computationally heavier and can be opaque for market participants. On the other hand, self-dispatch provides more flexibility to market actors and facilitate clearing processes, but are limited by inefficiencies associated with market orders (this point will be further discussed in Section 1.3). In any case, both systems lead to major differences in balancing management, reinforcing the heterogeneous aspect of European processes.

The link between balancing processes and local power systems compositions: brief comparison of German and French power systems

There is a wide diversity in local power system compositions across Europe, which partially influenced the design of local balancing processes. We can highlight this link by considering two specific areas with very distinctive balancing processes: Germany, and France.

Up until the 2010s, the power system of Germany was primarily composed of relatively flexible fossil-fueled power plants: gas, coal and lignite accounted for 50% to 70% of German installed capacities between 1990 and 2010[5]. Meanwhile, the share of vRES capacities increased significantly during the last two decades. The percentage of wind capacities steadily increased from 10% to more than 20%, while solar capacities went from less than 1 to more than 20% as well. Overall, Germany faced substantial balancing uncertainties linked with its high and increasing share of vRES capacities, and its power system was mostly composed of units that could provide secondary or fast tertiary reserves. This supports the choice of the reactive TSO strategy since, as mentioned above, it relies on these types of reserves. This also explains the absence of slow tertiary reserves in German balancing. Finally, developing a portfolio-based approach for the balancing stage was also interesting to help internalize vRES uncertainties.

Compared to the German area, the French power system is characterized by a large share of thermal units with a slow dynamic. Indeed, in 2022, nuclear power plants represented 43% of the installed capacities and accounted for 63% of the electricity generated. These shares were even greater two decades ago, before the clear beginning of the energy transition. Nuclear plants can participate in balancing processes, but are constrained by heavy physical limitations. In particular, they must stay at a constant power output for at least 2 hours between two power output variations, a constraint called minimum stable power duration (Jenkins et al., 2018, Petitet et al., 2019). To capture the potential of nuclear in balancing processes, it was then interesting to design longer products (i.e. slow tertiary reserves). The proactive strategy also pairs well with this type of operating constraints, as nuclear generation schedules can then be adapted in advance to respect their minimum stable power duration. Finally, it justifies using a unit-based dispatch system, to ensure that balancing activations do not violate operating constraints on individual units. This description is extended in Section 1.2.3, which proposes a detailed overview of the French historical balancing process.

1.2.2 Other disparities between balancing processes

On top of the systemic differences previously outlined, historical balancing processes differed in many more aspects, which are briefly presented in the current section.

[5]Extracted from the Fraunhofer Institute https://www.energy-charts.info/charts/installed_power/chart.htm?l=en&c=DE&chartColumnSorting=default&year=2015.

Variable remuneration schemes

Within historical balancing processes, three different remuneration schemes were used across Europe to compensate for balancing energy activations (van der Veen and Hakvoort, 2016). The *marginal* pricing method requires the use of a Common Merit Order List (CMOL). A uniform price is then defined, based on the price of the last reserve activated within the CMOL. This marginal price is then applied to all activated reserves. The *pay-as-bid* pricing remunerates each activated reserve according to the price indicated by the associated actor. *Regulated* pricing methods correspond to fixed prices, usually updated at a given frequency. Finally, *hybrid* pricing combines marginal / pay-as-bid pricings with regulated aspects.

Remuneration schemes varied not only according to the type of reserve, but also between areas for the same reserve type (ENTSO-E, 2021). Table 1.2 indicates the pricing scheme used for each type of reserve in Europe, excluding primary reserves[6]:

Remuneration scheme	Marginal price	Pay-as-bid	Regulated price	Hybrid
Secondary reserves	Bulgaria, Finland, Netherlands, Norway, Poland, Portugal, Romania, Sweden	Austria, Belgium, Bosnia & Herzegovina, Croatia, Germany, Hungary, Italy, Slovakia, Slovenia	Czech Republic, Denmark, France	Greece, Serbia, Spain, Switzerland
Fast tertiary reserves	Belgium, Bulgaria, Denmark, Estonia, Finland, Greece, Latvia, Lithuania, Netherlands, Norway, Portugal, Spain, Sweden	Austria, Bosnia & Herzegovina, Croatia, Czech Republic, France, Germany, Hungary, Romania, Serbia, Slovakia, Slovenia, Switzerland, United Kingdom	-	Ireland
Slow tertiary reserves	Czech Republic, Hungary, Poland, Portugal, Romania, Spain, Switzerland	France, Italy, United Kingdom	-	Ireland

Table 1.2: Remuneration schemes used by European countries for balancing activation processes

Temporal differences of activation processes

Balancing activation processes can differ on two key temporal aspects (van der Veen and Hakvoort, 2016). First, on the frequency of market execution and the balancing Gate Closure Time (GCT). The GCT is the limit of participation in wholesale markets for BRPs. Past this limit, TSOs are responsible for the supply-demand balance of their area. Consequently, a larger GCT attributes more balancing responsibility to the TSO, while a smaller one produces the opposite effect. Second, the temporal resolution of processes is also heterogeneous, and varies between.

Imbalance settlement processes and prices

Finally, multiple imbalance settlement processes are used across Europe. All share the same basic concepts. They involve two types of entities, Balancing Responsible Parties (BRPs) and TSOs. The former are financially responsible for respecting the commercial balance of a given perimeter that includes a set of generation and load units. After real-time and balancing processes, TSOs compute the imbalance of each

[6]In (ENTSO-E, 2021), data regarding primary reserves activation is unavailable for most European areas. In addition, remuneration schemes for the United Kingdom were extracted from the previous report (ENTSO-E, 2017), as they were unavailable in the updated version.

BRP by comparing their market commitments and the actual balance of their perimeter. This imbalance is then remunerated when positive (i.e. an excess of generation) or penalized when negative (i.e. a deficit of generation).

Although European settlement processes differ in many respects, (van der Veen et al., 2010) identifies the type of Imbalance Settlement Price (ISP) as the most important one. ISPs can be divided into two main categories: single imbalance pricing and dual imbalance pricing. With the single pricing method, positively and negatively imbalanced BRPS are settled based on the same price, which varies only according to the overall imbalance in the TSO area. This method usually rewards BRPs that are imbalanced in the opposite direction to that of the TSO area, incentivizing them to forecast system imbalances and assist in resolving them. Meanwhile, with the dual pricing, different prices are used to settle positively and negatively imbalanced BRPs. It encourages BSPs to stay balanced, as the price is usually penalizing in both directions.

1.2.3 A closer look at a balancing process: the French example

As described above, several design aspects define the different local balancing processes. They can be illustrated by focusing on the specific process employed by the French TSO RTE in its area, and detailing two of its main components: the balancing energy process, and the imbalance settlement process. Providing this closer look is interesting for two main reasons. First, it serves as a practical example of historical balancing processes, and from which differences with the new common balancing markets can be highlighted. The second reason is that both components presented here will be used as the reference when modeling historical balancing and imbalance settlement processes throughout this thesis.

The energy activation process: "Mécanisme d'Ajustement"

The "Mécanisme d'Ajustement", which can be translated to "Balancing Mechanism", is the historical balancing energy process used by the French TSO RTE, operational since the beginning of the 21^{st} century. We will call it FrBM, for French Balancing Mechanism, in the rest of the document.

The complete description of the FrBM is available at https://www.services-rte.com/files/live/sites/services-rte/files/documentsLibrary/RM-2-MECANISME_D_AJUSTEMENT-V01-20240401_3550_fr. It is also summarized in (RTE, 2017).

The role of the FrBM is to activate tertiary reserves to correct observed or forecasted supply-demand imbalances in the French area. It is executed at an hourly frequency, over a two-hour time frame T_{FrBM} illustrated in Figure 1.4.

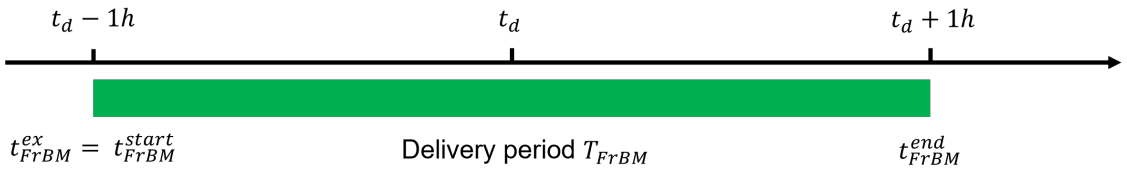

Figure 1.4: Time frame of the historical French Balancing Mechanism

As before, the notation t_d is used to designate a delivery date (i.e. the real time). On this timeline, t^{ex}_{FrBM} is the execution date of the process, and corresponds to the gate closure time of the French balancing

process. The effective time frame of the FrBM (between t_{FrBM}^{start} and t_{FrBM}^{end}) starts directly after the gate closure time: it corresponds to a period called "fenêtre opérationnelle" in French (which can be translated to "neutralization lead time"), during which the generation and consumption programs of units in the area are set. Only the TSO, through the FrBM, can modify these programs. The proactive strategy used in France is illustrated here, as the TSO is able to activate reserves *ahead of* the delivery date t_d, if it anticipates imbalances.

Each unit connected to the French transmission network is required to submit its entire available capacity to the FrBM, in both upward and downward directions, through reserve offers. These offers are considered "specific", as opposed to the "standard" market orders that will be part of common balancing markets (see Section 1.3.2.1). Indeed, on the FrBM, balancing offers indicate the price at which they should be activated (set by the units themselves) but do not specify any maximum or minimum quantity, nor any activation duration. Instead, each unit sends to the TSO its generation or load program, as well as all its operating constraints. The task of computing the feasible power range of each unit is then left to the TSO (a simplified example is illustrated in Figure 1.5, for a given unit).

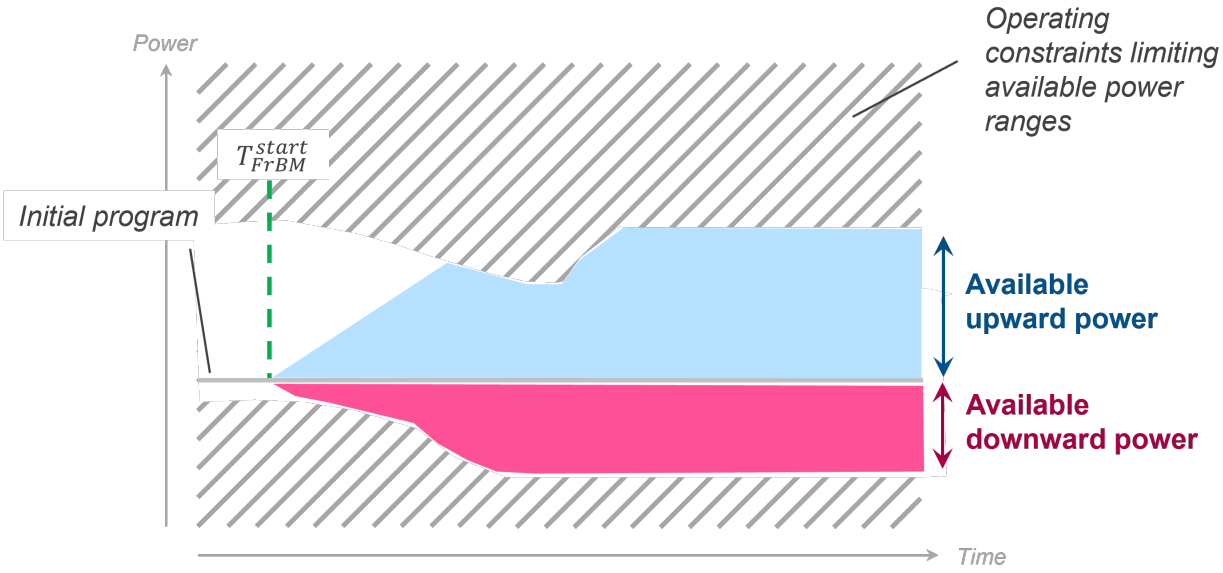

Figure 1.5: Illustration of the specific orders on the FrBM

After receiving all previous information from BSPs, RTE then proceeds to the balancing activations. The TSO first computes the projected local imbalance, based on generation and load plans of units in its area, as well as forecasts of variable assets. This imbalance is then resolved by activating energy among the offers sent by BSP, based on a merit order list that integrates all operating constraints. More formally, the resulting problem is similar to a unit commitment performed at the country scale, to resolve a given volume of balancing needs. In practice, it does include additional complexity, as internal network constraints are part of the computation. As discussed before, these aspects are not considered in the thesis.

At the end of the process, activated units are remunerated according to the "pay-as-bid" scheme, meaning at the price of their order multiplied by the activated energy.

Finally, we can provide numerical examples to help visualize the activated volumes involved in the FrBM. On average between 2010 and 2023, the yearly volume activated on this process was 3.58 TWh in the upward direction and 4.6 TWh in the downward direction[7].

The French imbalance settlement process

The French imbalance settlement process functions on the basis previously described: it remunerates BRPs that are positively imbalanced, while BRPs negatively imbalanced are required to pay for it.

This process is executed at the end of each month, and currently settles imbalances over a 30-minute period, which will soon be shortened to 15 minutes[8] (Figure 1.6).

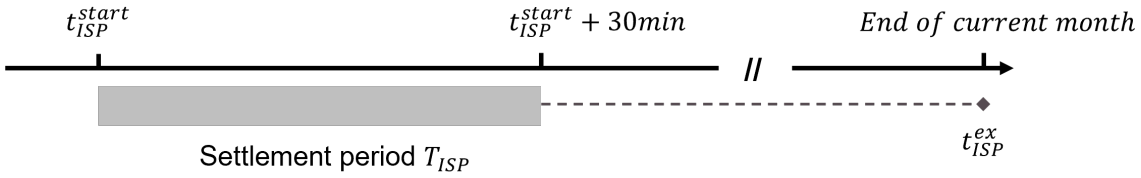

Figure 1.6: Time frame of the French imbalance settlement process

The official description of the Imbalance Settlement Price (ISP) used in the French process is available at https://www.services-rte.com/en/learn-more-about-our-services/becoming-a-balance-responsible-party/Imbalance-settlement-price.html.

Its computation can be summarized in Table 1.3:

	Imbalance direction in the French area	
BRP imbalance direction	**Upward needs**	**Downward needs**
Positive	$\lambda_w^{up} * (1 - \sigma_{\lambda_w^{up}} * k)$	$\lambda_w^{down} * (1 - \sigma_{\lambda_w^{down}} * k)$
Negative	$\lambda_w^{up} * (1 + \sigma_{\lambda_w^{up}} * k)$	$\lambda_w^{down} * (1 + \sigma_{\lambda_w^{down}} * k)$

Table 1.3: French imbalance settlement price computation

Where:

- $\lambda_w^{\bullet}$ is the volume-weighted average price of balancing activations in the $\bullet$ direction. These activations include primary, secondary and tertiary reserves, meaning that the weighted price takes into account activations performed by the FrBM.
- $\sigma_{\lambda_w^{\bullet}}$ indicates the sign of the weighted price ($= 1$ for a positive or null price, and $= -1$ for a negative price), and ensures that the ISP sends the same incentive to BRPs regardless of the sign of $\lambda_w^{\bullet}$.
- k is a coefficient defined ex-ante that aims to balance income and expenditure of the energy component of the balancing-imbalances account, based on historical data. This coefficient is occasionally updated, and has been set at 0.05 since 2019.

[7] Source: https://analysesetdonnees.rte-france.com/en/markets/balancing

[8] For more information: https://www.services-rte.com/en/learn-more-about-our-services/preparation-for-the-upcoming-amendments-related-to-the-transition-to-the-15-minute-imbalance-settlement-period-isp15.html

With this ISP, positively and negatively imbalanced BRPs are not settled with the same price, because of the $(1 \pm k)$ component. This is the distinctive aspect of a dual imbalance price scheme. Interestingly, the French ISP has both been described as single (ENTSO-E, 2021 or Roumkos et al., 2022) and dual (Vandezande et al., 2009 or Matsumoto et al., 2021) in the literature. This misclassification as a single price may come from the fact that the other component of the ISP–the weighted price of balancing activations $\lambda_w^{\bullet}$–displays characteristics usually associated with a single price scheme: this component does not depend on the BRP imbalance, but only on the direction of the overall French imbalance. Another possible explanation is the small value of the k coefficient, implying that prices for positively and negatively imbalanced BRPs are usually close. In any case, the French ISP as a whole should be considered as a dual price, and indeed conveys the usual incentives of this category as it encourages BRPs to stay balanced.

1.3 The future of balancing in Europe: common balancing energy markets

The design of the new European common balancing energy markets differs significantly from the heterogeneous processes described previously. This section provides a practical description of the designs of these new markets, to help highlight the challenges and opportunities of the ongoing balancing transition.

1.3.1 New harmonized types of reserves and new energy markets

The common balancing markets are structured around 4 harmonized types of reserves:

- Frequency Containment Reserve (FCR)
- automatic Frequency Restoration Reserve (aFRR)
- manual Frequency Restoration Reserve (mFRR)
- Replacement Reserve (RR)

Figure 1.7 shows the correspondence between this new nomenclature and the historical one, which was presented in Section 1.2.1. It also gives an overview of market geographical scopes, their official launching date and the name of their respective cross-border platform. In the figures, “operational members" correspond to actual market participants, while the other categories describe areas that are expected to or could join the market in the future. It should be noted that FCR is not part of an activation market, since their activation is directly tied to dynamic elements of the power systems. They retain the same geographical scope as primary reserves, i.e. the European synchronous area. In addition, both aFRR and mFRR markets only went into operation recently. While their number of participants is currently small (Germany, Austria and Italy for aFRR only), it is expected to grow significantly in the following years. The potential number of participants in the RR market is lower, which can be explained by the fact that only a part of European areas use slow tertiary reserves (as discussed in Section 1.2.1).

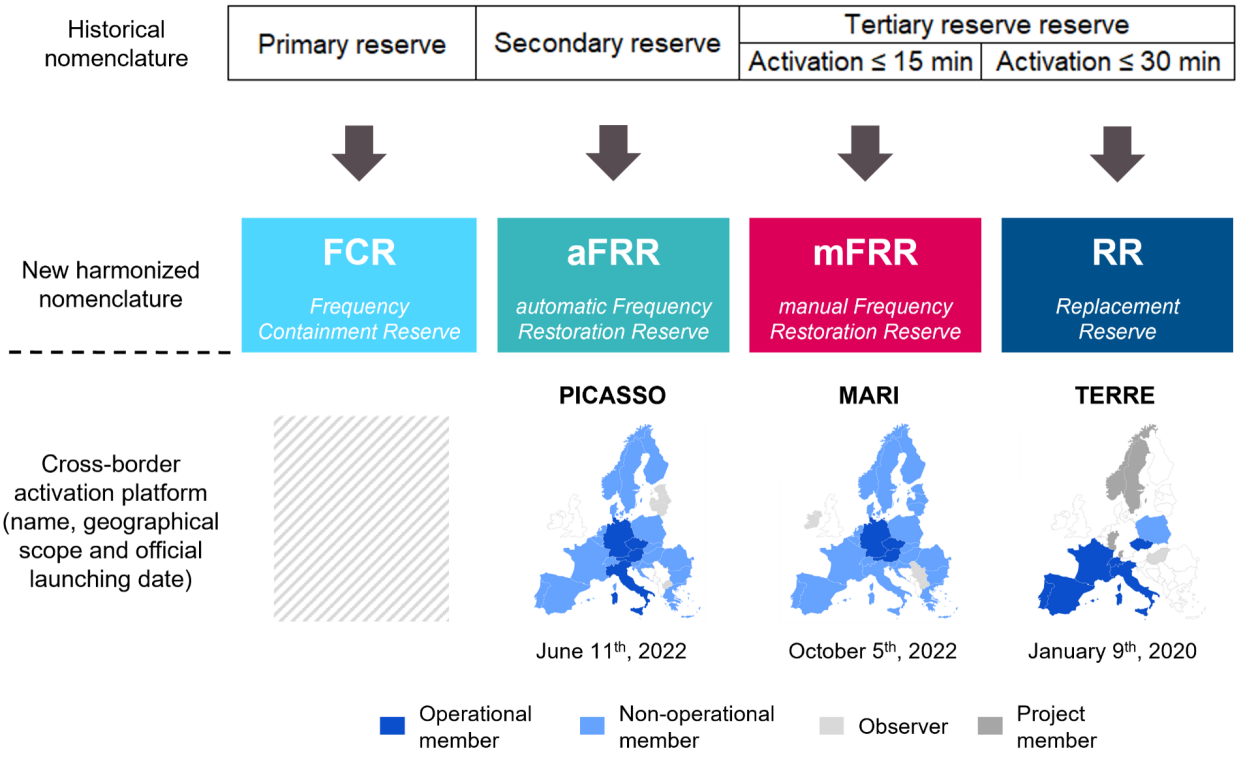

Figure 1.7: Nomenclature of harmonized European reserves (European maps are taken from https://www.entsoe.eu/)

Given that the focus of this thesis is set on manual reserves, only RR and mFRR markets will be detailed in the rest of this section.

1.3.2 Design of RR and mFRR energy markets

RR and mFRR markets share many similarities regarding their overall framework and market order standards, allowing for a common design overview. Details about the current designs of both the RR market and the TERRE platform can be found on https://www.entsoe.eu/network_codes/eb/terre/, notably the description of the clearing algorithm (ENTSO-E, 2023c). For the mFRR market and the MARI platform, one can refer to documents available at https://www.entsoe.eu/network_codes/eb/mari/, notably the description of the activation optimization function (ENTSO-E, 2023a).

An important remark is required concerning the mFRR market. In practice, it is characterized by two distinct operational modes: “scheduled activations" and “direct activations". The scheduled activations mode is a discrete market with a set delivery period occurring at a given frequency, similar to the RR market process. On the other hand, the direct activations mode corresponds to a continuous market, comparable to the process of European intraday markets. At any time, a TSO can submit balancing needs to the MARI platform, immediately met by a reserve activation. To limit the allow for a common analysis of RR and mFRR markets, the direct mode is not addressed in this thesis. In the rest of this document, any mention of the mFRR market will specifically refer to the scheduled mode.

1.3.2.1 Market framework and time frames

The high-level framework of both RR and mFRR markets is illustrated in Figure 1.8. They involve two main categories of market actors: Balancing Services Providers (BSPs), and TSOs.

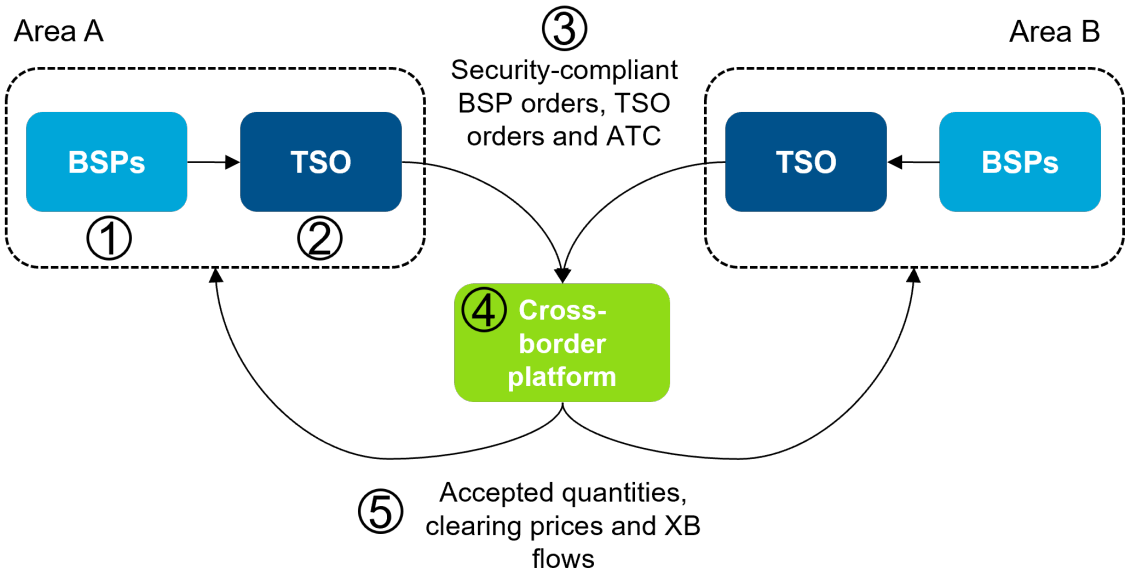

Figure 1.8: General framework of RR and mFRR markets

The overall process is divided into several steps:

1. BSPs create balancing energy offers, which may correspond to (i) previously procured capacity or (ii) voluntary bids, if they have available capacity (Poplavskaya et al., 2021). They then send their market orders to their respective TSO before the BSP Gate Closure Time (GCT^{BSP}), which is specific to each balancing product.

2. In a second time, TSOs perform two main tasks. First, they carry out a filtering process on BSP orders for safety reasons. This filter is notably performed to avoid internal network congestions[9] and to ensure future security of supply aspects in the case of TSOs with a margin approach to procurement[10]. TSOs also create their balancing need orders, computed according to the observed or forecasted imbalance in their area.

3. In a third step, TSOs submit all orders in their area, and the Available Transmission Capacities (ATC) on their cross-border transmission lines, to the cross-border platform before the TSO Gate Closure Time (GCT^{TSO}).

4. The fourth step is the so-called “Market Clearing". The cross-border platform first gathers market orders from all areas. At this stage, BSP and TSO orders are grouped together in purchase and sale

[9]European common balancing markets do not account for congestions within market areas. This aspect, and the TSO filtering, are not further considered in this thesis. A deeper look can be seen in (Girod et al., 2022) and (Girod et al., 2024)

[10]The margin approach is mainly used by the French TSO, and consists in an evolutive and close-to-real-time sizing of both procured and available reserves. Further details can be found in (Hary, 2018).

curves, thus becoming indistinguishable[11]. Sale and purchase orders are then selected and activated using a Common Merit Order List (CMOL), with the aim of maximizing social welfare. This principle is illustrated in Figure 1.9: all orders on the left side of the purchase and sale curves intersection are accepted.

Figure 1.9: Illustration of the clearing step in RR and mFRR common markets

This merging of BSP and TSO orders in similar curves has two practical implications. First, it allows matching TSO orders together, which is commonly known as netting between areas. In addition, BSP orders of opposite directions can also be matched, if their prices are suitable. This principle is called "counter-activation", and was deemed beneficial by (Marquet, 2018) after a study on the mFRR market. Consequently, it is to our knowledge available in both RR and mFRR markets.

Cross-border transmission line constraints are integrated into the Clearing process, using ATC values previously transmitted by TSOs. At the end of the Clearing, RR and mFRR market prices are determined according to the marginal pricing method.

5. Eventually, market results are sent back to all actors after the Clearing process. They include the quantities activated on each market order, the market clearing prices in all areas, and the updated power flows on all cross-border transmission lines. BSPs are then required to provide the activated quantities at the beginning of the delivery period of the market, within the so-called "Activation period".

While RR and mFRR markets include the same aforementioned steps, each possesses specific duration characteristics. Figure 1.10 represents their time frames and the different steps, illustrating the various durations. We should note that the scale of both time frames is not identical. It is enlarged for the mFRR for a better display, as it is much closer to real-time than the RR market. In addition, the mFRR market has

[11] The only exception to this rule are inelastic TSO orders, whose acceptation is prioritized over other orders.

a specific feature regarding its activation period, as it can overlap with its delivery period. The explanation of this feature will be detailed in Section 1.3.2.2.

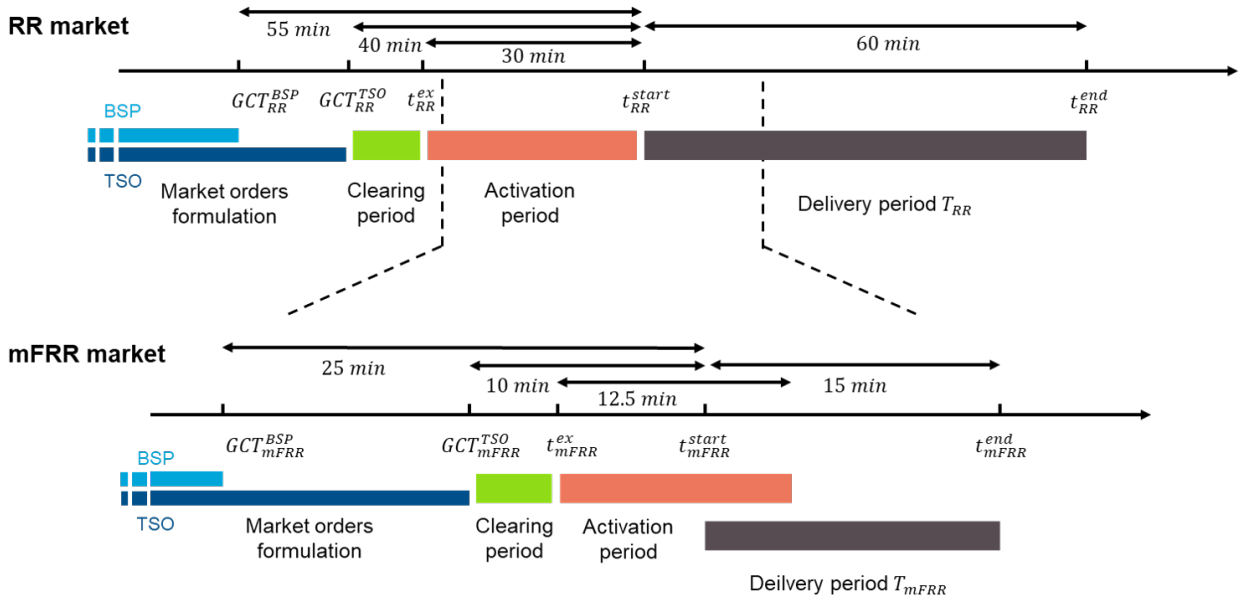

Figure 1.10: Illustration of RR and mFRR market time frames

On these time frames:

- t_m^{ex} is the execution date of the market $m \in \{RR, mFRR\}$, indicated by the end of the Clearing period.
- t_m^{start} and t_m^{end} are respectively the beginning and the end of the delivery period of market m. This period lasts for 60 minutes-divided in four time steps of 15 minutes–in the case of the RR market. Meanwhile, it only lasts for 15 minutes for the mFRR market and is comprised of a single time step.
- For the RR market, the value of the BSP Gate Closure Time GCT_{RR}^{BSP} depends on the area, as it is set by each TSO. It is usually comprised between 60 and 50 minutes before t_{RR}^{start}. For the mFRR market, GCT_{mFRR}^{BSP} is set at 25 minutes before t_{mFRR}^{start}.
- The TSO Gate Closure Time GCT_{RR}^{TSO} of the RR market is universally set at 40 minutes before t_{RR}^{start}. For the mFRR market, GCT_{mFRR}^{TSO} is set at 12.5 minutes before t_{mFRR}^{start}.

Both markets also differ in terms of frequency. Indeed, the RR market is executed at an hourly frequency, and the mFRR market at a 15-minute frequency. In practice, this implies that four mFRR markets are executed on the same delivery period as one RR market.

Finally, it is relevant to note that these markets do not manage the imbalance settlement process. It is still designed and operated locally by each TSO.

1.3.2.2 Standardization of market orders

Setting a European cross-border market requires a high degree of harmonization on the characteristics of market orders that can be traded. The chosen design of RR and mFRR markets imposes a standardization of

the shape of these orders: they correspond to a “rectangle" of available energy delimited by time and power bounds (Figure 1.11).

Characteristic	Description
t_o^{ex}	Creation date of order o
t_o^{start}	Start date of order o
t_o^{end}	End date of order o
q_o^{min}	Minimum power offered for order o
q_o^{max}	Maximum power offered for order o
p_o	Price of order o
σ_o	Boolean indicating the direction of order o $\sigma = 1$ for purchase, -1 for sale

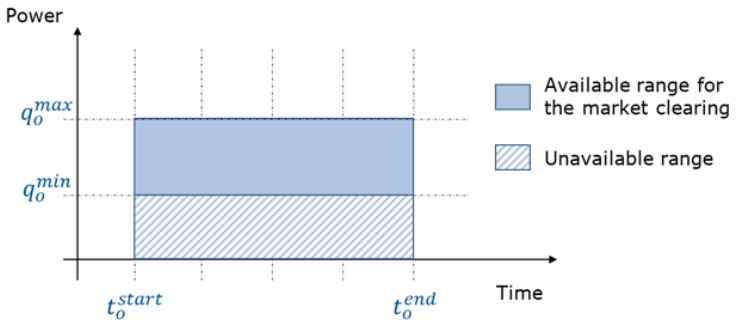

Figure 1.11: Characteristics and general shape of balancing energy market orders

These order characteristics are constrained by the requirements of RR and mFRR products. The types of requirements are once again similar across both markets, but their values differ according to the duration of each market. Figure 1.12 illustrates the types of temporal requirements, with the actual shapes of the RR order on the left side and of the mFRR order on the right side. It is complemented by Table 1.4, which indicates the values of the requirements for both types of reserve.

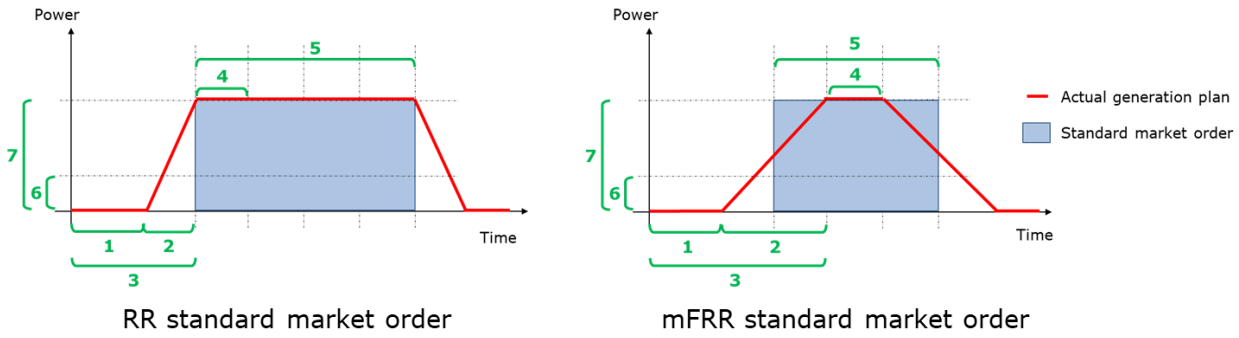

Figure 1.12: Types of temporal requirements of balancing market standard products

	RR		mFRR	
Requirement	**BSP order**	**TSO order**	**BSP order**	**TSO order**
Preparation period (1)	Between 0 and 30 min	/	2.5 min	/
Ramping period (2)	Between 0 and 30 min	/	10 min	/
Full Activation Time (3)	30 min	/	12.5 min	/
Minimum duration (4)	15 min	15 min	5 min	5 min
Maximum duration (5)	60 min	60 min	15 min	15 min
Minimum quantity (6)	1 MW	1 MW	1 MW	1 MW
Maximum quantity (7)	/	Up to the quantity of bids in the same direction submitted by BSPs in the TSO's area	/	/
Minimum price	-10,000 €/MWh	-10,000 €/MWh	-15,000 €/MWh	-15,000 €/MWh
Maximum price	10,000 €/MWh	10,000 €/MWh	-15,000 €/MWh	-15,000 €/MWh
Price resolution	0.01 €/MWh	0.01 €/MWh	0.01 €/MWh	0.01 €/MWh
Allowed order divisibility	Fully divisible Partially divisible Indivisible	Fully divisible	Fully divisible Partially divisible Indivisible	Fully divisible
Allowed coupling links	Exclusive Multi-part Linked in time	Linked in time	Exclusive Multi-part	/

Table 1.4: RR and mFRR markets standard product requirements

The requirements deserve further explanation:

- The preparation period (1), ramping period (2) and their sum, corresponding to the Full Activation Time (FAT) (3), set an initial limit to the delivery duration: starting when market results are sent back to the actors, an order is required to deliver the activated quantity within the FAT. These three requirements only concern physical units, i.e. BSPs, and are therefore not applied to TSO orders. On the RR market, a BSP can modulate its preparation (1) and ramping (2) periods at will to comply with the FAT (3). In contrast, the preparation (1) and ramping periods (2) are fixed for the mFRR product, to achieve the shape described in Figure 1.12. This shape is a notable feature of the mFRR product. It guarantees that the energy activated with the actual generation plan corresponds exactly to the volume of the standard market order, even when considering ramping periods[12].
- Minimum (4) and maximum (5) durations impose boundaries on the length of a market order. We've seen previously that the total delivery period of the RR market is divided into 4 time steps of 15 minutes. In this market, an order is required to last at least a time step, so a minimum duration of 15 minutes. It also cannot exceed the total delivery period (maximum duration of 60 minutes). For the mFRR market, these values are respectively equal to 5 minutes and 15 minutes.
- Minimum (6) and maximum (7) quantities constrain the maximum power q_o^{max} that can be offered in an order o. A specific requirement is applied to the maximum quantity (7) of TSO orders on the RR

[12] As the mFRR product is shorter, achieving this correspondence becomes more important than for the RR market. Keeping a shape similar to that of the RR product could lead to significant mismatches in energy activated.

market: it is limited by the sum of power of all orders submitted in the same direction by BSPs in their area. For instance, if the total volume of upward orders formulated by BSPs in the area of a given TSO is equal to 70 MW, this TSO will not be able to submit an upward order of more than 70 MW, regardless of its actual balancing needs[13].

- The price p_o of orders is limited by minimum and maximum price requirements. The price caps of the RR market ($\pm 15,000$€/MWh) are larger than those of the RR market, to emphasize moments with scarcity.

- The last two requirements are related to complex orders, and are discussed in the following section.

1.3.2.3 The notion of complex orders

Finally, two different tools are included in balancing markets to transcribe the physical limitations of units into standard orders. We will refer to them as “complex orders", as they add another layer of intricacy to market processes.

- The **divisibility** of order o refers to its possible acceptance ratio, which is bounded by its characteristics q_o^{min} and q_o^{max} (Figure 1.13). Three types of divisibility are possible. A fully divisible order corresponds to $q_o^{min} = 0$. A partially divisible order has $0 < q_o^{min} < q_o^{max}$. For an indivisible order, $q_o^{min} = q_o^{max}$.

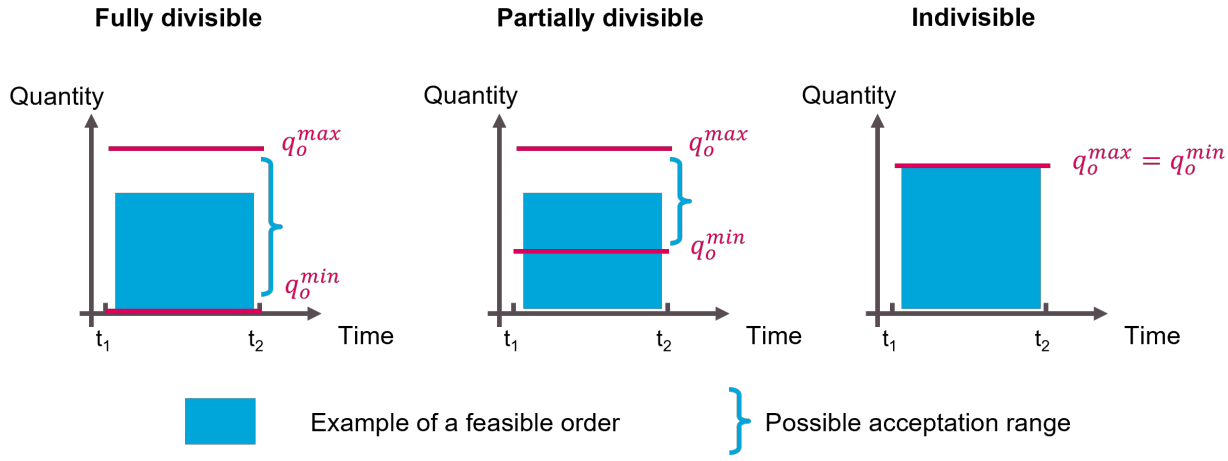

Figure 1.13: Order divisibility illustration

- Several types of **coupling links** can be used to link orders together (Figure 1.14). Among all orders linked by an *Exclusive* coupling, a single one can be activated. *Multi-part* couplings define a parent order, and a set of children orders. If any child order is accepted, then the parent order has to be accepted as well. Finally, orders *Linked in time* have to be accepted at the same quantity.

[13] More informations can be found in https://consultations.entsoe.eu/markets/rr_if_2nd_amendment/supporting_documents/202202_RRIF_2nd%20amendment.pdf.

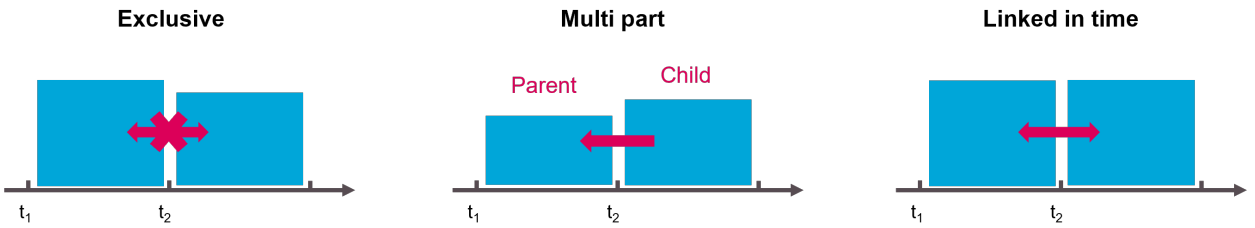

Figure 1.14: Coupling links illustration

A practical example can illustrate how these principles of complex orders are integrated into the BSP bidding process. Consider a unit with a minimum stable power duration constraint of 30 minutes (the same constraint that was discussed for nuclear units in Section 1.2.1) that wants to submit orders on the RR market. Because of this constraint, after a power output variation, the unit has to stay stable for at least 30 minutes before another power variation. As the RR market is divided into four different time steps of 15 minutes, formulating simple orders on each time step is not a possibility for the unit: the activation of a single order could violate its stable power constraint. To ensure that the RR activations will always be feasible, the BSP must link consecutive orders with the Linked-in-time coupling type. This example is illustrated in Figure 1.15.

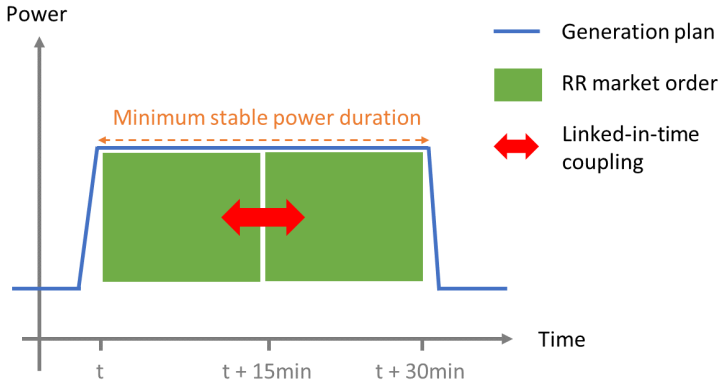

Figure 1.15: Illustration of a complex order integrating physical limitation of a generation unit

To summarize, the new common balancing markets should improve the efficiency of balancing activation processes, through exchanges at the European scale and a transparent and harmonized design facilitating the participation of new flexibility actors. It also requires significant adaptations from both the supply and the demand side, as the new design differs significantly from that of historical processes. Notably, the bidding process is completely different for BSPs because of the order standards previously described. For TSOs, this is even stronger as bidding on balancing markets is a novel environment.

1.4 Literature overview on balancing energy markets

Before introducing the key research questions of this thesis, a brief overview of the literature on balancing energy markets is proposed in this section. Its objective is not to be exhaustive, but rather to highlight

the key research fields already covered. More specific and in-depth reviews are carried out in the different chapters of this thesis. This review is divided into two sections: academic studies are discussed in a first section, while the different approaches to modeling balancing markets are introduced in a second section.

1.4.1 Academic studies on balancing energy markets

Design of common balancing energy markets

A part of the existing literature focuses on the design of the European balancing energy markets. The roots of this section of the literature are articles reviewing the diverse historical processes used in Europe. Some of them were already cited in Section 1.2. Both (Rebours et al., 2007a) and (Rebours et al., 2007b) combine to produce one of the first reviews of technical and economical aspects of balancing markets, including that of 7 European countries. (Håberg and Doorman, 2016) extended the comparison to the notion of TSO strategy, which was previously described.

(van der Veen and Hakvoort, 2016) produces a comprehensive high-level study of the various variables comprised in the design of a balancing process. The authors notably highlight the choices made in the diverse local balancing processes, with a detailed look at the Dutch system, They also exhibit possible trade-offs between design choices, which are used to define performance criteria helpful in comparing different market designs. Consequently, it can be used as a basis to study potential designs of common balancing markets. This design study is extended in (Rancilio et al., 2022), which emphasizes the analysis of regulatory trade-offs.

Complementing the previous approaches, several articles focus on a specific market design variable and try to conclude on the optimal choice. We can cite a few examples:

- The choice between marginal pricing and pay-as-bid methods is discussed by (Vandezande et al., 2010), (Akbari-Dibavar et al., 2020) and (Poplavskaya et al., 2020). The marginal pricing emerges as the better option compared to pay-as-bid, as it incites actors to bid at their true cost and consequently leads to lower system costs.
- The GCT of balancing processes has also been studied, notably by (Petitet et al., 2019). The authors compare the 1-hour GCT to the 15-minute GCT, two common design choices across European areas, and conclude that system costs are increased with the shorter GCT.
- Studies also reached topics just outside of the actual scope of common balancing markets, notably discussing the imbalance settlement process. We can cite (Van Der Veen et al., 2012), who compares different designs for the ISP and concludes that, although they lead to similar system imbalances, the single imbalance price is beneficial in terms of system and actor costs. Other articles on the subject notably include (T. W. Haring et al., 2015), (Bunn and Kermer, 2021) and (Matsumoto et al., 2021).

Benefits of market integration

Meanwhile, other articles focus on evaluating the benefits of integrating balancing energy markets. Two main methods are used in the literature (Newbery et al., 2016): analysis of the evolution of cross-border market flows before and after the integration, of simulations of not integrated and integrated configurations using

electricity market models. While the authors choose the first option, they also indicate that the latter is the most commonly found in the literature. In this overview, we will then focus on simulation studies.

Several studies of this type have been conducted at the regional scale, meaning across a few countries. We can cite (Zani and Migliavacca, 2014) which models the integration of Austria, Italy and Slovenia, (Frade et al., 2019) on the integration of RR reserves between France, Portugal and Spain, (Farahmand and Doorman, 2012) and (Gebrekiros and Doorman, 2014) in the Nordic area, or (Dallinger et al., 2018) in Central Western Europe. There are far fewer studies conducted at the European scale: to our knowledge, (Kannavou et al., 2019) and (Ortner and Totschnig, 2019) are the only article modeling the complete sequence of electricity markets (day-ahead, intraday and balancing) at this scale. Overall, all studies share common conclusions, notably that the integration leads to significant reductions in balancing costs (within the range of 30% to 75%).

For additional details, one can refer to the exhaustive review proposed in (Roumkos et al., 2022).

Studies on the behavior of actors in balancing market

The behaviors of actors in balancing energy markets is also investigated in the literature.

Some studies focus on the interaction with the ISP, trying to determine the optimal response given the type of incentives sent by the ISP design. For instance, (Chaves-Ávila et al., 2014) concludes that different designs lead to significant variations in optimal behavior for wind power plants. The impact of the ISP forecasting method precision on actor behavior is highlighted by (Bottieau et al., 2019), which demonstrates the intricacy of the forecast process.

Other articles consider the sequential state of electricity markets, and aim to derive optimal actor behavior from arbitrages between markets. An empirical analysis of the German power system is conducted by (Just and Weber, 2015) and finds that BSPs are performing stochastic arbitrages between the day-ahead and the balancing energy markets, leading to significant imbalances and price spikes. (Van den Bergh and Delarue, 2020) models day-ahead and balancing markets (both procurement and activation), and studies the impact of coupling/decoupling the procurement stage and the day-ahead market under different assumptions of vRES integration. (Poplavskaya et al., 2020) analyzes how decoupling procurement and activation stages impact the behavior of BSPs on aFRR markets. Other notable studies include (Brijs et al., 2019) or (Poplavskaya et al., 2021).

It is relevant to note that almost all articles looking at the behavior of actors focus on BSPs, while that of TSOs is seldom studied in the existing literature.

Integration of new actors in balancing markets

Finally, the integration of the new types of flexibility actors in balancing processes is explored by several studies, looking at both the opportunities resulting from their participation and the entry barriers.

The flexibility requirements induced by large integration of vRES capacities are notably detailed by (Holttinen et al., 2011) and (Huber et al., 2014), both articles finding an increase in these requirements that can be mitigated by aggregation in large areas (and consequently balancing market integration). Meanwhile, the conditions for efficient integration of large-scale vRES units are notably discussed in (Vandezande et al., 2010), (Hirth and Ziegenhagen, 2015), (Auer and Haas, 2016) or (Holttinen et al., 2016). A common conclusion across these studies is the interest in close-to-real-time products, that allow for a precise compensation

of forecast evolution.

As opposed to large-scale installations, distributed energy sources refer to decentralized small-scale assets, usually connected to the distribution system as opposed to the transmission system. They notably include electric vehicles, small-scale vRES units, demand-side response and storage systems. Their integration is discussed in a wide variety of articles. We can cite (Borne et al., 2018) which provides a comprehensive framework of entry barriers. This article is complemented by (Poplavskaya and De Vries, 2019) who focuses on Austrian, German and Dutch balancing systems to propose improvements for distributed energy resources integration.

1.4.2 Modeling approaches of balancing energy markets

A detailed classification of electricity market models is proposed in (Ventosa et al., 2005), and is comprised of three main categories. *Single-firm optimization problems* are suited for the modeling of a single entity, especially to perform profit maximization. *Market equilibrium models* are based on game theory principles (Nash equilibrium), and are able to represent electricity markets involving a few actors. However, they are less appropriate to model complex systems involving a wide variety of actors, as they are limited in the individual depiction of each participant. Finally, *Simulation models* are precisely relevant to represent complex systems, that cannot be encapsulated in a simple set of equilibrium equations. They are usually able to model individual agents with specific responses to the market state. Within them, a subcategory can be defined by the integration learning processes: in agent-based models, individual agents modify their strategy according to the results of previous markets (Weidlich and Veit, 2008), usually using reinforcement learning algorithms. Another category can be added to this initial classification: *System Dynamics models*, which are detailed in (Teufel et al., 2013). These models combine aspects of optimization and simulation categories, although they usually only model aggregates of actors and not individual agents (Poplavskaya, 2021).

As illustrated in Section 1.2 and 1.3, electricity market processes, and all the more so balancing energy markets are extremely intricate. Consequently, the usage of a simulation model appears to be a relevant choice when studying balancing markets, as it should be able to represent (i) the various types of actors, whose specific features are even more important in close-to-real-time markets and (ii) sequential processes that structure the balancing stage, notably the different market steps (bidding processes, clearing and energy activation stages). This is verified in practice, as simulation models have been used in the majority of articles on balancing markets (e.g. Abrell and Kunz, 2015, Petitet et al., 2019 or Ortner and Totschnig, 2019), with agent-based features in some (for instance Bublitz et al., 2014, Poplavskaya et al., 2020 or Qussous et al., 2022).

1.5 Research questions, thesis structure and main contributions

1.5.1 Main research questions

In an effort towards market design convergence, common balancing markets are a bridge between usual wholesale markets (day-ahead and intraday) and historical balancing processes. Their design adopts several

elements similar to that of wholesale markets, such as cross-border aspects, marginal price remuneration, and standardization of offers. However, they also differ in many respects, as they retain characteristics associated with balancing processes. This introduces challenges and opportunities to the balancing stage, both for the supply side (BSPs) and for the demand side (TSOs). The overview of the literature highlighted that many aspects of balancing energy markets have already been discussed. Still, several gaps are yet to be addressed.

First, when looking at close-to-real-time processes, the supply side is shaped by the physical limitations of units that compose the power system, which we will refer to as "operating constraints". Historically, local balancing processes were constructed to match the specific features of their power system, partially alleviating the impact of operating constraints by using adapted balancing designs. The French historical Balancing Mechanism, presented in Section 1.2.3, is a relevant example, as it operated on a two-hour window without any requirement to the shape of offers submitted by BSPs. Within common balancing energy markets, we saw in Section 1.3 that the requirements imposed on the shape of standard orders are much heavier: consequently, they can interact strongly with the operating constraints of physical units. While standard orders are also used in usual wholesale markets, this interaction can be managed more fluidly, since these markets operate on longer time frames and further away from real time. In the design of balancing markets, countermeasures were taken to mitigate the limitations imposed by standard requirements, especially the complex orders presented in Section 1.3.2.1. Even with these countermeasures, the interaction between operating constraints and order standardization could undermine the expected performances of common balancing markets, and is to our knowledge not approached in the existing literature. The first sub-question that arises is then the following:

Research question 1 - How do the operating constraints of units impact balancing energy market performance (notably market liquidity, balancing costs and social welfare), and is their representation in electricity market models relevant?

Balancing energy markets also introduce a new type of market actor within common markets: the TSOs. While TSOs were in charge of their local balancing processes, they did not participate in any common electricity market before. As they represent the demand side of balancing markets, their bidding process could impact market outcomes, and should consequently be a topic of interest. We notably saw that European TSOs employ two types of strategies (proactive and reactive), that could lead to different bidding behaviors on common markets. In particular, proactive TSOs activate reserves in anticipation of imbalances. Within sequential balancing energy markets, they could perform arbitrages between markets to activate the most economically optimal set of reserves. Hence, a correctly designed bidding method could lead to balancing cost reductions. However, as noted in the literature overview, this topic is almost entirely avoided. The sole exception is (Håberg and Doorman, 2017), which presents a first approach from a high-level perspective. Consequently, there is a significant gap that should be addressed, leading to the second sub-question of this thesis:

Research question 2 - How can we improve TSOs' bidding strategies on balancing energy markets? And what are the impacts of such methods on market outcomes and balancing costs?

Meanwhile, balancing energy markets are designed to facilitate decarbonization and the integration of vRES (variable Renewable Energy Sources) capacities in the European power system. Their cross-border aspect should significantly widen the pool of available reserves in all areas, and their transparency should encourage new actors to participate in them. However, the existing literature looking at long-term assessments

of the performance of balancing energy markets is rather scarce. It is then currently difficult to estimate if balancing energy markets will succeed in this task, and this points toward the need for quantitative analyses at long-term horizons. In addition, in the description of the general framework of RR and mFRR markets, we detailed the counter-activation aspect permitted by their design. These markets are not limited to matching TSO balancing demands with BSP reserves: they can also match orders of the same type of actors (TSOs or BSPs). The first consequence of this feature is the well-known netting between TSO orders, meaning using the energy excess in one area to supply an energy deficit in another. The second consequence is that, by matching BSP orders together, balancing markets can also act as close to real-time economic dispatch tools. Consequently, under the right conditions, market actors could use balancing energy markets to rebalance themselves, alleviating parts of the TSO balancing needs. These observations lead to the third and final sub-question of this thesis:

Research question 3 - What is the impact of the evolution induced by decarbonization on the European power system on both inputs and outputs of balancing energy markets? And what are the possible consequences of the self-balancing behavior of vRES actors at the 2050 horizon?

1.5.2 Thesis structure and main contributions

To address our 3 research questions, this dissertation is then divided into 3 main chapters.

In **Chapter 2**, the *research question 1* is addressed by focusing on thermal units, which are particularly subject to operating constraints. It leads to the following contributions:

- The identification of a list of operating constraints applied to thermal units, relevant for the time scale of balancing energy markets. Based on this list, a literature review of balancing energy market models is conducted. This literature review shows that most models only consider a small subset of the aforementioned list.
- A modeling approach formulating RR and mFRR orders for BSPs is proposed. It notably integrates all relevant operating constraints for thermal units, and complies with the order standards imposed by the common markets.
- A case study on European RR markets is carried out with the electricity market model ATLAS, assessing both individually and in combination the impacts of the different operating constraints on market inputs and outputs. The main findings show that an accurate representation of these constraints leads to a significant drop in market liquidity, as the volume offered by thermal units decreases. In particular, nuclear units are not able to participate in RR markets if the full set of constraints is taken into account. This liquidity drop induces an increase in TSO needs not fulfilled by RR markets, an increase in TSO balancing costs and a decrease in overall social welfare.
- The results advocate for the importance of including operating constraints in electricity market models, to avoid substantial overestimation of market performances (ability to respond to balancing needs, and eventual balancing costs).

Chapter 3 focuses on the demand side of balancing energy markets, and studies *research question 2*. It contributes to the existing literature in several aspects:

- An empirical analysis performed on RR markets over 2021 and 2022 highlights the price-inelastic behavior of TSOs in balancing energy markets, using the example of RTE. It illustrates that some TSOs are already formulating bidding curves on the RR market, which emphasizes the interest of studying their bidding behavior.

- A framework for bidding methods for TSOs on the RR market is proposed. It addresses three main complexities within the TSO bidding process identified by (Håberg and Doorman, 2017): the temporal resolution of the RR market, the existence of several types of RR market alternatives, and the uncertainty of TSO balancing need forecasts.

- These bidding methods are applied in a case study with the ATLAS model. The results show that a method integrating balancing needs uncertainty can yield balancing cost reductions. They also illustrate how a poor estimation of the alternative cost can render bidding methods ineffective.

- Overall, this chapter and the results of the case study confirm that the study of TSO bidding methods on balancing energy markets is a topic of interest. They also indicate that a regulatory framework could be necessary to avoid market distortions, either intentional (prioritizing a balancing process over others) or unintentional (because of inadequately tuned bidding methods).

In **Chapter 4**, both supply and demand sides are jointly analyzed through the prism of decarbonization, at both 2030 and 2050 horizons. Addressing the *research question 3*, it provides a novel quantification of long-term RR market performance that leads to two main contributions:

- Our analysis shows that the integration of vRES capacities indeed leads to significant increases in TSO balancing needs. But this increase is largely mitigated by (i) an increase in netted volume between market areas and (ii) an increase in the volume of BSP offers, driven by the new technologies of the energy transition (notably vRES, storage, or power-to-gas assets). Over the simulated periods, TSO balancing needs are always resolved by the RR market, which validates its role as a provider in terms of volume. However, we note that this conclusion relies on the strong participation of the aforementioned new technologies in the markets, and emphasizes the need to correctly incentivize these actors. A substantial increase in the variability of TSO balancing costs is also observed, especially in areas with large vRES installed capacities. Finally, the BSP-matching aspect of the RR market is found to generate a significant amount of social welfare, which is increased at the 2050 horizon because of the greater supply volumes and the increased balancing needs.

- A second part evaluates the impact of a self-balancing behavior for vRES actors at the 2050 horizon. We find that, under a dual imbalance pricing, this behavior should be economically profitable for these BSPs. While it could also lead to reductions in TSO balancing needs and costs, it would require improvements in the BSP-TSO communication to avoid a counterproductive effect. Without this improvement, our analysis shows that this behavior could have negative consequences on both balancing costs and security of supply.

Modeling contributions

The work proposed in this thesis is deeply associated with the electricity market model ATLAS (for Agent-based short-Term eLectricity mArkets Simulation), as it was used in all simulations performed. ATLAS is

developed by RTE, and inherits from the Optimate model/project (Weber et al., 2012). It aims to accurately simulate sequential short-term processes, ranging from day-ahead to real-time balancing. These modeled processes include common markets (day-ahead, intraday, balancing energy markets), but also local processes such as the French Balancing Mechanism. It also includes a detailed representation of market actors and allows for studying interactions between diverse BSPs, BRPs, and TSOs. According to the classification of Ventosa et al., 2005 presented in the literature overview, ATLAS belongs to the category of simulation models, which makes it a good candidate for detailed market simulations. We note that, while the model is able to represent individual agents with specific characteristics, it currently does not include learning behaviors which means that it is not an agent-based model. It should integrate this category in the future, with subsequent developments in learning processes. A detailed overview of ATLAS, and of the day-ahead and intraday processes, can be found in (Little et al., 2024).

The current section aims to clarify the perimeter of implementation that resulted from this thesis, as several parts of the model were already developed prior to its beginning. Its main contributions to ATLAS can be divided into two categories:

- **Implementation of the entire balancing activation stage.** At the beginning of this thesis, the ATLAS perimeter reached the intraday, but did not include closer to real-time processes. Consequently, the entire balancing section was implemented during the thesis.

  This section is flexible and is composed of the modules described in Figure 1.16. In ATLAS, a universal clearing module is used for all electricity markets. It was consequently *not developed* for the balancing stage. However, improvements were performed to link it with other balancing modules With the exception of the Clearing module, all the others were implemented during the thesis.

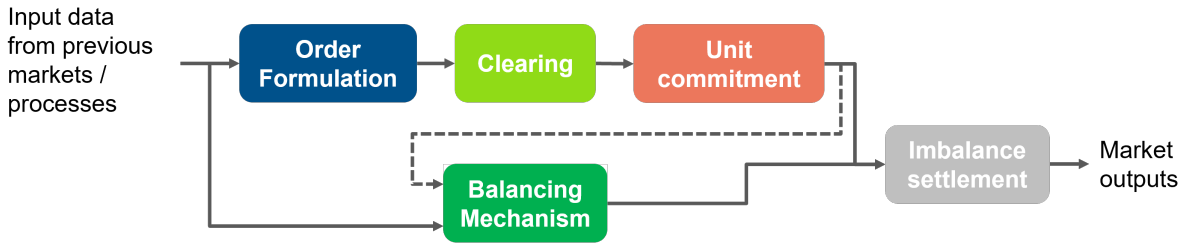

Figure 1.16: Usual steps of a market simulation in ATLAS

  A regular balancing energy market is depicted by modules of the top row. It is implemented to be able to simulate both RR and mFRR markets[14].

  A market order formulation step is executed first. This formulation is done in separate modules for BSPs and TSOs, as their processes differ significantly. These modules notably include academic contributions proposed in the different chapters of this thesis. The BSP order formulation module comprises the modeling approach integrating relevant operating constraints of thermal units (Chapter 2). In the TSO order formulation module, the bidding methods studied and proposed in Chapter 3 were implemented.

  After the Clearing module, a unit commitment module ensues. In ATLAS, while the day-ahead and intraday markets are modeled as portfolio-based self-dispatch, the balancing stage is modeled as a unit-based self-dispatch. Consequently, this module of balancing markets performs a unit-based commitment

[14]The mFRR market is modeled based on the scheduled activations mode, see Section 1.3.2 for more details

that verifies that quantities activated by the clearing process are feasible, and updates all relevant values (power outputs, reservoir levels notably) according to market results.

The last step of a balancing market process is the imbalance settlement, developed based on the French process described in Section 1.2.3.

In addition, a model of the French Balancing Mechanism presented in Section 1.2.3 was also implemented in ATLAS during this thesis. It was used as a reference when representing historical local balancing processes. It can be executed separately or following balancing energy markets.

A complete description of the balancing stage can be found in Appendix A, which is also available online (Cogen et al., 2024).

- **Harmonization and improvements of modules already developed.** In practice, sequential electricity markets are extremely complex. This complexity is also striking when creating close-to-reality market models. Hence, on top of the balancing stage implementation, a noteworthy part of this thesis was devoted to harmonizing, adapting and improving modules already developed. Although difficult to promote in the context of a thesis, this improvement work was necessary to simulate sequential markets and produce meaningful results.

Chapter 2

Impact of operating constraints on balancing market performances

Contents

Abstract Balancing energy markets are currently being implemented in the European power system, progressively replacing historical balancing processes that were designed at a local scale. Occurring within the last hour before real-time, these markets are consequently subject to specific constraints. Amongst these, operating constraints applied to generation and consumption units heavily conflict with the order formulation process of market actors. This paper curates a list of operating constraints–particularly related to thermal units–relevant to the balancing time frame, before highlighting the incomplete inclusion of these constraints in common energy market models. It then proposes a modeling approach that incorporates them in the electricity market model ATLAS, and demonstrates the impact of each one through a case study on the 2030 European power system. Results show that modeling operating constraints leads to a significant decrease in market liquidity (between 30% and 54%, depending on the reserve direction), and to subsequent impacts on market performances (notably a 114% increase in balancing costs and a doubling of the volume of unsupplied Transmission System Operator balancing demand). This advocates for the relevance of the inclusion of these constraints in balancing market models, and puts into perspective results obtained without them.

Acknowledgements: This chapter has benefited from the support of the Chaire European Electricity Markets (CEEM) of the Université Paris-Dauphine under the aegis of the Foundation Paris-Dauphine, supported by RTE, EDF, EPEX Spot, and Total Direct Energie. The views and opinions expressed in this paper are those of the authors and do not necessarily reflect those of the partners of the CEEM. All errors are my own.

Note for readers: As this chapter is based on a working paper published in the Chaire European Electricity Markets (CEEM), some sections present information similar to the general introduction. They are indicated in the text.

2.1 Context

European power systems have been undergoing a gradual liberalization since the beginning of the 21^{st} century, with the creation of electricity markets ever closer to real-time. The day-ahead spot market was implemented first, followed a few years later by the intraday market. These two markets were progressively extended to include more European areas. The intraday market was, until recently, the closest to real-time large-scale common market[1]. Indeed, during the period between the last intraday market and real-time, Transmission System Operators (TSO) are legally in charge of maintaining a balance between supply and demand, and were historically achieving this task by activating balancing reserves through local processes. European TSOs used diverse balancing processes tailor-made for their local area, with notable design differences in terms of market order type, clearing process or remuneration scheme. Various studies illustrate the deeply heterogeneous aspect of these processes (Rebours et al., 2007a, Rebours et al., 2007b, Håberg and Doorman, 2016, Ocker et al., 2016). This state of balancing processes in Europe presented both advantages and potential inefficiencies. On the one hand, they were adapted to the specific features of the local power system, and consequently able to able to align the best with the technical constraints of the regional options. On the

[1]Interzonal balancing markets existed in the Nordic area, but were not entirely homogeneous and harmonized (Khodadadi et al., 2020)

other hand, interconnected markets could achieve better economic performance thanks to a larger pool of offers and provide a more transparent and harmonized design.

To address these inefficiencies, the European regulation proposed to take another step in the path of liberalization by creating common European balancing markets, revolving around harmonized types of balancing reserves:

- Frequency Containment Reserve (FCR) that aims to stop any frequency deviation, by an automatic and proportional reaction to frequency deviations within a few seconds.
- automatic Frequency Restoration Reserve (aFRR), corresponding to the automatic activation of units within a few minutes to restore the frequency to its initial level.
- manual Frequency Restoration Reserve (mFRR), which serves the same purpose as aFRR but is activated manually in under 15 minutes.
- Replacement Reserve (RR) is eventually activated manually under 30 minutes to replenish all reserves described previously.

These reserves are part of a two-stage process: (i) a procurement stage taking place a few hours up to months before real time[2], during which both upward and downward power capacities are locked to make sure that enough reserves will be available in real-time, and (ii) an activation market occurring in real-time, which activates balancing energy to meet supply-demand imbalances. Because of the differences in time scales and activation methods (manual versus automatic), the set of technical and dynamic constraints associated with mFRR and RR reserves is quite distinct from that of aFRR and FCR reserves. This study does not look at the procurement stage, and focuses entirely on the activation of manual balancing reserves, traded on common cross-border platforms. On these platforms, Balancing Service Providers (BSPs) submit upward and downward reserve orders that correspond respectively to an increase and a decrease in power generation, whereas TSOs submit orders according to their balancing needs, computed using imbalance forecasts on their area. The existing literature on balancing markets discussed the optimal choices of variables and parameters of the design of balancing markets (for instance schedule time unit, gate closure times, method of procurement, balancing service pricing mechanisms, activation strategy or order requirements), and indicated the subsequent economic benefits of balancing markets compared to previous processes, notably significant gains in terms of balancing costs.

However, studies of this literature were mostly conducted on models that do not account for all the operating constraints applied to generation units, although these constraints have strong interactions with the order formulation process of balancing markets. Indeed, as shown in the General introduction, the high degree of order standardization required for operating a common European market limits the shape of market orders that can be submitted by both TSOs and BSPs. To comply with both order standardization and their operating constraints, BSPs often have to adapt the volume of balancing energy offered in their orders, and have to rely on several types of links between them–called order couplings–that add an extra level of complexity to market processes. Taking into account this phenomenon can influence simulation results, which directly impacts expected benefits and optimal design recommendations made by aforementioned studies.

[2]FCR reserves are procured as at European scale. Currently, the procurement of all other reserve types is still managed locally by TSOs, as there is currently no common European procurement market for it. This explains the diversity in terms of procurement timing.

The research question of this chapter is thus the following: *How do the operating constraints of thermal units impact balancing market performances, especially on indicators discussed in previous studies, and is their representation in market models relevant?* We chose to focus on thermal units to narrow the study to a reasonable number of operating constraints, while still studying a unit type that is heavily influenced by these constraints.

Studying this question leads to three main contributions to the literature. First, a literature review provides an overview of the theoretical design of balancing markets and their expected benefits, and establishes a list of relevant operating constraints for thermal units, as well as the state of their integration in balancing market models (Section 2.2).

Then, a model designed to emulate RR and mFRR markets is proposed in Section 2.3. It is integrated within the electricity market model ATLAS (exhaustively described in (Little et al., 2024) and (Cogen et al., 2024)), and it includes a detailed representation of operating constraints, by modeling with precision:

- The whole balancing process, starting from the market order (i.e. market bids) formulation by all market actors, followed by the Market Clearing stage, and eventually leading to a portfolio optimization done for each BSP to create generation programs. Additionally, a final local balancing process can be run after balancing markets to compensate for any remaining imbalance. It is based on the historical French Balancing Mechanism (FrBM).
- A detailed European power system including a diverse core of generating units, as well as an exhaustive list of operating constraints specific to the different types of units.
- The design chosen for each cross-border platform, along with the possibility of linking market orders during their formulation to account for operating constraints, and methods used to address these coupling links during the Clearing stage.

Finally, this model is applied in a case study that investigates the impact on market performances of integrating operating constraints in market models, looking at each constraint individually and also at their simultaneous inclusion. The methodology is detailed in Section 2.4, and the results of this study are discussed in Section 2.5, showing significant impacts on both market liquidity and outcomes.

2.2 Literature review

This literature review focuses on two main aspects: it first gives an overview of previous studies assessing the potential benefits of cross-border balancing markets, or analyzing their optimal design, and then details which operating constraints are relevant when looking at balancing markets and how they are taken into account in models of the literature.

2.2.1 Expected benefits of common balancing markets

Notes for readers: The following section displays similar information to Section 1.4 of the general introduction.

Several theoretical reasons for transitioning from local processes to common markets are presented in the literature. First, coupling multiple areas together offers two main advantages. A larger pool of orders should result in the activation of cheaper units, as was previously shown by (Farahmand and Doorman, 2012) on the balancing reserves procurement market in the northern region of Europe. A common market also functions as a built-in netting system that will avoid activation of reserves of opposite directions (i.e. upward and downward) from interconnected areas that share non-saturated transmission lines, which is studied by (Van der Veen et al., 2010) for instance. On top of theoretical gains from area coupling, the transition to common markets gives the opportunity to define a common optimal architecture, regarding design variables such as the order selection method, the pricing method, the gate closure time, or the schedule time unit of the market (Dallinger et al., 2018 and Gebrekiros et al., 2015). Finally, another key benefit is the improvement of market transparency. These last two points will notably be crucial to the integration of renewable energy sources by allowing their participation in the balancing process, through which they can mitigate the increase of balancing needs that they are expected to induce (Vandezande et al., 2010, Holttinen et al., 2011 and Koch and Hirth, 2019).

As explained in (Newbery et al., 2016), there are two main methods for evaluating the benefits of market integration: simulations using scenarios that incorporate different levels of integration, and the analysis of interconnector capacity usage based on empirical and projected data. The latter is chosen by the authors, and they concluded that coupling balancing energy markets in Europe could lead to considerable benefits (up to €2.4 billion/yr). It was also used in the study (Mansur and White, 2012) that empirically shows that the benefits of the transition from bilateral contracts to an auction-based market in day-ahead that occurred in 2004 in the US area of PJM outweigh the costs it induced. However, the main focus of our work is the simulation approach, which is the most common in the literature according to (Newbery et al., 2016).

A common method for estimating gains resulting from market evolution is the analysis of social welfare, which corresponds to the sum of the surplus of all market actors. This concept is broadly used for analyzing the day-ahead market (see Mansur, 2008 or Newbery et al., 2016), but remains rather unexplored in the exact context of balancing markets, as explained in (Zolotarev, 2017). In this article, the author details the computation method of social welfare, and justifies its theoretical increase from coupling areas together, although no practical application or quantified gain is given. To our knowledge, no further study has been conducted on this topic. A possible explanation lies in the difficulty of estimating the surplus of TSO demands. In (Zolotarev, 2017), the demand for balancing energy is supposed to be inelastic, and TSOs are assumed to have a preference price for their market orders. These assumptions could first be challenged, and in any case the preference price is difficult to determine properly, rendering the overall welfare computation problematic (see Section 2.5.2.2 for more details).

Expected benefits are consequently usually presented in the form of TSO balancing cost reduction. Reference (Zani and Migliavacca, 2014) compares 3 local balancing markets (corresponding to Italy, Austria and Slovenia) to a common one. The overall balancing cost reduction in the coupled scenario is estimated at 55%, while noticing different patterns in each area: costs are actually increasing in Austria and Slovenia, and are heavily decreased in Italy. Similar studies based on the Nordic area (including Norway, Sweden, Finland, Denmark, the Netherlands and Germany) can be found in (Abbasy et al., 2009) and (Gebrekiros and Doorman, 2014), where the yearly balancing costs are estimated to decrease by resp. 55% and 75% when energy markets are integrated. (Kannavou et al., 2019) widens the scope to Europe, and models day-ahead, intraday and balancing energy markets. The conclusions of this article are in line with the local studies presented

before, as the authors found balancing cost reductions of 76% across all areas. (Van der Veen et al., 2010) focuses on the netting aspect, and shows qualitatively the benefits of an Area Control Error netting.

2.2.2 Theoretical discussion and actual design of the RR market

Notes for readers: The following section displays similar information to Sections 1.3 and 1.4 of the general introduction.

A wide range of studies look at the theoretical optimal design of these new balancing markets. (van der Veen and Hakvoort, 2016) summarizes the different components and parameters of a market design, details commonly discussed choices for these parameters, and defines metrics that can be used to compare several designs. The authors determine 9 different performance criteria covering various themes (security of supply, economic efficiency, market facilitation).

In addition to this framework, research was also conducted to identify optimal values for nearly all design parameters. To only cite a few:

- (Van der Veen et al., 2010) illustrated the optimality of the selection of units according to a Common Merit Order List (CMOL).
- Regarding the choice of pricing method, several articles compare particular marginal pricing and pay-as-bid pricing, and conclude that the marginal pricing is economically more optimal since it encourages generators to bid at their generation costs, and leads to lower costs for consumers (Vandezande et al., 2010 and Akbari-Dibavar et al., 2020). This is completed by (van der Veen and Hakvoort, 2016), who add that a higher clearing frequency would likely lead to lower balancing prices in the case of marginal pricing.
- The Imbalance Settlement Price (ISP) is another commonly studied topic, even if it is currently not part of the design of cross-border platforms of RR and mFRR reserves[3], with (Hirst, 2001) concluding that this parameter is highly impactful on the performance of all electricity markets, even those further from real-time such as the Day-Ahead market.
- As a last example, (Petitet et al., 2019) considered different Gate Closure Times (GCT) for BSPs, corresponding to the deadline past which they cannot submit market orders anymore. The study demonstrated that a GCT of 60 minutes is better than a GCT of 15 minutes based on both the volume of balancing energy activated and overall balancing costs. This is largely due to BSPs' limited information about the current and future states of the whole power system, compared with a central actor.

As the case study of this chapter focuses on the existing RR market, an overview of the design is provided[4] (see (ENTSO-E, 2023c) for more details). For a given occurrence of the market that spans on a time frame that we will call T_{RR} (corresponding to the actual period of reserve activations), the following process is applied and illustrated in Figure 2.1:

[3] It is still managed locally by TSOs.
[4] This description is similar to the one included in the General Introduction, in Section 1.3

1. BSPs submit all their market orders to their respective TSO before their GCT, which varies between areas but is comprised between 60 and 50 minutes before the beginning of T_{RR}.

2. TSOs then transmit these orders along with their balancing needs to the TERRE market platform, before the TSO-associated GCT (which is universally set to 40 minutes before T_{RR}).

3. Market orders are selected and activated using a CMOL, and the market price is determined according to the marginal pricing method.

4. Eventually, market results are sent back to all actors 30 minutes before T_{RR}, and BSPs adjust the power output or the load of their portfolio to meet activation requirements.

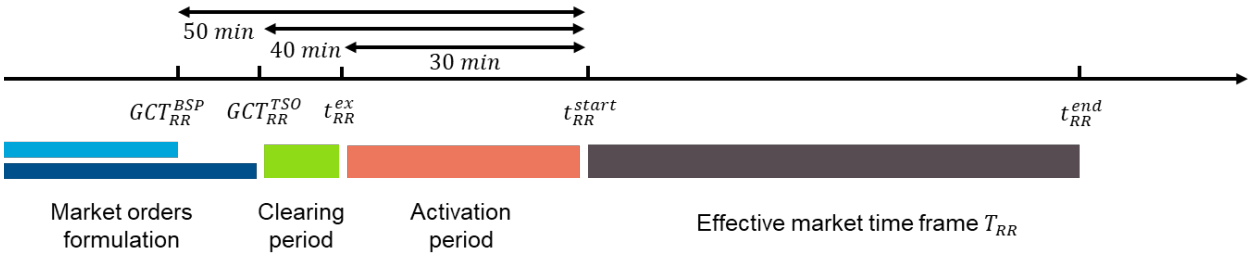

Figure 2.1: Illustration of the RR market time frame

Setting a European cross-border market also requires a high degree of standardization regarding the shape of market orders that can be traded. The standard chosen for RR market order is described in Table 2.1, associated with a schematic representation of a market order in Figure 2.2 that illustrates characteristics noted 1 to 7 in the table.

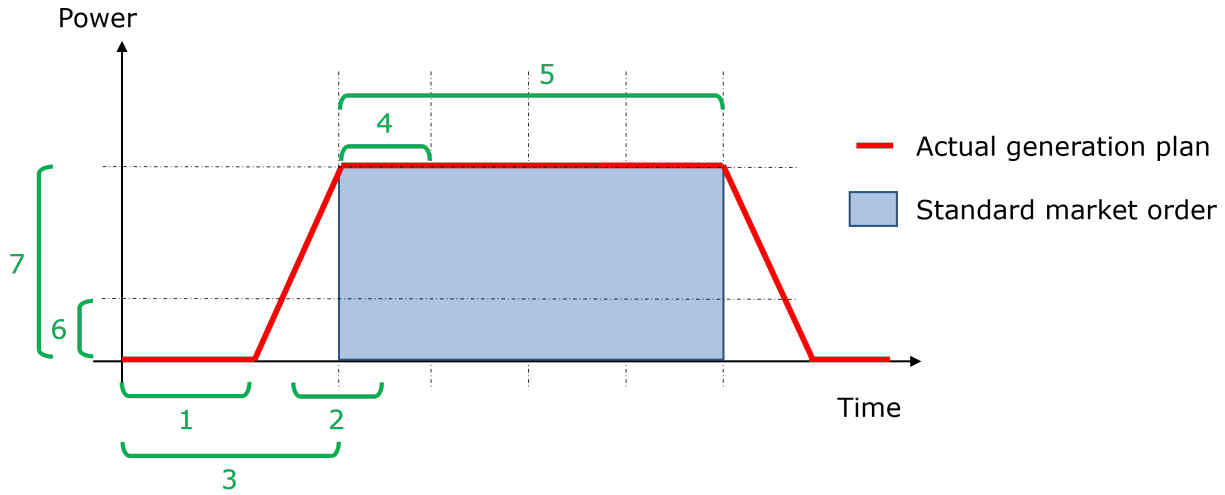

Figure 2.2: Schematic market order representation

Characteristic	**BSP order**	**TSO order**
Preparation period (1)	Between 0 and 30 min	/
Ramping period (2)	Between 0 and 30 min	/
Full Activation Time (3)	30 min	/
Minimum duration (4)	15 min	15 min
Maximum duration (5)	60 min	60 min
Minimum quantity (6)	1 MW	1 MW
Maximum quantity (7)	/	Up to the quantity of bids of opposite direction submitted by BSPs in the TSO's area
Minimum price	-10,000 €/MWh	-10,000 €/MWh
Maximum price	10,000 €/MWh	10,000 €/MWh
Price resolution	0.01 €/MWh	0.01 €/MWh
Order divisibility	Fully divisible Partially divisible Indivisible	Fully divisible
Coupling links permitted[5]	Exclusive Multi part Linked in time	Linked in time

Table 2.1: RR market standard product

The Preparation period, Ramping period and their sum, corresponding to the Full Activation Time (FAT), set an upper limit to the delivery duration: starting when market results are sent back to the actors, an order is required to deliver the activated quantity within the FAT, and can modulate its Preparation and Ramping periods at will in order to respect it. This only concerns physical units, and therefore is not relevant to TSO orders. A specific requirement is applied to the maximum quantity of TSO orders: it is limited by the sum of power of all orders submitted in the opposite direction by BSPs in their area. For instance, if the total volume of sale (resp. purchase) orders formulated by BSPs in the area of a given TSO is equal to 70 MW, it will not be able to submit a purchase order (resp. a sale order) of more than 70 MW, regardless of the imbalance volume it has computed. Minimum and maximum durations impose boundaries on the length of a market order. In the RR market, an order cannot last for less than 15 minutes and cannot exceed the total duration of the market time frame (60 minutes).

2.2.3 Operating constraints and their interactions with electricity markets

Previous sections illustrated the fact that the theoretical design of balancing markets and their expected benefits is already largely discussed in the academic literature. However, most studies tend to oversimplify certain operational or practical parameters, which may have a considerable impact on market performance. In particular, they usually only consider a few operating constraints on generating units, if any, and do not take into account the coupling links created between market orders by BSPs to represent these operating

[5]See Section 2.3.1.1 for details about coupling links and how they are translated in the model

constraints. The relevance of modeling operating constraints in power system simulations was already highlighted in other sections of the literature, which did not focus on electricity markets. It was for instance discussed by (Shortt et al., 2012) or (Poncelet et al., 2020), in the domain of capacity expansion models. The authors demonstrated that operating constraints on thermal units have significant impacts on model outputs. Given the extreme proximity to real-time of balancing energy markets (previously illustrated by Figure 2.1), we argue that it should be even more impactful in these markets.

(Morales-España et al., 2015) provides a list of operating constraints that are used in advanced thermal unit commitment problems:

- **Maximum power** output.
- **Minimum power** output, which is often strictly positive in the case of thermal units and implies a concrete distinction between the OFF state (during which the power output of the unit is 0) and the ON state (for which the power output of the unit is between its minimum and maximum power).
- **Maximum ramping**, imposing a ramping limit when increasing or decreasing the power output.
- **Minimum time ON**, indicating that the unit should be ON for at least a certain period after being started.
- **Minimum time OFF**, indicating that the unit should be OFF for at least a certain period after being shutdown.
- **Startup duration**, the duration required for the unit to go from an OFF state to its minimum power.
- **Shutdown duration**, the duration required for the unit to go from its minimum power to an OFF state.

The first 3 constraints of this list are the most basic ones. (Mansur, 2008) already highlighted their impact on market performances, and they were later included in most existing studies and models as Section 2.2.4 discusses. They are also not specific to thermal units, as opposed to the subsequent constraints.

In addition, (Petitet et al., 2019) models the following constraints:

- **Minimum stable power duration** for all thermal units, which indicates that the unit must keep a stable power output for a certain duration before ramping up or down again.
- **Notice delay**, representing the period required by a unit between the decision of a program modification (for instance a startup, or even a simple modification of the power output) and the moment when this unit is actually able to begin this modification. This corresponds to the Preparation period in the glossary in Table 2.1. Authors include this operating constraint in their representation of both thermal and hydro units, and it could be justified for demand flexibility as well.

Because of the prevalence of operating constraints for thermal units compared to other types of units, this study will focus solely on them. Nonetheless, constraints also exist for almost all unit types. In most models, hydro power plants take into account a maximum level for their water reservoir. Some include a minimum level as well, which may be different from 0 because of regulatory restrictions. In contrast, for Pumped Hydro Storage (PHS) plants, the transition duration constraint when switching between pumping and turbining states is, to the author's knowledge, never considered in any of these models. The impact of

this constraint could be studied later on using ATLAS, as it is already modeled in it. Demand response may also be constrained, mainly by daily energy limits, load postponement requirements or even significant notice delay for some categories of load units. However, these constraints are deeply heterogeneous amongst the wide variety of load units, and also difficult to evaluate because of a lack of empirical analysis. Storage units such as batteries are subject to storage level constraints and to charge and discharge efficiencies, which are usually modeled in the literature. Finally, renewable energy sources are only constrained by their ability to curtail their power output. Overall, the diversity of operating constraints, and its dependence on the unit type, implies that the generation mix plays a considerable role in the complexity of markets.

All these constraints become increasingly restrictive for close-to-real-time markets such as balancing markets, as they interact with standardization requirements detailed in Section 2.2.2 in two major ways:

- By restricting the power that can be offered by certain types of units on markets, or in the worst case entirely preventing them from participating. For instance, this would be the case for a unit that has a minimum stable power duration constraint greater than 60 minutes, as it would not be able to comply with the RR maximum duration constraint described in Table 2.1.
- Even for units that are able to formulate market orders, it is often still necessary to create “complex" orders to reflect their operating constraints. A unit with a minimum stable power duration of 30 minutes would be able to offer reserves on the RR market, but only over two consecutive time steps. This implies additional consideration: across which time steps to submit the offer, and how to manage interactions with other formulated offers.

The example given in the second point only demonstrates a specific case. In fact, many other parameters lead to the necessary application of complex orders. The complexity of balancing order standardization is illustrated by (Marneris et al., 2019) and (Fedele et al., 2020), both from the point of view of TSOs within a central-dispatch system (in Greece for the former article, in Italy for the latter). Indeed, with a central-dispatch system, it is the role of the TSO to create market orders for BSPs in its area, based on the operating constraints and the generation plan communicated to him. Notably, the first article looks at RR products, and shows how precise ramping constraints can conflict with order standardization.

To deal with these constraints, market actors can adjust the divisibility of their market orders and use several types of coupling links between them (cf. rows “Order divisibility" and “Coupling links permitted" in Table 2.1).

2.2.4 Integration of operating constraints in models of the literature

A detailed review of how operating constraints are taken into account in models simulating electricity balancing markets was conducted. Results of this review are exposed in Table 2.1[6].

[6]To our knowledge, we used the latest available description of unit bidding processes, in this review. Additional constraints have been implemented in the presented models since this review.

Model	Reference article and authors	Maximum power	Minimum power	Maximum ramping	Minimum time ON	Minimum time OFF	Startup duration	Shutdown duration	Minimum stable power duration	Notice delay
-	Gebrekiros and Doorman, 2014	✓	✓							
AMIRIS	Reeg et al., 2012	✓	✓							
powerACE	Fraunholz, Keles, and Fichtner, 2021 Fraunholz, Kraft, et al., 2021	✓	✓							
ElbaABM	Poplavskaya et al., 2021	✓	✓							
EMPS	Jaehnert and Doorman, 2010	✓	✓							
GAPEX	Cincotti and Gallo, 2012	✓	✓							
EDisOn	Burgholzer, 2016 Dallinger et al., 2018	✓	✓	✓						
EMCAS	Veselka et al., 2002	✓	✓	✓		✓				
MASCEM	Vale et al., 2011	✓	✓	✓	✓					
-	Aravena and Papavasiliou, 2016	✓	✓	✓	✓	✓				
HiREPS	Ortner and Totschnig, 2019	✓	✓	✓	✓	✓				
Dispa-SET	Quoilin et al., 2017	✓	✓	✓	✓	✓				
PRIMES-IEM	Kannavou et al., 2019	✓	✓	✓	✓	✓				
flexABLE	Qussous et al., 2022	✓	✓	✓	✓	✓				
COMPETES	van Hout et al., 2014	✓	✓	✓	✓	✓				
stELMOD	Abrell and Kunz, 2015	✓	✓	✓	✓	✓				
LUSYM	Van den Bergh et al., 2014	✓	✓	✓	✓	✓				
WILMAR	Tuohy et al., 2009	✓	✓	✓	✓	✓	✓			
AMES	Tesfatsion and Battula, 2020 Battula et al., 2020	✓	✓	✓	✓	✓	✓	✓		
OPTIMATE	Maenhoudt and Deconinck, 2013	✓	✓	✓	✓	✓	✓	✓		
SiSTEM	Petitet et al., 2019	✓	✓	✓	✓	✓	✓	✓	✓	✓

Table 2.2: Operating constraints on thermal units modeled in balancing market models

As illustrated in the table, models used in the literature only consider a subset of all operating constraints. In particular, startup/shutdown duration, minimum stable power duration and notice delay are almost always left out. The only notable exception to these observations is the SiSTEM model, used in articles (Petitet et al., 2019) and (Petitet, 2016), which is only missing the PHS transition duration from the list of constraints established before. However, this model is constructed to represent a single market area, and therefore is unable to simulate European common markets that require by definition multiple areas.

2.3 ATLAS model improvements

In order to assess the full impact of the inclusion of operating constraints, it was important to properly represent balancing processes. To that end, a model able to simulate both cross-border balancing markets and local balancing processes was developed and integrated with the existing electricity market model ATLAS.

The ATLAS (for Agent-based short-Term eLectricity mArkets Simulation) electricity model consists of a structured representation of a power system, and of a series of modules that model day-ahead, intraday and balancing (both RR and MFRR) markets by following the process of actual electricity markets. It was previously used to simulate day-ahead and intraday markets in the European project OSMOSE (Boehnke et al., 2022), and to study the interaction between balancing markets and real-time network constraints in (Girod et al., 2022). To keep the description relatively concise, the current section only highlights the key concepts of the balancing stage modules, that were entirely developed for this study (except for the Clearing, presented in Section 2.3.2). A complete description of these modules, as well as all other modules of ATLAS, can be found in a two-part documentation in (Little et al., 2024) and (Cogen et al., 2024).

A specificity of balancing energy markets is that they involve two kinds of actors that are fundamentally different from each other: BSPs and TSOs. Two distinct modules are consequently used to formulate both types of orders. The resulting structure of the balancing stage of ATLAS is illustrated in figure 2.3.

Figure 2.3: Macro overview of ATLAS balancing stage modules

The following notations will be used throughout this chapter (Table 2.3):

Sets	
Notation	**Description**
CA	Set of all control areas
U	Set of all units
U^i	Set of all units of type $i \in [g, l, th, h, st, w, pv]$. ($g$ = generation, l = load, th = thermal, h = hydro, st = storage, w = wind, pv = photovoltaic)
O	Set of all market orders
O^{up}	Set of all upward market orders
O^{down}	Set of all downward market orders
C^{excl}	Set of all coupling instances of type $Exclusion$
C^{pc}	Set of all coupling instances of type $ParentChildren$
C^{idr}	Set of all coupling instances of type $IdenticalRatio$
Temporal parameters	
t_m^{ex}	Execution date of the market m.
t^{start}	Start date of the effective period of the market.
t^{end}	End date of the effective period of the market.
Δt_m	Time step of the market m (in min)
T_m	Effective time frame of the market m, i.e. $T_m = [t_m^{start}, t_m^{start} + \Delta t_m, \ldots, t_m^{end} - \Delta t_m]$
id	Combinatorial index, formally written $id = \{\{t_{id}^{start}\}, \{t_{id}^{start} + \Delta t_m\}, \ldots, \{t_{id}^{end}\}\}$.
Decision variables	
$Q_{u,id}^{ResDir,max}$	Upper bound of the available power in direction $ResDir \in [up, down]$ of unit u, for the combinatorial index id
$Q_{u,id}^{ResDir,min}$	Lower bound of the available power in direction $ResDir \in [up, down]$ of unit u, for the combinatorial index id
$\delta_{u,id}^{SU}$	Binary variable indicating if unit $u \in U^{th}$ is starting on combinatorial index id.
$\delta_{u,id}^{SD}$	Binary variable indicating if unit $u \in U^{th}$ is shutting down on combinatorial index id.
Unit characteristics and input data	
$P_{u,t,t_m^{ex}}^{plan}$	Power output (in MW) of unit $u \in U$ at time $t \in T_m$, seen from time t_m^{ex}
$P_{u,t}^{max}$	Maximum power output (in MW) of unit $u \in U$ at time $t \in T_m$
$P_{u,t}^{min}$	Minimum power output (in MW) of unit $u \in U$ at time $t \in T_m$
$P_{u,t,t_m^{ex}}^{for}$	Forecast of the maximum power output (in MW) of unit $u \in [U^w, U^{pv}, U^l]$ at time $t \in T_m$
c_u^{var}	Variable cost (in €/MWh) of unit $u \in U$
c_u^{SU}	Startup cost (in €) of unit $u \in U$
$Res_{ut,t_m^{ex}}^{ResType,ResDir}$	Procured reserves of type $ResType \in [FCR, aFRR, mFRR, RR]$ in direction $ResDir \in [up, down]$ on unit u at time t, seen from t_m^{ex}
d_u^{SU}	Startup duration (in min) of unit $u \in U^{th}$
d_u^{SD}	Shutdown duration (in min) of unit $u \in U^{th}$
d_u^{minOn}	Minimum time on duration (in min) of unit $u \in U^{th}$
d_u^{minOff}	Minimum time off duration (in min) of unit $u \in U^{th}$

$d_u^{minStable}$	Minimum stable power duration (in min) of unit $u \in U^{th}$
d_u^{notice}	Notice delay (in min) of unit $u \in U$

Table 2.3: General notations

2.3.1 Market Orders Formulation

As presented in the General Introduction, a balancing energy market order has a set of characteristics (Table 2.4).

Notation	Description
t_o^{ex}	Creation date of order o
t_o^{start}	Start date of order o
t_o^{end}	End date of order o
q_o^{max}	Maximum quantity of power offered for order o, in MW
q_o^{min}	Minimum quantity of power offered for order o, in MW
q_o^{acc}	Accepted quantity of power offered for order o, in MW. This variable is an output of the Clearing module.
p_o	Price of order o, in €/MWh
σ_o	Sale / Purchase indicator order o, $\sigma = 1$ for sale, -1 for purchase.

Table 2.4: Characteristics of a balancing energy market order

In addition, market orders can be coupled with each other in several ways (c.f. Section 2.2.3) to represent operating constraints. In ATLAS, the following coupling types are implemented:

- *Exclusion*, which indicates that the Clearing stage can accept at most one order amongst the ones that are part of the Exclusion coupling group.
- *Parent-Children*, in which one order is classified as *Parent* and the other ones as *Children*, and that forces the Clearing stage to accept the *Parent* order if at least one of the *Children* is accepted. It is similar to the "Multi part" coupling type indicated in Table 2.1.
- *Identical Ratio*, which indicates that if the Clearing accepts one order o of this coupling group at a certain acceptance ratio $r = (q_o^{max} - q_o^{acc})/(q_o^{max} - q_o^{min})$, then all other orders of this group need to be accepted with the same acceptance ratio. It is similar to the "Linked in time" coupling type of Table 2.1.

The slight differences in terms of names or characteristics between coupling links in ATLAS and the ones in actual RR markets can be explained by the fact that, in ATLAS, coupling links are commonly used for all markets (day-ahead, intraday and balancing) and are therefore hybrids between coupling links that can be found in all of these markets.

2.3.1.1 BSP Orders Formulation

The objective of this module is to formulate, for each generation or load unit, balancing market orders that comply with the standards required for the target balancing market, while accounting for the generation plan determined from prior market phases, a complete set of operating constraints (that depends on the unit type) and reserves previously procured. The balancing formulation is unit-based: every unit is considered individually to determine the maximum upward and downward power it can offer.

In the ATLAS model, an optimal dispatch problem is implemented and was initially considered for the formulation process, similar to its usage in the formulation modules of day-ahead an intraday markets (Little et al., 2024). However, using this optimal dispatch in the context of balancing markets led to prohibitive computation times. Three main reasons have been identified: (i) the high frequency of balancing markets (24 RR markets per day, and 96 mFRR markets), which multiplies the number of optimization problems to be solved, (ii) the 15-minute time resolution of balancing markets, compared to the 1-hour time resolution of wholesale markets, leading to a significant increase in the number of optimization variables, and (iii) the platform in which the ATLAS modeled is developed, which induces latencies at the start and the end of each optimization problem.

Consequently, developing a heuristic method was required. This heuristic still models the same operating constraints as the dispatch optimization problem. It is overviewed in the current section, with the complete details given in Appendix (A.2). Our estimations indicate that it performs the order formulation 5 to 10 times faster than the optimal dispatch problem, rendering the simulation process more feasible.

2.3.1.1.1 Thermal units order formulation

Determination of combinatorial indexes

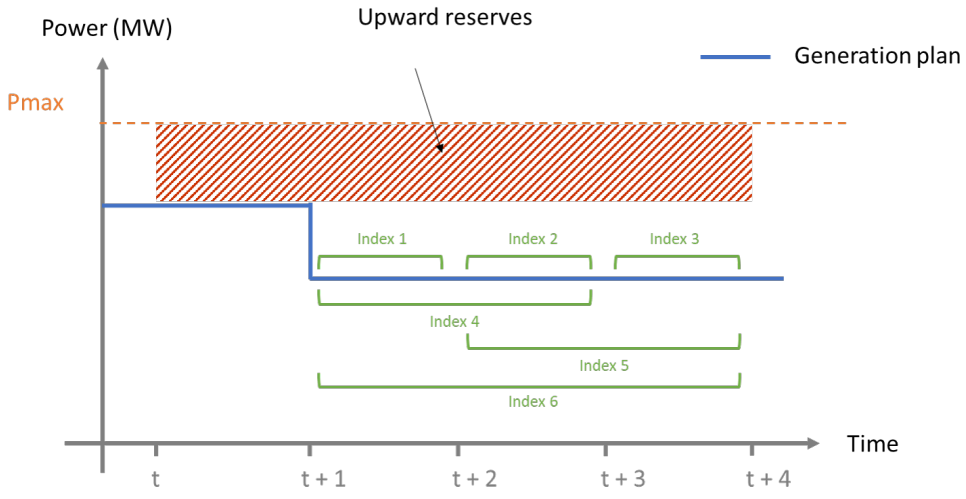

Figure 2.4: Definition of available time indexes

For each unit $u \in U^{th}$, the first step performed by the module is to define the set of “combinatorial" time

indexes $\{id\}$ within the delivery period of the studied market, for which orders will be formulated (Figure 2.4 illustrates with an example). Indeed, operating constraints can impose coupling links between orders over multiple time steps. To take that effect into account, the module identifies all available combinatorial indexes over which an order, or a "block" order (meaning an order that lasts over several time steps) could be formulated. This method allows for generating as many market orders as possible in the case of restrictive operating constraints, providing the highest possible liquidity to the market. Formally, a combinatorial index will be written: $id = \{\{t_{id}^{start}\}, \{t_{id}^{start} + \Delta t_m\}, \dots, \{t_{id}^{end}\}\}$. These indexes can overlap (for instance, indexes 4 and 5 in Figure 2.4), in which case their respective sets of orders will be linked by an *Exclusion* coupling link (see 2.A).

First, a verification is performed on unit u to see if any of the key duration constraints detailed in 2.2.3 is longer than the time step of the market. If not, it implies that operating constraints will not impose restrictions over multiple time steps in the order formulation process. Hence, there is no need to go through all combinatorial indexes and each time step of T_m is considered individually (Equation 2.1). In the other case, however, operating constraints are likely to impose restrictions on orders over multiple time steps. A set of combinatorial indexes is then computed by the function $Combinatorial()$ (Equation 2.2). An example of time steps computed by this function is illustrated in Figure 2.4.

$$\textbf{if } \Delta t_m \geq max(d_u^{SU}, d_u^{SD}, d_u^{minOn}, d_u^{minOff}, d_u^{minStable}, d_u^{notice}) \textbf{ then}$$
$$\{id\} = \{\{t_m^{start}\}, \{t_m^{start} + \Delta t_m\}, \dots, \{t_m^{end}\}\} \tag{2.1}$$
$$\textbf{else} \quad \{id\} = Combinatorial(T_m) \tag{2.2}$$

Then, for each index id, the range of available power is determined for three types of orders:

- For upward orders, the available power is bounded by $Q_{u,id}^{up,max}$ and $Q_{u,id}^{up,min}$. An upward order can induce a startup, which is tracked by $\delta_{u,id}^{SU}$.
- For downward orders, the available power is bounded by $Q_{u,id}^{down,max}$ and $Q_{u,id}^{down,min}$.
- If a shutdown is feasible, a shutdown order is formulated in addition to the regular downward order. The feasibility of such an order is tracked by $\delta_{u,id}^{SD}$.

The bounds of these ranges of available power are computed and successively updated by the steps in Algorithm 1, with:

- $P_{u,t,t_m^{ex}}^{plan}$ the power output of unit u at time t, seen from the execution date of the market t_m^{ex}.
- $P_{u,t}^{max}$ and $P_{u,t}^{min}$ respectively the maximum and minimum power of unit u at time t.
- ΔP_u^{max} the maximum ramping of unit u.

For better display, indicating the market m as an input of a function designates all of its characteristics, especially its execution date t_m^{ex}. Similarly, indicating the unit u as an input passes all of its parameters, such as the generation plan $P_{u,t,t_m^{ex}}^{plan}$ and all its operating constraints. Also, the addition of one or several time steps $t \pm n\Delta t_m$ is written $t \pm n$.

Algorithm 1 Order formulation steps for unit u on combinatorial index id, for balancing market m

Inputs: m, u, id

Initialization of lower bounds and startup / shutdown binaries

$Q^{up,min}_{u,id} \leftarrow 0$
$Q^{down,min}_{u,id} \leftarrow 0$
if $\forall t \in id,\ \ P^{plan}_{u,t,t^{ex}_m} = 0$ **then**
    $\delta^{SU}_{u,id} \leftarrow 1$
else
    $\delta^{SU}_{u,id} \leftarrow 0$
end if
if $\forall t \in id,\ \ P^{plan}_{u,t,t^{ex}_m} > P^{min}_{u,t}$ **then**
    $\delta^{SU}_{u,id} \leftarrow 1$
else
    $\delta^{SD}_{u,id} \leftarrow 0$
end if

Maximum and Minimum power constraints

$Q^{up,max}_{u,id} \leftarrow \min_{t \in id}(P^{max}_{u,t} - P^{plan}_{u,t,t^{ex}_m})$
$Q^{down,max}_{u,id} \leftarrow \min_{t \in id}(P^{plan}_{u,t,t^{ex}_m} - P^{min}_{u,t})$

Previously procured reserves

$Q^{up,max}_{u,id} \leftarrow Q^{up,max}_{u,id} - \max_{t \in id} \sum_{type \neq m} Res^{type,up}_{u,t,t^{ex}_m}$
$Q^{down,max}_{u,id} \leftarrow Q^{down,max}_{u,id} - \max_{t \in id} \sum_{type \neq m} Res^{type,down}_{u,t,t^{ex}_m}$

Notice delay

if $t^{start}_{id} - t^{ex}_m < d^{notice}_u$ **then**
    $Q^{up,max}_{u,id} \leftarrow 0$
    $Q^{down,max}_{u,id} \leftarrow 0$
end if

Maximum ramping constraint

$Q^{up,max}_{u,id} \leftarrow min(Q^{up,max}_{u,id}, \quad \Delta P^{max}_u * \Delta t_m - max(\Delta P^{plan}_{t^{start}_{id}, t^{start}_{id}-1}, \Delta P^{plan}_{t^{end}_{id}+1, t^{end}_{id}}))$
$Q^{down,max}_{u,id} \leftarrow min(Q^{down,max}_{u,id}, \quad \Delta P^{max}_u * \Delta t_m - max(\Delta P^{plan}_{t^{start}_{id}-1, t^{start}_{id}}, \Delta P^{plan}_{t^{end}_{id}, t^{end}_{id}+1}))$

Minimum stable power

if $MinStablePower(m, id, u) = False$ **then**
    $Q^{up,max}_{u,id} \leftarrow 0$
    $Q^{down,max}_{u,id} \leftarrow 0$
end if

Validity of a potential startup, applied when $\delta_{u,id}^{SU} = 1$
if $\delta_{u,id}^{SU} = 1$ **then**
  if $t_{id}^{end} - t_{id}^{start} < d_u^{minOn}$ **then** ▷ Check minimum time ON during the order
    $Q_{u,id}^{up,max} \leftarrow 0$
    $\delta_{u,id}^{SU} \leftarrow 0$
  end if
  if $MinTimeOff(m,u,id) = False$ **then** ▷ Check minimum time OFF before and after the order
    $Q_{u,id}^{up,max} \leftarrow 0$
    $\delta_{u,id}^{SU} \leftarrow 0$
  end if
  if $StartupDura(m,u,id) = False$ **then** ▷ Check startup duration before
    $Q_{u,id}^{up,max} \leftarrow 0$
    $\delta_{u,id}^{SU} \leftarrow 0$
  end if
  if $d_u^{SD} > \Delta t_m$ **then** ▷ Instant shutdown is required at the end of the order
    $Q_{u,id}^{up,max} \leftarrow 0$
    $\delta_{u,id}^{SU} \leftarrow 0$
  end if
end if

Validity of a potential shutdown
if $\delta_{u,id}^{SD} = 1$ **then**
  if $t_{id}^{end} - t_{id}^{start} < d_u^{minOff}$ **then** ▷ Check minimum time OFF during the order
    $\delta_{u,id}^{SD} \leftarrow 0$
  end if
  if $MinTimeOn(m,u,id) = False$ **then** ▷ Check minimum time ON before and after the order
    $\delta_{u,id}^{SD} \leftarrow 0$
  end if
  if $ShutdownDura(m,u,id) = False$ **then** ▷ Check shutdown duration before
    $\delta_{u,id}^{SD} \leftarrow 0$
  end if
  if $d_u^{SU} > \Delta t_m$ **then** ▷ Instant startup is required at the end of the order
    $\delta_{u,id}^{SD} \leftarrow 0$
  end if
end if

Finalization and order formulation
$CreateOrder(m,u,id,Q_{u,id}^{up,max}, Q_{u,id}^{up,min}, \delta_{u,id}^{SU}, Q_{u,id}^{down,max}, Q_{u,id}^{down,min}, \delta_{u,id}^{SD})$

Functions verifying operating constraints

In the previous algorithm, specific functions are applied to verify that making a block order on the index *id* does not violate operating constraints. Only an overview of these functions is presented here: in practice,

the heuristic approach leads to several case separations, that are not shown for length reasons. The full implementation is detailed in (Cogen et al., 2024), or in Section A.3.3.1.2 of the ATLAS Appendix A:

- $MinTimeOn()$ is called in the case of potential startup of shutdown orders. It verifies if the minimum time ON constraint of unit u is respected before and after the combinatorial index id. It returns $True$ if verified, and $False$ otherwise:

Algorithm 2 Definition of $MinTimeOn()$

Inputs: m, u, id

if $\exists t \in \{t_{id}^{start} - 1 - d_u^{minOn}, \ldots, t_{id}^{start} - 1\} \mid P_{u,t,t_m^{ex}}^{plan} = 0$ **then** ▷ Before id
  return $False$
else if $\exists t \in \{t_{id}^{end}, \ldots, t_{id}^{end} + d_u^{minOn}\} \mid P_{u,t,t_m^{ex}}^{plan} = 0$ **then** ▷ After id
  return $False$
else
  return $True$
end if

- $MinTimeOff()$ is called for potential startups and performs a similar task, with the minimum time OFF constraint:

Algorithm 3 Definition of $MinTimeOff()$

Inputs: m, u, id

if $\exists t \in \{t_{id}^{start} - 1 - d_u^{minOff}, \ldots, t_{id}^{start} - 1\} \mid P_{u,t,t_m^{ex}}^{plan} \neq 0$ **then** ▷ Before id
  return $False$
else if $\exists t \in \{t_{id}^{end}, \ldots, t_{id}^{end} + d_u^{minOff}\} \mid P_{u,t,t_m^{ex}}^{plan} \neq 0$ **then** ▷ After id
  return $False$
else
  return $True$
end if

- $StartupDura()$ checks if the startup duration is respected between the execution date of the market t_m^{ex} and the start of id. If it is respected, $\delta_{u,id}^{SU}$ is set to 1:

Algorithm 4 Definition of $StartupDura()$

Inputs: m, u, id

if $t_{id}^{start} - t_m^{ex} \geq d_u^{SU}$ **then**
  return $True$
else
  return $False$
end if

- *ShutdownDura*() checks if the shutdown duration is respected between t_m^{ex} and the start of id. If it is, $\delta_{u,id}^{SD}$ is set to 1:

Algorithm 5 Definition of *ShutdownDura*()

Inputs: m, u, id

if $t_{id}^{start} - t_m^{ex} \geq d_u^{SD}$ **then**
  return $True$
else
  return $False$
end if

- *MinStablePower*() verifies the minimum stable power constraint during, before and after id:

Algorithm 6 Definition of *MinStablePower*()

Inputs: m, u, id

if $t_{id}^{end} - t_{id}^{start} < d_u^{minStable}$ **then** ▷ During id
  return $False$
else if $\exists t \in \{t_{id}^{start} - 1 - d_u^{minStable}, \ldots, t_{id}^{start} - 1\} \mid P_{u,t,t_m^{ex}}^{plan} \neq P_{u,t_{id}^{start}-1,t_m^{ex}}^{plan}$ **then** ▷ Before id
  return $False$
else if $\exists t \in \{t_{id}^{end} + 1, \ldots, t_{id}^{end} + 1 + d_u^{minStable}\} \mid P_{u,t,t_m^{ex}}^{plan} \neq P_{u,t_{id}^{end}+1,t_m^{ex}}^{plan}$ **then** ▷ After id
  return $False$
else
  return $True$
end if

Market orders creation

At the end of Algorithm 1, the function *CreateOrder*() creates upward, downward and shutdown market orders o_i for all times $t \in id$ (Algorithm 7). Among the list of order characteristics presented in Table 2.4, some are always set in the same way: $t_{o_i}^{ex} = t_m^{ex}$, $t_{o_i}^{start} = t$, $t_{o_i}^{end} = t + \Delta t_m$. Consequently, they are not repeated in the description of the algorithm.

Startup and shutdown induce specific orders. For startup cases, two orders are created to allow for correct integration of startup costs: (i) an indivisible order (i.e. $q_o^{max} = q_o^{min}$) is created between 0 and the minimum power of the unit, and (ii) a flexible order is created between the minimum and the maximum power of the unit (it is assumed to be able to reach any power output between these values when starting). Startup costs (c_u^{SU}) are distributed over the indivisible order across the entire combinatorial index id, and the flexible part only takes into account variable costs (c_u^{var}). Shutdowns only necessitate one order (corresponding to the initial power output), but they also induce startup costs since the unit must restart at the end of the balancing market. These costs are consequently integrated into the price of shutdown orders.

Algorithm 7 Definition of $CreateOrder()$

Inputs: $m, u, id, Q^{up,max}_{u,id}, Q^{up,min}_{u,id}, \delta^{SU}_{u,id}, Q^{down,max}_{u,id}, Q^{down,min}_{u,id}, \delta^{SD}_{u,id}$

Upward orders
if $(Q^{up,max}_{u,id} > 0)$ **and** $(Q^{up,max}_{u,id} \geq Q^{up,min}_{u,id})$ **then** ▷ Check if upward orders are feasible
  if $\delta^{SU}_{u,id} = 0$ **then** ▷ Non-startup orders
    for $t \in id$ **do**
      Create $o_{id,t,up}$
      $q^{max}_{o_{id,t,up}} \leftarrow Q^{up,max}_{u,id}$
      $q^{min}_{o_{id,t,up}} \leftarrow Q^{up,min}_{u,id}$
      $p_{o_{id,t,up}} \leftarrow c^{var}_{u}$
      $\sigma_{o_{id,t,up}} \leftarrow 1$
    end for
  else ▷ Startup orders
    for $t \in id$ **do**
      Create $o_{id,t,up,1}$ ▷ Indivisible order
      $q^{max}_{o_{id,t,up,1}} \leftarrow P^{min}_{u,t}$
      $q^{min}_{o_{id,t,up,1}} \leftarrow P^{min}_{u,t}$
      $p_{o_{id,t,up,1}} \leftarrow c^{var}_{u} + \frac{c^{SU}_{u}}{P^{min}_{u,t} * (t^{end}_{id} - t^{start}_{id})/60}$ ▷ Integration of startup costs
      $\sigma_{o_{id,t,up,1}} \leftarrow 1$

      Create $o_{id,t,up,2}$ ▷ Flexible order
      $q^{max}_{o_{id,t,up,2}} \leftarrow P^{max}_{u,t} - P^{min}_{u,t}$
      $q^{min}_{o_{id,t,up,2}} \leftarrow 0$
      $p_{o_{id,t,up,2}} \leftarrow c^{var}_{u}$
      $\sigma_{o_{id,t,up,2}} \leftarrow 1$
    end for
  end if
end if

Downward orders
if $(Q_{u,id}^{down,max} > 0)$ **and** $(Q_{u,id}^{down,max} \geq Q_{u,id}^{down,min})$ **then** ▷ Check if downward orders are feasible
  for $t \in id$ **do**
    Create $o_{id,t,down}$
    $q_{o_{id,t,down}}^{max} \leftarrow Q_{u,id}^{down,max}$
    $q_{o_{id,t,down}}^{min} \leftarrow Q_{u,id}^{down,min}$
    $p_{o_{id,t,down}} \leftarrow c_u^{var}$
    $\sigma_{o_{id,t,down}} \leftarrow -1$
  end for
end if

Shutdown orders
if $\delta_{u,id}^{SD} = 1$ **then** ▷ Check if shutdown orders are feasible
  for $t \in id$ **do**
    Create $o_{id,t,shut}$
    $q_{o_{id,t,shut}}^{max} \leftarrow P_{u,t}^{plan}$
    $q_{o_{id,t,shut}}^{min} \leftarrow P_{u,t}^{plan}$
    $p_{o_{id,t,shut}} \leftarrow c_u^{var} + \frac{c_u^{SU}}{P_{u,t}^{plan} * (t_{id}^{end} - t_{id}^{start})/60}$ ▷ Integration of future startup costs
    $\sigma_{o_{shut}} \leftarrow -1$
  end for
end if

Coupling links creation

Finally, after the creation of market orders, coupling links are created when necessary. As described before, a *Parent-Children* coupling is used to link startup orders. In addition, all orders of the same combinatorial index *id* are linked by a *Identical Ratio* coupling. Finally, *Exclusion* coupling links are created between overlapping combinatorial indexes, and consecutive orders of opposite directions to respect the maximum ramping constraint. More details are provided in Appendix 2.A.

2.3.1.1.2 Formulation of orders for other types of units

As this study focuses on thermal units, the description of unit formulation of other types is less detailed in this chapter (but can be entirely found in (Cogen et al., 2024)):

- Hydro units are separated into 3 different categories, being Run of River (ROR), Reservoir and Pumped Hydro Storage (PHS). ROR units are considered non-dispatchable equipment, and therefore cannot provide any reserve. PHS are modeled as Storage units, and their bidding process is described in the corresponding part. Reservoir units have to comply with the following constraints: minimum and maximum power output, maximum and minimum reservoir level. Their maximum ramping capacity is assumed to be infinite.
- Storage units encompass batteries, electric vehicles and PHS. They can produce or consume energy, and follow constraints of maximum and minimum power output, maximum and minimum reservoir

level, maximum ramping capacity, while having charge and discharge efficiency parameters. Specific constraints are added for electric vehicles (to take into account the energy that was used for displacement and needs to be recharged, as well as variations of the number of vehicles connected at any given time), and for PHS (the transition duration constraint evoked in 2.2.3).

- Wind and Photovoltaic units share the same modeling rules. A forecast of their maximum power output limits the power they can produce, and it evolves as the forecast date gets closer to real-time. In addition, their power output can be curtailed up until a threshold that can be set for each unit. These units have no maximum ramping limit.

- Flexible load is able to provide reserve as well, and is only subject to maximum and minimum power output constraints.

2.3.1.2 TSO Order Formulation

The second stage of the balancing markets orders formulation is the creation of TSO orders. For every time step in the market time frame, each of them computes its balancing needs $bn_{ca,t,t_m^{ex}}$, corresponding to the imbalance within the control area ca it is responsible for (Equation 2.3).

$$\forall ca \in CA,\ \forall t \in T_m,\quad bn_{ca,t,t_m^{ex}} = \sum_{u^l \in U_{ca}^l} |P^{for}_{u^l,t,t_m^{ex}}| - \Big(\sum_{u^g \in U_z^g} P^{plan}_{u^g,t} + \sum_{u^{RES} \in U_{ca}^w \cup U_{ca}^{pv}} P^{for}_{u^{RES},t} \Big) \tag{2.3}$$

With:

- U_{ca}^l the set of all load type units in area ca.

- U_{ca}^w the set of all wind type units in area ca.

- U_{ca}^{pv} the set of all photovoltaic type units in area ca.

- U_{ca}^g the set of all generation units in area ca, excluding wind and photovoltaic units.

This imbalance is then converted into market orders, by taking into account a restriction imposed on TSO orders by balancing markets: the q_o^{max} of a sell (resp. buy) order o cannot exceed the total volume of buy (resp. sell) orders emitted by BSPs in their area[7]. In this chapter, the price of TSO orders is set as inelastic[8], meaning that it is equal to the price cap of the market (±10,000 €/MWh for the RR market, depending on the direction of the order). Eventually, an order o^{TSO} emitted by a TSO managing the market

[7]This is indicated in https://consultations.entsoe.eu/markets/rr_if_2nd_amendment/supporting_documents/202202_RRIF_2nd%20amendment.pdf

[8]This assumption will be challenged in Chapter 3

area z at time t has the following characteristics:

$$\forall t \in T, \quad \textbf{if} \quad bn_{ca,t,t_m^{ex}} > 0, \quad \textbf{then} \quad \begin{cases} q_{o^{TSO}}^{max} = \min(|bn_{ca,t,t_m^{ex}}|, \sum_{o \in O_{z,t}^{BSP} | \sigma_o = 1} q_o^{max}) \\ q_{o^{TSO}}^{min} = 0 \\ p_{o^{TSO}} = 10000 \\ \sigma_{o^{TSO}} = -1 \end{cases} \tag{2.4}$$

$$\forall t \in T, \quad \textbf{if} \quad bn_{ca,t,t_m^{ex}} < 0, \quad \textbf{then} \quad \begin{cases} q_{o^{TSO}}^{max} = \min(|bn_{ca,t,t_m^{ex}}|, \sum_{o \in O_{z,t}^{BSP} | \sigma_o = -1} q_o^{max}) \\ q_{o^{TSO}}^{min} = 0 \\ p_{o^{TSO}} = -10000 \\ \sigma_{o^{TSO}} = 1 \end{cases} \tag{2.5}$$

2.3.2 Market Clearing

The Market Clearing stage aims to accept or reject market orders and to fix the market price, which ultimately conditions the remuneration of all involved market actors. It is based on clearing algorithms used in actual day-ahead or balancing markets (respectively EUPHEMIA[9] and TERRE (ENTSO-E, 2023c) algorithms). The order acceptance is performed through a social welfare maximization, subject to constraints regarding transmission capacities and coupling links between market orders.

The Market Clearing stage was already developed in ATLAS before this study, for day-ahead and intraday markets, and is described extensively in (Little et al., 2024). As it was designed to be generic, it is also used for balancing markets. Its main interaction with operating constraints comes from the coupling links described in Section 2.3.1.1, as these links can interfere with both the order activation and the clearing price determination process.

2.3.3 Generation and load plans update

After receiving the results of the Clearing module, all units update their generation or load plan. In the day-ahead or intraday market, a portfolio optimization occurs here. However, given the short response time imposed by balancing markets (see Section 2.2.2), a unit-based activation is assumed. Consequently, all market actors respect exactly what has been activated on each unit by the Clearing module, and update their dispatch accordingly.

2.3.4 Balancing Mechanism

Economic or technical reasons can lead to market areas still being imbalanced after balancing markets. A last module is used to correct any remaining imbalance. It is based on the historical local process used by

[9] Complete description of the EUPHEMIA algorithm: https://www.nordpoolgroup.com/globalassets/download-center/single-day-ahead-coupling/euphemia-public-description.pdf

the French TSO RTE called "Balancing Mechanism" (FrBM hereafter), which currently still runs after the RR market, and has been developed in ATLAS (Cogen et al., 2024).

This process considers each TSO individually, along with its control area. Every unit in this area is required to communicate to its TSO its generation or load plan, alongside all of its operating constraints, and an activation price. The TSO then computes the remaining imbalance in its area, and solves an optimization to identify the units that need to be activated to correct the imbalance at the least cost, while taking into account all operating constraints. Each activated unit is then remunerated (or has to pay, if it was activated as a downward reserve) according to a pay-as-bid method. In this study, it is assumed that the activation price communicated by the units corresponds to their variable cost, in line with the assumption made on balancing markets. A detailed description of the Balancing Mechanism is given in Appendix A.5.

2.4 Methodology

The literature review presented in Section 2.2.4 highlighted that the operating constraints associated with thermal generation units are only partially taken into account in the articles modeling electricity markets. To quantify the impact on market performance of this simplified view, a market simulation on a European-wide power system was performed using the ATLAS model, following a methodology described in this section.

2.4.1 Input data

The input dataset comes from the 2030 scenario of the Energy Pathways to 2050 study (RTE, 2022). It represents the European power system in a simplified way, while capturing its local particularities by modeling it with 32 interconnected areas based on official European bidding zones, each with specific generation and consumption assets. Transmission lines and capacities are derived from the current system and from European as well as national network development plans. The resulting map is shown in Figure 2.5a.

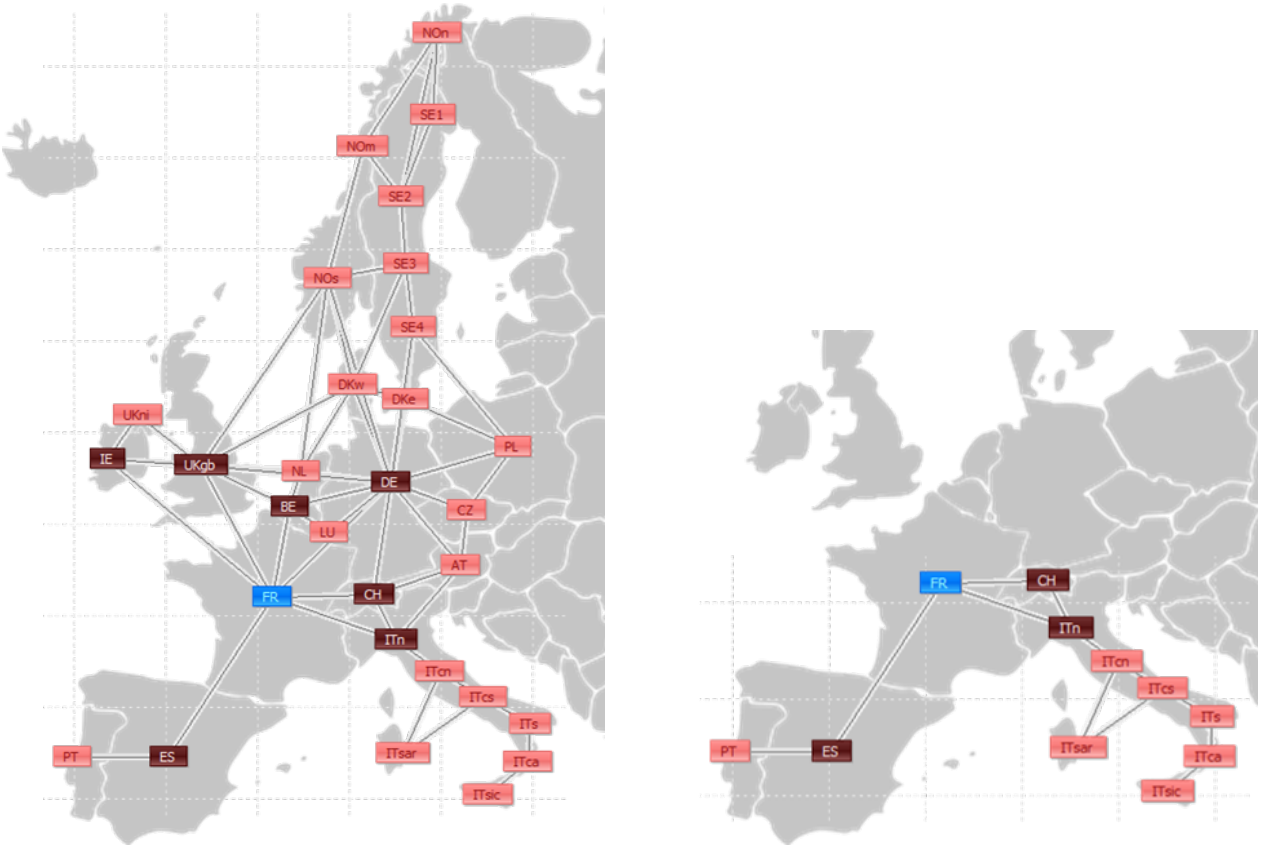

(a) Complete European power system

(b) Market areas included in RR market simulations

Figure 2.5: Map of the European power system in the 2030 representation used in the ATLAS case study

A subset of this power system will be used for RR market simulations (Figure 2.5b), including all countries that are currently participating in RR markets with the exception of Czech Republic[10].

The composition of the European generating fleet, alongside installed capacities in power-to-gas (P2G) technologies, are given in Table 2.5. It is also detailed for each area in Appendix 2.B (Table 2.9). Most thermal units are clustered at an almost national scale (CCGT in Germany or the United Kingdom for instance), meaning that the results presented in this chapter are probably still underestimating the impact of operating constraints.

Storage assets stand out amongst other types of generation assets because of the following particularities:

- Batteries and PHS can withdraw energy on top of injecting it into the network, which is indicated in the table by a negative value. In the case of an identical maximum power in both directions, the sign $\pm$ is used.
- The capacity of electric vehicles connected to the network is always fluctuating, and is comprised within the ranges given for each area. In this study, electric vehicles are assumed to be unable to function in

[10] Czech Republic is not currently not directly connected to the other participants of the RR market, and essentially consists in a local closed RR market

the so-called "vehicle to grid" mode, meaning that they can only consume energy to charge (and not act as generation units).

Technology	**Thermal**				**Hydraulic**	**Storage**			**Wind**	**Solar**	**P2G**	**Other**
Sub-technology	Gas	Oil	Coil	Nuclear	/	Batteries	PHS	Electric Vehicles	/	/	/	/
Total installed capacity (GW)	229	2.6	52.7	85.7	145.5	0.5	48.5	2.8	358.9	321.5	25.5	20.5

Table 2.5: Synthetic view of European installed capacity of generation and P2G technologies in the input dataset

Regarding unflexible load, each area contains exactly one asset of this type. The peak load of each one over the simulated period is represented in Table 2.8 of Appendix 2.B. The only exception is the French (FR) zone, which also contains one unit of heavy electric vehicles (trucks and buses), modeled as a pure consumption asset with a capacity of 1750 MW.

Finally, all thermal units in the different areas have their own characteristics, and in particular their specific operating constraints depending on their fuel type (Figure 2.6). They are consistent with operating constraint values chosen in other works of the literature (Schill et al., 2017, Petitet et al., 2019).

Unit type / Fuel type	**Minimum time ON**	**Minimum time OFF**	**Startup duration**	**Shutdown duration**	**Minimum stable power duration**
New CCGT	120	120	60	60	15
Old CCGT	180	180	60	60	15
OCGT	0	0	25	25	15
Conventional gas	300	300	30	30	15
New lignite	480	480	600	600	30
Old lignite	660	660	600	600	30
Coal	300	300	60	60	30
Oil	0	0	15	15	0
CHP oil / heavy oil	180	180	15	15	0
Nuclear	720	720	600	600	120
French nuclear	1440	1440	600	600	120

Table 2.6: Qualitative values (in minutes) of operating constraints in the input dataset

2.4.2 Scenarios

In order to capture the individual effects of every operating constraint on thermal units, as well as their influence when modeled together, the following 6 scenarios are studied (Figure 2.7).

Scenario / Operating constraints	Minimum constraints	Basecase (BS)	BS + MinTimeOn/Off	BS + Startup/Shutdown	BS + MinStablePower	All constraints
Maximum power/ Minimum power	✓	✓	✓	✓	✓	✓
Maximum ramping	✗	✓	✓	✓	✓	✓
Minimum time ON / Minimum time OFF	✗	✗	✓	✗	✗	✓
Startup duration / Shutdown duration	✗	✗	✗	✓	✗	✓
Minimum stable power duration	✗	✗	✗	✗	✓	✓

Table 2.7: Scenarios simulated

A few points should be highlighted regarding these scenarios:

- When an operating constraint is described as inactive in a scenario, it means that its value is set at 0 for every thermal unit in the input data set (assuming that a maximum ramping of 0 MW/min corresponds to an infinite ramping potential).
- Minimum time ON and minimum time OFF constraints are grouped into the same scenario, as they are usually symmetrical (in the sense that the same value is chosen for both constraints) and that they are usually implemented together since they are based on the same concepts. The same logic was applied for startup duration and Shutdown duration constraints.
- The second scenario is considered as the base case, because as Figure 2.2 showed, nearly all models include at least the Minimum power, Maximum power and maximum ramping constraints. The first scenario, referred to as *Minimum constraints*, was simulated to evaluate the impact of removing the maximum ramping constraint. Similar sensitivity scenarios could not be carried out for maximum power and minimum power constraints, as they are required for ATLAS market simulation modules to run properly.
- The notice delay constraint is not included in these simulations. Given that the values found for the different fuels in (Petitet et al., 2019) are almost all in the [5min, 30min] range, the impact of this constraint on RR market processes can be deemed negligible. However, it would become prevalent if mFRR markets were simulated, given their short time frame.

2.4.3 Simulations details

Because of computation time constraints, the entire sequence of short-term electricity markets (i.e. day-ahead, intraday, RR and mFRR markets) could not be simulated over the whole year of data. 3 days were selected because of their characteristics: an autumn day with rather standard load and renewable energy generations across all areas (Day A), a winter day stressed by high load and low photovoltaic generation (Day W), and a summer day with low load and high photovoltaic generation (Day S).

At first, a day-ahead market was simulated for each scenario, for each of these 3 days, on the complete European system depicted in Figure 2.5a. Results of day-ahead markets are detailed in Section 2.5, which

shows that all market indicators studied are almost identical for all scenarios. However, even minor differences in day-ahead results can lead to important variations regarding indicators observed for subsequent markets (notably market liquidity indicators). Consequently, and to better understand the impact of operating constraints on balancing markets specifically, a single day-ahead market that includes all operating constraints presented in Figure 2.7 was taken as the basis for balancing simulations for each day. These balancing simulations consist of 24 sequences of an RR market followed by a FrBM (one for each hour of the day), this time performed for each scenario independently and on the reduced power system presented in Figure 2.5b. This simulation framework is illustrated in Figure 2.6.

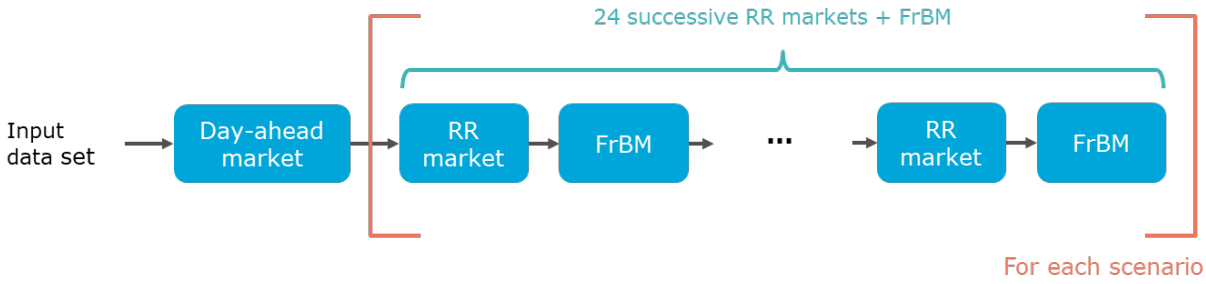

Figure 2.6: Simulations framework

For computation time reasons, intraday markets were not simulated here. Consequently, the imbalance seen by TSOs when formulating market orders for RR markets is greater than the one they would have computed if intraday markets were included. The following verifications were performed to make sure that this simplification does not drastically change results:

- Average balancing needs of the French TSO for products corresponding to RR reserves were estimated to be equal to 0.9 GW over 2022 in (Pichoud, 2023). In our simulations, in the French area, the average upward (resp. downward) balancing need is equal to 1.66 GW (resp. 1.59 GW). All things considered, while greater on average, these simulated need volumes seem reasonable, especially since the power system studied is based on the projected 2030 system that incorporates more renewable energy sources than in 2022 (leading to increased balancing needs, as discussed in Section 2.2.1).

- There is no clear discrepancy between imbalance volumes calculated for the first RR market of the day and for the last market (meaning that TSO needs on the last RR market of the day are not substantially different, on average, from needs on the first one of the day).

2.5 Results

The results section illustrates the impacts of integrating specific operating constraints in an electricity market model on market performance, and is divided into two main categories: first a rapid overview of impacts on the day-ahead market in Section 2.5.1, followed by a more detailed analysis of impacts on the RR market in Section2.5.2.

2.5.1 Day-ahead market results

The main change induced by operating constraints is the market liquidity, which consequently modifies market outcomes. Figure 2.7 represents the liquidity in the day-ahead market over the 3 days simulated by plotting the total volume submitted on this market (corresponding to the sum of q_o^{max} of market orders). On top of each histogram the evolution compared to the Basecase scenario is shown.

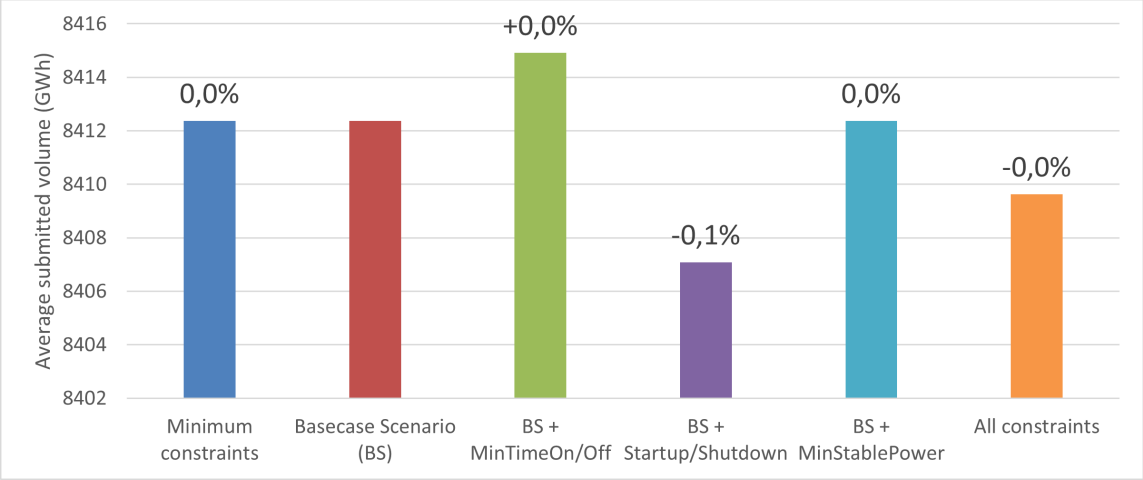

Figure 2.7: Total volumes (GWh) offered on the day-ahead market, for each scenario

There is almost no difference in terms of market liquidity (at most a difference of 0.1% of submitted volume). The small increase observed for scenarios *BS + MinTimeOn/Off* compared to the *Basecase* can be explained by must-run situations. As Minimum Time On/Off duration can restrict a unit from shutting down for a short period and restarting after, it may be forced to offer power during this period even if its price forecast indicates that it is better for the unit not to produce. In other scenarios (except for All constraints), this situation does not exist as the unit can simply choose not to offer power on the period.

These results provide an explanation as to why modeling advanced operating constraints in electricity markets was mostly overlooked before: while they still constrain the shape of generation plans of units, they have little impact on the volume of orders submitted, and consequently on actual performances of markets such as the day-ahead.

2.5.2 RR market results

On the other hand, the RR market exhibits many more differences between the operating constraint inclusion scenarios, as the results of this section show.

2.5.2.1 Market liquidity

Market liquidity varies heavily with the different scenarios, as illustrated in Figure 2.8 and Figure 2.9[11]. Upward and downward orders are differentiated, as they compensate for different types of system imbalances (a lack of downward reserves, for instance, cannot be filled by an excess of upward reserves) and therefore should not be aggregated in the same indicator. It should be noted that certain types of thermal assets are not formulating orders in a specific direction. For instance, this is the case for nuclear assets that are not making upward orders. This is not due to advanced operating constraints, but rather to the fact that they are all already producing at their maximum power output at the end of the day-ahead market. On the opposite side, oil assets are not formulating downward orders because they were not activated by the day-ahead market.

There is a significant market liquidity drop between the scenarios with a simplified view of operating constraints and the others, especially the *All constraints* scenario: -30% for upward reserves, and up to -54% for downward reserves compared to the *Basecase* scenario. Here it is worth noting the relationship between specific operating constraints and unit/fuel types:

- The minimum stable power duration constraint is a prime example of this, as it is deeply associated with nuclear assets. In Figure 2.8b and Figure 2.9b, it can be seen that volumes in the scenario *BS + MinStablePower* are close to those of the *Basecase* scenario for all fuels except nuclear. In our simulations, since these assets happen not to provide upward reserves because of day-ahead market results (see previous paragraph), overall market liquidity impacts vary considerably between upward and downward reserves. Note that in the last two scenarios, a nuclear asset not functioning at its maximum power would not be able to provide upward reserves, even if the case does not arise in our simulations. Overall, this means that the minimum stable power duration constraint completely prohibits nuclear assets from participating in RR markets.
- Minimum time on/off constraints are particularly relevant for CCGT units, whose flexibility and installed capacities make them a major provider of RR reserves. If this constraint is taken into account, previously turned-off CCGT units cannot formulate orders on the RR market, as this would conflict with their minimum time on requirement. Additionally, already turned-on CCGT units cannot make shutdown orders because this would violate their minimum time off constraint.

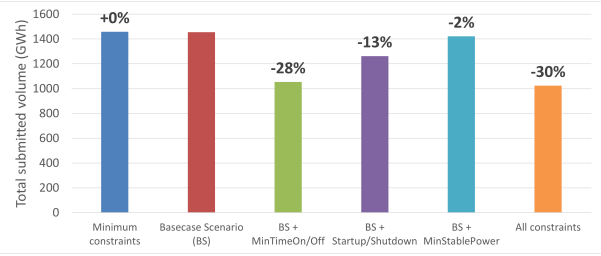

(a) Overall market liquidity

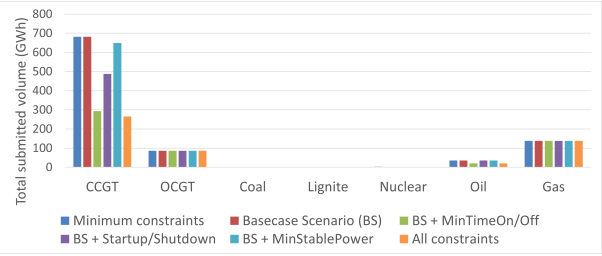

(b) Thermal units volumes, for each fuel type

Figure 2.8: Daily volume of upward RR orders per scenario, in GWh

[11]The formulation process can lead to simultaneous orders (for overlapping combinatorial indexes). This is integrated into market liquidity indicators: only the largest order is considered in that case.

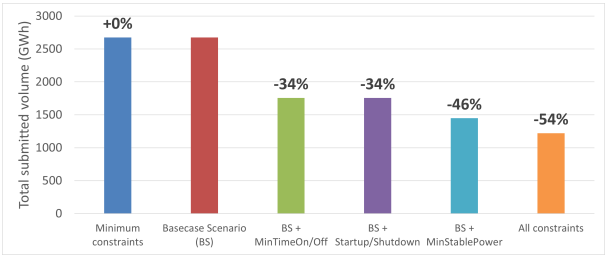

(a) Overall market liquidity

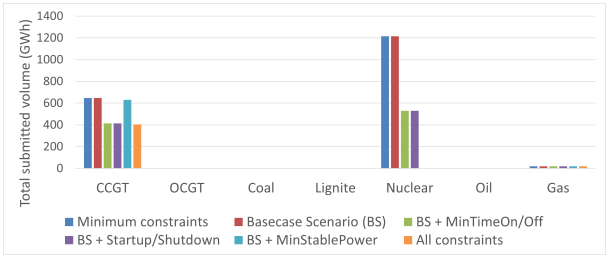

(b) Thermal units volumes, for each fuel type

Figure 2.9: Daily volume of downward RR orders per scenario, in GWh

Day-by-day liquidity results are displayed in Appendix 2.C. Although trends are similar, differences can still be observed between them, as the state of the power system at the end of the day-ahead market determines the range of possible RR market offers. This is particularly clear for day W (the winter day), as most CCGT units are already turned on in the day-ahead market to meet the important winter demand. Consequently, their ability to provide reserves on the RR market is much less impacted by minimum time on/off constraints (notably for upward reserves), resulting in smaller differences between scenarios.

A graph showing differences between countries[12] is displayed in Figure 2.10. The average volume submitted by thermal units, as well as the separation between upward and downward orders, are plotted for scenarios *Basecase* and *All constraints*. It can be seen that impacts on liquidity differ between areas and directions, which was to be expected given the diverse generation mixes. France and Switzerland experience drastic decreases in the volume of downward orders submitted between both scenarios, mainly because of them having large installed capacity of nuclear assets. The relative importance of CCGT units in the Spanish thermal generation fleet leads to a greater decrease in upward orders formulated, compared to downward orders. Italy or Portugal are less impacted by these liquidity variations.

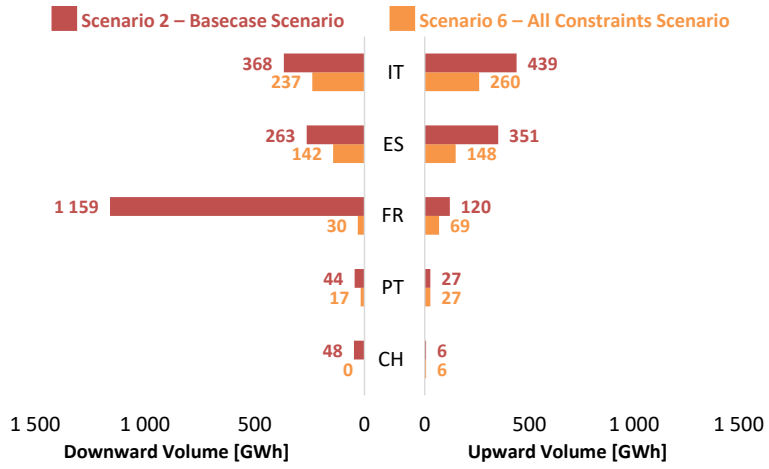

Figure 2.10: Volumes of RR orders submitted by thermal units per country for scenarios *Basecase* and *All constraints*, in GWh

[12]Market areas of Italy are regrouped together, for clarity purposes.

2.5.2.2 Impact on market outputs

The previous section demonstrated the impact of operating constraints on market liquidity, and this section studies the outcome of these liquidity variations on market results, based on 3 indicators: security of supply, TSO balancing costs and social welfare.

Security of supply

First, an important outcome of markets is the security of supply, evaluated in this study through the volume of TSO balancing demands that are not supplied by the market. This indicator is linked with the limitation imposed by the RR design on the maximum demand that can be submitted by TSOs, explained in Section 2.2.2: in nominal state, they cannot exceed the volume of reserves offered by BSPs in their area. If the latter is not sufficient in a given area, the associated TSO may not be able to ask its entire balancing needs on the market. The average daily quantity of unsupplied (i.e. unsubmitted) needs of all TSOs is shown, for each scenario, in Figure 2.11.

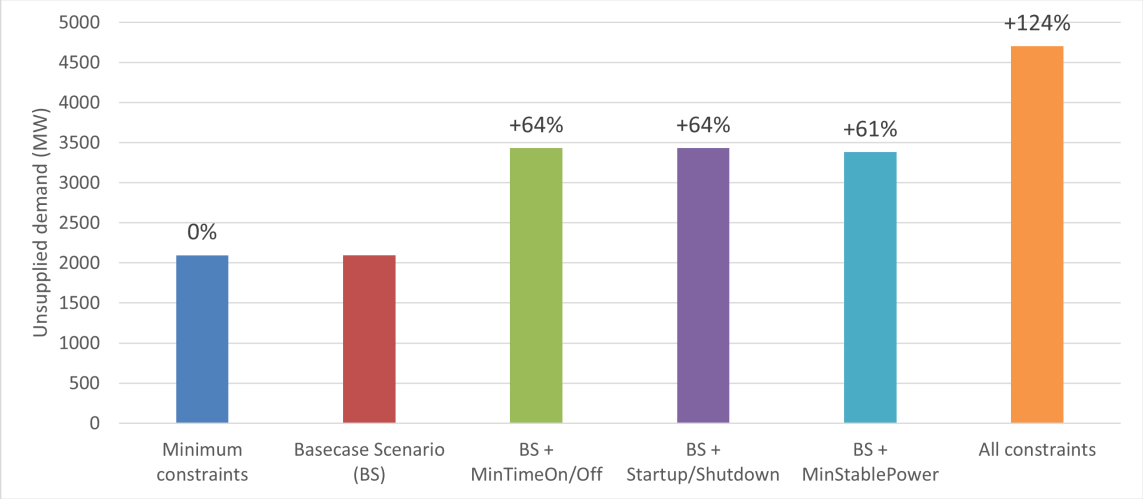

Figure 2.11: Daily quantity of unsupplied TSO demands (in MW), per scenario

Compared to the *Basecase*, scenarios with additional constraints lead to a considerable increase of unmet TSO demands, around 120% more for the *All constraints* scenario. This result should be taken in a qualitative way rather than quantitative, since in our case study TSOs did not procure RR reserves in advance and only rely on the energy activation stage. It mainly advocates for the importance of the reserve procurement process: because of operating constraints and the associated liquidity decrease, the balancing energy market may not be able to provide all the balancing needs required without prior procurement. It should be noted that operating constraints also impact the procurement stage, by extension: given the current design of the RR product, nuclear units would still be unable to be activated even if they had procured power.

TSO balancing costs

In addition, we looked at the overall balancing costs of TSOs c^{TSO} for each scenario, which is the sum of two components: their costs or benefits coming from the RR market, as well as the cost of resolving any remaining imbalance after each RR market using the FrBM (noted c^{FrBM}_{t,TSO_i} hereafter, for the TSO associated with market area i). The RR market component is further subdivided into two parts: the revenue coming

from accepted orders, and benefits associated with congestion rents[13].

$$c^{TSO} = \sum_{t} \sum_{i \in Z} \left[\sum_{o \in O_{i,t}^{TSO}} q_o^{acc} * (-\sigma_o) * \lambda_{t,i} - \sum_{mb_{i,j} \mid j \in Z} (\lambda_{t,i} - \lambda_{t,j}) * (\Delta q)_t^{mb_{i,j}} \right] * \frac{\Delta t_m}{60} + c_{t,TSO_i}^{FrBM} \quad (2.6)$$

Where:

- Z is the set of all market areas.
- $O_{i,t}^{TSO}$ is the set of all TSO orders on area i at time t.
- $\lambda_{t,i}$ is the market clearing price at time t in area i.
- $mb_{i,j}$ is the market border between areas i and j.
- $(\Delta q)_t^{mb_{i,j}}$ is the power flow in market border mb_{ij} (from i to j) at time t.

Average TSO balancing costs over the 3 days, for all scenarios, are indicated in the second column of each graph of Figure 2.13 (as part of the social welfare computation). We can observe that average costs are always higher for scenarios including more operating constraints than the *Basecase* scenario. In particular, there is a significant increase of 114% in balancing costs between scenario *Basecase* (average of 2.26 M€) and scenario *All Constraints* (average of 4.85 M€).

Furthermore, Figure 2.12 plots the evolution of balancing costs for each day of each scenario, compared to the same day of scenario *Basecase*. Despite the differences between simulated days that were discussed in Section 2.4.3, the pattern of balancing cost increase is similar across all days, which reinforces our trust in the observed consequence of including operating constraints. The scale of this increase still depends on the day, with Day A (the autumn day) displaying the largest for all scenarios.

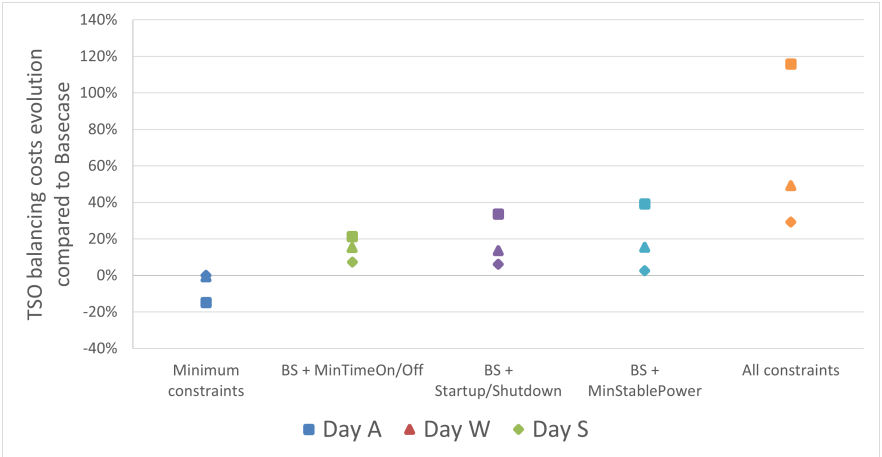

Figure 2.12: TSO balancing costs evolution compared to *Basecase* scenario for all 3 days simulated

[13]Congestion rents are generated when a transmission line (also called a market border) between two market areas is saturated by market activations.

Social welfare

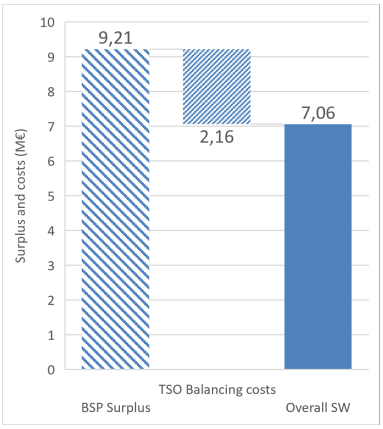

(a) *Minimum constraints*

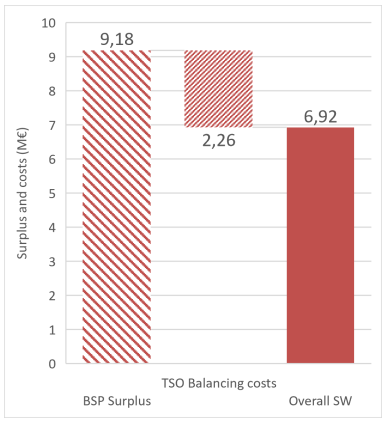

(b) *Basecase*

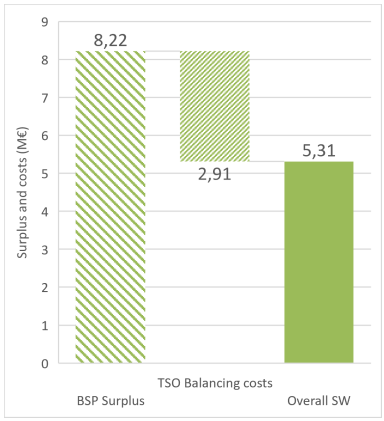

(c) *BS + MinTimeOn/Off*

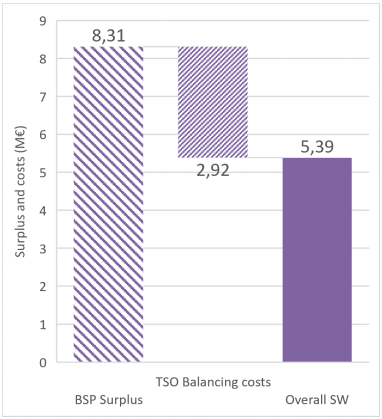

(d) *BS + Startup/Shutdown*

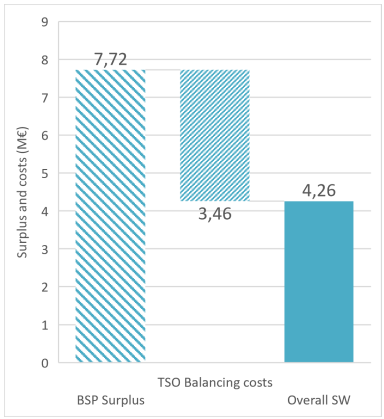

(e) *BS + MinStablePower*

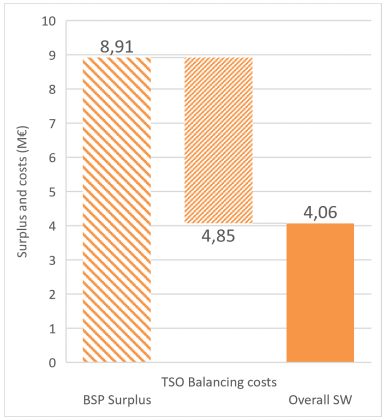

(f) *All constraints*

Figure 2.13: Social welfare per scenario and its decomposition, in M€

Finally, we computed the social welfare for each scenario. On electricity markets, the classic definition of social welfare is composed of two parts (Zolotarev, 2017): (i) the order surplus that represents the difference between the amount that the actor was willing to pay/receive and its actual payment/benefits, (ii) the congestion rents received by TSOs. This is given in Equation 2.7:

$$SW = \frac{\Delta t_m}{60} * \sum_t \sum_{i \in Z} \left[\sum_{o \in O_{i,t}} q_o^{acc} * \sigma_o * (\lambda_{t,i} - p_o) + \sum_{mb_{i,j} \mid j \in Z} (\lambda_{t,i} - \lambda_{t,j}) * (\Delta q)_t^{mb_{i,j}} \right] \tag{2.7}$$

However, this definition is not appropriate for this study, as TSO orders are assumed to be formulated at all costs (i.e. at $p_o = \pm 10,000$€/MWh). If it was applied, the TSO orders surplus term $\sum_{o \in O_{i,t}^{TSO}} q_o^{acc} * (-\sigma_o) * (p_o - \lambda_{t,i})$ would lead to enormous inflation of the indicator, given that market prices λ are comprised

between 50 €/MWh and 100 €/MWh in our simulations. Instead, we used the social welfare computation of Equation 2.8, which corresponds to the difference between the BSP order surplus and the TSO balancing costs previously computed.

$$SW = \sum_{t \in T_{RR}} \left[\sum_{i \in Z} \sum_{o \in O_{i,t}^{BSP}} q_o^{acc} * \sigma_o * (\lambda_{t,i} - p_o) * \frac{\Delta t_m}{60} \right] - c^{TSO} \tag{2.8}$$

Figure 2.13 details average social welfare results over the simulated days, including the values of both BSP and TSO components. As presented before, TSO balancing costs are higher for scenarios that include advanced operating constraints. The BSP surplus tends to decrease in scenarios with advanced constraints, although the BSP surplus of scenario *All constraints* is relatively close to that of scenario *Basecase*. Its evolution is harder to describe, as it is simultaneously influenced by variations in market prices and by the type of BSP orders limited by operating constraints. Indeed, if units with low production costs are prevented from participating in RR markets by these constraints, and more expensive units are activated instead, the resulting BSP surplus will decrease.

2.6 Conclusion

This chapter puts past studies on electricity balancing markets into perspective by focusing on the inclusion of operating constraints of thermal units in electricity markets models, with a focus on balancing markets and more specifically on the RR product. Indeed, interactions between operating constraints and strong requirements in terms of order standardization associated with the definition of RR products can lead to significant overestimation of market liquidity, and consequently of market performances.

We first compiled a list of relevant operating constraints for the time scale of balancing markets. Based on it, a literature review of the integration of operating constraints in electricity balancing market models used was conducted, and it reveals that almost all of them incorporate only a subset of this constraint list.

To address this issue, a new model of balancing markets was developed and integrated into the ATLAS electricity market model. It is then used to study the impact of such model simplifications on simulated market inputs and outputs: a day-ahead market, followed by 24 RR markets are simulated for 3 representative days from different seasons, based on 6 scenarios. Each one of them gradually introduces additional operating constraints in the simulation. Even if the intraday market was not simulated, the order of magnitude of TSO balancing needs formulated on the RR market was assessed and is quite representative.

Results of these simulations indicate that taking into account the complete set of constraints has a major impact on market liquidity, with decreases of 30% (upward) and 54% (downward) of volumes of RR orders compared to the *Basecase* scenario that only includes basic constraints (maximum and minimum power, as well as ramping limit). This liquidity decrease induces several variations in market outcomes (values indicated are the comparison between the *Basecase* and *All constraints* scenarios):

- An average increase in TSO balancing costs of 114% (2.59 M€).
- An overall decrease of 40% of social welfare, taking into account the fact that TSOs formulate inelastic demands in our study.

- A reduction of the level of security of supply, illustrated by a 120% increase in the volume of TSO balancing needs that are not fulfilled by RR markets.

These effects are similar in all 3 days simulated, despite their notable differences in terms of load and renewable generation, thermal unit availability and eventually TSO balancing needs volume and direction. This reinforces our trust in the presented results. We also observed a notable link between the different constraints and the composition of the power system. In areas with a major share of CCGT units (e.g. Germany), minimum time on/off constraints are particularly influential. With the current design of RR markets, the minimum stable power duration constraint prohibits almost entirely the participation of nuclear units: including this constraint has greater impacts on power systems with high nuclear capacities (e.g. France).

Following this study, the authors note that taking into account operating constraints, especially on thermal generation units, has a significant impact on outcomes of close-to-real-time market simulations, and should be considered when studying these types of markets in accordance with the power system modeled. It is also worth noting that this study was done on the least restrictive balancing reserve type. Indeed, mFRR markets impose heavier requirements in the standardization phase since these reserves are closer to real-time than RR, and the impact of operating constraints will be even stronger.

Further research topics will include an extension of this study to estimate the impact of the energy transition on indicators presented here, by using an input dataset that represents the 2050 European power system (which will include a large share of renewable energy sources, batteries and demand response). Additionally, the behavior of market actors in balancing markets should be refined: all reserve providers were assumed to act in perfect competition in our simulation, by offering all their available capacity at their production cost. Previous studies showed that this is probably not the case in the actual power system, which could accentuate our results. We are also planning to study the potential behavior of TSOs in balancing markets, deepening the simple modeling presented in this chapter.

2.A Appendix A - Coupling links in the RR market model in ATLAS

The creation of coupling orders by the Balancing markets BSP orders formulation stage is detailed here.

- *Identical Ratio* links are created between orders of the same combinatorial index id (Equation 2.9, with $\bullet \in \{up, down\}$). Equation 2.10 deals with the case of startup orders, where it is only necessary to link the flexible orders.

$$\forall id \mid \delta^{SU}_{u,id} = 0, \quad \exists\, c^{idr} \in C^{idr} \mid \forall t \in id, \quad o_{id,t,\bullet} \in c^{idr} \tag{2.9}$$

$$\forall id \mid \delta^{SU}_{u,id} = 1, \quad \exists\, c^{idr} \in C^{idr} \mid \forall t \in id, \quad o_{id,t,up,2} \in c^{idr} \tag{2.10}$$

- *Parent-Children* coupling links are created for orders inducing the startup or the shutdown of a unit $u \in U^{th}$, as explained in Section 2.3.1.1.1. It is written in Equation 2.11, where C^{pc} is the set of *Parent-Children* coupling links.

$$\forall u \in U^{th}, \ \forall id \mid \delta^{SU}_{u,id} = 1, \ \forall t \in id, \quad \exists\, c^{pc} \in C^{pc} \mid \{o_{id,t,up,1}, o_{id,t,up,2}\} \in c^{pc} \tag{2.11}$$

A visual example is given in Figure 2.14. Using such a coupling has 2 main interests. First, it ensures that the power activated by the Clearing respects the minimum power constraint, as it is forced to activate the "bottom" order entirely (as the order is indivisible) to be able to activate the "top" order. This feature could have been obtained in a simpler fashion with a single order, partially divisible (with $q^{min}_o = P^{min}_{u,t}$ and $q^{max}_o = P^{max}_{u,t}$). However, properly distributing the startup cost with this simple method would not have been possible. With the *Parent Children* coupling, this fixed cost can be distributed over the relevant part, i.e. the indivisible "bottom" order.

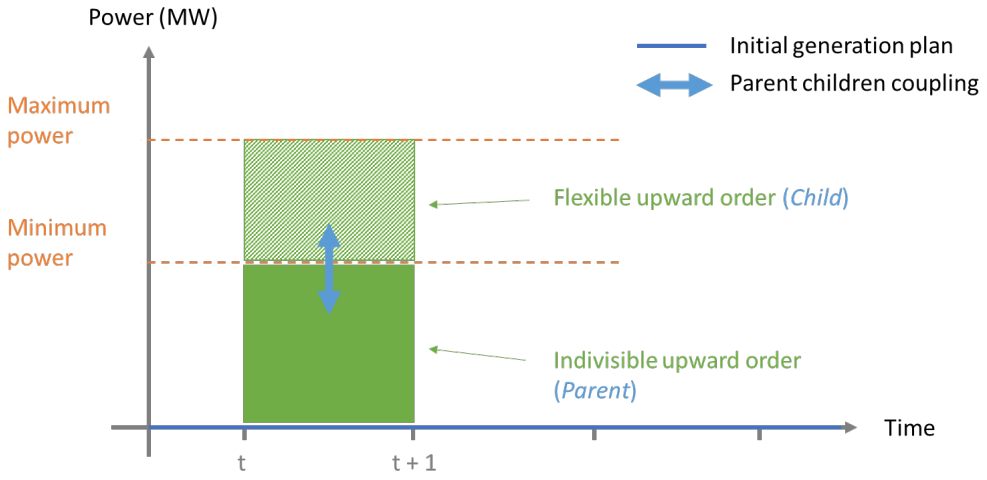

Figure 2.14: *Parent Children* coupling between startup orders

- *Exclusion* links are created between consecutive orders in opposite directions. As Figure 2.2 shows, the real generation plan of the unit induces ramping before and after the actual start date and end date of the market order. This means that activating consecutive orders in opposite directions (upward, then downward, or the contrary) could lead to violation of the maximum ramping constraint (Figure 2.15).

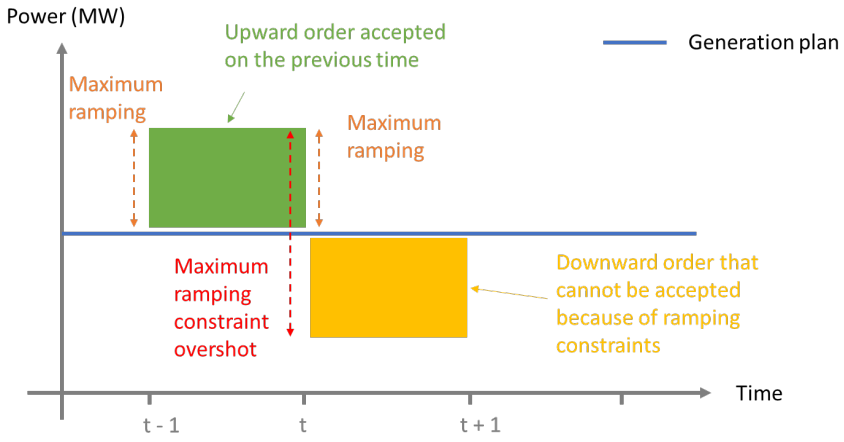

Figure 2.15: Possible maximum ramping issue induced by consecutive orders of opposite direction

- Finally, *Exclusion* links are created between overlapping orders of the same direction (for instance orders of separated time indexes, or downward / shutdown orders on the same time step).

2.B Appendix B - Detailed description of installed capacities in the 2030 input dataset

Table 2.8 indicates the peak load in each area, for all simulated days (see Section 2.4.3 for more details).

Area	AT	BE	CH	CZ	DE	DKe	DKw	ES	FR	IE
Day A peak load	8227	10479	5343	7851	63231	1661	3034	34305	56221	5051
Day W peak load	13723	14290	11669	12157	96320	2811	5317	44148	93729	7026
Day S peak load	10744	12353	6176	9163	77023	2047	3810	39566	69068	5477

Area	ITca	ITcn	ITcs	ITn	ITs	ITsar	ITsic	LU	NL	NOm
Day A peak load	841	3908	7446	23107	3354	1308	2731	1161	12845	3164
Day W peak load	1053	4575	9143	29692	3968	1595	3270	1548	21185	5579
Day S peak load	1088	5110	9693	29425	4153	1696	3481	1314	15922	3383

Area	NOn	NOs	PL	PT	SE1	SE2	SE3	SE4	UKgb	UKni
Day A peak load	2455	11455	20689	7110	1179	1880	8998	2345	32657	1247
Day W peak load	4220	18890	29082	9043	2008	3344	15955	4162	56098	1961
Day S peak load	2582	11721	23739	9990	1314	2047	9791	2607	38729	1433

Table 2.8: Peak load in each area in MW, for all simulated days

Table 2.9 indicates the installed capacity in MW for each type of generation, and in brackets the number of units across which this capacity is spread (when there is more than one unit). The initial dataset contained clusters of units at national levels, especially large clusters of CCGT plants. For instance, the entire CCGT fleet of Spain was originally modeled as a single unit in ATLAS. Since this level of clusterization renders operating constraints very difficult to accurately represent, we separated the largest CCGT clusters amongst countries included in the RR simulations into smaller clusters for which the operating constraints application would be less of an approximation.

	Thermal							Hydraulic		Storage			Wind		Solar		Other non dispatchable			
Area	CCGT	OCGT	Gas other	Oil	Coal	Lignite	Nuclear	ROR	Reservoir	Batteries	PHS	Electric Vehicle	Onshore	Offshore	Photovoltaic	Thermodynamic	Waste	Biomass	GeoThermal	Other
AT	2824	40	1501	168	0	0	0	7800	6300	0	3159	[21-54]	4478	0	3054	0	57	331	0	0
BE	6436	294	2109	158	541	0	0	100	0	0	1395	[49-104]	4611	4253	11004	0	20	300	0	0
CH	0	0	660	0	0	0	2565	3800	8200	0	3989	[26-55]	255	0	5500	0	0	0	0	555
CZ	1310	0	1140	14	0	4981	4055	1000	1100	0	0	[42-90]	960	0	3936	0	13	490	10	0
DE	18860	2932	18749	841	8968	9562	0	4200	2900	0	7811	[231-493]	81501	21093	91300	0	0	4086	0	251
DKe	39	62	110	633	1248	0	0	0	0	0	0	0	752	1963	2143	0	0	19	0	0
DKw	523	169	290	209	363	0	0	0	0	0	0	0	4072	3365	3151	0	3	71	0	0
ES	24501	0	3980	0	0	0	3041	7100	10100	0	8465	[196-419]	48350	200	38404	7300	0	0	0	1050
FR	6692	649	4197	990	0	0	59400	7400	8400	470	3800	[248-624]	33201	5200	35100	0	251	377	0	775
IE	1616	446	140	324	0	78	0	400	0	0	292	[20-44]	6000	3500	400	0	0	112	0	0
ITca	3283	223	20	0	0	0	0	0	0	0	800	0	1858	300	1078	0	0	114	0	0
ITcn	920	142	1240	0	0	0	0	307	821	0	0	[39-83]	232	0	5125	0	0	75	760	0
ITcs	5625	1029	1483	0	0	0	0	380	664	0	2538	[39-83]	3600	0	8508	0	0	199	0	0
ITn	22167	1019	3968	0	0	0	0	6025	7171	0	4205	[46-99]	150	0	24185	0	0	867	0	0
ITs	3539	503	1590	0	0	0	0	132	1091	0	450	0	6800	300	6346	440	0	293	0	0
ITsar	590	0	300	0	0	0	0	33	161	0	240	0	2176	300	2278	0	0	89	0	0
ITsic	2401	646	790	866	0	0	0	23	191	0	1158	0	3583	300	3600	440	0	55	0	0
LU	0	0	100	0	0	0	0	0	0	0	1310	0	428	0	280	280	13	31	0	0
NL	10339	794	3770	0	3381	0	486	0	0	0	0	[65-140]	7800	13257	27150	0	0	0	0	216
NOm	0	0	20	0	0	0	0	0	4931	0	±84	0	2106	0	0	0	0	0	0	0
NOn	0	0	200	0	0	0	0	0	5540	0	±1	0	2567	0	0	0	0	0	0	30
NOs	0	0	50	0	0	0	0	0	24000	0	1030	[19-41]	3091	0	1500	0	35	2	0	0
PL	5001	0	6400	0	12164	7434	0	600	400	0	1495	0	10199	3600	7737	0	72	914	0	431
PT	2839	0	780	0	0	0	0	1300	6700	0	3554	[58-123]	9304	287	9383	334	64	320	16	381
SE1	0	90	0	0	0	0	0	0	5315	0	0	0	5719	0	17	0	2	127	0	0
SE2	0	54	0	0	0	0	0	0	6795	0	0	0	6622	0	200	0	5	461	0	0
SE3	0	1010	0	0	0	0	6835	0	1972	0	0	[54-114]	3938	979	3005	0	297	1640	0	0
SE4	0	501	0	660	0	0	0	0	237	0	0	0	2581	420	1125	0	58	509	0	0
UKgb	34688	2128	7487	335	3984	0	9281	1900	0	0	2744	[102-219]	15494	24826	16433	0	1504	824	6	1202
UKni	1001	12	10	389	0	0	0	0	0	0	0	0	2036	317	722	0	19	65	0	2

Table 2.9: Installed capacities in MW by generation type, for each area of the power system

2.C Appendix C - Liquidity results for each simulated day

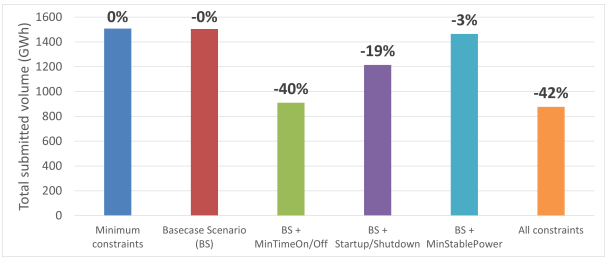

(a) Overall volume per scenario

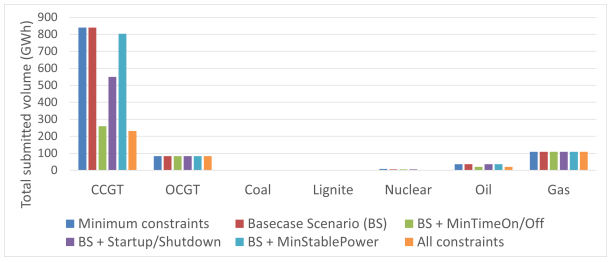

(b) Volume per scenario, for every fuel type

Figure 2.16: Volumes of upward RR orders formulated by thermal units per scenario for day A, in GWh

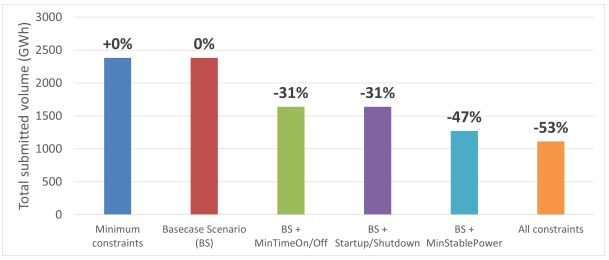

(a) Overall volume per scenario

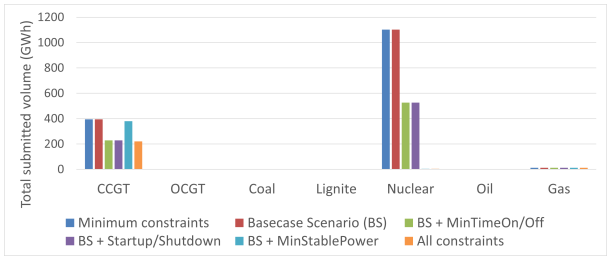

(b) Volume per scenario, for every fuel type

Figure 2.17: Volumes of downward RR orders formulated by thermal units per scenario for day A, in GWh

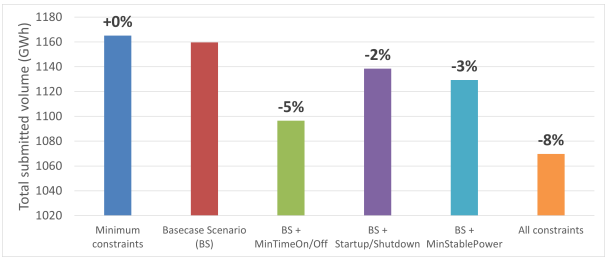

(a) Overall volume per scenario

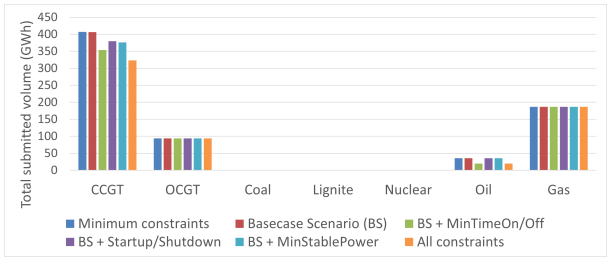

(b) Volume per scenario, for every fuel type

Figure 2.18: Volumes of upward RR orders formulated by thermal units per scenario for day W, in GWh

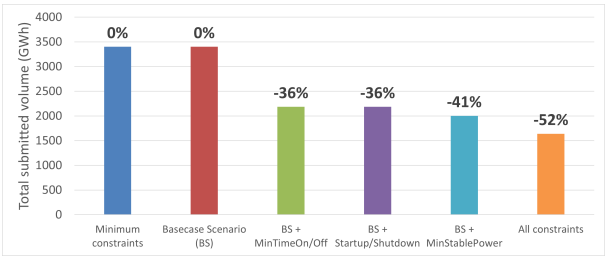

(a) Overall volume per scenario

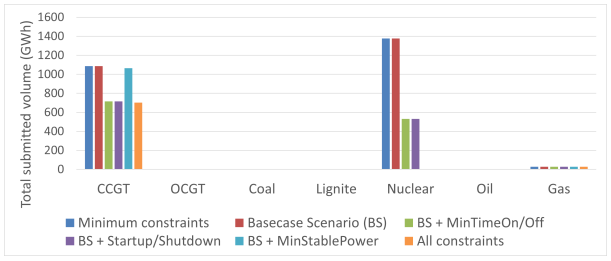

(b) Volume per scenario, for every fuel type

Figure 2.19: Volumes of downward RR orders formulated by thermal units per scenario for day W, in GWh

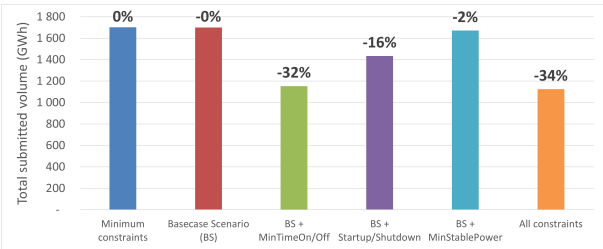

(a) Overall volume per scenario

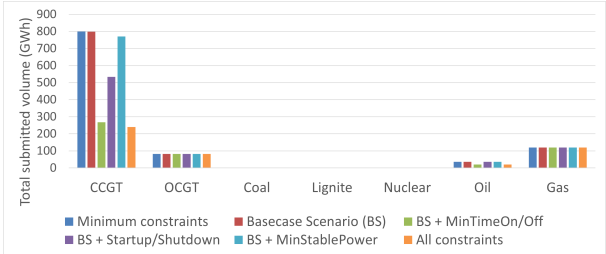

(b) Volume per scenario, for every fuel type

Figure 2.20: Volumes of upward RR orders formulated by thermal units per scenario for day S, in GWh

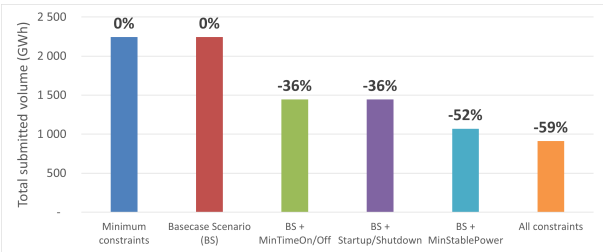

(a) Overall volume per scenario

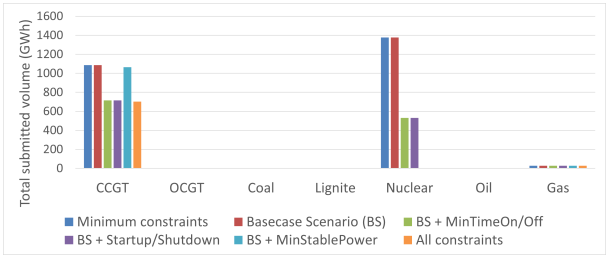

(b) Volume per scenario, for every fuel type

Figure 2.21: Volumes of downward RR orders formulated by thermal units per scenario for day S, in GWh

Chapter 3

Bidding strategies for Transmission System Operators on balancing markets

Contents

Abstract Common European balancing energy markets are progressively integrated into the wholesale electricity markets. These new types of markets differ from classic day-ahead and intraday markets on several levels. In particular, they include a new type of market actor: the Transmission System Operators (TSOs). While the bidding process of reserve providers on balancing markets is commonly studied and modeled in the existing literature, to our knowledge, a single article approached bidding strategies for TSOs. (Håberg and Doorman, 2017) proposed an opportunity costs-based bidding strategy, that relied on balancing market alternatives. In other studies, the TSO demand is always considered to be price-inelastic. This chapter challenges this assumption, leading to 4 main contributions. It first provides an empirical analysis of the operational RR balancing market using the example of the French TSO RTE, which emphasizes that TSOs are not price-inelastic in practice. The analysis of the possible RR market alternatives is then deepened, and a new category of alternatives is identified. Building on the opportunity cost-based method, we propose a new bidding method adapted for TSOs on the RR market that integrates balancing needs volume uncertainty. This method also considers different types of RR market alternatives, for which specific opportunity cost functions are used. Finally, the performance of the different bidding methods (price inelastic, basic price elastic and price elastic with volume uncertainty) are compared through a case study on the ATLAS electricity market model. We illustrate the types of demand curves created, their impact on RR market performances, and their benefits in terms of balancing costs. Results show that cost reductions can be achieved by using correctly tuned bidding methods, and advocate for further research on this topic.

Acknowledgements: A first version of this chapter was published at the 2023 19th International Conference on the European Energy Market (EEM) (Cogen et al., 2023). It has been significantly reworked in the manuscript.

3.1 Context

The balancing activation stage of the European power system is currently undergoing a profound transition. It was historically operated locally by Transmission System Operators (TSOs), who are in charge of maintaining the balance between supply and demand at all times in their own area. To improve economic efficiency (Van der Veen et al., 2010 and Akbari-Dibavar et al., 2020) and to allow better integration of Renewable Energy Sources (RES) by providing an adapted and transparent market design (Hirth and Ziegenhagen, 2015), the European Commission decided to harmonize the balancing stage with the creation of 4 standard types of balancing reserves. Among these types, 3 stand out as they will be part of new common European energy markets:

- The automatic Frequency Restoration Reserve (aFRR), which is activated automatically in under 5 minutes on the cross-border platform PICASSO.
- The manual Frequency Restoration Reserve (mFRR), which is activated manually under 15 minutes on the cross-border platform MARI.

- The Replacement Reserve (RR), which is activated manually under 30 minutes on the cross-border platform TERRE.

On these activation markets, two main categories of actors can be distinguished: Balancing Services Providers (BSPs), which make both upward and downward reserve offers, and TSOs who submit balancing needs. Offers and needs (referred to together as market orders) are then cleared and activated using a common merit order method, and all actors are remunerated or required to pay according to the marginal clearing price. This chapter focuses on the RR market, whose design has been detailed in Section 1.3.

The distinction between both types of actors is important. Indeed, as the introduction of the manuscript hinted at, TSOs are a new type of actors in common electricity markets. Consequently, when looking at the literature on the bidding behaviors of market actors in balancing markets, a clear discrepancy arises between BSPs and TSOs. While the strategies of BSPs are studied by a wide variety of articles, to our knowledge, the question of TSO bidding behavior has only been approached by a single article (Håberg and Doorman, 2017). Since this article, this topic has not been further studied, and the behavior of TSOs has always been modeled as price-inelastic. We believe that this assumption should be once again challenged.

Indeed, within sequential electricity markets, the RR market is followed by closer-to-real-time balancing processes, with overlapping delivery periods. These processes can be seen by the TSOs as *alternatives* to the RR market in that any imbalance remaining after a given RR market can be managed by future alternative processes. TSOs can then rely on arbitrages with alternatives to estimate opportunity costs on the RR market, which can be translated into prices for their RR balancing needs. This is especially relevant for TSOs using a proactive strategy, as one of their main objectives on the RR market is to compensate for forecasted future imbalances (see Section 1.2.1 for the differences between proactive and reactive strategies).

(Håberg and Doorman, 2017) proposed a method using the aforementioned concepts of alternatives and opportunity costs to create TSO demand curves the RR markets, but also detailed a number of complicating issues that should be addressed:

1. The existence of several types of alternatives to the RR market.
2. The temporal resolution of TSO balancing needs, which was assumed to be one hour in the article.
3. The uncertainty on the volume of balancing needs forecasted by the TSO.
4. The complexity of estimating the opportunity costs of an alternative, stemming from (i) the limited information on the supply side of future markets, and (ii) the complexity of balancing energy markets, especially the order complexity presented in the General introduction (Section 1.3.2.1).

In addition, this article did not provide an application of the proposed bidding method, which could evaluate its impact on balancing performance.

Building on their work, this chapter aims to study the following research questions: How can we improve TSOs' bidding methods on balancing energy markets? And what are the impacts of such methods on market outcomes and balancing costs?

By investigating these questions, this work contributes to the literature in four main ways:

- We conducted an empirical analysis of the orders formulated by the French TSO on the RR market over 2021 and 2022. It provides statistics and examples of demand curves formulated, emphasizing the interest of studying the price elasticity of TSO demands.
- Possible alternatives to RR markets are discussed in detail. We argue that a possible alternative to RR markets was not considered by (Håberg and Doorman, 2017): historical balancing processes. An extension of the previous empirical analysis studies the reliability of this new alternative type, through the example of the historical French balancing process. It indicates that this process is still stable enough to be considered a relevant alternative for the French TSO.
- We propose a framework for TSO bidding strategies on the RR market that addresses the complicating issues previously mentioned. It notably integrates volume uncertainty of balancing needs, and considers different types of alternatives.
- A case study is performed, using the ATLAS electricity market model. We compare the performance of our proposed volume uncertainty method to both the usual price-inelastic assumption and the method proposed in (Håberg and Doorman, 2017), for two different alternative types. Results demonstrate the benefits in balancing costs of our proposed bidding strategy. They also highlight the importance of an adequate alternative cost estimation, by showing that a poor estimation can have a significant impact on the performance of price-elastic strategies.

This chapter is then divided into 4 sections. In Section 3.2, a literature review shows the scarcity of articles looking at TSO bidding strategy. It is complemented by an empirical analysis of the RR market, highlighting the price elasticity of TSO balancing demands on actual RR markets. The different types of RR market alternatives are discussed in Section 3.3. Section 3.4 examines the existing literature on bidding strategies for actors in sequential electricity markets, and extracts relevant concepts used to integrate volume uncertainty in TSO bidding curves on RR markets. The ATLAS model and the study case methodology are described in Section 3.5. Finally, Section 3.6 provides and discusses the study case results.

3.2 TSO bidding strategies on balancing energy markets: literature review and empirical evidence

3.2.1 Literature review of bidding strategies for actors on balancing energy markets

The strategic behavior of BSPs resulting from the sequential state of short-term electricity markets is studied in a wide variety of articles, mainly from a theoretical point of view. (Guo et al., 2022) looks at bidding strategies of generation companies on the day-ahead market are studied. (Silva et al., 2022) explores the bidding processes of renewable energy assets in both day-ahead, intraday and balancing markets, while (Pei et al., 2016) focuses on microgrids in real-time markets.

Empirical research has also been conducted, such as in (Just and Weber, 2015) where strategic behavior of German BSPs is observed between 2006 and 2011, or in (Ocker and Ehrhart, 2017) where authors study

the influence of a new intraday market design on the German balancing process, and how BSPs progressively adapted their bidding strategies to this evolution over several years.

In addition, the impacts of transitioning from local, historical balancing processes to common balancing markets on BSP strategic behavior have been analyzed in multiple articles. (Poplavskaya et al., 2020) uses the Elba-ABM agent-based model to simulate aFRR markets under different combinations of assumptions regarding the pricing type (pay-as-bid and marginal), the overall market design (the historical process compared to the proposed aFRR market), the number of BSPs, and finally their bidding behavior. Two bidding strategies are compared, one that reflects true balancing costs and the other where each actor seeks a profit maximization by taking into account past aFRR prices using a Q-learning reinforcement algorithm. In the subsequent article (Poplavskaya et al., 2021), authors study how allowing BSPs to formulate voluntary bids on aFRR energy markets (meaning offering energy outside of previously procured capacity) impacts their bidding strategies, and concludes that this design rule encourages BSPs to bid at their true costs.

In contrast, the behavior of TSOs in balancing markets seems to be a rather unexplored topic. (Marneris et al., 2019) focus on the Greek central dispatch system, and study the role of the associated TSO in the RR market. In this type of system, the TSO has to compute both its balancing demands and the reserve offers of all units in its area on balancing markets. This article deals with the second aspect, especially on the integration of units' operating constraints in the formulation process; it does not look at the formulation process of TSO balancing needs. (Fedele et al., 2020) extend this study to the Italian system, which is also functioning as a central dispatch, and more specifically detail the adaptations required to formulate balancing orders on the mFRR market for units in the Italian area. This article also does not address the formulation of TSO balancing needs.

To the authors' knowledge, the only article looking at this topic is (Håberg and Doorman, 2017), which was presented in the introduction. It was published in 2017 and since then, the formulation process of TSOs has not been further studied, and their demand is always modeled as price inelastic. In the meantime, the official launch of balancing energy markets occurred (in 2020 for the RR market, and in 2022 for both mFRR and aFRR markets). One could then wonder whether TSOs are price-inelastic in actual RR markets, and if not, whether they submit demand curves, similar to the method of (Håberg and Doorman, 2017).

3.2.2 TSO price-elasticity on actual RR markets: empirical evidence

This section provides answers to the previous questions, first using results from recent market reports published by ENTSO-E[1], then complemented by an empirical analysis that we conducted on operational RR markets.

Evidence from ENTSO-E market reports

The ENTSO-E balancing report (ENTSO-E, 2022) presents analyses of balancing markets empirical data for 2021. Figure 3.1, taken from this report, indicates the share of TSO balancing needs submitted as price-inelastic versus that submitted as price-elastic on the RR market. We can see that every TSO formulated more than 90% of their demand as price elastic.

[1]ENTSO-E is the association gathering European TSOs for a coordinated view of the power system

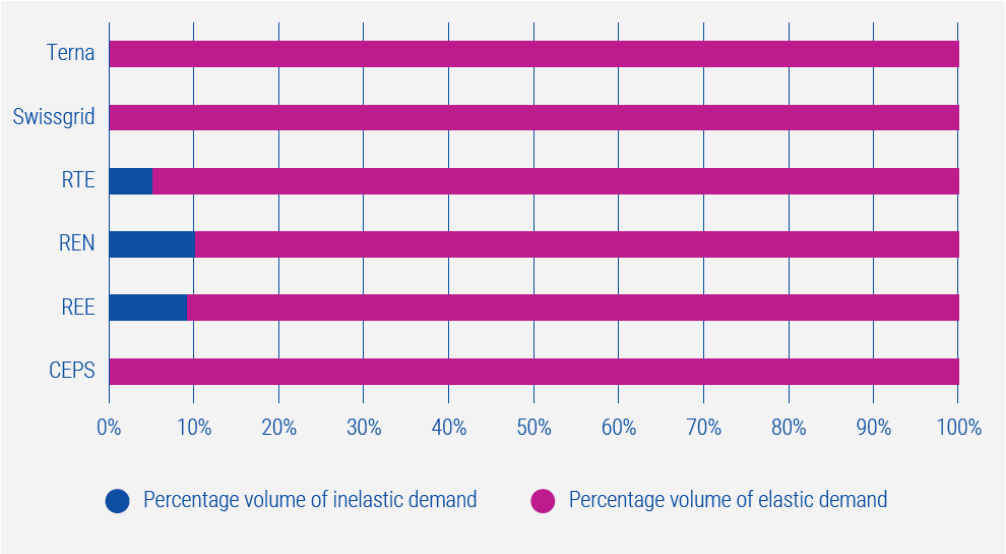

Figure 3.1: Share of price-inelastic versus price-elastic TSO demand on RR markets over 2021. From ENTSO-E, 2022, Figure 44 of Section 5.4

This observation is even stronger in the market report published the following year (ENTSO-E, 2023b), as it can be seen in Figure 3.2 that almost all TSOs exclusively formulate elastic demands over 2022 (RTE being the TSO that formulate the most inelastic orders, only approximately 5% of the time).

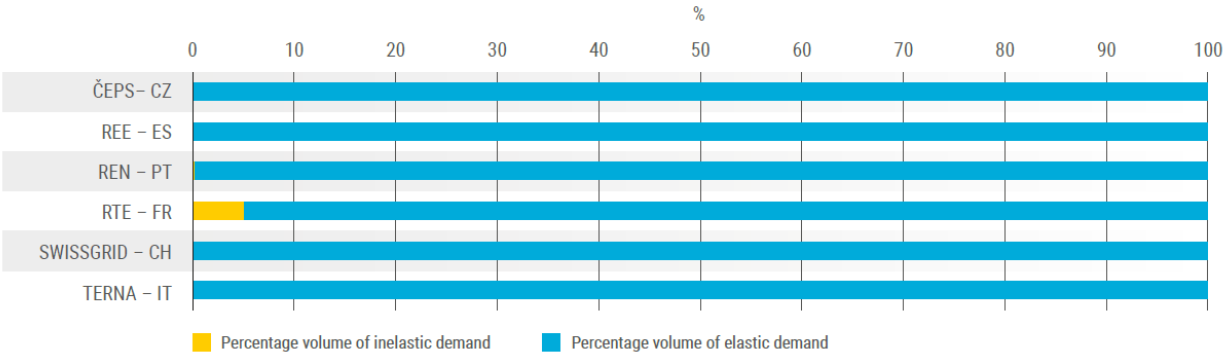

Figure 3.2: Share of price-inelastic versus price-elastic TSO demand on RR markets over 2022. From ENTSO-E, 2022, Figure 6.3.4.6

Results are stricking: TSOs should definitely be considered as price elastic on the RR market.

Empirical analysis of operational RR markets

ENTSO-E's market reports indicate that TSOs are price-elastic in practice, but do not provide additional information about the prices or the shape of these TSO demands. In this section, we deepen the first results of these reports, using data from actual RR markets published by RTE on their public data portal[2]. The other participating TSOs were not included in this empirical analysis due to a lack of publicly available data.

[2]Available at https://www.services-rte.com/en/download-data-published-by-rte.html, in category Market and subcategory Balancing energy

First, the normalized price distribution of RTE's RR orders over 2021 and 2022 is represented in Figure 3.3. Upward orders (i.e. demands for additional energy) are plotted in red, while downward orders are in purple. It can be immediately noted that this distribution corresponds to a price elastic behavior, as order prices are relatively spread between -100 €/MWh and 1500 €/MWh. If the TSO was behaving in a price-inelastic manner, upward order prices would all be equal to the upper price cap of the TERRE platform (+10,000 €/MWh), and all downward orders would be priced at the lower price cap (-10,000 €/MWh). In some cases, upward orders are formulated at the price cap, which is represented by the spike in the distribution happening at +10,000 €/MWh. This matches the information from ENTSO-E's market reports, as RTE formulated price inelastic orders 5 to 10% of the time.

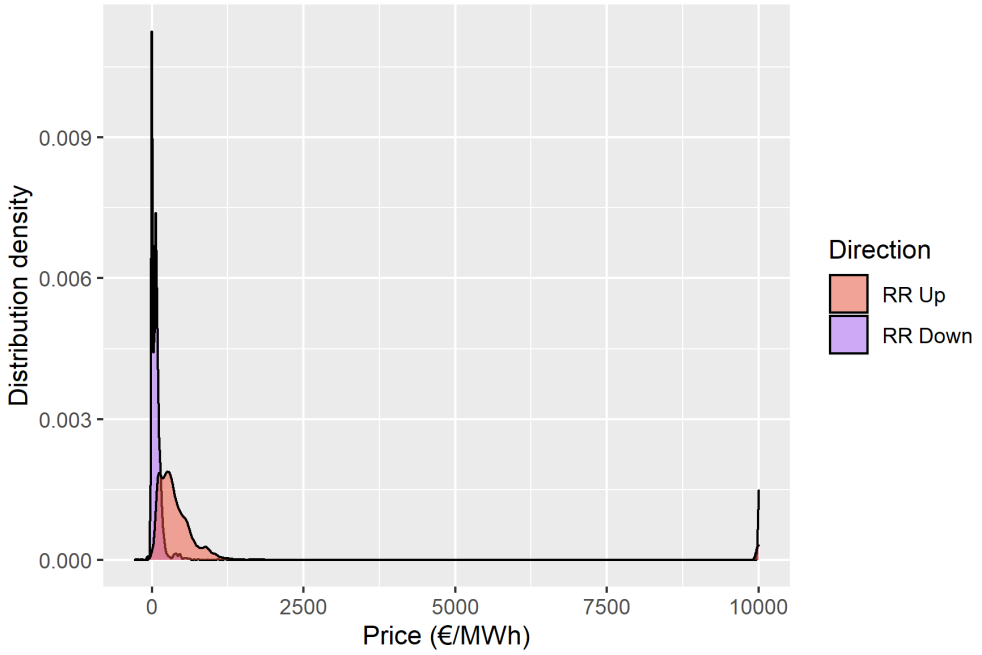

Figure 3.3: French TSO RR orders price distribution

In addition, Figure 3.4 plots the number of market orders formulated for a single time step by RTE over 2021 and 2022. As we can see, even if RTE formulated a single order for the majority of time steps across these two years, it did formulate multiple market orders for approximately 9% (resp. 3%) of time steps for which it had upward (resp. downward) balancing needs, effectively creating demand curves for these time steps.

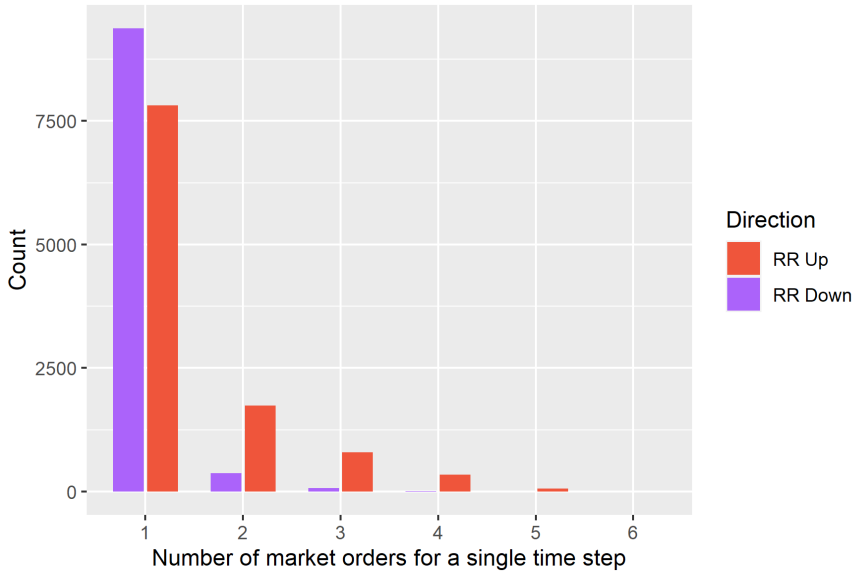

Figure 3.4: French TSO number of RR orders formulated for a single time step

These demand curves are illustrated in Figure 3.5a for upward orders, and Figure 3.5b for downward orders. The price amplitude within these demand curves is still relatively small, compared to the total range available: for time steps when 5 orders were formulated, the average price difference between the first order and the last order is 24.5 €/MWh.

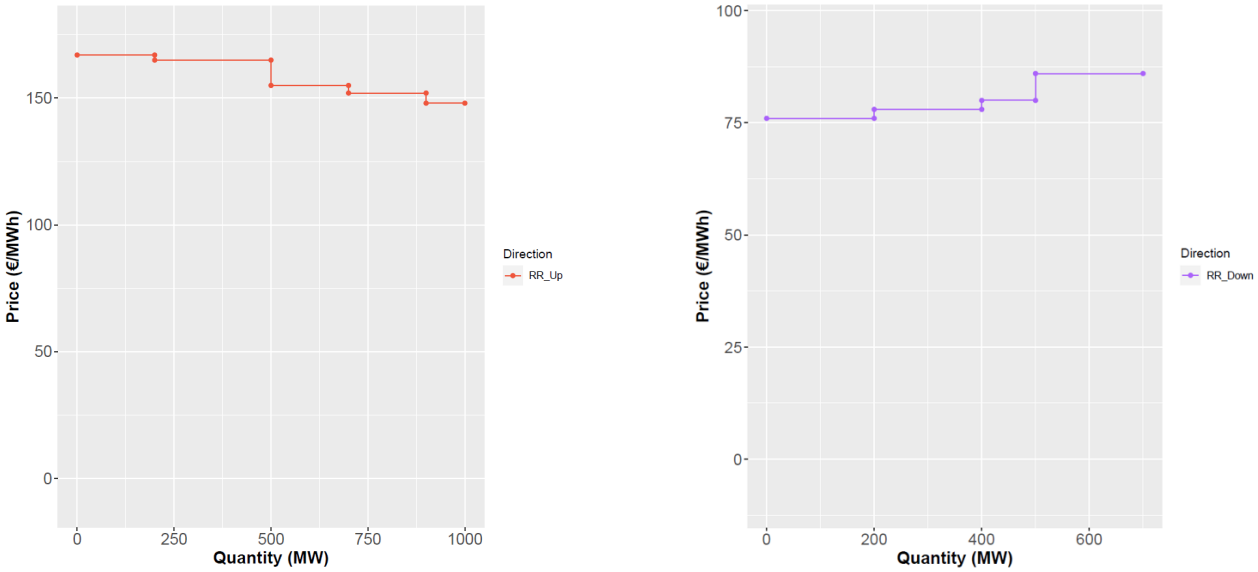

(a) Upward orders, 2022/01/09 at 10:15:00

(b) Downward orders, 2021/01/06 at 11:00:00

Figure 3.5: Examples of RR demand curves formulated by the French TSO

Finally, Table 3.1 summarises the acceptance state of all RTE's orders given their position in the demand curve. Despite the relatively tight price differences between them, a clear evolution can be observed and

demonstrates the impact of the curve formulation: the acceptance ratios are much lower for orders positioned further in the demand curve.

Position in bidding curve	Number of submitted orders	Ratio of fully accepted orders	Ratio of partially accepted orders	Ratio of rejected orders
First	20584	71%	18%	11%
Second	3400	49%	15%	36%
Third	1282	39%	12%	49%
Fourth	416	35%	15%	50%
Fifth	68	28%	19%	53%

Table 3.1: RTE's orders acceptance status

To summarize, empirical results emphasize that the usual price inelasticity assumption associated with TSOs should be challenged, as demand curves are already being formulated on RR markets similar to the suggestion of (Håberg and Doorman, 2017). Consequently, we aim to address the complicating issues presented in this article in the following sections.

3.3 Analysis of the different types of alternatives to the RR market

3.3.1 Discussion of the different alternative types

As explained in the introduction, TSOs can rely on alternatives to estimate their willingness to pay on the RR market. (Håberg and Doorman, 2017) noted that the existence of multiple types of alternatives is a complicating issue, as each alternative has its specific characteristics. Therefore, TSOs must be able to identify which ones can be considered relevant.

The current section details the different types of alternatives that can be considered, and discusses their relevance. In particular, it introduces local processes as a new category of alternatives, as it was not included in (Håberg and Doorman, 2017) which focused on common balancing markets. In the current European market structure, we then argue that two main categories of RR market alternatives can be distinguished:

- European common balancing energy processes, namely the mFRR and aFRR markets, and the FCR activation process. Figure 3.6 illustrates them in a timeline, which displays their delivery periods and their execution date[3]. These alternatives were already discussed in (Håberg and Doorman, 2017). The authors noted that, while FCR is a possible alternative, it should not be considered as such given that it would entail major safety risks. We also stand behind that point.

  Meanwhile, aFRR could be a viable alternative, depending on the philosophy of each area. It seems reasonable in areas that rely heavily on this type of reserve for their balancing (i.e. with reactive strategies, such as Germany or Belgium, see Section 1.2.1 of the manuscript introduction). In these areas, the large procured capacities and pool of orders would usually be sufficient to cover for balancing

[3]The execution date of aFRR markets is not represented, as it is a nearly continuous market that is cleared every 4 seconds.

needs not accepted on the RR market. In areas with proactive strategies, however, the aFRR is usually tightly sized. Considering it as an alternative seems more questionable in that case, as a possible shortage of aFRR could lead to costly last-resort actions, such as load shedding.

Finally, there is a larger pool of mFRR reserves in Europe. The mFRR market will also gather most European areas in the near future (see Section 1.3.1 of the general introduction), which supports its availability.

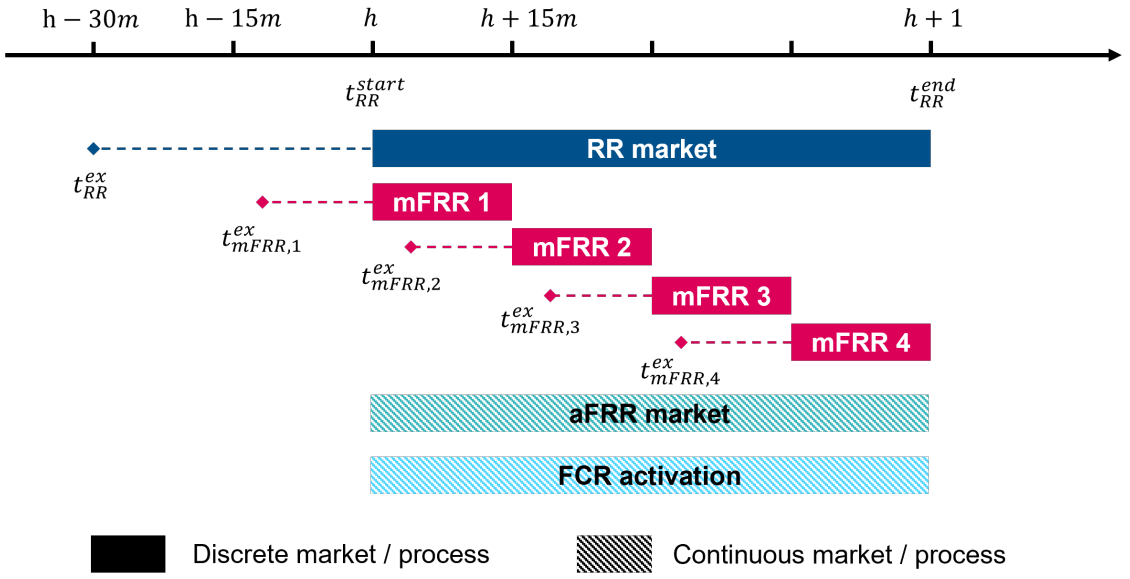

Figure 3.6: mFRR, aFRR and FCR alternatives timeline

- Local processes, illustrated in Figure 3.7 with the example of the French area. They notably include the historical balancing processes, such as the French Balancing Mechanism (FrBM) which is currently still being used in France alongside common markets. The reliability of historical balancing processes as an alternative can be questioned, as they “compete" with common balancing markets. Indeed, if all the available capacity in an area is submitted and accepted on common balancing processes (such as RR or mFRR markets), the local process might experience a reserve shortage. This question is addressed for the French local process in Section 3.3.2.

Finally, voluntary and involuntary load shedding could also be considered as alternatives. However, similar to the FCR case, both would probably be socially unacceptable or extremely expensive[4], so they are not recommended.

[4]The value of loss varies across areas and between studies, but is usually in the range of 10,000 to 30,000 €/MWh. Hence, it is above the price caps of the RR market: using it as an alternative would result in formulating price-inelastic needs.

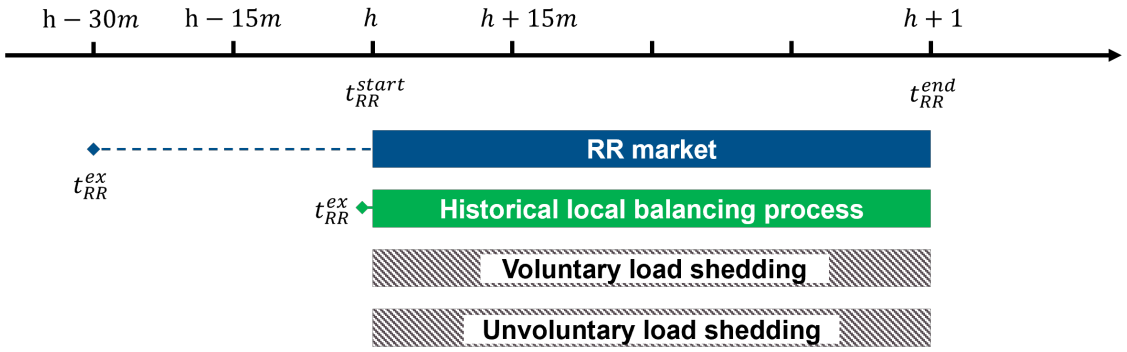

Figure 3.7: Local alternatives timeline

This chapter focuses on the proactive point of view. Given the previous discussion, this narrows the choice of possible alternatives to two: the mFRR market, and the local balancing process. Ideally, a TSO should consider a combination of all the relevant alternatives during its cost opportunity estimation. In this work, we will only consider each one independently, but their combination could be studied in the future.

3.3.2 Reliability of the French Balancing Mechanism as an RR market alternative

This section analyzes the French Balancing Mechanism (FrBM) as a reliable alternative to RR markets for the French TSO. As presented in the previous section, the FrBM can be executed between the last RR market and real-time. It is then necessary to verify that the volume of reserves available on the FrBM is still sufficient and relatively stable. To achieve this, two different indicators are compared over 2022:

- The volume of RR market orders formulated by all French BSPs, in both upward and downward directions. This data was extracted from the ENTSO-E Transparency platform.
- The capacity submitted by the same BSPs on the FrBM at most 40 minutes before real-time, to match the time frame of the RR market. Since all French BSPs are required to transmit their entire available capacity to the FrBM, this gives a relevant approximation of the theoretical maximum volume that could have been submitted on the RR market[5]. This data was gathered from internal RTE sources.

Figure 3.8 plots the average value per time step of both indicators, for each month of the year as well as the yearly averages in dotted lines. It shows that, over 2022, the volume of RR upward (resp. downward) orders is approximately 50% (resp. 15%) of the volume that is eventually submitted on the FrBM, i.e. the theoretical volume that could have been submitted on RR markets. In addition, despite the monthly variations of volumes submitted–with notably a clear seasonal impact during the summer–, this ratio of capacity submitted on RR markets versus the total available capacity stays relatively stable throughout the year.

[5]As presented in the general introduction of the manuscript (Section 1.2.3), the BSP capacity available on the FrBM is calculated by RTE. This is why we refer to this quantity as an *approximation* of the total volume available on the RR market.

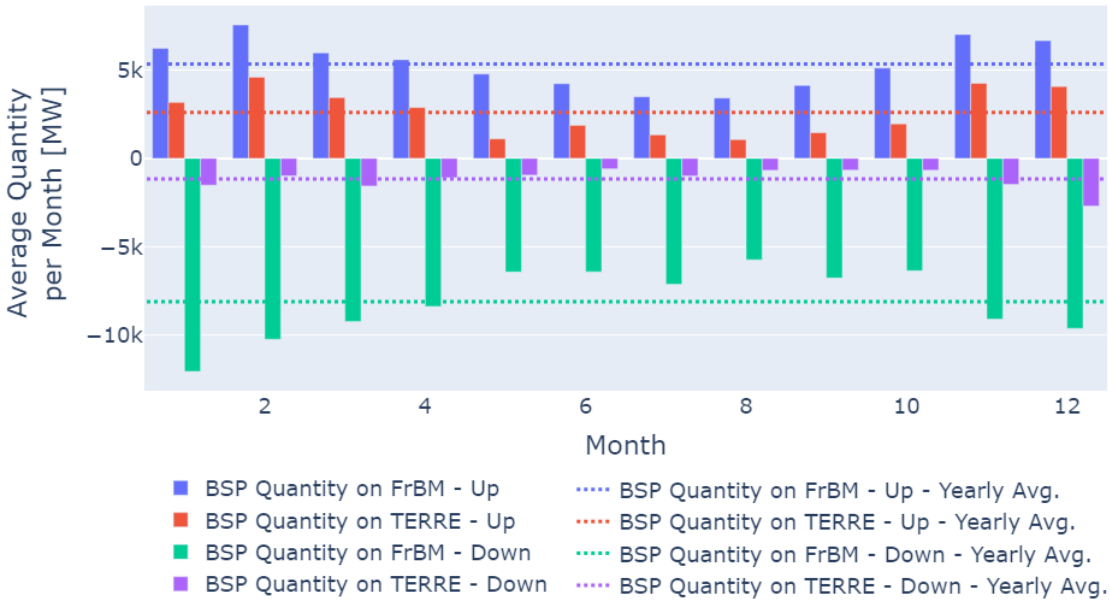

Figure 3.8: Comparison of BSP volumes submitted on the RR market and the French Balancing Mechanism

The share of available capacity directly submitted to the FrBM is significant, and its stability over the entire year indicates that the FrBM can currently be considered a reliable alternative for the French TSO.

Finally, it is also relevant to question the durability of this alternative. Indeed, the balancing stage is currently still in transition. We could imagine that local balancing processes would be stopped, or that all BSPs would eventually submit their entire available capacity to the RR market.

First, a European phase-out from local balancing processes does not seem on the agenda in the short term. To investigate the durability of the observed BSP behavior, the main question that arises is then the following: what are the reasons that cause this large proportion of French BSPs' available capacity to not be submitted on RR markets? And can we expect this situation to remain the same in the future?

We identified three reasons that could lead to the observed lack of RR orders, which are discussed in detail in Appendix 3.A:

- BSPs could still be progressively entering the RR market, which would be plausible since it was only launched in 2020. However, Section 3.A.1 discusses this possibility and shows that there is no sign of an increase in French BSP participation over 2022.
- It could be a choice directly driven by market prices, in the case where the FrBM is on average more profitable than the RR market for BSPs. However, comparisons of the prices of both processes (Section 3.A.2) indicate that this does not seem to be the case in practice: a BSP would make more profits on average by offering its capacity on the RR market.
- Finally, the complexity of balancing market processes and the potential required investment costs could be refraining French BSPs from participating in the RR market. This idea is discussed in Section 3.A.3.

To summarize, there is currently no sign that the reliability of the FrBM as an RR alternative will change in the short term. Overall, using the example of the French area, this empirical analysis illustrated how local balancing processes–that are currently still running alongside common balancing markets–could be considered relevant balancing market alternatives.

3.4 Creation of TSO need curves on balancing markets

In the previous section, we discussed the multiple types of alternatives to the RR market, which is one of the complicating issues raised by (Håberg and Doorman, 2017). In this section, we aim to address the complicating issues directly related to the TSO balancing need formulation process, by proposing a novel TSO bidding framework on the RR market (Figure 3.9).

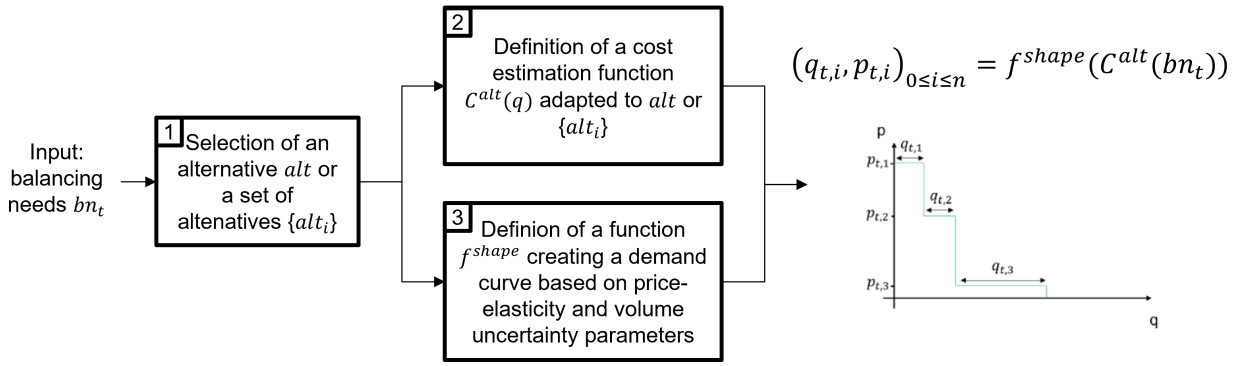

Figure 3.9: Framework for TSO RR bidding

In (Håberg and Doorman, 2017), the TSO directly deduces its RR bidding curve from its forecast of the supply curve of the mFRR market. However, the authors noted that this forecast may be difficult in practice, notably because a local TSO lacks information about the state of power systems in other areas. Our proposed framework differs from this method in the following ways:

- Several types of market alternatives can be chosen (step 1).
- A novel approach to the estimation of opportunity costs is considered, as it depends on the type of alternative chosen (step 2).
- The shape of the bidding curve is determined not only by the cost estimation of step 2, but also by a function f^{shape} that integrates volume uncertainty concerning the TSO balancing needs (step 3).

As previously mentioned, we choose to look at the mFRR market and the FrBM independently, which settles step 1 in our case. We then model specific cost estimation functions for each: since they need to be adapted to the simulation context, we detail them in the case study methodology (Section 3.5.5). In the rest of the current section, we focus on the integration of volume uncertainty in the formulation process (step 3), by defining the function f^{shape} in several cases.

To do so, we first propose an extension of our literature review, by focusing on the integration of volume uncertainty in bidding methods for usual actors on sequential electricity markets (Section 3.4.1). Section 3.4.2

then describes the implementation of the usual price-inelastic method, the method developed in (Håberg and Doorman, 2017) and our proposed method with volume uncertainty.

3.4.1 Current state of the art: bidding strategies on sequential electricity markets with volume uncertainty

A wide range of studies look at the bidding strategies for actors (owners of generation units or retailers) participating in sequential electricity markets. First of all, we can note that using arbitrage between different markets to compute opportunity costs is a common practice in these articles. This is for instance studied in (Poplavskaya et al., 2021), where opportunity costs are explicitly defined in the bidding process of BSPs that participate in the day-ahead market and in both aFRR capacity and energy markets. In this article, the aFRR capacity market occurs before the day-ahead market. Consequently, when BSPs bid a given quantity on the capacity market, they set their price by estimating the opportunity costs of not being able to bid this quantity on the day-ahead market. Similar inclusion of opportunity costs between day-ahead and balancing markets can be found in (Just and Weber, 2015) and (Ocker et al., 2018) which are focusing on the German system, or by (Boomsma et al., 2014) in the Nordic area. It is then relevant to apply the same concepts to TSOs in the RR market.

In addition, bidding strategies for retailers or generation units relying on power forecasts (mainly wind and photovoltaic assets) have been studied in several articles. We can exhibit similarities between these types of actors and pro-active TSOs bidding on balancing energy markets, when looking at the market order formulation process. Indeed, all of their market orders depend on the estimation of a certain quantity ahead of real-time: the consumers' load in the case of retailers, the expected generation in the case of wind or photovoltaic farms, and local imbalance in the case of pro-active TSOs. This quantity is continuously evolving with different forecast horizons, and eventually reaches a final value in real time. Any resulting deviation from volumes previously traded is then settled, which can induce benefits or costs for the associated market actor. This phenomenon is notably studied by (Zhang et al., 2012) who propose and compare three bidding strategies for wind power plants in the day-ahead market, based on forecasts of real-time market prices and on the distribution of power output forecast errors. Solutions to the profit maximization problem described in the article are then analytically computed. A similar problem was approached using fuzzy optimization in (Dukpa et al., 2010), and with a risk-constrained method in (Heydarian-Forushani et al., 2014).

The ability to extract an analytical solution to the profit maximization problem is tied to key assumptions made in the modeling of wind power plants: they are assumed to be price-takers on wholesale markets, which is justified by their small scale. Consequently, real-time prices are independent of the bidding behavior of these plants, and are modeled by a random variable following a known distribution. This is a significant difference between usual market actors and TSOs. In this chapter, TSOs are assumed to be price-makers in balancing processes, because they represent an important part of the demand side and their number is relatively small in balancing markets (there are, for instance, only 40 different TSOs in Europe, and some of them are not participating in common balancing markets).

Finally, we note that risk aversion is studied with a wide variety of tools: shortfall costs are used for retailers in (Fleten and Pettersen, 2005); fuzzy optimization was used for wind power plants in (Xue et al., 2008) and (Dukpa et al., 2010); a combination of stochastic power forecasts and price scenarios are associated

with the Conditional Value at Risk (CVaR) in (Botterud et al., 2010) for wind power plants and in (Xu et al., 2015) for retailers. We did not include risk aversion in this first approach to volume uncertainty TSO bidding methods. Nonetheless, we believe that it could be an interesting component of the TSO bidding process and we are looking to include it in future work. Indeed, TSOs are legally in charge of maintaining the supply-demand balance in their area, and facing important costs or even load shedding in the case of extreme situations would damage their reputation and public trust. Consequently, amongst methods proposed by studies, it seems especially relevant to consider those that aim at limiting potential extreme losses–instead of maximizing profits on a given set of scenarios–in the TSO bidding process[6].

3.4.2 Definition of f^{shape} for different types of price-elasticity and volume uncertainty

In this section, key concepts extracted from the literature on bidding strategies presented in the previous section are applied to define the function f^{shape}. We place ourselves from the point of view of a given TSO in a control area aiming at formulating a set of demand orders o_i for time $t \in T_{RR}$ on an RR market executed at time t^{ex}_{RR}. Following our framework, it is assumed that the TSO has calculated its projected balancing needs bn_t, has chosen a given alternative alt and is able to estimate $C^{alt}(q)$, the cost of resolving the volume of imbalance q using alt. Its objective is now to compute a finite set of tuples $(q_{t,i}, p_{t,i})$ defined for $i \in \{1, \dots, n\}$, where n is the number of slices into which the total balancing needs are going to be divided. $q_{t,i}$ corresponds to the quantity of slice i, and $p_{t,i}$ to its price.

The price-inelastic bidding method, which is the usual way to represent TSO bidding in the literature, is presented in sub-section 3.4.2.1. It will be used as a first benchmark to evaluate the performance of our proposed bidding method. Then, a price-elastic method similar to the one proposed by (Håberg and Doorman, 2017) is described in sub-section 3.4.2.2, creating demand curves solely based on opportunity costs. Finally, sub-section 3.4.2.3 proposes a price-elastic strategy that takes into account volume uncertainty in addition to opportunity costs, with a methodology inspired by (Zhang et al., 2012).

3.4.2.1 Price-inelastic bidding

For a price-inelastic TSO, only one market order is formulated ($n = 1$) and the quantity/price couple associated is:

$$(q_t, p_t) = (|bn_t|, \sigma_t * 10,000) \tag{3.1}$$

Where σ_t is a binary that indicates the balancing need direction ($\sigma_t = 1$ if $bn_t > 0$, -1 otherwise). Here, the TSO submits its entire forecasted need at the maximum (resp. minimum) price permitted by the market, for an upward (resp. downward) balancing need. The absolute value of the balancing need is used, as the standard RR market order requires a positive value for the quantity submitted; the direction of the order is given by its characteristic σ_o.

[6]For instance, based on the results of (Xu et al., 2015), we would recommend the CVaR method instead of the VaR method because of its loss limiting properties.

3.4.2.2 Basic price-elastic bidding using opportunity costs

A price-elastic TSO can instead consider the opportunity costs stemming from possible alternatives to RR markets (either closer to real-time markets or local balancing process, as was discussed in Section 3.3.1). This is in line with the method proposed in (Håberg and Doorman, 2017).

In our case, we do not assume that the TSO can accurately predict the supply curve of the alternative. Consequently, we will consider that the size of each slice, i.e. the quantity of each market order, is set exogenously to a given value V_s. The only exception to this rule will be the "top" slice, so that the entire balancing need can be converted into market orders (an example of slice determination is given in Figure 3.10).

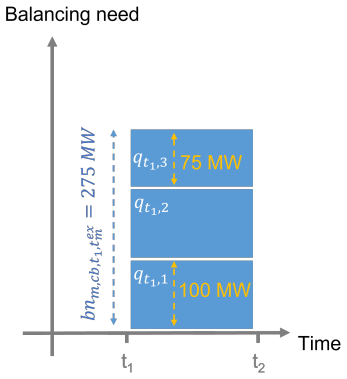

Figure 3.10: Example of need slices for the basic price-elastic bidding method with $V_s = 100MW$

The choice of maximum quantity defines the number of slices n at each time t, with Equations 3.2 and 3.3 linking the slice sizes with the overall need:

$$\forall t \in T, \ \ \forall i < n, \quad q_{t,i} = V_s \tag{3.2}$$

$$\forall t \in T, \quad \sum_{i \leq n} q_{t,i} = bn_t \tag{3.3}$$

With this hypothesis on slice sizes, the bidding strategy only revolves around the determination of the $p_{t,i}$ of a given slice of need i. This is realized by estimating the opportunity cost of resolving the stack, $St_{t,i} = \sum_{1 \leq j \leq i} q_{t,j}$, with its chosen alternative alt, which is given by the following equation:

$$\forall t \in T_{RR}, \ \ \forall i \leq n, \quad p_{t,i} = \sigma_t * \frac{C^{alt}(St_{t,i})}{St_{t,i}} \tag{3.4}$$

Where $C^{alt}(q)$ is the estimation of the cost of balancing quantity q using alternative alt.

3.4.2.3 Integrating volume uncertainty in the price-elastic bidding method

The bidding method proposed in this chapter uses the same general process as the basic price-elastic method: estimation of opportunity costs, and formulation of a bidding curve by dividing the total balancing need into slices. However, this method considers that the estimated volume of balancing needs is not certain, and could be under- or over-estimated. The volume uncertainty is represented by a forecast error function, similar to the method used in (Zhang et al., 2012). In this section, examples will be illustrated using a normal distribution for this function. However, our proposed method can accept any distribution as input, as it only relies on its quantiles. For instance, in our case study (Section 3.5), specific endogenous forecast error functions are computed according to the alternative type.

The general idea of this method is to create a bidding curve in which the size of each slice i is directly defined by the distribution quantiles, and its price integrates the costs of under- or over-estimation of needs in addition to the cost of the stack $St_{t,i}$. It is comprised of the following steps:

1. Determining the distribution of the error made by the TSO when forecasting its balancing needs between two different dates: the execution date of the RR market, and the execution date of its chosen alternative. This can be performed by using either real or simulated data, but it requires a large volume of forecasts in any case.

2. Using quantiles of this distribution to compute the size of each slice and the associated probability of occurrence. This step is illustrated in Figure 3.11, using an arbitrary normal distribution. Quantiles ϵ_i of probability $\alpha_i \in [0.1, \ldots, 0.9]$ are displayed, bounded by extreme quantiles ϵ_0 of probability $\alpha_0 = 0.01$ and ϵ_n of probability $\alpha_n = 0.99$ that will be used as references for outer bounds. In this example, n is arbitrarily set to 10 for clarity purposes, meaning that 9 quantiles are considered outside of the extremes. However, the proposed method can function for any value of n.

   The quantile i indicates that the real forecast error ϵ made by the TSO has a probability α_i of being below the associated quantity ϵ_i, and a probability $(1 - \alpha_i)$ of being above this value:

$$\forall i \in [0, \ldots, n], \quad P[\epsilon \leq \epsilon_i] = \alpha_i \tag{3.5}$$

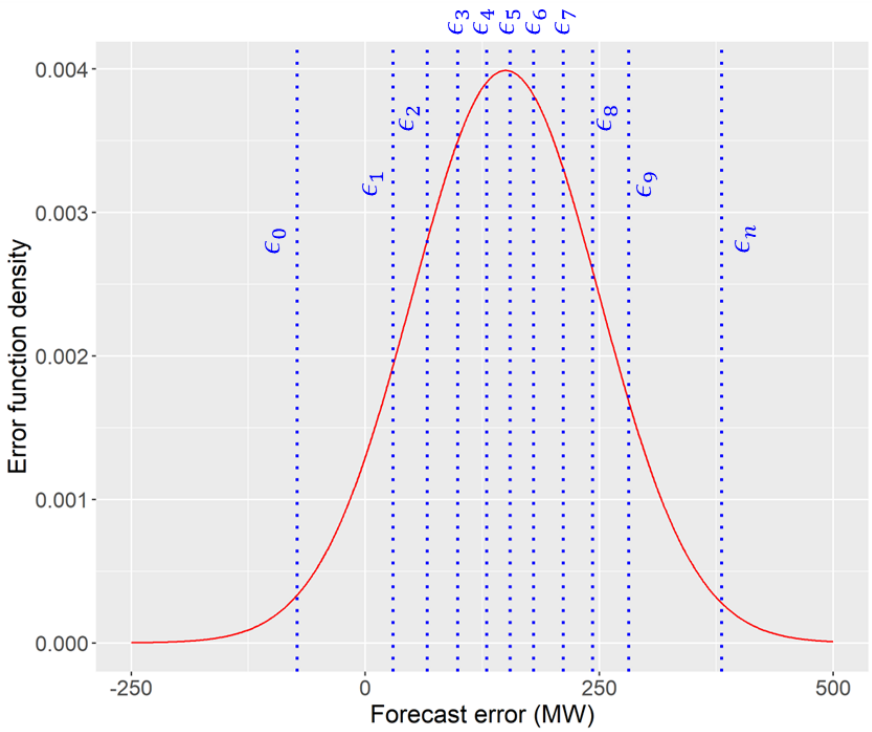

Figure 3.11: TSO forecast error distribution example (for readability concerns, we will note $i \in [1, \dots, 9]$)

Information carried by quantiles can then be translated into the quantity of each slice of need submitted to the RR market. If we look at a given forecasted balancing need in the upward direction ($bn_t > 0$), then $bn_t + \epsilon_i$ should give the imbalance that is likely to be reached with an α_i probability. However, depending on the values of bn_t and ϵ_i, this calculated imbalance volume can be in the opposite direction as bn_t. This makes sense from a practical point of view: if the forecasted imbalance is low (and/or if the margin of error is high), then there is a decent chance that the actual balancing need is eventually in the opposite direction. But it also introduces another layer of complexity when determining the volume of each slice, as it leads to 3 different cases:

- If $bn_t > 0$ and $bn_t + \epsilon_1 \geq 0$, then it is the simple case where the balancing need submitted is always positive, even when taking into account the possible forecast errors. In that situation, the first slice of need ranges from 0 up until $bn_t + \epsilon_1$. The quantity of every subsequent slice of need i is equal to the quantity between the two successive quantiles ϵ_{i-1} and ϵ_i.

$$\forall t \in T_{RR}, \;\; if \;\; (bn_t > 0) \;\; \& \;\; (bn_t + \epsilon_1 \geq 0),$$
$$\begin{cases} q_{t,1} = bn_t + \epsilon_1 \\ q_{t,i} = \epsilon_i - \epsilon_{i-1}, \quad \forall i \in [2, \dots, n-1] \end{cases} \tag{3.6}$$

- If $bn_t < 0$ and $bn_t + \epsilon_{n-1} \leq 0$, then this is the mirror case of the first one, with submitted needs

being always negative.

$$\forall t \in T_{RR},\ \ if\ (bn_t < 0)\ \ \&\ \ (bn_t + \epsilon_{n-1} \leq 0),$$
$$\begin{cases} q_{t,i} = \epsilon_i - \epsilon_{i+1}, \quad \forall i \in [1, \dots, n-2] \\ q_{t,n-1} = bn_t + \epsilon_{n-1} \end{cases} \tag{3.7}$$

- If $bn_t > 0$ and $bn_t + \epsilon_1 < 0$, or if $bn_t < 0$ and $bn_t + \epsilon_{n-1} > 0$, then some need slices submitted should be negative and other should be positive. It is then important to identify where submitted balancing needs shift from being negative to being positive when browsing through values of i, and between which consecutive slices it happens. Let's note these consecutive slices i_{s1} and i_{s2}, such that:

$$\begin{cases} \nexists\ i \in]i_{s1}, i_{s2}[\\ bn_t + \epsilon_{i_{s1}} < 0\ \ \&\ \ bn_t + \epsilon_{i_{s2}} > 0 \end{cases} \tag{3.8}$$

  As Equation 3.9 describes, for slices lower than i_{s1}, submitted balancing needs are always negative. For slices higher than i_{s2}, submitted balancing needs are always positive. Finally, slices i_{s1} and i_{s2} are dealt with in specific cases:

$$\forall t \in T_{RR},\ \ if\ \big(\ (bn_t > 0)\ \ \&\ \ (bn_t + \epsilon_1 < 0)\big)\ |\ \big(\ (bn_t < 0)\ \ \&\ \ (bn_t + \epsilon_{n-1} > 0)\big),$$
$$\begin{cases} q_{t,i} = \epsilon_i - \epsilon_{i+1}, \quad \forall i \in [1, \dots, i_{s1} - 1] \\ q_{t,i_{s1}} = \epsilon_{i_{s1}} \\ q_{t,i_{s2}} = \epsilon_{i_{s2}} \\ q_{t,i} = \epsilon_i - \epsilon_{i-1}, \quad \forall i \in [i_{s2} + 1, \dots, n-1] \end{cases} \tag{3.9}$$

3. Computing the price of each slice i, taking into account both the opportunity cost of the associated stack of needs $St_{t,i} = \sum_{1 \leq j \leq i} q_{t,i}$, and the potential costs of over-/under-estimation of balancing needs. If we still look at upward balancing needs bn_t for the sake of the explanation, the following reasoning is applied:

   - Opportunity costs associated with the volume of this stack of needs are directly given by the cost estimation function, and are equal to $C^{alt,up}(St_{t,i})$.
   - In addition, there is a α_i chance that the actual imbalance volume is lower than $St_{t,i}$, meaning that the TSO will have to compensate in the downward direction with its alternative if the market activates it. To be precise, the formula giving the expected cost of overestimation compensation $C^{alt,over}$ would be:

$$C^{alt,over}(St_{t,i}) = \int_0^{\epsilon_i} (\alpha_i - \alpha_\epsilon) * C^{alt,down}(\epsilon_i - \epsilon) d\epsilon \tag{3.10}$$

     Where α_ϵ is the probability of error ϵ. As this integral cannot be theoretically solved without any more information on the cost function C^{alt}, an approximation is used here and the associated costs are estimated at:

$$C^{alt,over}(St_{t,i}) = \sum_{0 \leq j < i} (\alpha_{j+1} - \alpha_j) * C^{alt,down}(\epsilon_{j+1} - \epsilon_j) \tag{3.11}$$

- On the other hand, there is a $(1-\alpha_i)$ chance that the actual imbalance volume is higher than $St_{t,i}$, meaning that the TSO would have to ask for additional upward power with its alternative. Similar to overestimation costs, underestimation costs are approximated at:

$$C^{alt,under}(St_{t,i}) = \sum_{i<j\leq n-1} (\alpha_j - \alpha_{j-1}) * C^{alt,up}(\epsilon_j - \epsilon_{j-1}) \tag{3.12}$$

By gathering all parts together, the price of slice i can be written in Equation 3.13:

$$\begin{aligned} &\forall t \in T_{RR},\ \ \forall i \in [1,\dots,n-1], \\ p_{t,i} = \frac{1}{St_{t,i}} * \Bigg[& C^{alt,up}(St_{t,i}) + \\ & \sum_{0\leq j<i} (\alpha_{j+1} - \alpha_j) * \ C^{alt,down}(\epsilon_{j+1} - \epsilon_j) + \\ & \sum_{i<j\leq n-1} (\alpha_j - \alpha_{j-1}) * C^{alt,up}(\epsilon_j - \epsilon_{j-1}) \Bigg] \end{aligned} \tag{3.13}$$

With

$$St_{t,i} = \begin{cases} \sum\limits_{1\leq j\leq i} q_{t,i} & if\ \ bn_t > 0 \\ \sum\limits_{i\leq j\leq n-1} q_{t,i} & if\ \ bn_t < 0 \end{cases} \tag{3.14}$$

3.5 Case study: Methodology

The previous section described a theoretical framework to formulate price-elastic TSO orders on RR balancing markets. To illustrate its practical implications and potential impact on market performances, simulations were conducted on the ATLAS electricity market model with the three pricing methods presented, and with two different alternatives: the FrBM and the mFRR market. This section provides an overview of the ATLAS model and describes the simulation framework and scenarios. Notably, it details the hypotheses taken for the cost estimation functions associated with each alternative, and the data used to compute forecast error functions for the volume uncertainty method.

3.5.1 Overview of the ATLAS electricity market model

ATLAS is an electricity market model, developed on the foundations of the OPTIMATE model (Maenhoudt and Deconinck, 2010). It aims at modeling close-to-reality day-ahead, intraday and balancing markets by integrating a wide range of technical constraints and by representing all the different steps of actual electricity markets. It has been previously used in the OSMOSE European project to investigate flexibilities in the power system (Kolkmann et al., 2019), and to study network constraints associated with balancing markets in (Girod et al., 2022). It is comprehensively explained in (Little et al., 2024) and (Cogen et al., 2024). The balancing stage of the ATLAS model represented in Figure 3.12 was developed in this thesis. The Balancing Mechanism module implemented in ATLAS is based on the French balancing process FrBM, which implies this process is taken as a reference for local balancing processes in all simulations done with ATLAS. This

chapter focuses on the TSO Orders Formulation module and consequently does not explain other modules of the balancing stage. Their exhaustive description is given in general Appendix A.

Figure 3.12: Macro overview of ATLAS balancing stage modules

The TSO Orders Formulation takes place in two main phases. The first phase is the computation of balancing needs $bn_{ca,t,t_m^{ex}}$ for each TSO associated with a control area ca, for time t seen from the execution time t_m^{ex} of a market m:

$$\forall ca \in CA, \ \forall t \in T_m, \quad bn_{ca,t,t_m^{ex}} = \sum_{u^l \in U_{ca}^l} |P^{for}_{u^l,t,t_m^{ex}}| - \Big(\sum_{u^g \in U_{ca}^g} P^{plan}_{u^g,t,t_m^{ex}} + \sum_{u^{RES} \in U_{ca}^w \cup U_{ca}^{pv}} P^{for}_{u^{RES},t,t_m^{ex}} \Big) \quad (3.15)$$

Where:

- $P^{plan}_{u,t,t_m^{ex}}$ is the generation (or consumption) plan of unit u at time t, seen from t_m^{ex}.
- $P^{for}_{u,t,t_m^{ex}}$ is the generation (or consumption) forecast of unit u at time t, seen from t_m^{ex}.
- U_{ca}^l the set of all load type units in control area ca.
- U_{ca}^w the set of all wind type units in control area ca.
- U_{ca}^{pv} the set of all photovoltaic type units in control area ca.
- U_{ca}^g the set of all generation units in control area ca.

These balancing needs are then converted into market orders in the bidding phase, which is developed based on the framework presented in Section 3.4. It includes the 3 different bidding strategies (price inelastic, basic price elastic and volume uncertainty price elastic). Finally, both RR and mFRR markets, as well as the local French balancing process FrBM can be simulated in the ATLAS balancing phase, which makes it able to consider either the mFRR market or the FrBM as an alternative to RR markets.

3.5.2 Study case input dataset

The input dataset is the same as the one used in Chapter 2. It is described in detail in Section 2.4.1, and is derived from RTE's report Energy Pathways to 2050 (RTE, 2022). A realistic and robust 2030 European power system was constructed for this report using the Antares adequacy simulator, and was then converted into ATLAS format. It includes 32 interconnected market areas (usually 1 for each country, with the exception

of Italy, Sweden and Norway which are divided into several market areas to match bidding zones of the actual system), each of them containing a specific composition of generation and consumption assets with a precise description of their operational constraints. The entire European system in Figure 3.13a was taken into account for both day-ahead and intraday market simulations, while the reduced version of Figure 3.13b was used for balancing market simulations[7].

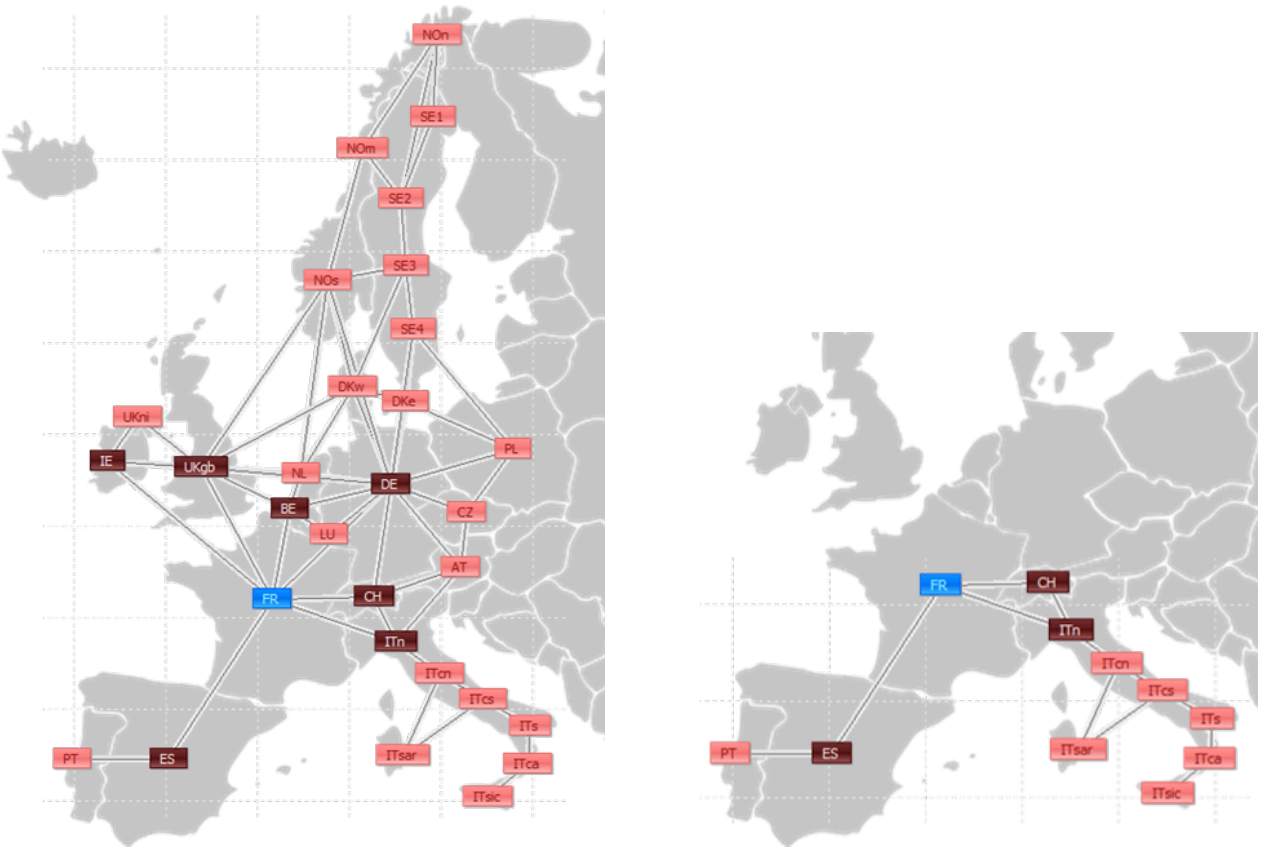

(a) Complete European power system

(b) Market areas included in RR market simulations

Figure 3.13: Map of the European power system in the 2030 representation in Antares / ATLAS used in this study

3.5.3 Scenarios and simulation framework

The objective of this case study is to compare several features of the TSO order formulation:

- Price-inelastic and price-elastic demand formulation.
- For price-elastic scenarios, the basic bidding method described in Section 3.4.2.2 and the bidding method that introduces volume uncertainty of Section 3.4.2.3.
- For price-elastic scenarios, two different types of alternatives: the FrBM and the mFRR market. The former is an approach that could currently be used by all TSOs that are not yet participating in the

[7]These areas correspond to the zones that are currently participating in the RR market. The exception is the Czech Republic, which is currently participating in the market but does not share any direct transmission line with other participants, hence having its own closed RR market. Consequently, this area was not included in our RR market simulations.

mFRR market, which began very recently. The latter is suited for TSOs that are participating in both RR and mFRR markets.

Table 3.2 summarizes all the different scenarios and their features. For computational time reasons, the various bidding methods were only applied to the French TSO. All other TSOs in the dataset are set to always be price-inelastic.

Scenario	Alternative	Demand elasticity	Formulation type
Inel_local	FrBM	Inelastic	-
FrBMalt_basic	FrBM	Elastic	Basic
FrBMalt_vol	FrBM	Elastic	Volume uncertainty
Inel_market	mFRR market	Inelastic	-
mFRRalt_basic	mFRR market	Elastic	Basic
mFRRalt_vol	mFRR market	Elastic	Volume uncertainty

Table 3.2: Summary of all scenarios

An entire day of electricity markets was then simulated using ATLAS (Figure 3.14). It is composed of a day-ahead market, followed by an approximation on an intraday market[8], setting the state of the power system for the core of the study. Based on this, 24 instances of RR markets followed by a post-RR market balancing process were simulated for all scenarios previously described. The role of the post-RR balancing process is to correct any remaining imbalance after the RR market. The type of process used is coherent with the alternative chosen for price-elastic scenarios. In addition, the price-inelastic scenario was balanced after the RR market using both processes, in order to serve as a valid comparison for all scenarios.

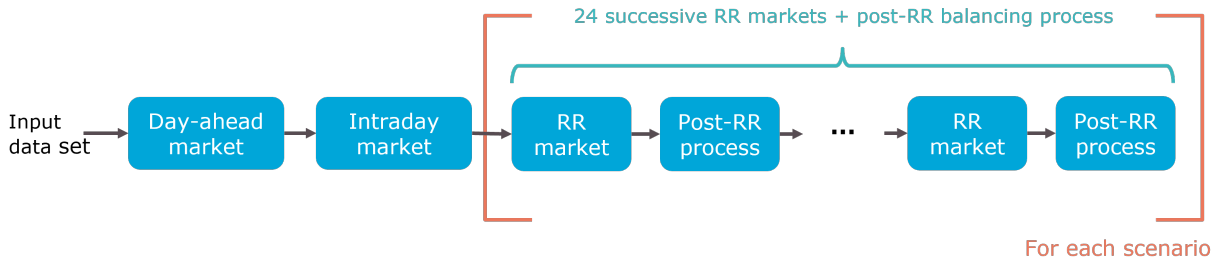

Figure 3.14: Simulations framework

The resulting execution timelines for every balancing sequence–RR market followed by the post-RR balancing process–are illustrated in Figure 3.15 (for scenarios using the FrBM as the post-RR process) and 3.16 (for scenarios using the mFRR market as the post-RR process):

[8]In reality, the intraday market is supposed to be continuous over the entire day. This feature is quite difficult to model in a simulation process, which is why the intraday market is modeled as a discrete market in ATLAS. In addition, a single intraday market was performed for each day of the simulation to limit computation time, as this is not the main focus of our study. This intraday market proxy however takes into account the system vision actors have 2 hours before real-time for each hour of the day.

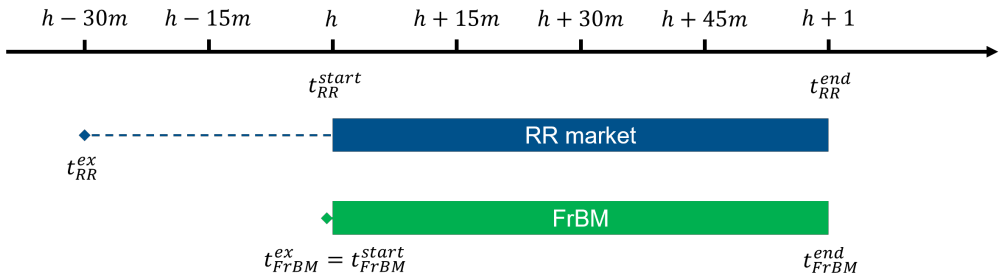

Figure 3.15: Timeline of the balancing sequence of scenarios with the FrBM process

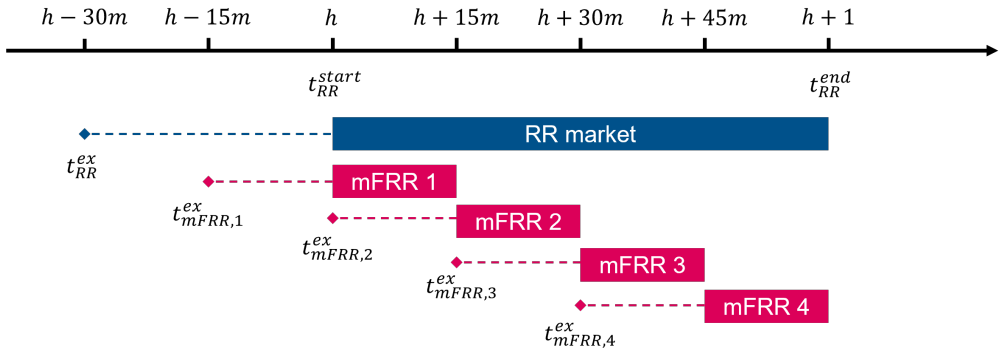

Figure 3.16: Timeline of the balancing sequence of scenarios with the mFRR market process

To further clarify the process, one can take the example of one sequence with the mFRR market alternative, focusing on actions made by the TSO:

1. The TSO formulates its RR balancing needs at t_{RR}^{ex}. During this process, it estimates the opportunity cost of its alternative, the mFRR market, for each time step of the RR market. This estimation is realized given the information available at t_{RR}^{ex} (generation and load programs, and forecasts of solar, wind and load assets).
2. The RR market is then immediately cleared.
3. The post-RR balancing process is applied, in this case the mFRR market. The 4 mFRR markets are then simulated with their respective execution date $t_{mFRR,i}^{ex}$. Consequently, these simulations take into account updated visions of the system.

These simulations also address the temporal resolution issue pointed out by (Håberg and Doorman, 2017): RR markets are simulated with a 15-minute time resolution, each of them being subdivided into 4 periods. RR market orders also follow the same resolution, which corresponds to the design of actual RR markets. Finally, all generation and consumption plans and all forecasts are performed at 15-minute time steps as well.

3.5.4 Hypotheses taken for f^{shape} functions

This section describes the input parameters chosen for the f^{shape} functions of both price-elastic bidding methods.

Definition of the exogenous maximum slice size for the basic price-elastic formulation

For scenarios using the basic price-elastic formulation, the only parameter of the f^{shape} function is the maximum size V_s of each slice. It is exogenously set at 200 MW. This value was chosen according to expert opinions in RTE, to produce a sufficient number of slices given the usual balancing need volumes, while keeping the computational time of the bidding process at a reasonable level.

Definition of the forecast error distribution functions for the volume uncertainty bidding method

For scenarios using the volume uncertainty formulation, the f^{shape} function relies on a distribution of the TSO forecast error function. As both RR alternatives are associated with different lead times (see Figures 3.15 and 3.16), specific error functions are computed for each one, based on forecast data available in our input dataset[9]. An entire year of forecast data is used in the computation process to ensure statistical relevance. Figure 3.17b gives the distribution and relevant quantiles for the error function of the FrBM alternative, between the execution date of the RR market and that of the FrBM. Figure 3.17a displays the same information for the error function of the mFRR alternative, between respective execution dates of RR and mFRR markets. The values of all quantiles are indicated in Table 3.3.

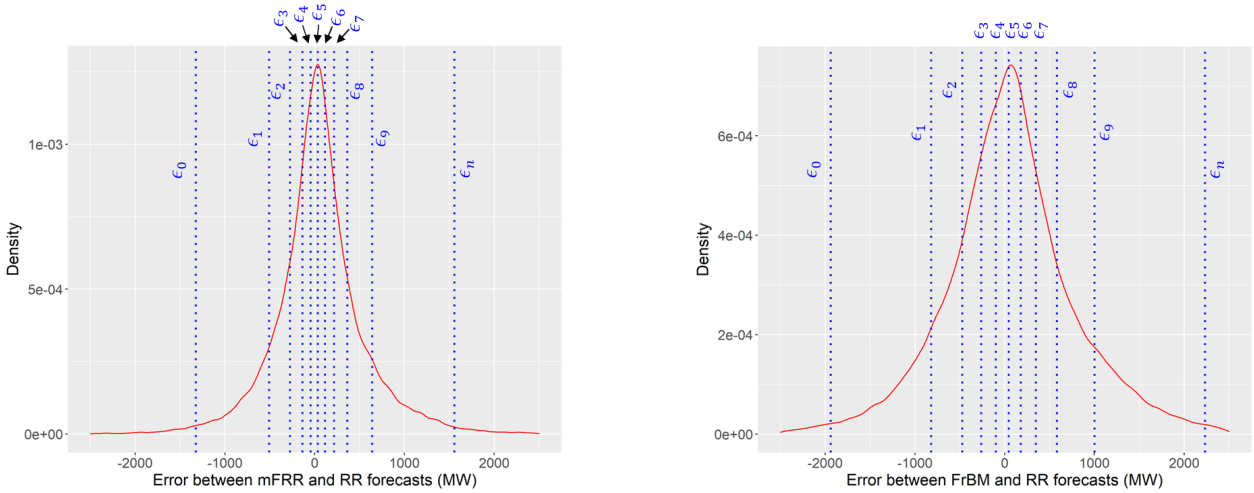

(a) RR - mFRR forecasts error

(b) RR - FrBM forecasts error

Figure 3.17: Distribution of ATLAS forecasts error functions for both alternatives to the RR market

Alternative	ϵ_0	ϵ_1	ϵ_2	ϵ_3	ϵ_4	ϵ_5	ϵ_6	ϵ_7	ϵ_8	ϵ_9	ϵ_n
mFRR	-1323	-508	-275	-137	-44	36	115	216	363	641	1157
FrBM	-1939	-821	-472	-261	-99	45	180	348	582	1002	2232

Table 3.3: ϵ_i quantile values (in MW) for both mFRR and real-time / FrBM alternatives

[9]These forecast data cover wind and solar generation, as well as load.

3.5.5 Hypotheses taken for opportunity cost computation of alternatives

In the framework described in Section 3.4, we purposefully did not settle the opportunity cost computation function C^{alt}, as it can vary according to the chosen alternative. We argue that common market and local process alternatives should be considered differently:

- When using local balancing processes as its alternative, the TSO has access to a significant level of information. Consequently, it can compute accurate opportunity cost estimations by simulating its local balancing process.
- For common market alternatives such as mFRR or aFRR markets, the information at his disposal is considerably reduced, as pointed out by (Håberg and Doorman, 2017). In that context, using market price predictions seems relevant. Most articles modeling sequential markets presented in Section 3.4.1 employ this method, usually in the form of stochastic price scenarios.

In both cases, as discussed previously, the TSO should be considered a price-maker on the alternative: the volume and direction of its balancing demands impact the prices or the costs of each alternative.

3.5.5.1 FrBM alternative

In scenarios relying on the FrBM alternative, the cost estimation is computed by performing endogenous simulations of the projected FrBM. The computation $C^{FrBM}(q,t)$, for a given imbalance quantity q, is given by Equation 3.16. The complete description of the module that simulates the FrBM in ATLAS is available in Section A.5 of general Appendix A.

$$C^{FrBM}(q,t) = min \sum_{u \in U_{ma}} P^{act}_{u,t} * p_{u,t} * \frac{\Delta t_{FrBM}}{60} + E^{VoLL}_{ma,t} * VoLL + E^{spill}_{ma,t} * p^{spill} \tag{3.16}$$

$$s.t. \qquad \sum_{u \in U_{ma}} P^{act}_{u,t,t^{ex}_{FrBM}} + (E^{VoLL}_{ma,t} - E^{spill}_{ma,t}) * \frac{60}{\Delta t_{FrBM}} = q$$

Where:

- ma is the area of the TSO.
- $P^{act}_{u,t}$ is the power activated by the FrBM process on unit u, at time t.
- $p_{u,t}$ is the activation price of unit u at time t. In the simulations of this chapter, units are always assumed to bid at their true cost, on common markets and on the FrBM. Consequently, the activation price corresponds to the variable cost of each unit, plus startup costs if required. This assumption could be challenged in future work.
- $E^{VoLL}_{ma,t}$ is the unsupplied energy in area ma, at time t.
- $VoLL$ is the Value of Loss Loads, set at 26,000 €/MWh in the French area.
- $E^{spill}_{ma,t}$ is the solar and wind spilled energy in area ma, at time t.

- p^{spill} is the penalty for spillage, set at 100 €/MWh in our simulations.

Using a local balancing process as an alternative still relies on an important assumption. As the empirical analysis of Section 3.3.2 discussed, the volume of available capacity on the local process has to be reliable. This analysis found that, in the French area, more than 50% of the available BSP capacity was not submitted on the RR market, and directly transmitted to the FrBM. In our simulations, we used this observation as a reference, which has two main impacts:

- First, all scenarios share the same hypothesis: only approximately 50% of the BSP available capacity is submitted on RR markets. Units prevented from formulating RR orders are selected randomly. The 50% threshold is applied independently to each type of unit–thermal, hydraulic, storage. Thermal units are also separated according to their fuel category. This was done to avoid rejecting most or all orders from a specific type of unit or fuel, which could cause significant price disturbances[10].
- During the TSO order formulation, the TSO uses the same assumption of 50% of available capacity on the FrBM. Once again, units assumed to be able to participate in these projected FrBMs are selected randomly, using the process described above. They may be different from the 50% selected during the BSP order formulation process, to represent the

3.5.5.2 mFRR market alternative

For scenarios using the mFRR market alternative, the opportunity cost computation is based on estimated mFRR market prices. Multiple options were then considered for this estimation.

Historical prices of actual mFRR markets could have been used. However, the mFRR market had only been operational for a year when we performed our simulations (as it was launched on October 5th, 2022); data from the RR market showed that this is not enough time to reach a stable state for the market, as both BSPs and TSOs are still progressively entering it and experimenting with it (see Appendix 3.A.1). It could also not be suited for simulation using fictive or prospective input data sets, as historical prices are tied to the current European power system state.

Another potential basis would have been the prices of mFRR markets simulated in ATLAS. Indeed, by generating price scenarios with the input data set used for the current study, the resulting estimations should be rather accurate. However, this would have required large numbers of simulations of mFRR markets to generate sufficient data, and this option was currently ruled out for computational time reasons.

Since the two previous options were ruled out for this study, the data we chose to use for the estimation of mFRR prices was extrapolated from the historical FrBM over 6 years, between 2018 and 2023[11]. Within these datasets, we used two columns that indicate the weighted average prices of mFRR-type activated offers, for upward and downward needs separately, and for each time step of the year. When constructing our mFRR price estimations, we paid attention to two elements:

[10]The empirical data that was used in Section 3.3.2 is aggregated, and we cannot use it to identify if there is a technology bias in these unsubmitted volumes.

[11]This data is public and was downloaded from the RTE services website https://www.services-rte.com/en/home.html, categorizedinMarket/BalancingEnergy/Prices

- To better fit with our simulation dataset and be less dependent on the general electricity price level, we used the ratio between mFRR-type offers and the day-ahead price for each time step.
- We wanted to capture the price-maker aspect of TSOs on mFRR prices. To achieve this, time steps of the selected years and all associated mFRR/day-ahead ratios previously calculated were classified according to 6 ranges of TSO imbalance volume on this time step. Average ratios per imbalance range were then calculated, and are displayed in Table 3.4.

Imbalance volumes ranges (MW)	**Ratio$^{\mathbf{Down}}$**	**Ratio$^{\mathbf{Up}}$**
0 - 300	0.81	1.28
300 - 600	0.76	1.33
600 - 900	0.73	1.36
900 - 1200	0.7	1.37
1200 - 1500	0.7	1.38
1500 - ∞	0.59	1.47

Table 3.4: Price ratio in France between day-ahead and mFRR prices over 2018-2023

Eventually, the price estimation $\tilde{\mu}^{mFRR,ResDir}$ of the mFRR for an imbalance q in the direction $ResDir \in \{Down, Up\}$ is given by:

$$\tilde{\mu}^{mFRR,ResDir}(q) = \mu^{DA} * Ratio^{ResDir}(q) \tag{3.17}$$

Where μ^{DA} is the day-ahead price endogenously obtained within the simulation process described in Section 3.5.3.

This leads to the following cost estimation for the mFRR market alternative for a given imbalance quantity q, where σ_q is a boolean variable indicating the direction of q ($\sigma_q = 1$ if $q >= 0$, and $\sigma_q = -1$ otherwise):

$$C^{mFRR}(q) = \sigma_q * q * \tilde{\mu}^{mFRR,ResDir}(q) \tag{3.18}$$

Despite the effort to adapt mFRR price estimation to our simulation dataset, the method finally chosen has a disadvantage similar to that of the first method mentioned (use of actual mFRR prices): the resulting price estimations can still be inaccurate, as they were calibrated on the historical prices of the French area alone. Indeed, our 2030 dataset includes more flexible assets than the historical French power system, which is likely to lead to lower spreads between day-ahead and balancing market prices. In addition, all BSPs are assumed to bid at their true costs in our simulations, which may not have been the case on the historical FrBM. Because of these limits, we expect the mFRR price estimations to be higher than the actual simulated prices, and will look at the consequences during the result discussion.

3.6 Case study: Results and discussion

Market simulations were performed based on the methodology presented in the previous section. The current section presents and discusses the relevant results extracted from this case study. First, the demand curves

generated in the different scenarios are illustrated in Section 3.6.1, and finally the subsequent market outcomes are highlighted in Section 3.6.2.

3.6.1 Market inputs: Shape of TSO demand curves and discussion of order prices

Among the 96 time steps of the simulated day of RR markets, a subset of 3 time steps is selected to illustrate the order curves created in the different scenarios. These 3 time steps encompass 3 different balancing needs situations: large upward needs ($t = 04H45$), large downward needs ($t = 21H45$) and small upward needs ($t = 14H00$) for which the forecast error distribution suggests that upward and downward needs are actually possible.

Both scenarios with inelastic TSO demands (**Inel_local** and **Inel_market)** create the exact same orders[12]. As expected, their demand curve consists of a single order at the maximum (resp. minimum) price authorized on the market, with a quantity equal to forecasted upward (resp. downward) balancing needs, which can be seen in Figures 3.18a to 3.18c. Notably, in the case of small upward needs, the order price is still equal to 10,000 €/MWh. Given their extreme prices, they were not plotted alongside other scenarios as it would completely squash the other demand curves.

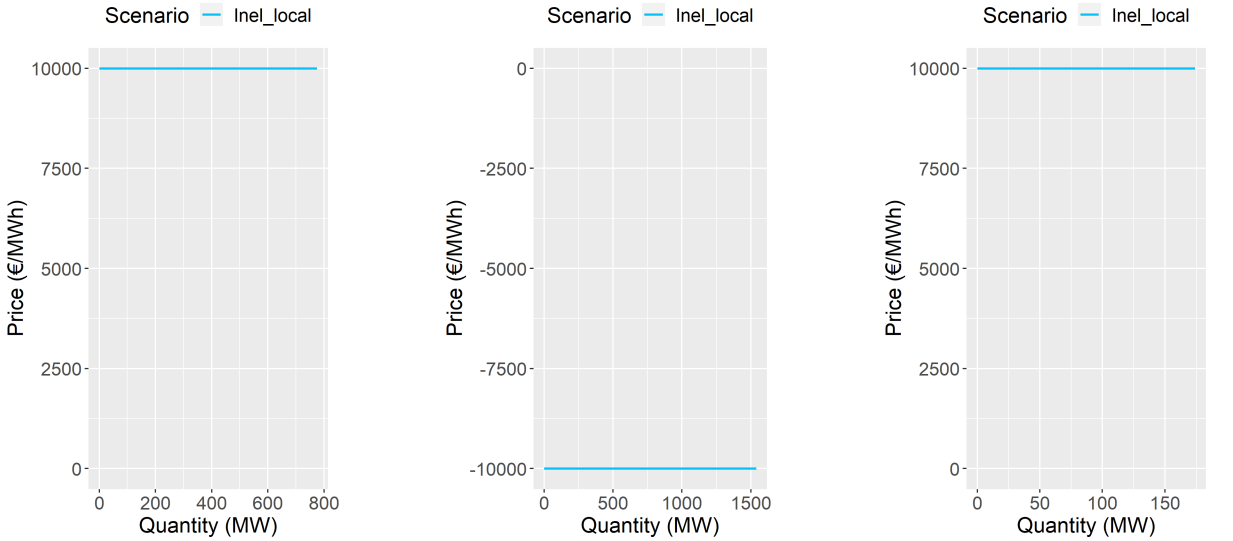

(a) $t = 04H45$ (Upward) (b) $t = 21H45$ (Downward) (c) $t = 14H00$ (Small downward)

Figure 3.18: Examples of demand curves formulated for **Inel_local** and **Inel_market** scenarios

Introducing the basic elastic bidding method with both possible alternatives leads to the creation of order curves represented in Figures 3.19a to 3.19c, for scenarios **FrBMalt_basic** (in green) and **mFRRalt_basic** (in red). Compared to inelastic orders, the same overall volume is formulated. However, the range of order prices is completely different in these new order curves, being much closer to commonly seen prices of

[12]The only difference between them corresponds to the post RR market balancing process.

electricity markets. These order curves are also comparable in shape and range to the examples of actual RR orders formulated by RTE, which were illustrated in Figure 3.5.

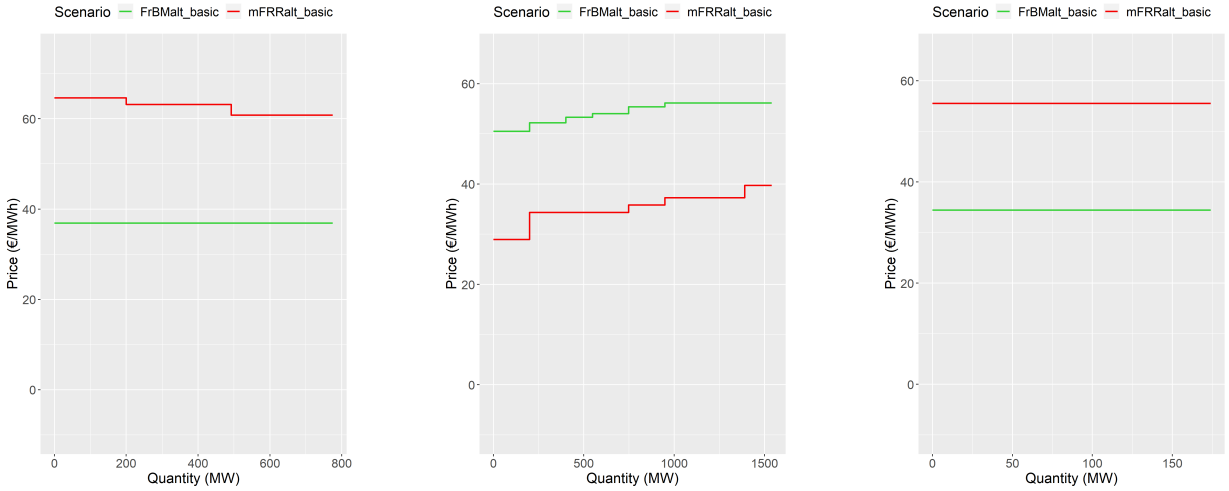

(a) $t = 04H45$ (Upward) (b) $t = 21H45$ (Downward) (c) $t = 14H00$ (Small downward)

Figure 3.19: Examples of demand curves formulated for scenarios **FrBMalt_basic** and **mFRRalt_basic**

Order curves generated for scenarios **FrBMalt_vol** (dark green) and **mFRRalt_vol** (dark red) are added to the previous graph in Figures 3.20a to 3.20c. These scenarios always lead to larger volumes of submitted needs, which was expected as they take into account the fact that the volume of balancing needs could be underestimated by the TSO. They also display a wider spread of prices compared to scenarios without volume uncertainty, with certain slices of needs being submitted with noteworthy prices according to their associated probability of under-/over-estimation. For instance, in Figure 3.20a, the first slice of both the **FrBMalt_vol** scenario and the **mFRRalt_vol** is associated with $\alpha_1 = 0.1$, so a 10% probability of over-estimation, and a 90% probability of under-estimation. Its price is consequently set at the high value in both scenarios by the bidding methods (respectively 179.07 €/MWh and 93.61 €/MWh, compared to prices of 48.63€/MWh for the first slice of **FrBMalt_basic** and 64.62 €/MWh for the first slice of **mFRRalt_basic**). In contrast, the last slice has a high chance of being an overestimation of balancing needs and requiring compensation in the other direction with the alternative. Its price integrates this information and is consequently way lower for upward needs (and or higher for downward needs), thus making it less likely to be accepted by the RR market.

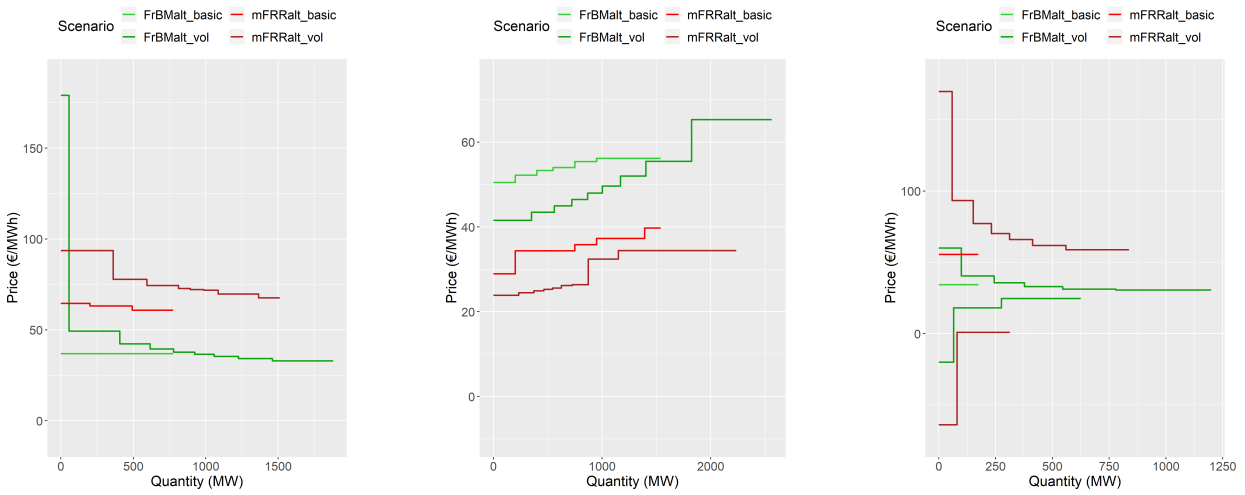

(a) $t = 04H45$ (Upward) (b) $t = 21H45$ (Downward) (c) $t = 14H00$ (Small downward)

Figure 3.20: Examples of demand curves formulated for all scenarios with elastic demand

Another noteworthy point is the 3rd situation (Figure 3.20c). With the volume uncertainty method, both sell and buy orders are simultaneously submitted. Some buy and sell orders can naturally net themselves: in practice, but it could be preferable for the TSO to net them before submitting its needs to the market (this pre-netting was not performed in our simulation). If the estimated balancing needs are small compared to the error range, it could even be better for the TSO not to submit orders at all. This could be investigated in further studies.

Finally, Figures 3.21a and 3.21b plot the prices of RR orders submitted for all scenarios, respectively for upward and downward directions.

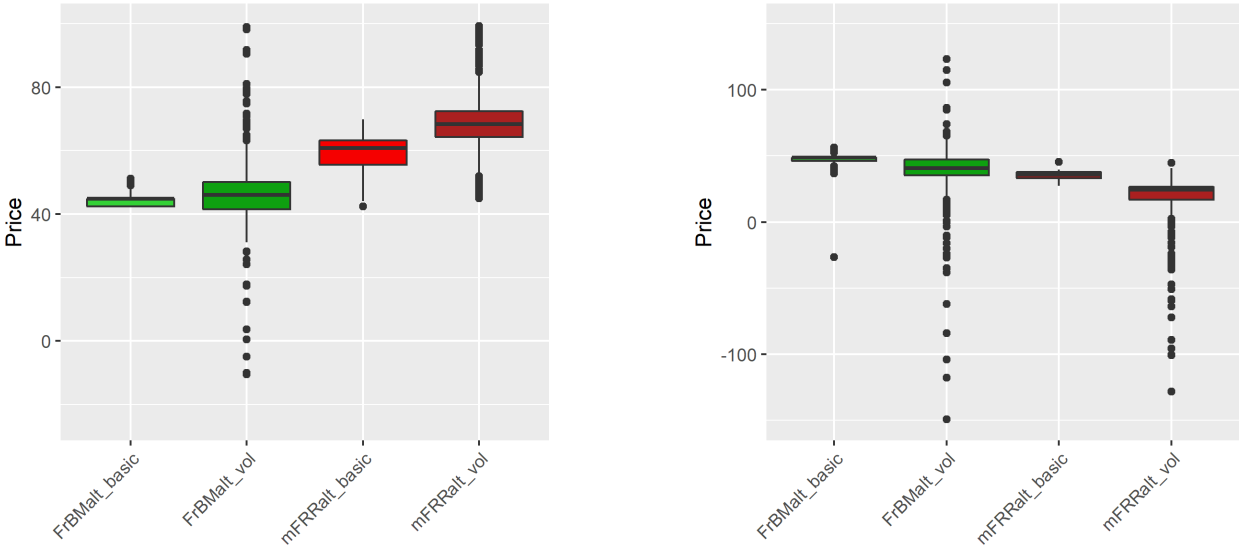

(a) Upward orders (b) Downward orders

Figure 3.21: RR order prices boxplot for all scenarios

Boxplots confirm the larger dispersion observed for volume uncertainty scenarios. For certain time steps, this method also formulates orders with a negative price, especially in the downward direction. In that direction, this phenomenon happens for orders associated with a high probability of (downward) need underestimation: the bidding method estimates that, on average, the TSO will have to sell a large additional volume of energy on its alternative, and is consequently even willing to pay for the RR order to be accepted.

The most important result is that scenarios using the mFRR market alternative, and especially the **mFRRalt_vol** scenario, tend to exhibit higher prices for upward orders and lower prices for downward orders (also visible in the examples of Figure 3.20). This is a direct consequence of the inaccuracy of the mFRR price estimation that was discussed previously. Table 3.5 indicates the average and the range of upward mFRR prices estimated with the exogenous historical data, and the same information resulting from the actual simulations of mFRR markets extracted from the **mFRRalt_vol** scenario, for both directions of balancing needs. As we can see, in the upward direction, mFRR price estimations are way higher than the simulated mFRR prices, both on average and for the upper bound. Meanwhile, estimations in the downward direction are much more accurate.

Direction	**Estimated $\tilde{\lambda}^{mFRR}$ average**	**Estimated $\tilde{\lambda}^{mFRR}$ range**	**Simulated λ^{mFRR} average**	**Simulated λ^{mFRR} range**
Upward	62.16	[42.41 - 82.72]	43	[41.22 - 52.39]
Downward	32.56	[19.55 - 45.58]	30.77	[0 - 52.39]

Table 3.5: Accuracy of the mFRR price estimation function (**mFRRalt_vol** scenario)

Consequently, the bidding method overestimates the mFRR alternative prices when formulating upward orders. The following section discussing market results shows that this phenomenon has significant impacts.

3.6.2 Market results discussion and overall balancing costs

While the previous section highlighted the impact of each bidding method on RR market inputs, the current section focuses on the output results of RR markets and post-RR balancing processes for all scenarios. All results presented only concern the studied TSO. Since scenarios **Inel_local** and **Inel_market** create the same RR market orders, they also produce the same market outcomes and are consequently grouped together when looking at RR market results.

3.6.2.1 RR market clearing prices and TSO accepted needs

RR market clearing prices

Figure 3.22 plots the RR market prices in the French area for all scenarios. For the majority of time steps, scenarios exhibit identical market prices (this is especially true for price-inelastic and basic price-elastic scenarios). It can be explained by the fact that the pricing methods were only applied to the French TSO, meaning that balancing demands in all other areas remain identical between scenarios.

A notable exception is the period from 14h to 15h, where higher prices are observed for the **FrBMalt_vol** scenario (and to a lesser extent the **mFRRalt_vol** scenario). During these time steps, the French area has a

deficit of energy, resulting in upward balancing needs. In the price-inelastic and basic price-elastic scenarios, these needs are entirely compensated by solar and wind generation which have variable costs of 0 €/MWh. Consequently, for these scenarios, the local RR clearing price is 0 €/MWh. However, as seen before, the volume uncertainty bidding method generates larger volumes of orders (upward orders in these time steps, given the direction of balancing needs). The renewable generation assets are not sufficient to compensate for the additional volume of TSO orders, thus hydro units are activated. The marginal price then rises to around 20 €/MWh.

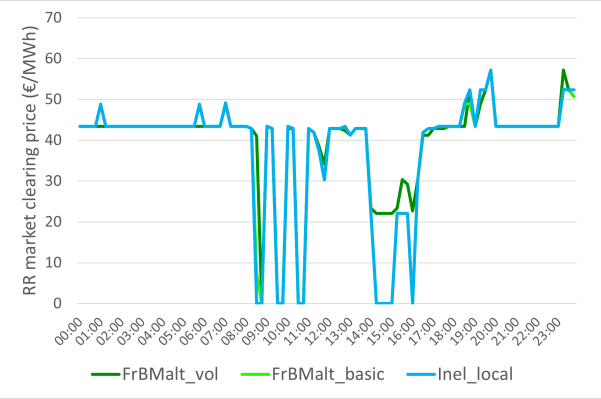

(a) FrBM alternative

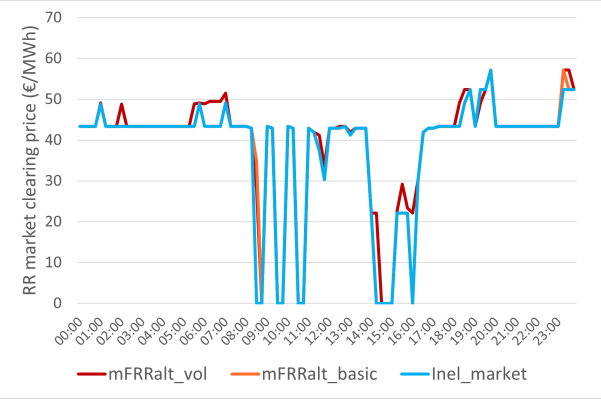

(b) mFRR market alternative

Figure 3.22: RR market prices in France

TSO accepted needs

Another outcome of the RR market is the volume of TSO demands accepted. Important differences between scenarios can be observed, resulting from the differences in both submitted volumes and order prices. Accepted and rejected quantities for both upward and downward orders are displayed in Figure 3.23a for scenarios with the FrBM alternative, and in Figure 3.23b for scenarios with the mFRR market alternative.

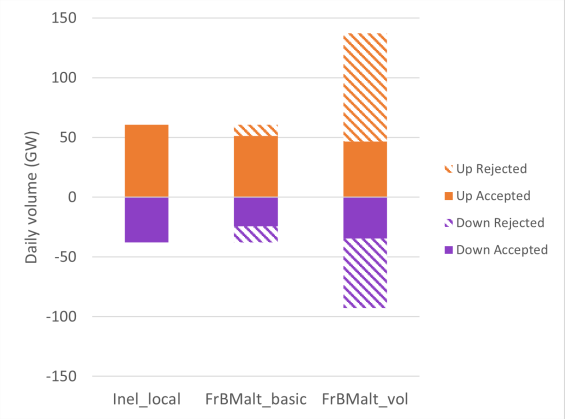

(a) FrBM alternative

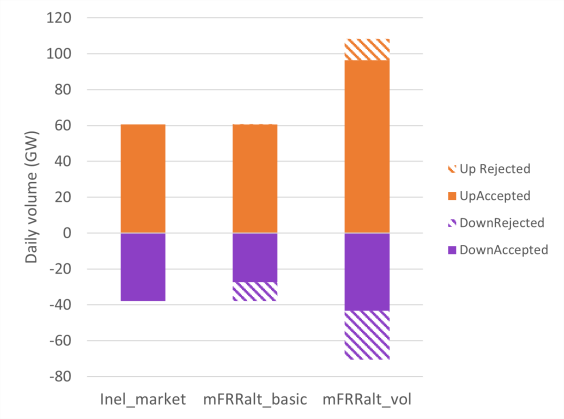

(b) mFRR market alternative

Figure 3.23: Accepted and rejected quantities of TSO orders (in GW) by scenario, with upward and downward orders separated

For the price-inelastic scenarios, all the orders submitted are accepted. It indicates that there is no

shortage of balancing energy during the simulated day. In addition, it can be seen that the TSO's position is short on average for the simulated day, as the total volume of upward balancing needs (61 GW) is greater than the total volume of downward needs (38 GW).

The same amount of volumes is submitted for the price-elastic scenarios with basic formulation. However, we can see that a part of these orders is not accepted by the market: with the FrBM alternative, 16% of upward orders and 36% of downward orders are rejected; with the mFRR alternative, 28% of downward orders are rejected. This is induced by the order price estimated from the alternative opportunity costs, and it indicates the share of balancing needs for which the basic price-elastic bidding method estimates that the alternative is a better option than the RR market.

Finally, scenarios using the volume uncertainty bidding method lead to much greater submitted volumes, which comes from the fact that they formulate slices of potential under- or over-estimation of balancing needs that exceed the initial forecasted volume. However, the difference in acceptance ratios between both alternatives is striking. With the FrBM alternative, the majority of orders are rejected by the clearing (66% of upward orders and 63% of downward orders), eventually leading to accepted quantities similar to those of **Inel_local** and **FrBMalt_basic** scenarios. On the other hand, with the mFRR market alternative, the volume-uncertainty method leads to significantly high volumes accepted, especially in the upward direction: 96 GW are accepted during the day (versus 61 GW of initial balancing needs, as indicated by the price-inelastic scenarios). This is a direct consequence of the high prices of formulated upward RR orders observed in Figure 3.21, associated with the clearing prices detailed in Figure 3.22b. It implies that, for upward needs, the bidding method considers that the mFRR market is a much worse option compared to the RR market, as most slices associated with a high probability of being an over-estimation (i.e. $\alpha > 0.5$) are accepted by the RR market.

3.6.2.2 Overall TSO balancing costs

To conclude, overall TSO balancing costs are computed for all scenarios, for the French TSO. It corresponds to the sum of costs associated with RR markets and costs of balancing using the post-RR market alternative, according to Equation 3.19:

$$\forall alt \in \{FrBM, mFRR\}, \quad C^{TSO,alt} = \sum_{t} C^{TSO}_{RR,t} + C^{TSO}_{alt,t} \tag{3.19}$$

Costs associated with markets are composed of two parts. First, the obvious part is the amount paid or received by the TSO on the market through its activated orders. In addition, TSOs receive an additional amount called congestion rent, which is generated when a transmission line (also called a market border) between two market areas is saturated by market activations. Both of these components are indicated formally in Equation 3.20 that focuses on a given TSO with its associated market area ma:

$$\forall m \in \{RR, mFRR\}, \ \forall t \in T_m,$$
$$C^{TSO}_{m,t,ma} = \lambda^{m}_{t,ma} * \sum_{o \in O^{TSO}_t} [q^{acc}_o * (-\sigma_o) * \frac{\Delta t_m}{60}] - \frac{1}{2} * \sum_{mb_{ma,j}} (\lambda^{m}_{t,ma} - \lambda^{m}_{t,j}) * (\Delta q)^{mb_{ma,j}}_t * \frac{\Delta t_m}{60} \tag{3.20}$$

Where:

- $\lambda^{m}_{t,ma}$ is the clearing price of market m in market area ma, at time t.
- O^{TSO} is the set of all market orders submitted by the given TSO.
- $\sigma_o = 1$ for sale orders (downward needs in the case of TSO), and $\sigma_o = 1$ for purchase orders (upward needs for TSOs).
- $mb_{i,j}$ is the market border between market areas i and j.
- $(\Delta q)^{mb_{i,j}}_{t}$ is the power flow at time t on mb_{ij}, taken as positive in the direction i to j.

This formula is applied for the cost computation of the RR market, and of the mFRR market when it is chosen as the post-RR balancing process. Finally, for scenarios using the FrBM as the post-RR balancing, balancing costs are a direct output of the simulation, computed as described in A.5.5.

We will look at the results of each alternative separately, as they are quite different from each other. Overall social welfare results were also computed and are discussed in Appendix 3.B. They follow a similar trend to that of TSO balancing costs.

FrBM alternative

First, Table 3.6 summarizes the daily balancing costs for the French TSO for the FrBM alternative, while detailing the values of the different components. It is completed by the boxplots in Figure 3.24 that indicate the dispersion across all time steps. It can also be noted that the mean values are over the median for all scenarios, as the distribution of balancing costs is slightly skewed towards positive values.

Scenario	RR market costs	FrBM costs	Total costs
Inel_local	331.2	105.4	436.6
FrBMalt_basic	305.9	100.8	406.7
FrBMalt_vol	54.4	203.2	257.6

Table 3.6: Total balancing costs (in k€) for all scenarios with FrBM post-RR balancing process

- Balancing costs of the **FrBMalt_basic** scenario are pretty close to that of the price-inelastic scenario, even if we look at the two components individually. Overall, it does display a slight cost reduction. The boxplots indicate that their dispersion is also smaller.

- The **FrBMalt_vol** scenario stands out more as it yields significant reductions in terms of total costs. In particular, the RR market-associated costs are reduced, while the FrBM costs are increased. This means that, on average, this bidding method manages to arbitrate correctly between the RR and the FrBM by identifying when the FrBM becomes a better option than the RR market. This cost reduction is also visible in boxplots of Figure 3.24, scenario **FrBMalt_vol** has a lower median, as well as a tighter distribution with fewer outliers. However, for 3 time steps during the day, this scenario exhibits significantly higher costs (indicated by the positive outliers on the boxplot). This result supports the idea of studying risk aversion in future work, as a TSO would be willing to avoid such cost spikes.

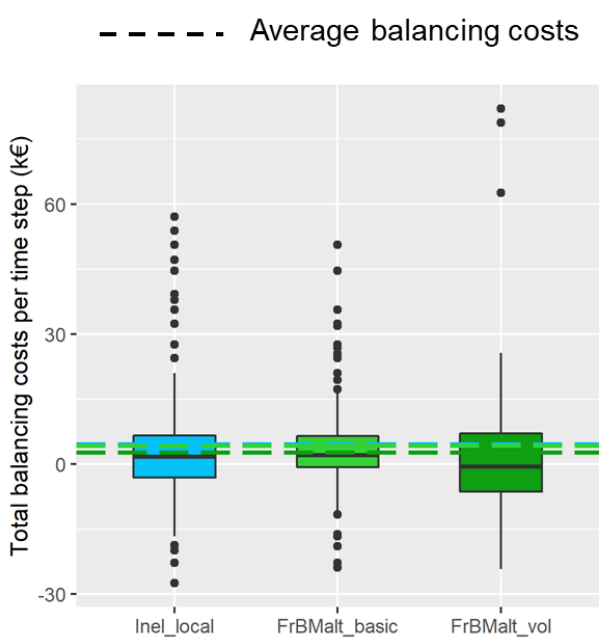

Figure 3.24: Boxplots of balancing costs with the FrBM alternative

mFRR market alternative

Results of the mFRR market alternative are displayed in Table 3.7 for daily balancing costs and in Figure 3.25 for the associate boxplots.

First, it should be noted that mFRR market costs are largely negative for all scenarios using this alternative (Table 3.7). This is caused by the exogenous evolution of load, wind and solar forecasts between t^{ex}_{FrBM} and the t^{ex}_{mFRR} of the four following mFRR markets. In approximately 80% of time steps of the simulated day, this evolution leads to downward balancing needs in the mFRR market, and consequently negative daily costs.

In addition, the main result for the mFRR market alternative is that the performance of the volume uncertainty bidding method is worse than the other two, even the price-inelastic method. It was previously shown that the price of upward orders was overestimated by this bidding strategy, leading to significantly high volumes accepted by the RR market. In Table 3.7, the RR market costs resulting from this are clear, as the **mFRRalt_vol** scenario displays much higher costs. These costs are only partially compensated on mFRR markets, when the TSO sells its energy excess. Figure 3.26 shows the balancing costs boxplot for time steps of upward RR balancing needs, and confirms the increased balancing costs for the last scenario in this case.

Scenario	RR market costs	mFRR market costs	Total costs
Inel_market	331.2	-349.8	-18.6
mFRRalt_basic	329.8	-349.1	-19.1
mFRRalt_vol	550.6	-423.5	127.1

Table 3.7: Total balancing costs (in k€) for all scenarios with mFRR post-RR balancing process

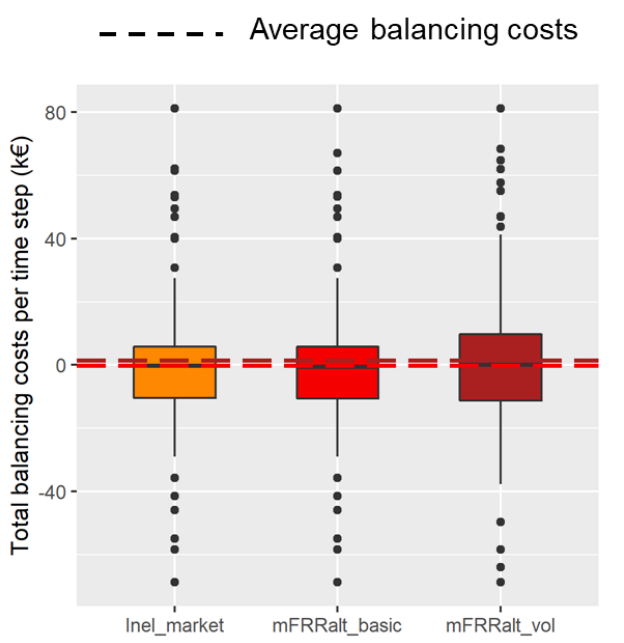

Figure 3.25: Boxplots of balancing costs with the mFRR market alternative

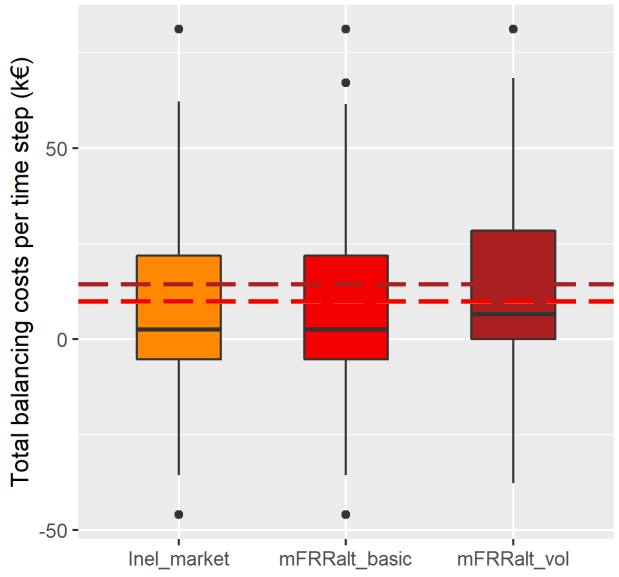

Figure 3.26: Boxplots of balancing costs with the mFRR market alternative for upward balancing needs

To summarize, two main conclusions can be drawn from the case study:

- The proposed bidding methods, and especially the method including volume uncertainty, can lead to significant reductions in balancing costs.
- The accuracy of the cost estimation function has a considerable impact on the performance of the

volume uncertainty method, and should be adapted to the chosen alternative.

3.7 Conclusion

This chapter focuses on the demand formulation process of proactive Transmission System Operators (TSOs) in balancing energy markets, and more specifically on the common European RR market. To the author's knowledge, TSO demand has only been studied in a single article (Håberg and Doorman, 2017) in the existing literature. Since then, no further research has been conducted on this topic, and TSO demand has been modeled as price-inelastic in all subsequent articles. In contrast, recent market reports published by ENTSO-E tend to indicate that TSOs are price elastic on actual balancing markets. This chapter then builds on the initial work of (Håberg and Doorman, 2017), addressing the complicating issues raised by the authors and improving their opportunity cost-based method. In doing so, we contribute to the literature in four main ways.

First, we complemented the ENTSO-E market reports with an empirical analysis of the actual RR market, based on data published by the French TSO RTE. Results confirm the actual price-elastic behavior of TSOs with the example of RTE. They also provide additional details regarding the shape and prices of its market orders which show that demand curves are already being formulated on balancing energy markets.

Furthermore, this chapter discusses the different RR market alternatives, based on which opportunity costs can be estimated. Notably, we analyzed the relevance of historical local balancing processes as alternatives, which were not considered by (Håberg and Doorman, 2017). This analysis is supported by empirical data on the French Balancing Mechanism (FrBM), the historical process that is still used alongside RR markets in France. It concludes that this process can currently serve as a relevant alternative to RR markets.

Since the challenges faced by TSOs when trying to determine the prices of their demand orders on RR markets resemble those faced by forecast-dependant assets (wind, photovoltaic or load assets) on interrelated wholesale electricity markets, we investigated associated bidding strategies studied in the literature. Based on this review, we proposed a new methodology to construct demand curves for TSOs by integrating uncertainty associated with the volume of balancing needs. This methodology relies on the estimation of the error made by the TSO when forecasting its balancing needs.

This new methodology was applied in a case study on the ATLAS electricity market model, in which our proposed bidding method was compared to both the price inelastic formulation and the method proposed by (Håberg and Doorman, 2017). Two different alternatives to the RR market are studied: the local FrBM process, and the mFRR common European market. Results demonstrate that the volume uncertainty bidding method can yield significant balancing cost reductions. They also illustrate that the accuracy of the cost estimation of the alternative has a substantial influence on the bidding method performance, and that it needs to be tuned properly.

The work on bidding strategies presented in this chapter improves on the only approach previously published in the literature for TSO balancing needs bidding methods on balancing markets. We believe that this research topic should be deepened, as our results showed the potential in balancing cost reductions as well as the inefficiencies that could result from an inaccurate design. Future research avenues could look

at refining the opportunity cost computation method, in particular by integrating risk aversion regarding alternative price estimations or volume uncertainty in the TSO bidding process. A combination of several alternatives could also be studied (for instance, local balancing processes and the mFRR market). BSPs were always assumed to bid at their true cost in our simulations, in both energy markets and local balancing processes. This hypothesis should be refined in the future, to grasp how BSP learning behaviors could interact with the TSO formulation process.

In addition, the TSO balancing needs forecast error function is another topic of interest. In this study, we focused on uncertainty stemming from wind and solar generation, and load forecasts, to compute the error function. We did not model fortuitous events on thermal units that can induce unforeseen unavailabilities, which could be included in future studies. Finally, we believe that it would be important to work on a regulatory framework to avoid significant market distortions resulting from TSO strategic behavior, either wanted (prioritizing the local balancing process over common markets) or unwanted (like the inaccuracy of the mFRR alternative cost estimation of our studies).

3.A Appendix A - Discussions on the participation of French BSPs to the RR market

Section 3.3.2 showed that a large portion of the theoretical available capacity of French BSPs is not formulated on RR markets, and is instead directly sent to the FrBM. Possible reasons are analyzed in detail in the current appendix.

3.A.1 Evolution of BSPs' participation in new RR markets

This section discusses the possibility that French BSPs are still entering the RR market, based on the market reports (ENTSO-E, 2022) and (ENTSO-E, 2023b).

The former displays data from 2021, with volumes in the French area highlighted in blue for better readability. It is particularly interesting, as the beginning of 2021 corresponds almost exactly to the connection of the French area to the RR market which happened on December 2nd, 2020[13]. During this first full year, French BSPs were indeed progressively entering the market, as a clear increase in submitted volumes can be seen in Figure 3.27. Submitted volumes in the upward (resp. downward) direction are almost equal to 0 until July 2021 (resp. September 2021), where an increase in volume can be noted for each month until the end of the year. By the end of the year, we can graphically see that French BSP submitted around 350 GWh/month in the upward direction and around 700 GWh/month in the downward direction.

[13] https://www.services-rte.com/en/learn-more-about-our-services/terre.html

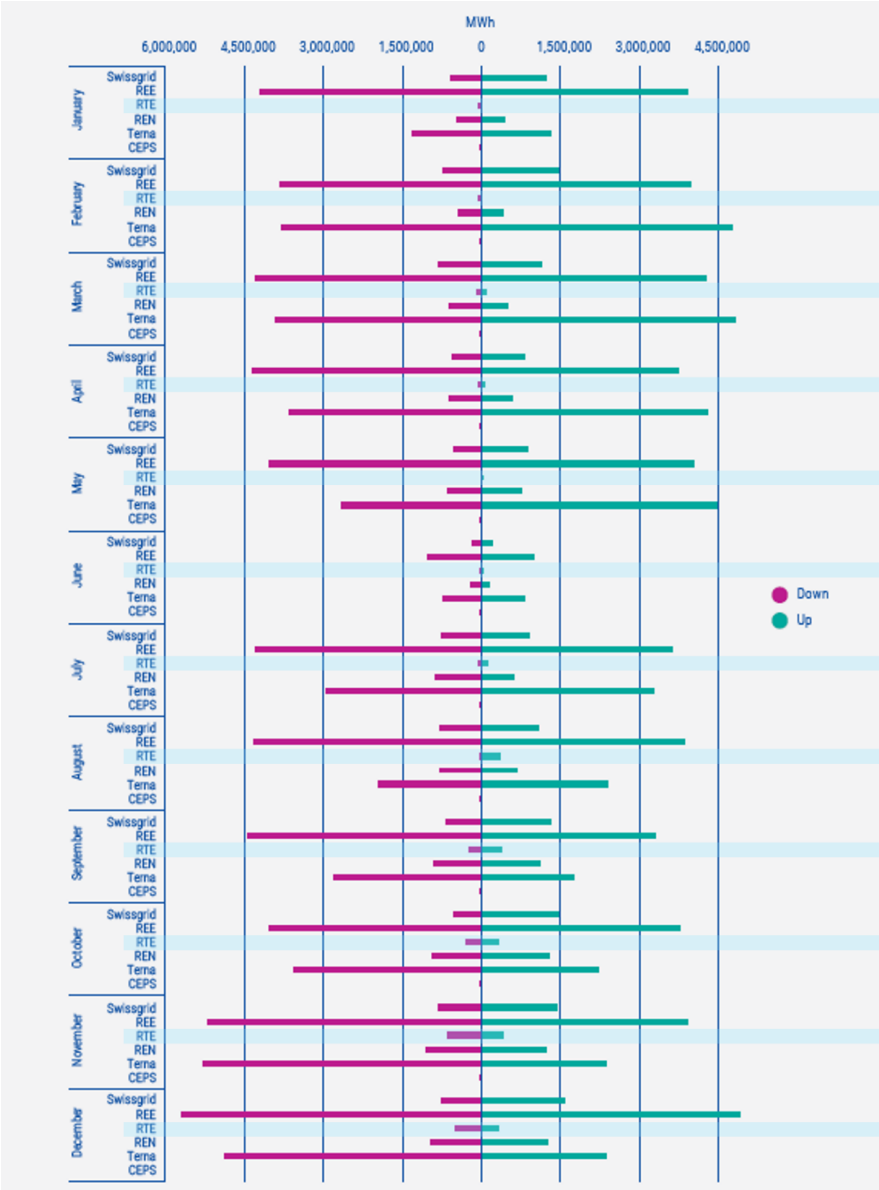

Figure 3.27: Volumes of RR BSP bids per area in 2021 (from (ENTSO-E, 2022))

In 2022 however, there is no overall increase in volumes submitted by BSPs. We can observe a seasonal variation in Figure 3.28 (Figure 38 of (ENTSO-E, 2023b), but the volumes submitted at the end of the year are similar to those at the beginning.

Consequently, it seems that French BSPs were entering the RR market during the second half of 2021, but that they reached a rather stable point since. The data does not suggest that the submitted volume is increasing.

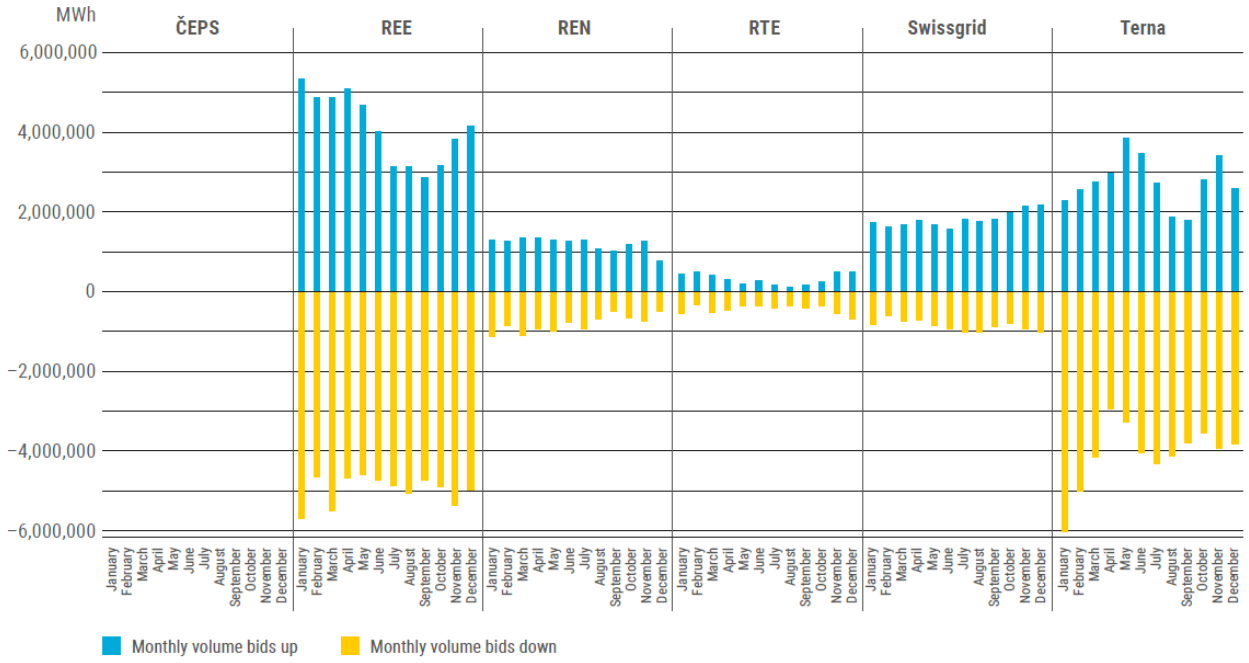

Figure 3.28: Volumes of RR BSP bids per area in 2022 (from (ENTSO-E, 2023b))

3.A.2 Comparison of FrBM and RR market prices

This section compares RR market prices to activation prices on the FrBM, to see if the FrBM is economically more attractive for BSPs. This analysis is not straightforward, for two main reasons: first, the FrBM is using a pay-as-bid method, and second it blends RR and mFRR reserves together (as they both correspond to what was historically called "reserve tertiaire" in the French balancing process). To tackle these problems, we computed two indicators $\lambda_t^{FrBM,RR,\bullet}$, based on FrBM activation prices in direction $\bullet$ that are available on the RTE data portal[14]. They correspond to the weighted price of reserves activated on units that can participate in the RR market but not in the mFRR market, because of operating constraints limiting their flexibility (Equation 3.21). The separation between units able to participate on the mFRR or not is already provided in the dataset, and we will note u^{RR} a unit that can only participate in the RR market.

$$\forall t, \quad \lambda_t^{FrBM,\bullet} = \frac{\sum_{u^{RR}} p_{t,u^{RR}}^{\bullet} * q_{t,u^{RR}}^{FrBM,\bullet}}{\sum_{u^{RR}} q_{t,u^{RR}}^{FrBM,\bullet}} \tag{3.21}$$

Where:

- $q_{t,u^{RR}}^{FrBM,\bullet}$ corresponds to the quantity activated by the FrBM on the unit u^{RR} in direction $\bullet$, at time t.
- $p_{t,u^{RR}}^{FrBM,\bullet}$ corresponds to the price at which unit u^{RR} is remunerated for the FrBM activation in direction $\bullet \in \{Up, Down\}$, at time t.

[14] https://www.services-rte.com/en/download-data-published-by-rte.html?category=market&type=balancing_energy&subType=prices

Figure 3.29 presents monthly boxplots of this indicator over 2022, for upward and downward FrBM activations, alongside monthly boxplots of the RR clearing price. We note that it is limited to the price range [-400 €/MWh, 800 €/MWh] for better readability, and that it cuts the outlier tail of the distribution in certain months.

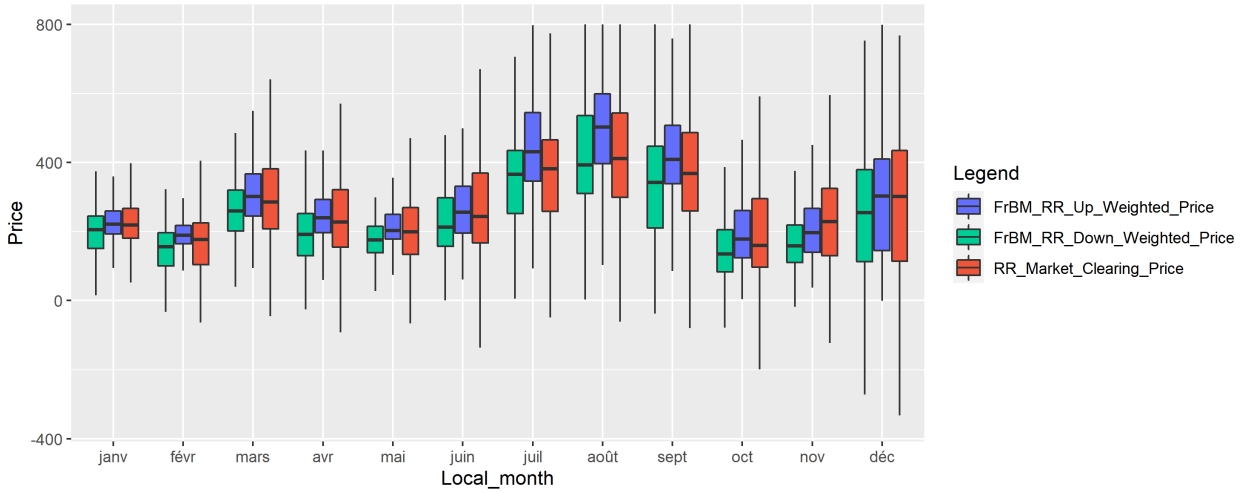

Figure 3.29: Monthly boxplots of RR clearing price and FrBM weighted activation prices of RR type reserves

The median value of the RR market clearing price is relatively close to that of FrBM weighted prices. However, RR clearing prices are more spread and can reach significantly higher or lower values. This is highlighted by Figure 3.30, which plots the distribution densities of these prices over 2022 (for better readability, the range is limited to [-1000 €/MWh, 1500 €/MWh], even if RR market prices outside of this range were observed in 2022). Extreme quantiles (0.01, 0.1, 0.9 and 0.99) are indicated for each distribution.

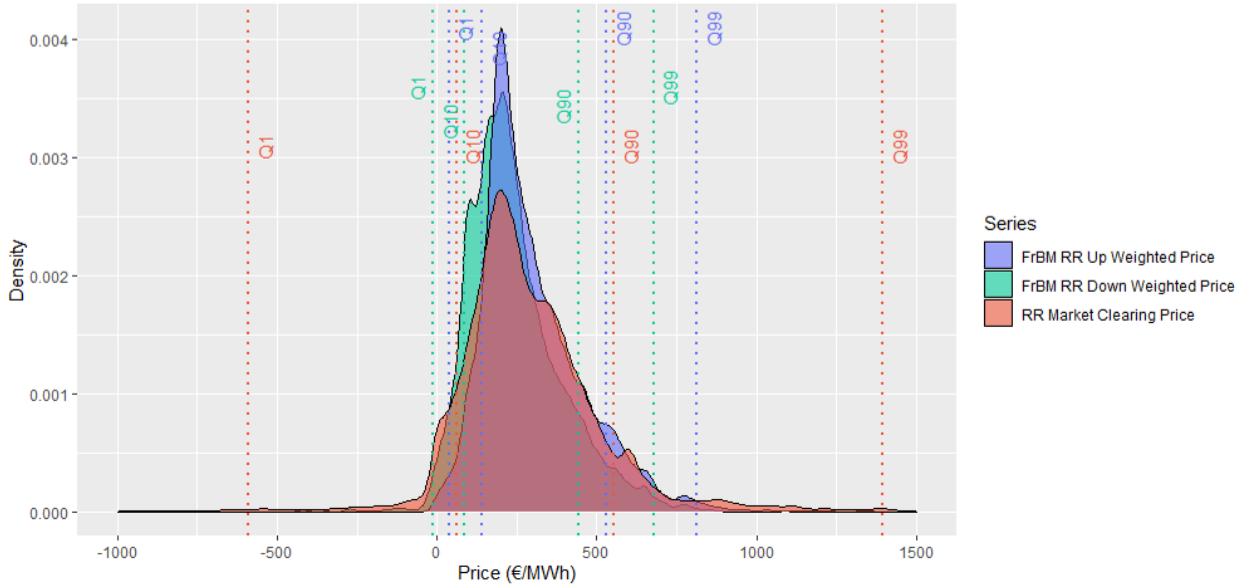

Figure 3.30: Distribution density of RR market clearing prices and FrBM weighted activation prices of RR type reserves

Quantiles 0.01 (Q1 on the graph) and 0.99 (Q99) are much more spread for the RR market clearing price, confirming that extreme prices are more common on the RR market than on the FrBM. In these cases, because of the remuneration associated with the marginal pricing system, the BSP would receive a significant benefit from participating in the RR market.

To give a final idea of the potential benefits of both processes, we took the illustrative example of a fictive unit that can offer $q = 10MW$ of power in both directions, for each time step of the year. Under different hypotheses of production cost c, we computed the benefits that this unit would make by offering either on the RR market or on the FrBM (assuming that it is always fully activated). Benefits B are computed according to the following equation (accounting for the conversion power to energy, hence the division of q by 4):

$$\begin{cases} B^{RR,Up} = \sum_t \max\big(0,\ \ q/4 * (\lambda_t^{RR} - c)\big) \\ B^{FrBM,Up} = \sum_t \max\big(0,\ \ q/4 * (\lambda_t^{FrBM,Up} - c)\big) \\ B^{RR,Down} = \sum_t \max\big(0,\ \ q/4 * (c - \lambda_t^{RR})\big) \\ B^{FrBM,Down} = \sum_t \max\big(0,\ \ q/4 * (c - \lambda_t^{FrBM,Up})\big) \end{cases} \tag{3.22}$$

Results are given in Table 3.8, and show that the unit makes more profits by submitting on the RR market, mainly by capturing the extreme prices presented before:

Production cost (€/MWh)	Upward RR market benefits	Upward FrBM benefits	Downward RR market benefits	Downward FrBM benefits
50	22,744	22,030	1,959	212
100	18,915	17,795	2,454	579
200	12,360	10,337	4,545	3,021
300	7,921	5,682	8,752	8,212

Table 3.8: Example of potential benefits (in k€) of a fictive units on balancing processes over 2022

In conclusion, it seems that market/process prices are not the main drivers explaining the lack of participation in the RR market.

3.A.3 Participating in balancing energy markets: A complex process for BSPs

For BSPs, the new balancing markets change the core of the balancing stage. In the historical balancing process used in France for instance, they were only required to indicate their generation plans and technical constraints applied to their units, along with an activation price, leaving the optimization task to the TSO. Now, BSPs are responsible for creating feasible orders, which is a task made complex by two main factors:

- The order standardization explained in Introduction 1.3.2.1 is not straightforward, especially the elements 1 to 5 of Figure 1.12. Indeed, it can conflict with operational constraints applied to their units, and it introduces multi time step dependencies. This complexity is notably highlighted in Chapter 2 for BSPs, and from the point of view of a TSO in a central dispatch system in Marneris et al., 2019.

- While they already had to create feasible orders on day-ahead and intraday markets, it was easier to manage both simultaneously, as the day-ahead market is only run once a day. Interactions between the RR markets and all the others, or even between consecutive RR markets create intricate unit commitment problems. This is illustrated from the point of view of a BSP in Figure 3.31, which is still a very simplified view since it only represents a few markets. One notable element is the indeterminacy period that exists for every market: after its order formulation, a BSP cannot know how much of the order is going to be activated by the market, until the end of the Clearing stage, and this adds another layer of complexity to the overall process.

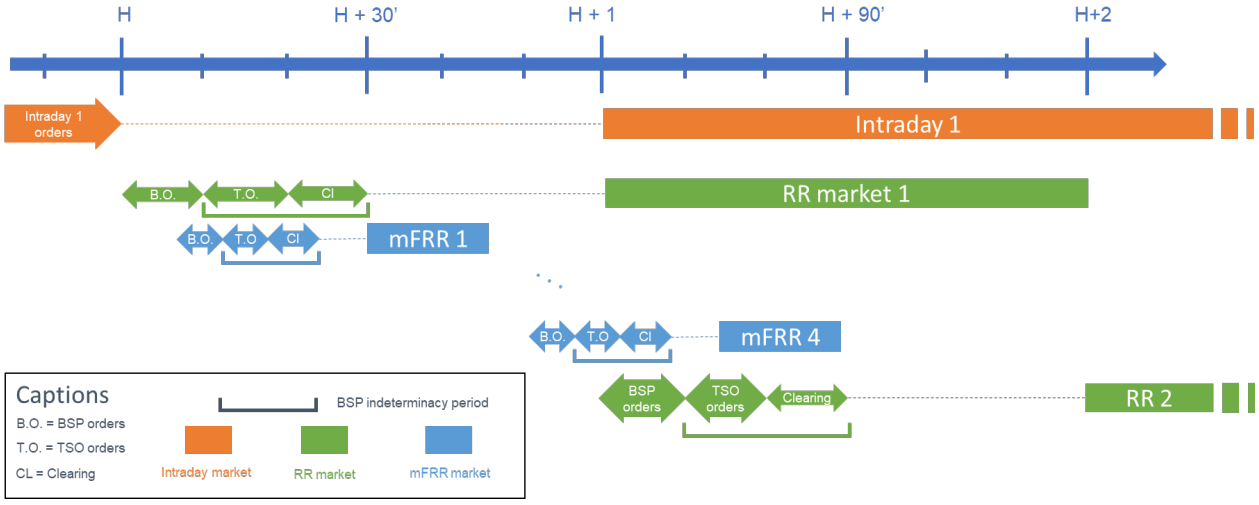

Figure 3.31: Electricity markets complex interactions for BSPs

Solving this process correctly requires heavy investments in workforce and IT systems notably (algorithms able to quickly determine feasible orders, based on frequently evolving inputs), and this could be a reason as to why many BSPs are not, or not yet at least, formulating orders on the RR market, and prefer to still rely on local processes: from a global perspective, the costs of entering the RR market could outweigh the benefits it provides, especially for small scale actors who have less opportunity to recover the aforementioned fixed costs. Indeed, the final example of Section 3.A.2 illustrated that the benefits difference between participating in the RR market and in the FrBM are real but not extremely high.

3.B Appendix B - Social welfare results

Because simulations includes TSO price-inelastic orders, the social welfare has to be computed as the sum of the BSP surplus and the TSO balancing costs (this social welfare formulation was discussed in detail in Chapter 2). In this chapter, the alternative cost is also included within TSO balancing costs. The overall social welfare of a given alternative can then be expressed as:

$$SW^{alt} = \sum_{ma \in Z} \left[\sum_{t \in T_{RR}} \left(\sum_{o \in O^{BSP}_{ma,t}} q^{acc}_{o} * \sigma_o * (\lambda^{RR}_{t,ma} - p_o) * \frac{\Delta t_{RR}}{60} \right) - C^{TSO,alt}_{ma} \right] \tag{3.23}$$

Where:

- Z is the set of all market areas.
- $O^{BSP}_{ma,t}$ is the set of all BSP market orders in area ma, at time t.
- q^{acc}_{o} is the quantity accepted on order o.
- σ_o gives the direction of order o (=1 for sale orders, and =-1 for purchase orders).
- p_o is the price of order o.
- Δt_{RR} is the time step of the RR market, hence 15 minutes.
- $C^{TSO,alt}_{ma}$ are the balancing costs for TSO associated with area ma, computed according to Equation 3.19

Tables 3.9 and 3.10 summarize the results for each alternative type. It is relevant to note that the TSO balancing costs presented here are the sum over all areas. This is why the values differ from those indicated in Section 3.6.2, which corresponded to the French TSO only.

Scenario	BSP surplus	TSO balancing costs	Social welfare
Inel_local	2,859	1,450	1,419
FrBMalt_basic	2,851	1,415	1,446
FrBMalt_vol	2,832	1,229	1,614

Table 3.9: Total social welfare (in k€) for all scenarios with the FrBM alternative

Scenario	BSP surplus	TSO balancing costs	Social welfare
Inel_market	2,859	930	1,939
mFRRalt_basic	2,833	910	1,933
mFRRalt_vol	2,860	1066	1,804

Table 3.10: Total social welfare (in k€) for all scenarios with the mFRR market alternative

The evolution between scenarios is mostly driven by the evolution of TSO balancing costs. Indeed, BSP surpluses are not significantly modified across all scenarios. This can be linked with the relatively low impact on market prices observed in Figure 3.22: in most time steps, the variations in volumes of balancing needs accepted for the French TSO only modify the accepted quantity of the marginal BSP order, but do not induce a change of marginal cost. Consequently, the BSP surplus remains the same in these situations, as this marginal BSP order is not generating any social welfare ($p_o = \lambda^{RR}$).

Chapter 4

Evolution of balancing energy markets with the energy transition: a 2050 case study

Contents

Abstract

The new European balancing energy markets were designed in part to facilitate the integration of Variable Renewable Energy Sources (vRES) in the power system, by mitigating the increase of balancing needs

their uncertainty is expected to induce. Their design also allows for matching Balancing Services Providers (BSPs) orders together, which creates new opportunities for market actors: using balancing markets as a self-balancing tool, by formulating their imbalance as market orders. This is particularly relevant for vRES assets in long-term studies, given their aforementioned uncertainty. This chapter evaluates the impact of decarbonization on balancing energy markets between the 2030 and 2050 horizons, including the notion of vRES self-balancing. Simulations of a day-ahead, intraday and RR balancing markets are performed using the ATLAS electricity market model. Key findings indicate that RR markets can compensate for the expected increase in balancing needs at the 2050 horizon, under the assumption of significant market participation of flexible technologies, but also reveal an increase in balancing cost variability. In addition, we show that the self-balancing behavior is economically beneficial for vRES actors when a dual imbalance pricing scheme is used. However, without communication between BSPs and proactive TSOs about these self-balancing orders, this behavior can be detrimental to the security of supply and increase balancing costs. Consequently, we propose a regulatory evolution: self-balancing orders should be clearly identified by BSP to their TSO to avoid a potential overcompensation of imbalances.

4.1 Context

The energy transition is a key component towards a sustainable world. Its impact on the European power system is already noticeable, especially on the installed capacities of variable Renewable Energy Sources (vRES): between 2000 and 2019, they increased from 6 GW to 165 GW for wind capacities and from less than 1 GW to 110 GW for solar capacities[1]. Looking ahead to the 2050 horizon, this trend is set to intensify and profoundly reshape the power system. vRES are notably projected to represent the most important share of installed generation capacities, and to produce the majority of electricity consumed in Europe. These changes will significantly interact with power system management, notably with the balancing stage of electricity markets. Indeed, the growing share of wind and solar power is expected to lead to a significant increase in balancing needs, due to the uncertainty of their power output forecasts. This is notably illustrated by (Doherty et al., 2009), (Holttinen et al., 2011), (Heggarty et al., 2019) and (Goodarzi et al., 2019).

As described in previous chapters, the European balancing stage has historically been managed locally by the different Transmission System Operators (TSOs). It is now undergoing a transition towards common balancing markets structured around 4 different types of reserves (namely FCR, aFRR, mFRR and RR). One of the main challenges of these new markets is to facilitate the aforementioned large integration of RES in the power system, by relieving the additional balancing stress they are expected to induce. This can be achieved directly through the increase of the pool of available reserves and the exchanges between areas (Ortner and Totschnig, 2019), and by implementing an appropriate and transparent market design (Vandezande et al., 2010) (Hirth and Ziegenhagen, 2015). In particular, both RR and mFRR markets are designed not only to meet the balancing needs of TSOs. As evoked in the general introduction of the manuscript, these markets can also play the role of dispatch optimization markets, similar to that of day-ahead and intraday markets but even closer to real-time. Indeed, they can match Balancing Services Providers (BSPs) reserve offers of opposite directions if their prices are suitable (Marquet, 2018). This implies that actors can use RR or mFRR markets to balance themselves, notably if the imbalance settlement process in their area incites them to stay

[1] From https://ec.europa.eu/eurostat/statistics-explained/index.php?title=Electrical_capacity_for_wind_and_solar_photovoltaic_power_-_statistics#Increasing_capacity_for_wind_and_solar_over_the_last_decades

balanced. Because of their variable power output, vRES are particularly concerned by this phenomenon, which makes it a relevant inclusion in our long-term study of balancing markets.

The contributions of this chapter to the literature are twofold.

First, a quantification of the evolution of the RR balancing energy market with the energy transition is performed. More precisely, we model and compare European power systems representative of local political targets for the 2030 and 2050 horizons, using the electricity market model ATLAS. A detailed look at the evolution of both market inputs and outputs is proposed, providing insights into how the offer and demand curves could be affected by the energy transition, and the subsequent market outcomes (notably the security of supply, balancing costs, and social welfare). Overall, we try to estimate if common balancing energy markets can achieve their objective of facilitating the integration of vRES in the power system by mitigating their impact on balancing needs.

A second set of contributions is associated with the investigation of the potential self-balancing behavior of vRES actors. We show that, under the hypothesis of dual imbalance pricing, it is beneficial for vRES actors to choose this self-balancing behavior. The systemic impact of this behavior is also analyzed, to assess the potential impact of this behavior on balancing needs and costs. Finally, the regulatory aspect of this behavior is discussed, as the communication processes between BSPs and TSOs should be framed to avoid potential overcompensation of imbalances.

A literature review is proposed in Section 4.2, showing existing analyses of balancing processes evolution associated with energy transition to identify a gap around balancing energy markets. It also details previous works performed on the interaction between imbalance settlement and market actor behavior in balancing processes, underlining that the self-balancing behavior of vRES actors has never been considered. Section 4.3 details the methodology of the simulations performed in this chapter. It includes an overview of the model, a description of both datasets representing current and 2050 European systems, the simulation framework, and the scenarios. Finally, the results are discussed in Section 4.4.

4.2 Literature review

4.2.1 Overview of studies quantifying the impacts of decarbonization on European balancing processes

Quantifications of the impact of the energy transition on European balancing processes have already been conducted, with both empirical and prospective approaches.

Several empirical analyses look at the effect of the beginning of this transition, i.e. between 2000 and 2020. (Batalla-Bejerano and Trujillo-Baute, 2016) highlights the increase in balancing costs in Spain associated with the integration of vRES between 2011 and 2014, concluding that this increase is mainly linked to the uncertainty of vRES (as opposed to their intermittency, which has a lesser impact). (Goodarzi et al., 2019) studies the relation between vRES forecast errors and day-ahead spot prices in Germany over 2014, concluding that wind forecast errors have a higher impact than errors on solar generation. As a last example,

the integration of vRES in the Turkish system between 2016 and 2019 is analyzed by (Sirin and Yilmaz, 2021): the authors conclude that this integration led to an increase in positive system imbalances.

Meanwhile, long-term analysis of inertia and primary frequency control at a 2050 horizon can be found in (Agathokleous and Ehnberg, 2020), which quantifies the need for inertia in the European system, and in (Seck et al., 2020) that focuses on France and quantifies the technical feasibility and required investments of a 100% RES system. Balancing reserve procurement in the Baltic area is studied in (Petrichenko et al., 2022), using 2050 projections of the local power system. (Lorenz, 2017) widens the scope to the European scale between 2020 and 2050, using a dynamic investment model to investigate the future cost of reserve procurement. Finally, (Nordström et al., 2022) conducted a high-resolution analysis of the Nordic area in a 2045 scenario to estimate the future need for balancing power. The authors included a netting effect but did not simulate energy markets.

When looking at balancing energy markets of tertiary reserves (mFRR and RR), the existing literature is scarce. (Farahmand and Doorman, 2012) models day-ahead and balancing processes in the Nordic area based on a 2030 scenario. Although the authors modeled the energy activation processes, the focus of the article is set on the impact of cross-border reserve procurement. (Dallinger et al., 2018) proposes a comprehensive analysis of aFRR and mFRR balancing markets, modeling both procurement and activation in the Central-Western Europe region in a 2030 scenario. As for the previous article, this work focuses mainly on the procurement side. (Ortner and Totschnig, 2019) produced one of the first analyses of future balancing market performances at the European scale focused on energy activation, based on different scenarios of generation mix and interconnection development at the 2030 horizon. The scope of this work is mainly set on potential revenues per technology type, while our objective is to assess the future market liquidity, balancing performances and security of supply.

To our knowledge, there is a gap in the literature regarding the assessment of long-term European balancing energy markets performance, which we aim to address in this chapter.

4.2.2 Projected evolution in the types of technologies participating in balancing processes

To perform a long-term analysis of European balancing energy markets, it is important to understand how the power system flexibilities are likely to evolve.

In the current power system, short-term flexibilities are mainly provided by gas- or oil-fueled power plants, pumped hydro storage and reservoir-based hydro (Poncela et al., 2018). Nuclear plants can also be added to this list, as their benefits in short-term balancing management are notably highlighted by (Jenkins et al., 2018) and (Cany et al., 2018).

This state of power system flexibility options will change in the future. The participation of certain types of technologies previously mentioned is going to decrease. In particular, a large part of fossil-fueled power plants is expected to be shut down in the energy transition process. To compensate for this flexibility loss, and accommodate for the increased system variability induced by vRES, new types of technologies are expected to participate in future balancing processes. We can notably cite vRES themselves, storage, demand-side response and power-to-gas assets (Lund et al., 2015) (Joos and Staffell, 2018).

First, even though vRES units are expected to be the main drivers of imbalances in long-term power systems, they can also provide balancing services. This is notably highlighted by (Hirth and Ziegenhagen, 2015), who studies their potential participation in German balancing processes and concludes that they are mostly suited to offer downward reserves. Indeed, they would need to be operated below their optimal power output to provide upward reserves. (Joos and Staffell, 2018) deepens the technical and economical assessments of vRES participation in balancing processes, by considering the United Kingdom system in addition to the German one. The article points out that certain technical limitations must be addressed for efficient participation, notably improvements in system inertia management and in forecasting tools. Overall, both studies underline the economic potential of vRES balancing participation in future power systems, with system balancing cost reductions estimated between 20% and 50%.

Storage units could act as local buffer tools to compensate for unforeseen variations in vRES generation, relieving some of the role of transmission lines (De Jonghe et al., 2011). These units can be classified into three different categories: mechanical, electro-chemical and electrical storage. Batteries, belonging to the second category, are notably studied by (Bussar et al., 2016), which focuses on their impact within a future European power system with large vRES capacities. (Mileva et al., 2016) links the potential of batteries to the share of installed solar capacity. In addition, electric vehicles are often considered a relevant flexibility option for long-term scenarios (Teng et al., 2016, Colmenar-Santos et al., 2019 or Lauvergne et al., 2022), albeit subject to more constraints than regular batteries and dependant on the behavior of consumers.

The continuous development of smart devices for load management opens up the possibility for both aggregators and end-consumers to participate in balancing processes. On top of the response to vRES variability, it should help in peak load management. (Gils, 2014) assesses the potential of demand-side response at the European scale, and identifies a range of $\pm 60GW$ that can be covered by this flexibility type. Local assessments have also been carried out. For instance, (Kirkerud et al., 2021) analyzes the potential participation in Nordic balancing processes and concludes that heating (both for space and water) has the most potential there among demand-side response tools. When looking at future power systems, the integration of demand-response in investment models toward a 2050 power system has been conducted in several articles. We can cite (Mier and Weissbart, 2020), which concludes that investments in short-term demand response can reduce the gas installed capacity by 50%, while (Marañón-Ledesma and Tomasgard, 2019) finds that demand-side response mainly supports other technologies and can reduce the need for large storage capacities.

Finally, numerous articles look at the potential of power-to-gas as a flexibility tool in future power systems, especially hydrogen produced by electrolysis. To only cite a few, the economic viability of their participation in aFRR-type balancing processes is identified by (Grueger et al., 2017), in the German power system. (Lux and Pfluger, 2020) widens this scope to the European system at a 2050 horizon, and confirms the potential of hydrogen as a flexibility option (notably reducing the usage of storage assets by 45%).

4.2.3 Interaction between the imbalance settlement price and actor behavior on balancing markets

While several types of imbalance settlement processes are used across European areas, they all function based on the same principles. They involve two kinds of actors, Balancing Responsible Parties (BRPs) and TSOs.

BRPs are responsible for the commercial balance of a given perimeter of generation and consumption assets. Before the final gate closure time of balancing processes, BRPs declare to their TSO their balance state, i.e. the difference between their market commitments and the actual generation-load balance of their perimeter. Any imbalance is then settled ex-post, using an Imbalance Settlement Price (ISP) that is usually based on the price of the energy activated by the TSO during the balancing processes. BRPs are remunerated for positive imbalances (an excess of generation), and pay for negative imbalances (a deficit of generation).

In practice, the perimeter of a BRP is composed of several BSPs. Hence, the behavior of BSPs and BRPs in balancing energy markets is closely linked. To simplify the analysis, in the rest of this chapter, we will consider that a BRP is "equal to" a BSP, meaning that each perimeter contains only one BSP. I will use the term BSP to designate them both.

The relationship between ISPs and BSP behavior in balancing energy markets is already highlighted in the literature. Several studies focus on the different types of ISPs, and try to determine the optimal design to send the right incentives to market actors. This is for instance the case of (Vandezande et al., 2010), (T. Haring et al., 2012) or (Jacobsen and Schröder, 2012). The two main categories of ISPs are dual imbalance pricing and single imbalance pricing. A dual imbalance pricing usually penalizes actors for being imbalanced, by decreasing the remuneration (for positive deviations) and increasing the cost (for negative deviations) compared to balancing processes. Consequently, it incites actors to stay balanced. Meanwhile, a single imbalance pricing rewards deviations that naturally help to balance the power system, and penalize deviations in the other direction. Such an ISP encourages BSPs to predict the system imbalance, and voluntarily put themselves in imbalance in a way that would help the system.

Other studies take the point of view of BSPs, and seek to maximize their profits under a given ISP. We can notably cite (Bottieau et al., 2019), which details how actors' behavior is influenced by their ability to forecast the ISP, and then proposes a new method to accurately perform this prediction. (Schneider and Roozbehani, 2017) studies systems that penalize this vRES for deviating from their day-ahead generation plan in real-time, using market-based imbalance pricing. The authors derive optimal bidding strategies for this type of actor from a two-stage game theory model. These studies, and most of the existing literature focus on how actors can adapt their balancing position *before* the gate closure time of balancing processes.

A scarcer section of the existing literature instead considers the possible actions of BSPs *after* the latest gate closure time. This point of view is notably studied in (Klyve et al., 2023), where the authors focus on the Nordic system and evaluate the cost efficiency of performing a portfolio internal redispatch to correct the forecast evolution of vRES assets. This internal redispatch is realized by dispatchable assets, such as storage or thermal units, and is done at the expense of formulating energy offers on mFRR markets with these dispatchable units. The authors then conclude that it is always more profitable for the actor not to correct its imbalance internally, and rather to offer the available energy of its dispatchable units on mFRR markets.

Interestingly, (Klyve et al., 2023) discusses the fact that vRES forecast evolution could be offered on the mFRR market, which would alleviate their imbalances. However, the authors chose not to model this behavior, mainly because they deemed it risky for the vRES actors as they face the possibility of the TSO not activating their self-balancing offers. While logical in the Nordic balancing system, we argue that this risk is reduced for vRES actors within European balancing energy markets, first because of the larger area, but more importantly given the design features detailed in the introduction. Indeed, their self-balancing offers

can match with other BSP offers: not only does this provide a larger pool of possible matches, but it also almost guarantees that reserve offers will be available in the opposite direction, which was an issue if they could only match TSO needs.

Consequently, and given the large integration of vRES capacities associated with decarbonization, it appears relevant to include the self-balancing behavior of this type of unit in studies at the 2050 horizon, and to evaluate its systemic impacts.

4.3 Methodology

We used the electricity market model ATLAS to investigate the impact of the energy transition on balancing energy markets. The model was previously presented in Section 2.4, and the description of all components specific to the balancing stage is available in Appendix A while all other aspects are detailed in (Little et al., 2024). It is suited for simulations of day-ahead, intraday and balancing markets, modeling close-to-reality processes.

4.3.1 Scenarios and simulation framework

Time horizons and seasonal considerations

Two different datasets were used as inputs, respectively representing the 2030 and 2050 European power systems. They are detailed in Section 4.3.2. To capture various market situations, we conducted our simulations over several days of two different periods: winter and summer.

Overview of vRES behavior scenarios

Additional scenarios are included for the 2050 time horizon to model the self-balancing behavior previously described. It is illustrated in Figure 4.1, considering the example of a vRES unit that forecasted a given power output q when formulating its offers on a previous market–say, the day-ahead market–, and successfully sold this quantity. When approaching real-time and the balancing energy markets, the vRES sees an evolution Δq of its generation forecast. Depending on the sign of Δq, several situations arise:

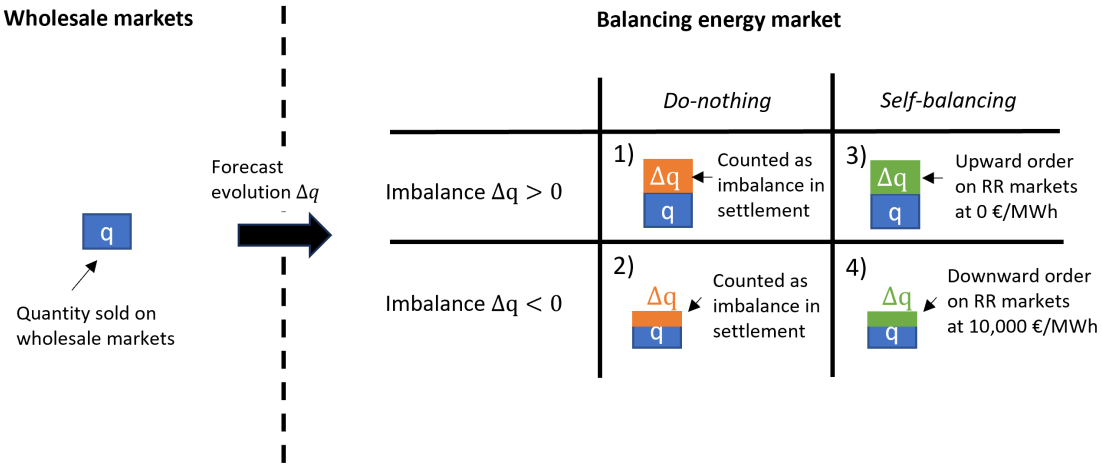

Figure 4.1: Schematic view of potential vRES behaviors

The *Do-nothing* behavior will be considered as the basis[2], and will notably be applied to all 2030 simulations. With this behavior, the vRES unit does not act according to the forecast evolution. The resulting imbalance is then counted as such in the imbalance settlement process, and be remunerated (situation 1) or paid (situation 2) according to the chosen ISP, detailed later in this section.

In contrast, with the *Self-balancing* behavior, the vRES actor submits its forecast evolution to the RR market in an upward order for positive imbalances (situation 3), and in a downward order for negative imbalances (situation 4). An important case needs to be discussed: if the self-balancing order of a vRES actor is not accepted on the RR market, then the actor will be imbalanced in real time as its power output would be equal to $q + \Delta q$ while the sum of its market commitments is still equal to q. In that case, this imbalance will be settled according to the imbalance settlement process, similar to the previous behavior scenario. Conservative order prices were chosen for these self-balancing orders in this first approach, 0 and 10,000 €/MWh for upward and downward self-balancing orders, respectively. This implies that the unit considers the RR market to always be more profitable than the ISP.

Finally, the *Self-balancing* behavior can strongly interact with the RR balancing needs computation of a proactive TSO. Indeed, as discussed in the general introduction of the manuscript, the RR balancing needs of this type of TSO represent their forecast of imbalances, which includes the evolution of vRES power output. Consequently, if the TSO is not informed that vRES actors are formulating self-balancing orders, the same imbalance could be asked twice on the RR market (both by the BSP and the TSO). To study the resulting impact, two possible BSP-TSO interactions will be considered. If there is communication between the TSO and BSPs in his area about self-balancing orders, the TSO will not consider the associated volume in his computation. On the other hand, if there is no communication, the TSO is not informed of self-balancing orders and conducts his calculation as usual[3]. The practical implementation of both variants is detailed in Section 4.3.4. We will not study the BSP-TSO communication with the *Do-nothing* behavior, as the usual computation method of the TSO is already fitted for this behavior.

Scenarios

Eventually, gathering the two different time horizons, the two seasons, the possible vRES bidding behaviors and the BSP-TSO communication leads to 8 different scenarios summarized in Tables 4.1 and 4.2:

Time horizon	2030	
Season type	Summer	Winter
vRES behavior	*Do-nothing*	*Do-nothing*
BSP-TSO communication	\	\
Scenario name	2030_S	2030_W

Table 4.1: Scenarios 2030

[2]This is the behavior currently used by vRES actors in France.

[3]In the current design of RR markets, BSP balancing orders are first sent to their TSO, which performs safety filtering. Consequently, he could theoretically extract the information from BSP orders, based on their previous market commitments and power output forecasts. However, we argue that this task would be particularly complex without communication since the TSO cannot ensure that his power forecasts match those of the unit. For instance, a vRES unit could voluntarily sell less than its forecast on wholesale markets to offer RR reserves. Distinguishing this from a self-balancing behavior would be almost impossible for the TSO.

Time horizon	2050					
Season type	Summer			Winter		
vRES behavior	*Do-nothing*	*Self-balancing*		*Do-nothing*	*Self-balancing*	
BSP-TSO communication	\	Yes	No	\	Yes	No
Scenario name	2050_S_DoN	2050_S_Self	2050_S_Self_NC	2050_W_DoN	2050_W_Self	2050_W_Self_NC

Table 4.2: Scenarios 2050

Simulation framework

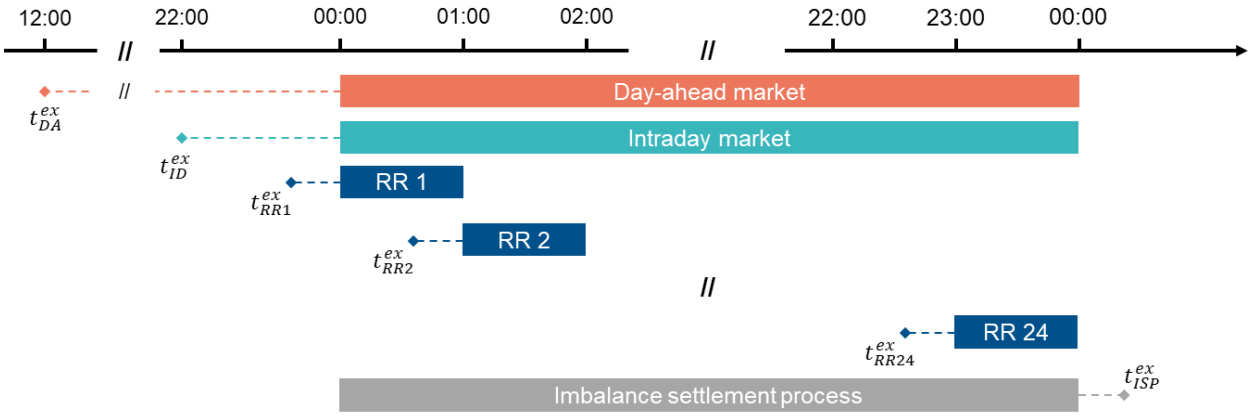

Figure 4.2: Simulations framework

For each scenario, we simulated a sequence of electricity markets (Figure 4.2) for 3 consecutive days, each one including:

- A day-ahead market, executed at 12:00 of the previous day.
- An approximation of the intraday market, which takes as input the forecasted view of the power system two hours before real-time. This hypothesis on system view is rather conservative, notably compared to (Ortner and Totschnig, 2019) which uses hour-ahead forecasts. It can be justified by the self-balancing aspect studied in this chapter: if actors can balance themselves on balancing markets, they could be inclined to prioritize this market and not systematically participate in the latest intraday markets.
- 24 instances of RR markets, executed 30 minutes before real time.
- Eventually, the imbalance settlement process ais performed ex-post, over the entire day. We chose to use a dual imbalance pricing, which is commonly used in Europe (ENTSO-E, 2021). This method incites actors to stay balanced, which justifies the self-balancing behavior. The modeled settlement process is based on the French ISP, which was presented in the General introduction (Section 1.2.3). The official description of this ISP is available at https://www.services-rte.com/en/learn-more-about-our-services/becoming-a-balance-responsible-party/Imbalance-settlement-price.html, and its computation can be summarized in Table 4.3:

	French system imbalance	
BRP imbalance direction	**Upward needs**	**Downward needs**
Positive	$\lambda_w^{up} * (1 - \sigma_{\lambda_w^{up}} * k)$	$\lambda_w^{down} * (1 - \sigma_{\lambda_w^{down}} * k)$
Negative	$\lambda_w^{up} * (1 + \sigma_{\lambda_w^{up}} * k)$	$\lambda_w^{down} * (1 + \sigma_{\lambda_w^{down}} * k)$

Table 4.3: French imbalance settlement price computation

In this table, $\lambda_w^{\bullet}$ is the volume-weighted average price of balancing activations in the $\bullet$ direction. $\sigma_{\lambda_w^{\bullet}}$ indicates the sign of the weighted price ($= 1$ for a positive or null price, and $= -1$ for a negative price), and ensures that the ISP sends the same incentive to BRPs regardless of the sign of $\lambda_w^{\bullet}$. Finally, k is a coefficient "defined ex-ante with the aim of balancing income and expenditure of the energy component of the balancing-imbalances account based on historical data."[4]. This coefficient is occasionally updated, and has been set at 0.05 since 2019.

Since a single balancing process is used in these simulations–the RR market–, in practice there is no need for volume-weighted average prices in both directions. The only price of balancing energy activation is then the RR clearing price λ^{RR}, which simplifies the ISP computation in our simulations (Equation 4.1, with $k = 0.05$):

$$\forall u \in U, \ \forall t, \quad \begin{cases} \lambda_{u,t}^{ISP} = \lambda_t^{RR} * (1 - \sigma_{\lambda_t^{RR}} * k) & if \ \Delta q_{u,t}^{imb} > 0 \\ \lambda_{u,t}^{ISP} = \lambda_t^{RR} * (1 + \sigma_{\lambda_t^{RR}} * k) & if \ \Delta q_u^{imb} < 0 \end{cases} \tag{4.1}$$

A simplification is assumed in this framework. Indeed, the evolution of vRES power output forecasts between its order formulation of the RR market and the RR delivery period is not considered (it would correspond to a difference of 30 minutes). In practice, forecast evolution during this period could be problematic for a vRES unit that sold upward reserves on the RR market. It could lead to reserve delivery failure, which is usually penalized heavily. This notably concerns the *Self-balancing* behavior. Challenging this assumption will be discussed in future research avenues.

4.3.2 Input datasets

The long-term composition of the European power system is subject to many uncertainties, which will naturally impact the balancing stage. For time constraints reasons, we only studied one scenario for both the 2030 and 2050 time horizons, which is a limitation of this chapter. This limit should be addressed in further work, by considering additional long-term scenarios.

If a single scenario is considered, we believe that it makes sense to choose it to be as close as possible to European national projections. Indeed, given the high inertia of power systems evolution, current national projections and decisions can shape the system for several decades. Both datasets used in our simulations are extracted from RTE's *Energy pathways to 2050* (RTE, 2022), and are based on such national projections.

[4]From https://www.services-rte.com/en/learn-more-about-our-services/becoming-a-balance-responsible-party/Imbalance-settlement-price.html

The report constructed these scenarios from public documents that are part of the European Commission's Long-Term Strategies[5], and on simulations performed for ENTSO-E's Ten Year Network Development Plans.

The 2030 dataset is the same as the one previously used in Chapters 2 and 3. It was extensively described in Section 2.4.1.

For the 2050 horizon, the reference publication proposes several scenarios for the French power system development. The power systems of other countries remain the same across all scenarios. Out of these, the 2050 input dataset corresponds to the so-called N2 scenario. This choice was driven by the recent French political decisions regarding energy, which guided the development of the French toward the maintenance of nuclear assets. The N2 scenario fits this evolution, as it includes 37 GW of installed nuclear capacities in France.

Comparison of 2030 and 2050 hypotheses on power systems

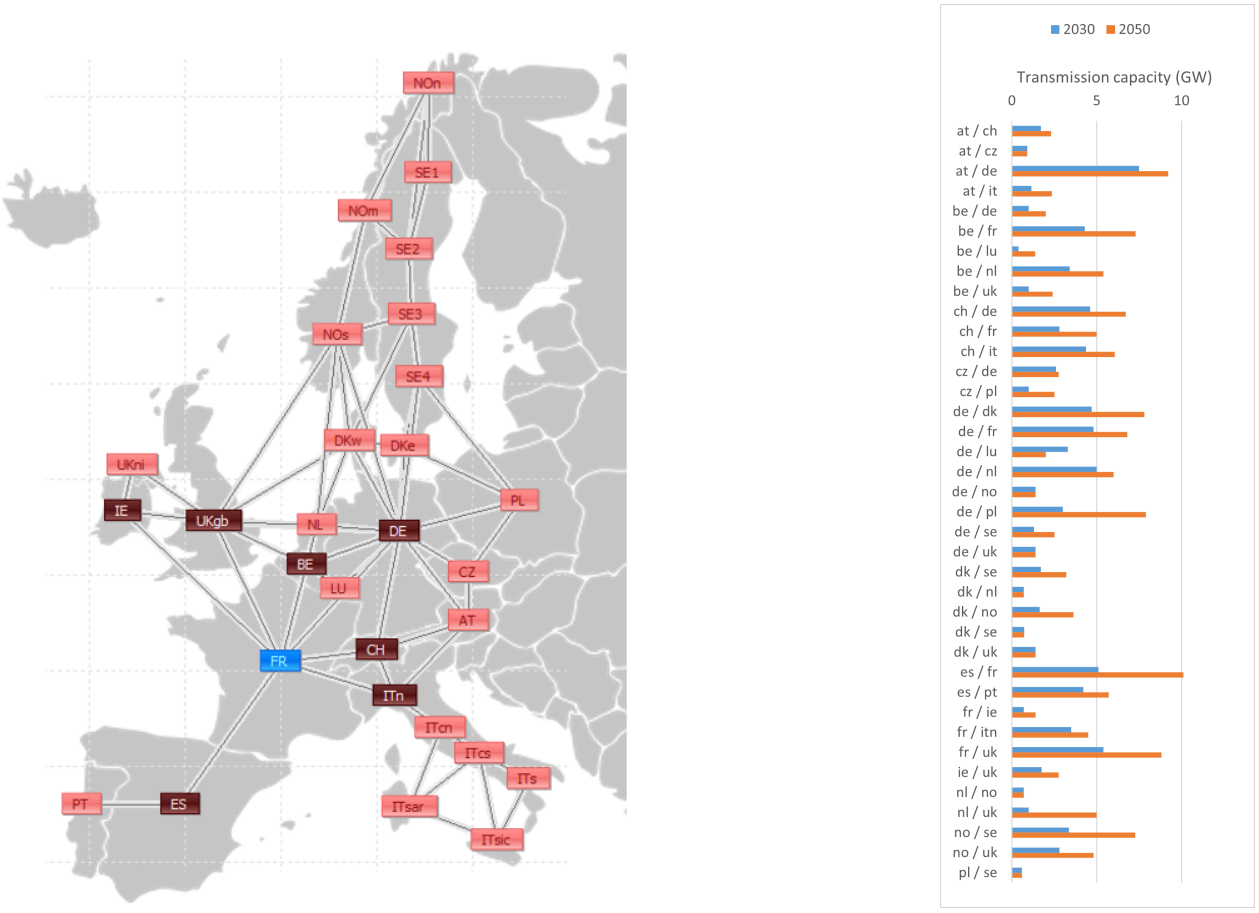

(a) European power system map

(b) Transmission capacities

Figure 4.3: Map of the European system in both datasets

The map of the European power system is identical between both time horizons, and includes 32 inter-

[5]Available at https://commission.europa.eu/energy-climate-change-environment/implementation-eu-countries/energy-and-climate-governance-and-reporting/national-long-term-strategies_en

connected market areas based on the current official European bidding zones (Figure 4.3a). In this study, we assume that balancing energy markets will be integrated in most European countries at the 2050 horizon[6]. The capacities of transmission lines also evolved between these two scenarios, which is represented in Figure 4.3b. For clarity purposes, and since local results presented in Section 4.4 are aggregated at the scale of each country, the evolution of internal transmission lines is not displayed here. As a general indicator, the total sum of European cross-border capacities is increased by 58%.

The European installed capacities of all technologies in both scenarios are compared in Figures 4.4a to 4.4c. Notable changes between these two scenarios are: (i) a decrease in installed capacities of thermal units, including a complete phase-out of oil- and coal-powered plants; (ii) an increase in storage capacities, especially for smart charging able electric vehicles[7] and usual batteries; (iii) an increase in flexible load, which is particularly strong for power-to-gas (P2G) units in this scenario; (iv) an increase of the inflexible load, represented by the peak load across all simulated periods, which is driven by the electrification of uses. Qualitatively, these evolutions are in line with the expected new flexibility types presented in the literature review (Section 4.2.2).

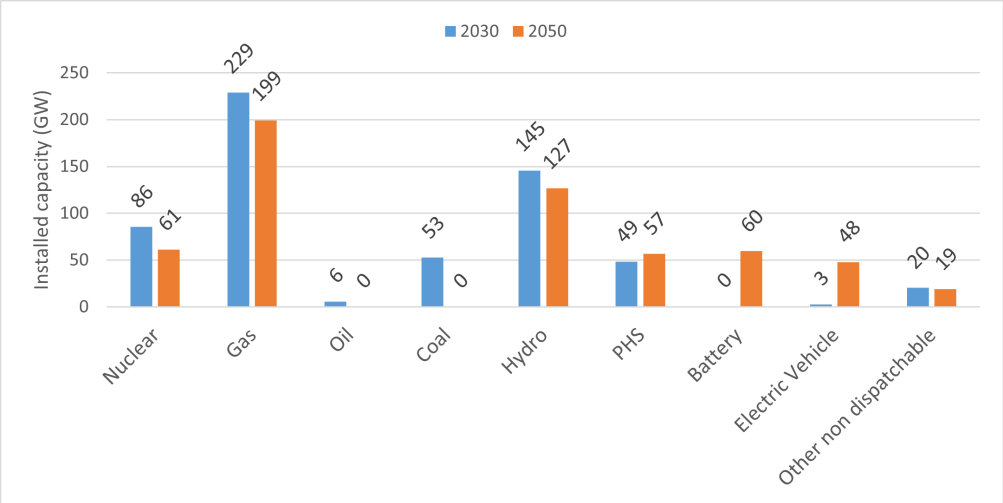

(a) Generation capacities (excluding vRES)

[6]Currently, common balancing markets are still in an integration phase. Only a subset of European countries are participating in them

[7]Other types of electric vehicles are classified as inflexible load.

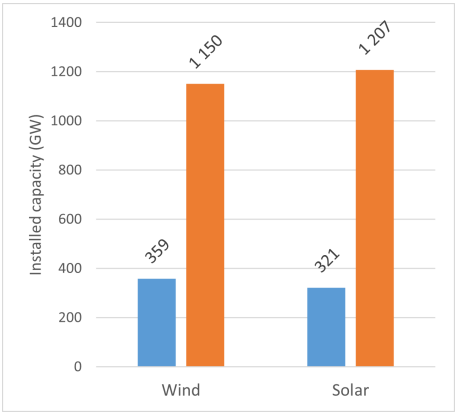

(b) vRES capacities

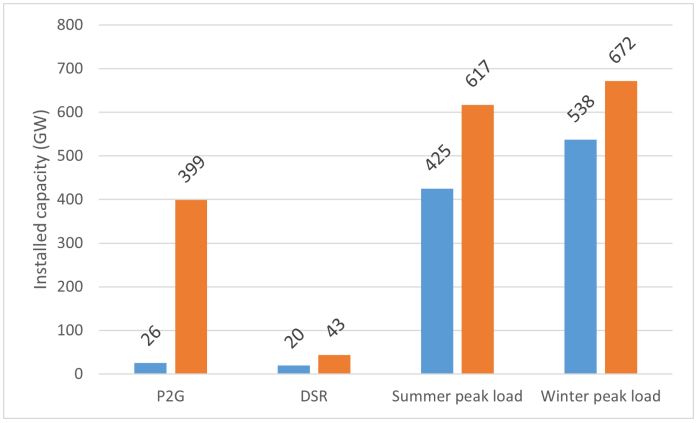

(c) Load capacities

Figure 4.4: Comparison of European installed capacities (in GW) between 2030 and 2050 datasets

The detail of installed capacities in all areas is provided in Appendix 4.A.

vRES forecasts and uncertainties

An important component of the simulations is the wind, solar and load evolutive forecasts, which represent the uncertainty associated with these technologies. In both datasets, an initial hourly load factor is estimated for each forecast-associated unit. Forecast errors at different time horizons are then generated for each unit, using a predictive function trained on historical forecast data and then applied to the initial load factor. The methodology is described in (Little et al., 2024).

Forecast errors resulting from applying this methodology in our datasets are illustrated in two sets of figures. They represent yearly boxplots of forecast errors at different lead times, for all areas:

- Figures 4.5 illustrate forecast errors between the day-ahead and the RR market for both input datasets. If we note ϵ_{DA-RR} this error, it corresponds to: $\epsilon_{DA-RR} = P_{DA}^{for} - P_{RR}^{for}$
- Figures 4.6 illustrate errors between the intraday market and the RR market: $\epsilon_{ID-RR} = P_{ID}^{for} - P_{RR}^{for}$. As a reminder, intraday markets are executed 2 hours before real-time in the simulations. As actors use them to rebalance their forecast evolution, this set of figures gives a relevant indication of the level of imbalances then faced by TSOs on RR markets.

For both lead times, the largest forecast errors are associated with wind plants, which matches the results of (Ortner and Totschnig, 2019). The uncertainty on solar power output is lower, and on average it tends to correspond to an overestimation. This indicates a small bias in the historical forecast data used to calibrate the predictive function. Once again, the same observation was made in (Ortner and Totschnig, 2019), indicating that this historical bias is reasonable. Finally, since the evolution of load consumption between 2030 and 2050 is much smaller than the evolution of wind and solar installed capacities, both time horizons exhibit similar forecast errors.

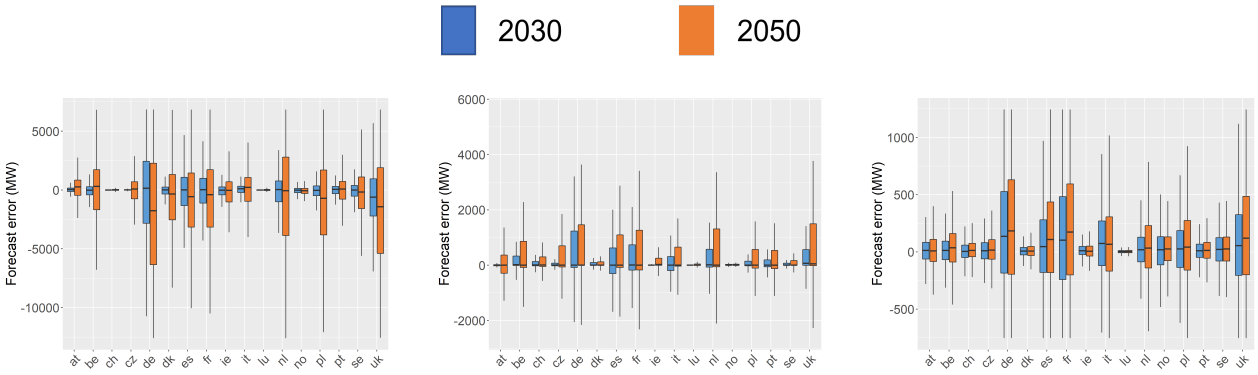

(a) Wind (b) Solar (c) Load

Figure 4.5: Forecast errors (in MW) between day-ahead markets and RR markets

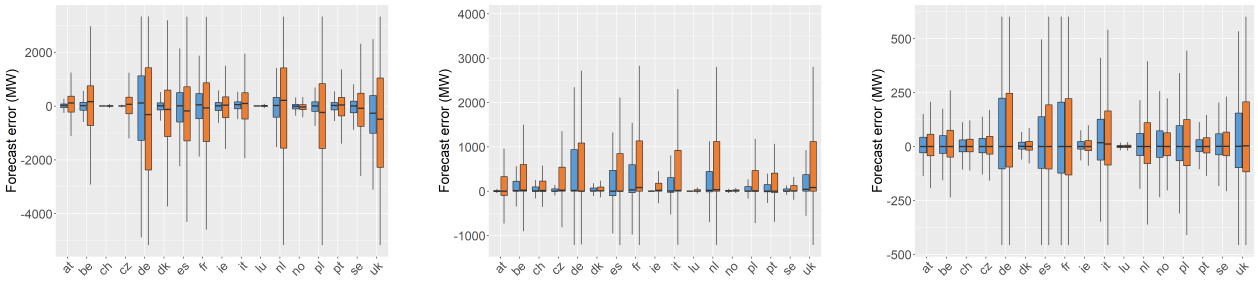

(a) Wind (b) Solar (c) Load

Figure 4.6: Forecast errors (in MW) between intraday markets and RR markets

We note that this modeling could be perfected in the future, by integrating improvements in forecast prediction accuracy for long-term scenarios, as well as geographical diversification within areas. Given that these changes are likely to reduce uncertainty, the current study should offer an upper bound of uncertainty (and consequently of balancing needs) at the 2050 horizon.

Load, solar and wind forecasts constitute the main source of uncertainty in the ATLAS model. Thermal unit outages were not modeled: they were deemed to have a rather low impact on overall imbalances in the 2030 European power system modeled by (Ortner and Totschnig, 2019). It is likely to be the case in our 2050 power system as well given the decreased installed capacities of thermal units. In addition, run of river hydraulic generation is modeled as deterministic, with inflows locally scaled to the 2050 horizon in each area (taking into account estimations of the local impact of climate change). Tables 4.5 and 4.6 of Appendix 4.A indicate that this scaling corresponds to a lower generation on average.

4.3.3 Hypotheses on the costs and flexibility of units

This section gives an overview of the assumptions taken to model the RR market bidding process of each technology type. A complete description of day-ahead and intraday market bidding processes can be found in (Little et al., 2024), while the balancing bidding is further detailed in Section A.2 of Appendix A.

The main hypothesis taken for this process is that units bid in a pure and perfect competition. It has two main implications *for our modeling*.

- All units bid at their true costs. For instance, thermal units directly rely on their variable and startup costs to estimate their true generation costs. Other types cannot rely on such tangible parameters– hydro or storage units notably–and need to consider intertemporal aspects in their cost computation, which requires the use of different methods.
- All units offer their entire available capacity in balancing energy markets, both in upward and downward directions. This is a strong assumption, notably in light of the empirical analysis of Chapter 3 that identified the current deficit of market orders submitted by French BSPs on the RR market. Consequently, the simulations will represent an upper bound of the supply curve, that could be achieved if all technologies are sufficiently incited to participate in balancing markets.

The market orders formulated by all actors respect the requirements and shape of standard RR orders presented in the general introduction.

Thermal units

In the model, thermal units reflect their generation cost with a combination of their variable and startup costs (Equation 4.2):

$$\forall u \in U^{th}, \ \forall t, \quad p_o = c_u^{var} + \sigma_o^{SU} \frac{c_u^{SU}}{P_{u,t}^{min} * \Delta t_m / 60} \tag{4.2}$$

With:

- o a market order.
- U^{th} the set of all thermal units.
- σ_o^{SU} a variable indicating if order o generates a startup ($= 1$), cancels a startup ($= -1$) or has no effect on the startup state ($= 0$)
- c_u^{var} and c_u^{SU} respectively the variable and startup costs of unit u.
- $P_{u,t}^{min}$ the minimum power output of unit u at time t.
- Δt_m the time step of market m (in our simulation, $1h$ for day-ahead and intraday markets, $15min$ for RR markets.

It is relevant to note that variable costs of gas-fueled units are assumed to change significantly between the 2030 and 2050 scenarios. In our 2030 dataset, they are powered by natural gas, and their variable cost is typically in the range [45 €/MWh, 80 €/MWh]. Meanwhile, in the 2050 dataset, these units are powered by biogas and hydrogen, which are assumed to be more expensive. The usual range of 2050 thermal units variable cost is then [100 €/MWh, 170 €/MWh].

The quantity of thermal unit offers is computed according to their initial power output, resulting from day-ahead and intraday markets, and to their operating constraints. To comply with RR standards, it uses coupling links to represent operating constraints when needed. All operating constraints analyzed in Chapter 2 are included in this process.

Hydro units

The bidding process of hydro units is based on their marginal storage value, which attributes an economical value to the energy currently stored in their hydraulic reservoir. Marginal storage values integrate the potential future value of the stored energy, and allow the unit to decide when to produce (if the marginal storage value is lower than market prices) and when to keep energy (if the marginal storage value is higher than market prices). These values are computed ex-ante for each area separately, using a method based on Bellman's algorithm (Bellman, 1966) which takes into account 20 yearly scenarios of local inflows and market price forecasts.

In ATLAS, hydro units are modeled by a single asset in each area. In practice, each individual hydro unit in a given area would compute its own water values, since each has a specific reservoir-size-to-power ratio. To account for this zonal simplification in the bidding process, clustered hydro units divide their available capacity into fragments priced around their calculated water value. Each fragment is then submitted individually on markets.

Finally, these units are considered to be highly flexible: they are only constrained by their maximum power output and reservoir levels.

Storage units

The intricacy of formulating storage units on balancing markets that only span over an hour is that, intrinsically, the offer or demand prices of these units depend on forecasts of market prices in other periods. Indeed, during the day-ahead market formulation, an optimization is performed over an extended period to compute storage offer prices for each hour of the studied day (Little et al., 2024). These prices are calculated to achieve at least neutral benefits over the extended period. During intraday processes, these prices are updated to account for the evolution of price forecasts (Little et al., 2024). For consistency reasons, the price of storage units on balancing markets is set to the average of all previous market clearing prices: in this case study, this corresponds to the average of day-ahead and intraday clearing prices.

Like hydro units, storage units are modeled as flexible assets, limited by their maximum and minimum power outputs and by their reservoir capacity. However, their minimum power can be negative, as they can both generate and consume electricity. In addition, their reservoir capacity is more constraining compared to hydro units, as their reservoir is typically much smaller.

vRES units

In our simulations, all wind (resp. solar) assets in a market area are gathered in a single unit. The minimum power output of this unit is modeled as a ratio of its actual maximum power output, to represent physical curtailment limits. For both time horizons, the curtailment limit of the aggregated wind power plant is set at 20% of its maximum output. This value corresponds to an approximation of the lower bound of wind generation, below which wind units have to stop. For the aggregated solar unit, the curtailment limit is set at 40% of their maximum output, which approximates the share of rooftop solar plants owned by individual users[8].

The quantity of vRES orders on RR markets depends on the type of bidding behaviors chosen, and on their forecast evolution between the last market cleared (in our simulations, the intraday market) and the execution date of the RR market. With the *Do-nothing* behavior, vRES units only submit downward orders,

[8]We assume that, as is the case today, the TSO ability to switch off diffuse solar power has not been put in place.

up until their curtailment limit. With the *Self-balancing* behavior, they first submit a self-balancing order that corresponds to the aforementioned forecast evolution. Then, they formulate a second order, which is the downward order up to their curtailment limit.

The price of vRES (wind and solar) RR orders is set to their variable costs of 0 €/MWh, except for the downward self-balancing order with is set to the price cap of the RR market, hence 10,000 €/MWh (as explained before in Section 4.3.1).

Power-to-gas units

In our simulations, power-to-gas (P2G) units are modeled as flexible load assets. Notably, we assumed that they are connected to a common hydrogen network, which allows us to define a variable cost based on hydrogen prices for each time step: the criteria upon which they decide to buy electricity or not is an arbitrage between the expected price on hydrogen markets and electricity prices. In our simulation, hydrogen prices are set exogenously based on data from (RTE, 2022).

Finally, these units are considered fully flexible, as they are only constrained by their maximum consumption. We also assume that they are willing to participate fully in RR markets. Both assumptions could be challenged in future work. Indeed, we currently lack sufficient knowledge on P2G modulation, notably on potential assets aging that could change either the physical flexibility or the behavior of P2G units. In addition, regulatory incentives could also impact their behavior.

Other load units

Demand side response is modeled as fully flexible, only limited by maximum and minimum level constraints. Their bidding price is exogenously set at a high value, 350 €/MWh for both time horizons.

Unflexible load units do not formulate offers on balancing markets in ATLAS. Their forecast evolution is taken into account in the TSO balancing needs (see next sub-section).

4.3.4 Hypotheses on balancing needs of TSOs

In these simulations, TSO balancing needs $bn_{z,t}$ in area z at time t correspond to their forecasted zonal imbalances over the delivery period T_{RR} of the RR market. In the regular case, i.e. the *Do-nothing* behavior for vRES units, balancing needs are computed according to Equation 4.3, which notably takes into account their latest forecast of vRES generation.

$$\forall z \in Z,\ \forall t, \quad bn_{z,t} = \sum_{u^l \in U_z^l} |P_{u^l,t}^{for}| - \Big(\sum_{u^g \in U_z^g} P_{u^g,t}^{plan} + \sum_{u^{RES} \in U_z^{vRES}} P_{u^{RES},t}^{for} \Big) \tag{4.3}$$

Where:

- $P_{u,t}^{for}$ is the latest forecast of unit u at time t.
- $P_{u,t}^{plan}$ is the generation plan of unit u at time t.
- U_z^l the set of all load type units in area z.

- U_z^g the set of all generation units in area z, except of vRES units.
- U_z^{vRES} the set of all vRES units in area z.

When vRES actors are using the *Self-balancing* behavior, two different computations can be considered depending on their communication with the TSO. Without any communication, the TSO proceeds as usual, following Equation 4.3. If the TSO knows about the self-balancing orders, he will instead compute its needs according to Equation 4.4, by considering the latest generation plan of vRES actors (and not their forecast).

$$\forall z \in Z, \ \forall t, \quad bn_{z,t} = \sum_{u^l \in U_z^l} |P_{u^l,t}^{for}| - \Big(\sum_{u^g \in U_z^g} P_{u^g,t}^{plan} + \sum_{u^{RES} \in U_z^{vRES}} P_{u^{RES},t}^{plan} \Big) \tag{4.4}$$

Finally, TSOs are modeled as price-inelastic in these simulations. While the results from the previous chapter showed potential gains from price-elastic TSO bidding, calculating these bidding curves is computationally expensive. Additionally, they demonstrated that using this type of bidding strategy requires precise estimations of the alternative costs, which cannot currently be provided for a dataset at the 2050 horizon. For this analysis therefore, we simulate only the RR market to treat the full imbalance, ignoring the alternatives discussed in the previous chapter, and as a consequence, choose not to include price-elastic bidding for TSOs.

4.4 Results and discussion

The case study results are presented and discussed in this section. First, we provide a comparison between 2030 and 2050 datasets, considering only the *Do-nothing* vRES bidding behavior (Section 4.4.1). The impact of the two vRES behaviors is then presented in Section 4.4.2.

4.4.1 Comparison of 2030 and 2050 time horizons

4.4.1.1 Balancing markets inputs: Energy needs and bids

We first quantified the evolution of market inputs, and more precisely the volume of TSO balancing needs and the characteristics of BSP supply curves.

TSO balancing needs

The average hourly volume of TSO balancing needs at the European scale is represented in Figure 4.7. As expected, absolute balancing needs (the sum of full and striped sections) increase significantly between the two scenarios. The volume of downward balancing needs[9] in the winter period is particularly high, which is a consequence of a skewed wind forecast evolution during this period (discussed later on).

This increase in absolute needs is already partially compensated by the increased benefits of the netting between market areas. The netting corresponds to TSO-TSO orders activation, in which the energy deficit

[9]Downward needs correspond to an excess of generation in the TSO control area, while upward needs correspond to a deficit of generation.

of a TSO is directly compensated by the energy excess of another one[10]. The striped sections in both graphs represent the average netting volume, which is improved by 250% to 400% (depending on the period and direction) between 2030 and 2050 in our scenarios. However, in the end, the final balancing needs (post-netting) are still considerably larger in 2050 compared to 2030.

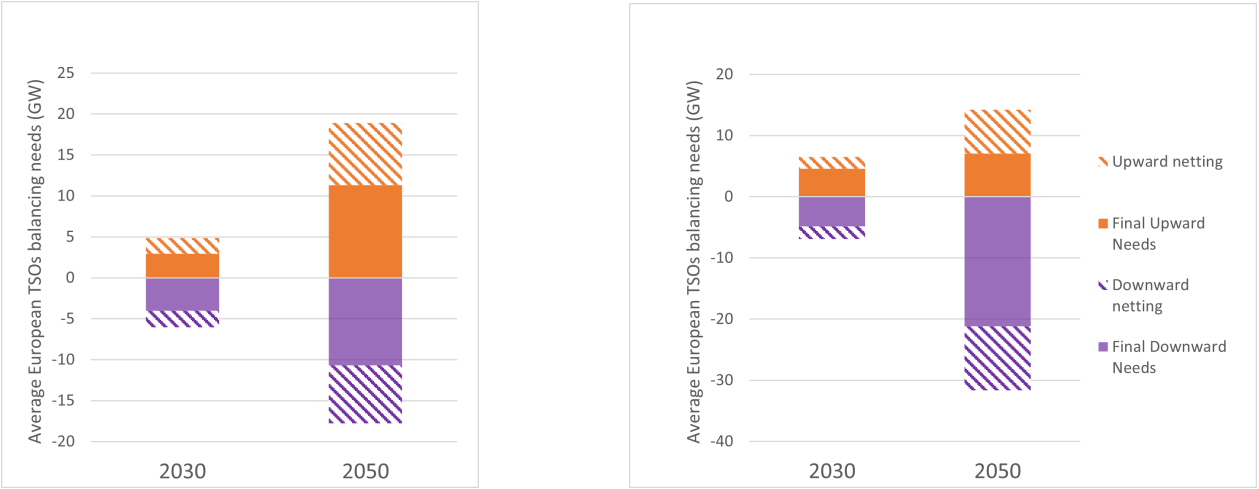

(a) Summer period

(b) Winter period

Figure 4.7: Hourly BSP submitted volume - European

Previous graphs displayed balancing needs aggregated at the European scale. By scaling down, noteworthy differences between areas can be observed in the absolute need boxplots of Figures 4.8 and 4.9. The volume of balancing needs is correlated with the installed capacity of vRES capacities and their forecast errors:

- Wind units have a higher load factor in winter, which translates to a greater impact on balancing needs. This can be clearly seen for Germany in the 2050 winter period (Figure 4.9b), as they possess by far the largest wind capacities. On top of this, we can also observe in the same sub-figure the skewed wind power forecasts that were previously evoked: in Germany notably, but also in the United Kingdom or the Czech Republic for instance, balancing needs are mostly downward during the 3 days simulated.

- On the contrary, the impacts of the load factor and of solar units are higher in summer. This explains why Italy, with its significant solar capacities, faces higher balancing needs in the 2050 summer period (Figure 4.8b)

[10] Assuming that they are linked by a non-congestioned transmission line.

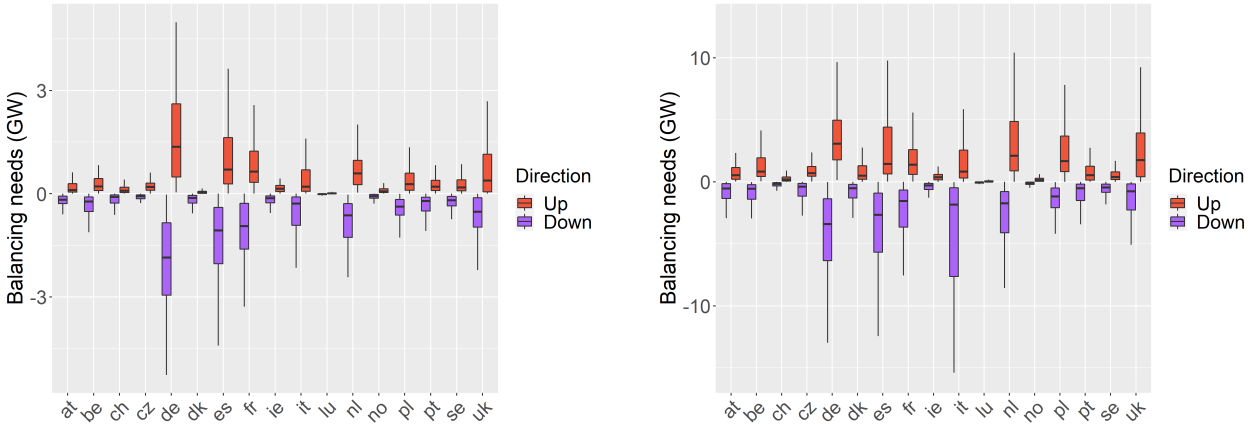

(a) 2030 (b) 2050

Figure 4.8: TSO balancing need boxplots per area - Summer period

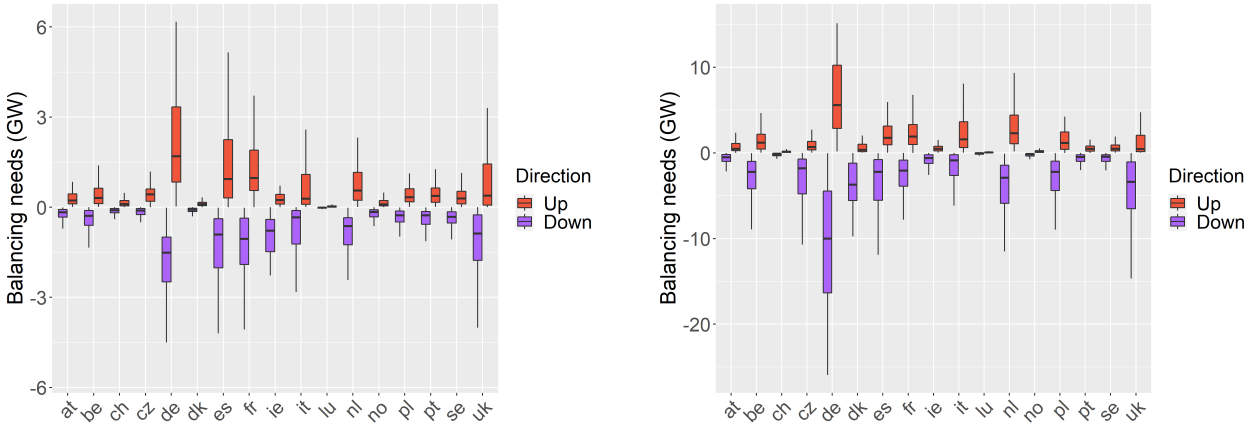

(a) 2030 (b) 2050

Figure 4.9: TSO balancing need boxplots per area - Winter period

BSP offer curves

The average hourly volume submitted by BSPs in the entire European system is represented in Figure 4.10, for both periods. To complement the averages of the aggregated figure and provide a view of the actual shape of the supply curves, two additional sets of figures are presented: (i) separated upward and downward supply curves for a subset of specific time steps, in which the different technologies are depicted (Figures 4.11), and (ii) bundles of European offer curves for all time steps simulated in Figure 4.12.

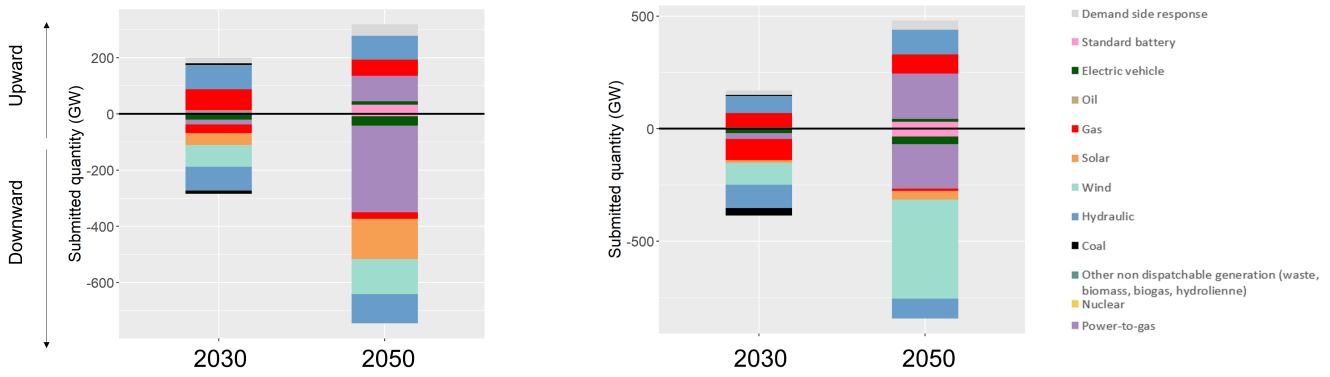

(a) Summer period (b) Winter period

Figure 4.10: Hourly BSP submitted volume - European

There is a substantial increase in volumes offered between 2030 and 2050, in both directions and for both seasons (in volume, a 59% increase for upward reserves and 162% increase for downward reserves in the summer period; 185% increase for upward reserves and 118% increase for downward reserves in the winter period).

Two main categories of technologies drive this increase:

- The power-to-gas units account for a large share of offered volumes in our 2050 simulation, in both directions. This can be explained by three main assumptions: the large installed capacities in the input dataset, their complete flexibility (described in Section 4.3.3) which makes them able to participate in all balancing energy markets, and the fact that they offer their entire available capacity (i.e. they are economically incited to participate in balancing markets). We can also observe in Figure 4.11 that power-to-gas units generate wide levels within BSP offer curves (purple sections), which implies that they are more likely to be the price setters than other types of technologies.

- vRES (wind and solar) units are the main providers of downward reserves in terms of volume. However, as 4.11b illustrates, the price of their downward orders is set to their variable cost of 0 (orange and light blue sections). It places them at the tail end of the "buy" curve, and they consequently serve as a last resort to answer downward balancing needs. The type of season also directly impacts the availability of vRES units, with solar units mostly participating in the summer while the participation of wind units is accentuated during the winter period.

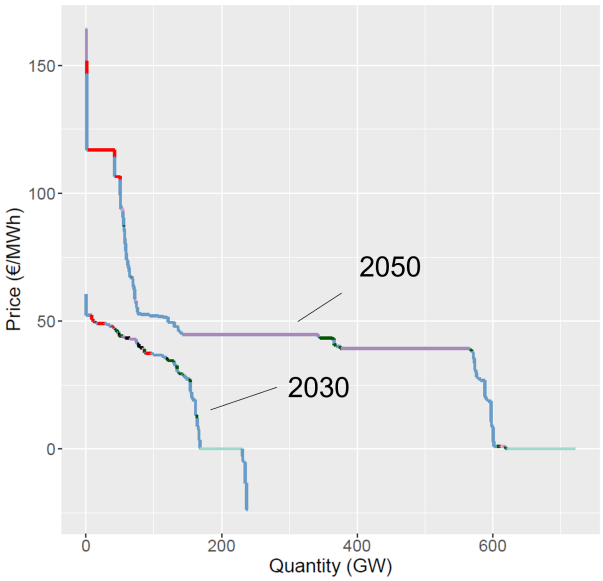

(a) Summer period, 04h00 of the first day (buy curve)

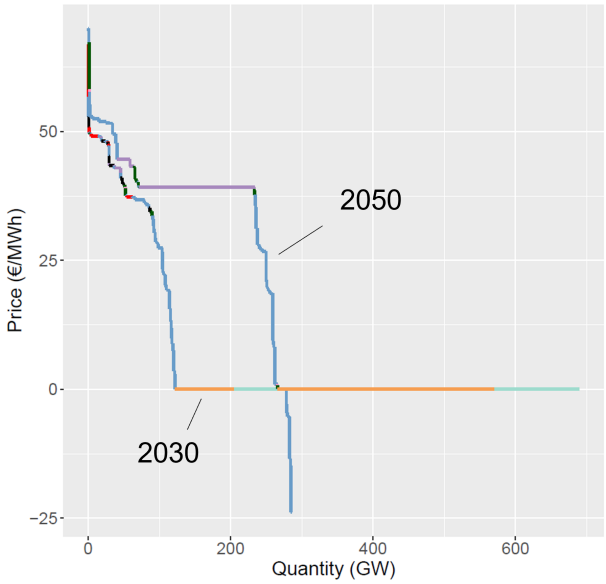

(b) Summer period, 14h00 of the first day (buy curve)

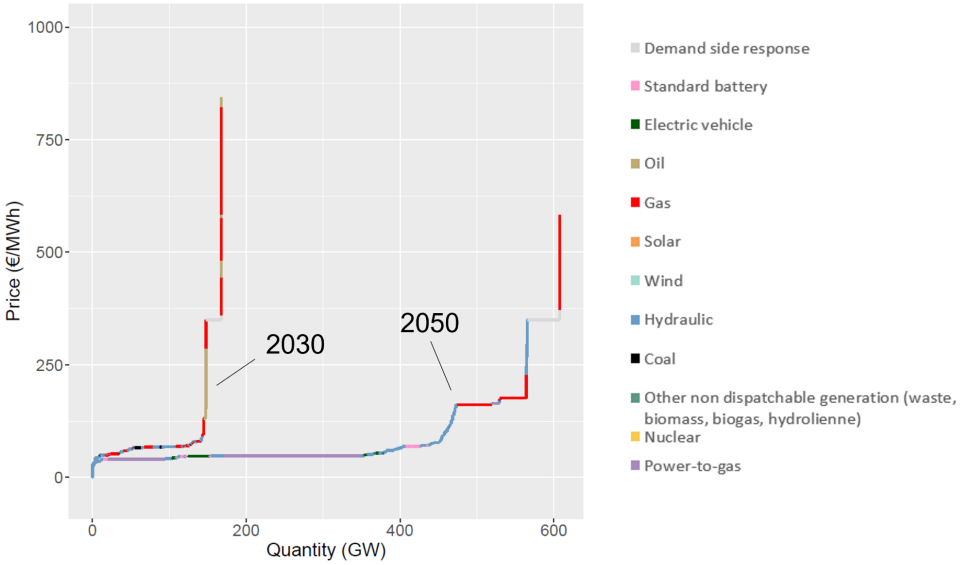

(c) Winter period, 12h00 of the first day (sell curve)

Figure 4.11: Specific examples of BSP offer curves

The other types of technologies also experience changes between the two time horizons:

- The volume of reserves offered by thermal units is decreasing, albeit still important in the upward direction in 2050.
- Storage units play a larger role in the 2050 offer curves in both directions (electric vehicles and standard batteries notably).
- The demand-side response also has a notable contribution to the total volume of BSP upward orders in our 2050 scenarios, when it was almost not contributing in 2030. It acts as a last-resort option given

their position in the offer curve (grey sections of the offer curves in Figure 4.11c as an example).

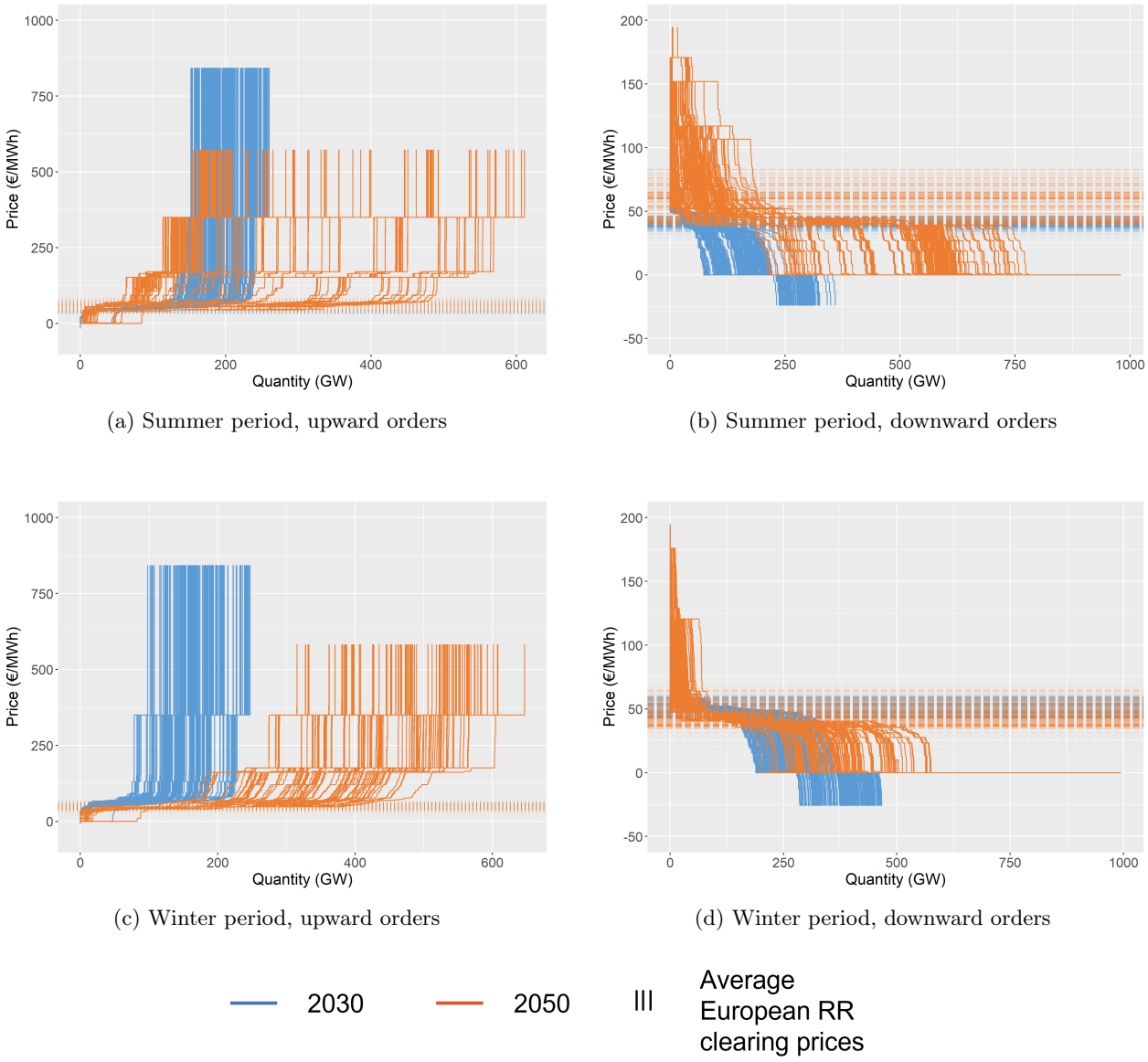

(a) Summer period, upward orders

(b) Summer period, downward orders

(c) Winter period, upward orders

(d) Winter period, downward orders

Figure 4.12: BSP offer curves bundles

The bundles in Figures 4.12 gather the supply curves of all simulated time steps for a given scenario, along with the range of average RR clearing prices across all areas. These figures can help in visualizing the variability of both supply curves and market prices. First, supply curves are mostly shifted "to the right" in 2050. They also usually display lower average prices for upward curves, and higher average prices for downward curves. A notable exception to these observations is the first group of upward curves in the 2050 summer period (Figure 4.12a), which appears to be shifted "to the left" compared to 2030. This could result in higher market prices and balancing costs for this scenario. We also see that the spread between all order curves in a scenario is much greater at the 2050 horizon. This important spread is caused by the availability of the main flexibility drivers described previously (power-to-gas and vRES). Finally, the RR market price

variability is increased for both seasons. It is notably visible in the downward order curves (on the right side), where the range of prices is easier to see.

Overall, the main conclusions extracted from the analysis of RR market inputs are the following. The absolute volume of balancing needs increases between 2030 and 2050, but it could be compensated by two components on the market. First, by the increased value of netting between areas, which is achieved thanks to investments in transmission capacities between the two time horizons. Then, by the increase in the volume of BSP offers submitted to the market, which depends on the ability to encourage the participation of new technologies in balancing energy markets. However, these results of market inputs need to be confirmed by analyses of market outputs, which is the purpose of the next section. Indeed, because of possible congestion in transmission lines between areas, parts of the supply and demand curves may only be available in specific areas.

4.4.1.2 Balancing market outputs

As a first and important market outcome, TSO balancing needs are always entirely accepted by RR markets in our simulations, for all scenarios with the *Do-nothing behavior*. This validates the observations made in the previous section, about the ability of these markets to cope with the increase in balancing needs. However, it is still tied to the participation of new technologies in the market. As a sensitivity analysis, we simulated the 2050 scenarios with no RR orders from vRES, power-to-gas, demand-side response and new storage assets (electric vehicles and batteries). These simulations exhibit multiple instances of reserve shortage, in approximately 5% of time steps.

TSO balancing costs

TSO balancing costs have been computed according to the following equation (previously used and described in Chapter 2, Section 2.5.2.2):

$$c^{TSO} = \sum_{t} \sum_{i \in Z} \left[\sum_{o \in O_{i,t}^{TSO}} q_o^{acc} * (-\sigma_o) * \lambda_{t,i} - \sum_{mb_{i,j} \mid j \in Z} (\lambda_{t,i} - \lambda_{t,j}) * (\Delta q)_t^{mb_{i,j}} \right] * \frac{\Delta t_m}{60} \tag{4.5}$$

Where:

- Z is the set of all market areas.
- $O_{i,t}^{TSO}$ is the set of all TSO orders on area i at time t.
- q_o^{acc} is the quantity accepted by the market on order o, and σ_o its direction ($\sigma_o = -1$ for buy orders, and $\sigma_o = 1$ for sell orders).
- $\lambda_{t,i}^{RR}$ is the RR market clearing price at time t in area i.
- $mb_{i,j}$ is the market border between areas i and j.
- $(\Delta q)_t^{mb_{i,j}}$ is the power flow in market border mb_{ij} (from i to j) at time t.
- Δt_{RR} is the time step of the RR market, i.e. 15 minutes.

Figure 4.13 displays the average hourly TSO balancing costs for each area, with the European average indicated with the dashed lines. The 2030 horizon is displayed in blue and the 2050 horizon in orange. The

following convention is chosen: positive balancing costs indicate actual spending for TSOs, and negative costs indicate revenues.

The evolution of average TSO balancing costs is not easy to quantify. It depends on the seasons and on overall balancing needs. In the 2050 winter period, balancing costs are negative for most TSOs in Europe. This is logical given that average balancing needs were in the downward direction during this period, because of the aforementioned skewed wind forecast. In summer, costs are increasing on average between the 2030 (-3.6 k€/h) and 2050 (10.8 k€/h) scenarios, even though overall balancing needs were mostly equilibrated between upward and downward directions (Figure 4.7a). This last result indicates that balancing could be more expensive in the future in certain situations, even if the RR markets ensure the security of supply thanks to the large pool of reserves.

The most important observation is the significant variability of balancing costs in both periods at the 2050 horizon, as they can reach very high values in both directions. This is especially amplified in areas with large capacities of wind units: Germany is the prime example, along with Spain, France, Italy, the Netherlands and the United Kingdom.

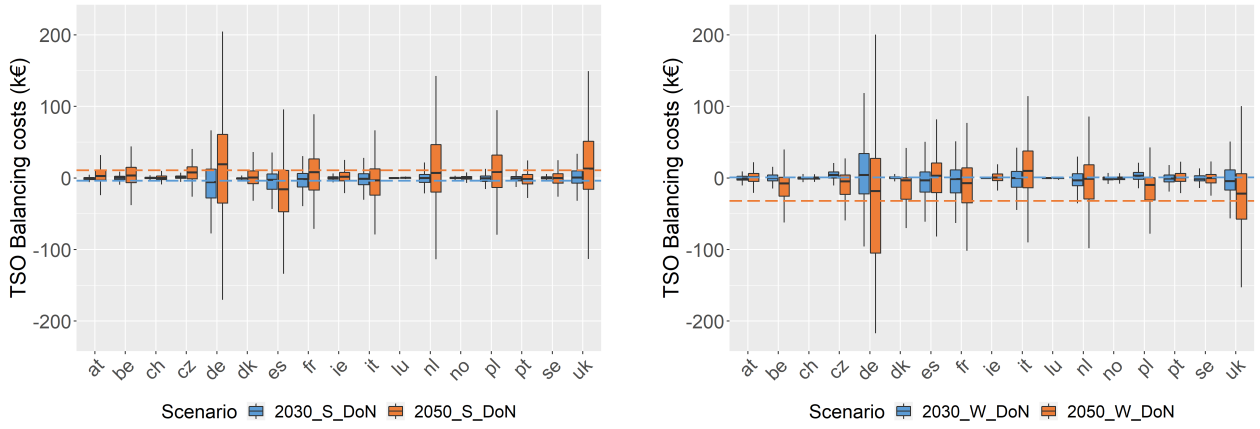

(a) Summer

(b) Winter

Figure 4.13: TSO balancing costs boxplots per area

Overall social welfare

Since TSO balancing needs are formulated as price inelastic, the social welfare is computed as the sum of the BSP surplus and TSO balancing costs (see Section 2.5.2.2 of Chapter 2 for more details). Its daily value across all areas is represented in Figures 4.14 (summer period) and 4.15 (winter period). On these graphs, the TSO balancing costs are represented negatively (positive values indicate revenues for TSOs). Two main results are consistent:

- The overall social welfare is positive in all scenarios. It indicates that the welfare generated by BSP-BSP order activations, i.e. the dispatch optimization performed by the RR market, is greater than the costs induced by activations to resolve imbalances. This is in line with the findings of (Marquet, 2018).
- The surplus of BSPs is rising between 2030 and 2050, due to (i) the increase in the volume of balancing needs accepted, and consequently in the volume of BSP orders accepted to resolve them, and (ii) an

increase in the volume of dispatch optimization performed by the RR market. In both periods of the 2050 horizon, the volume of BSP-BSP order activation increases by 250% to 300% compared to the 2030 horizon. The second aspect can be linked to the increase in the overall system variability. Indeed, the dispatch resulting from previous markets is more likely to be sub-optimal considering the new forecasts. Its re-optimization in the RR market can induce significant interzonal variations. This is illustrated in Appendix 4.B, which provides additional analyses of the export-import balances and transmission line usage rates. It notably shows that the latter increases between our 2030 and 2050 scenarios.

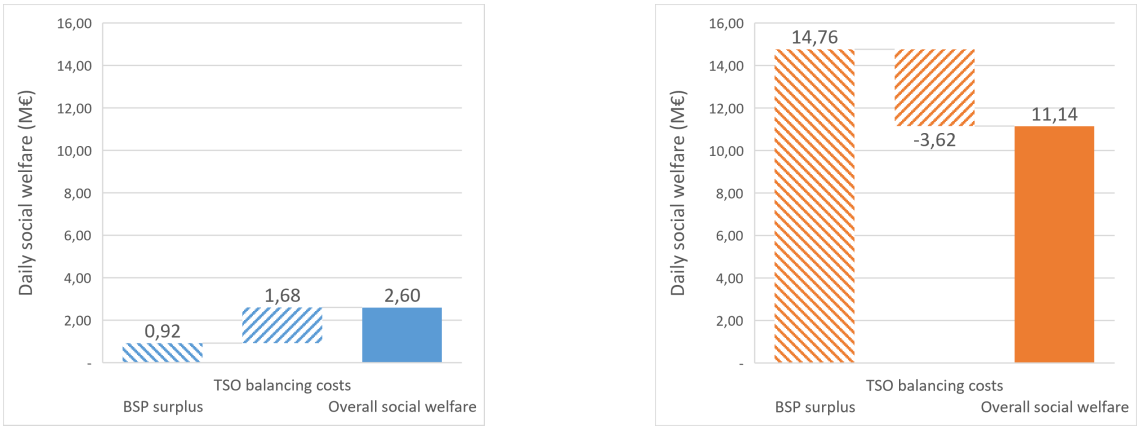

(a) 2030 (b) 2050

Figure 4.14: Daily social welfare - Summer period

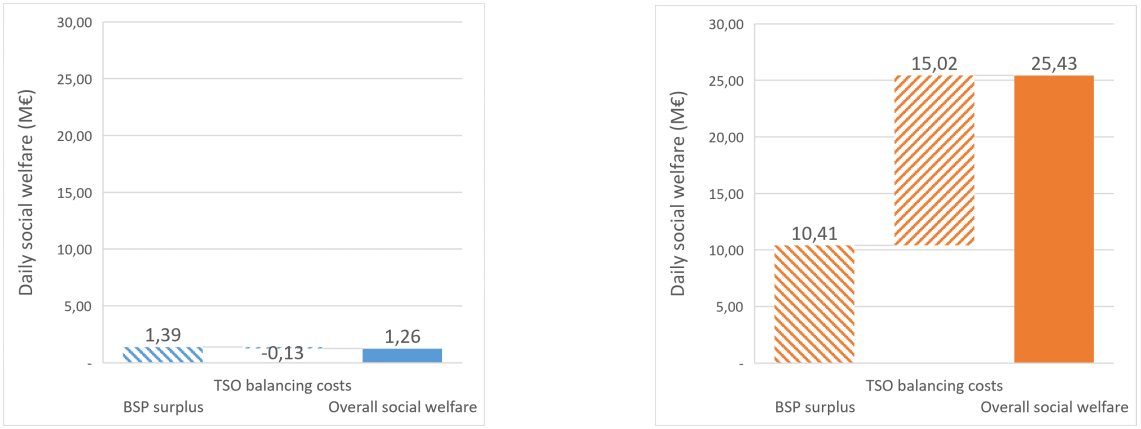

(a) 2030 (b) 2050

Figure 4.15: Daily social welfare - Winter period

To summarize this section, the key findings about market outcomes are the following:

- All TSO balancing needs are entirely accepted in all scenarios, which validates the performance of the RR market in mitigating the increase in balancing needs. However, this result is tied to the significant participation of new flexibilities.

- The impact on average balancing costs is unclear, but their variability is heavily accentuated by the energy transition. Areas with large installed capacities of vRES are particularly impacted by this phenomenon.
- In all scenarios, the overall social welfare is increased between 2030 and 2050. This increase is driven by the growing interest in near real-time re-optimization associated with vRES variability. This re-optimization can be performed by the RR market through BSP-BSP orders activation.

4.4.2 Impact of the vRES behavior

The current section focuses on the changes induced by the different types of vRES bidding behavior at the 2050 horizon. As a reminder, all results previously discussed correspond to a scenario with the *Do-nothing* behavior (indicated by a "DoN" suffix in the rest of this section), for which vRES actors do not try to rebalance themselves on the RR market. Additional simulations at the 2050 horizons were performed, with the *Self-balancing* behavior vRES actors: they formulate RR market orders to compensate for imbalances stemming from their forecast evolution (scenarios with a "Self" suffix). Two variants are considered for this behavior, one with BSP-TSO communication and another without (the latter being indicated with an additional "NC" suffix). To lighten the figures, the no communication variant is only displayed when relevant (notably, it does not affect supply curves).

TSO balancing needs and BSP offers

Figure 4.16 represents the TSO balancing needs for both seasons. The left scenario is the *Do-nothing* behavior, the middle is the *Self-balancing* behavior with BSP-TSO communication and the right scenario is the *Self-balancing* behavior without BSP-TSO communication.

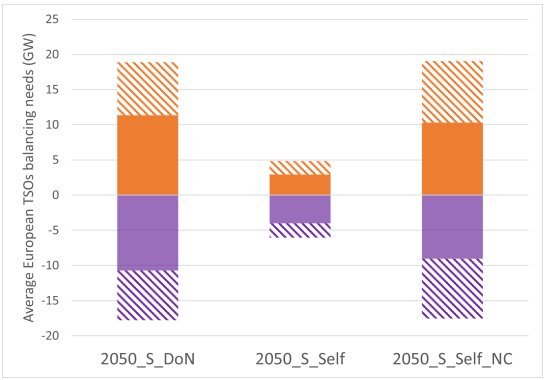

(a) Summer period

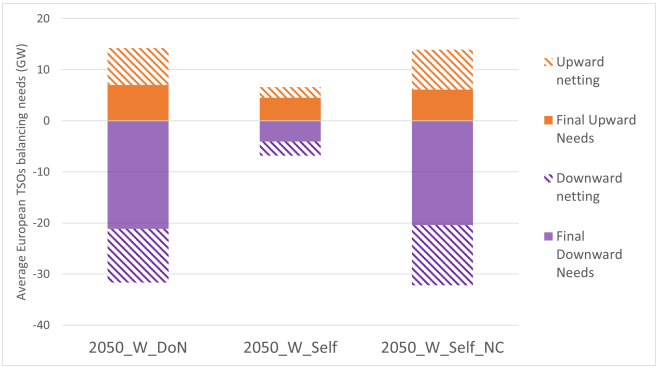

(b) Winter period

Figure 4.16: Hourly TSO balancing needs with vRES behaviors - European

The evolution of balancing needs between *Do-nothing* and *Self-balancing* scenarios is significantly affected by the communication hypothesis:

- With BSP-TSO communication, the amount of TSO balancing needs is greatly reduced in both directions. Indeed, vRES actors internalize their imbalance with this behavior, meaning that TSOs only have to consider (i) load forecast evolution and (ii) imbalances resulting from BRPs deviating from

previous market commitments. On average, absolute TSO balancing needs are reduced by 53% up to 78%, while netted TSO balancing needs are reduced by 35% up to 81%.

- Meanwhile, balancing needs for the *Self-balancing* behavior without BSP-TSO communication are equal to those of the *Do-nothing* scenario. This is logical since TSOs use the same balancing needs computation method in both scenarios (they take into account their forecast of vRES units power output). It illustrates the fact that TSOs are still trying to compensate for the imbalance that BSPs offer in the RR market, which will impact market results.

If we focus on the supply side, the average overall volume of BSP offers is not significantly changed between both behaviors (Figure 4.17). The scenario without BSP-TSO communication is not displayed here, since the supply curves are not affected by the communication variant. There is a slight shift from downward orders to upward orders between both behaviors. The volume of this shift corresponds to the excess of energy due to forecast evolution in the upward direction. With the *Do-nothing* behavior, vRES simply follow their forecast, and this volume is consequently offered as regular downward orders. Meanwhile, with the *Self-balancing* behavior, vRES units offer this volume as self-balancing upward orders on the RR market.

(a) Summer period (b) Winter period

Figure 4.17: Hourly BSP submitted volume with vRES behaviors - European scale

As for the actual shape of BSP offer curves, we can exhibit larger differences between scenarios in both directions. Figure 4.18 illustrates this by looking at the supply curves for noteworthy steps of the summer period, characterized by high vRES forecast evolution. For a better display, the price of self-balancing buy orders are set to 300 €/MWh *in these figures only* (their actual price in our simulation is still 10,000 €/MWh). With the *Self-balancing* behavior, supply curves are shifted to the right compared to the curves of the *Do-nothing* behavior. It is notably important to remark that all self-balancing orders are placed at the beginning of supply curves, meaning that they are the first orders accepted by the RR market, according to the common merit order list. This position is induced by the order prices chosen in our simulations (see Section 4.3.3), and reduces the risk in security of supply associated with these self-balancing orders. In contrast, if they were placed further to the right of supply curves, the possibility of being rejected by the clearing process on a purely economical basis would be greater, resulting in possible security of supply issues.

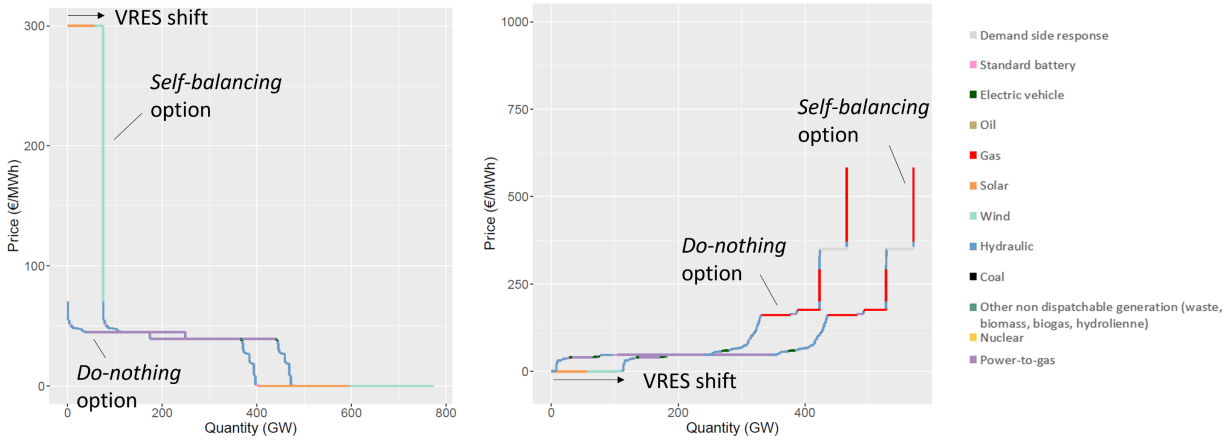

(a) Buy curves (b) Sell curves

Figure 4.18: Specific examples of BSP offer curves

Market outcomes: vRES revenues and balancing costs

When looking at market outcomes, several aspects are notable.

First, the overall revenues of vRES actors in balancing processes are computed for both scenarios, to evaluate if this behavior is profitable for them. For a given unit u, these revenues correspond to the sum of two terms: (i) the sum of its revenues and costs on the RR market, and (ii) the results of the imbalance settlement process conducted after the RR market (Equation 4.6).

$$Rev_u = \sum_t \left[\sum_{o \in O_{u,t}} \sigma_o * q_o^{acc} * \lambda_t^{RR} + \Delta q_{u,t}^{imb} * \frac{\Delta t_{RR}}{60} * \lambda_{u,t}^{ISP} \right] \tag{4.6}$$

Where:

- $O_{u,t}$ is the set of RR market orders of unit u at time t.
- σ_o is the direction of order o, and is equal to 1 for sell orders and -1 for buy orders.
- q_o^{acc} is the quantity accepted by the RR market on order o.
- λ_t^{RR} is the RR market clearing price at time t.
- $\Delta q_{u,t}^{imb}$ corresponds to the power imbalance on unit u at time t, calculated as the difference between the final power output and the sum of all market commitments.
- $\lambda_{u,t}^{ISP}$ is the imbalance settlement price detailed in Section 4.3.1.

Figure 4.19 plots the difference between (i) hourly balancing revenues of vRES actors in scenarios with the *Self-balancing* behavior (light green represents the variant with BSP-TSO communication, and dark green the variant without) and (ii) hourly balancing revenues of vRES actors with the *Do-nothing* behavior. Formally, the information displayed corresponds to $\sum_u Rev_u^{Self} - Rev_u^{DoN}$, using the revenue formulation described above. A positive value indicate that the *Self-balancing* scenario is more profitable than the *Do-nothing* scenario.

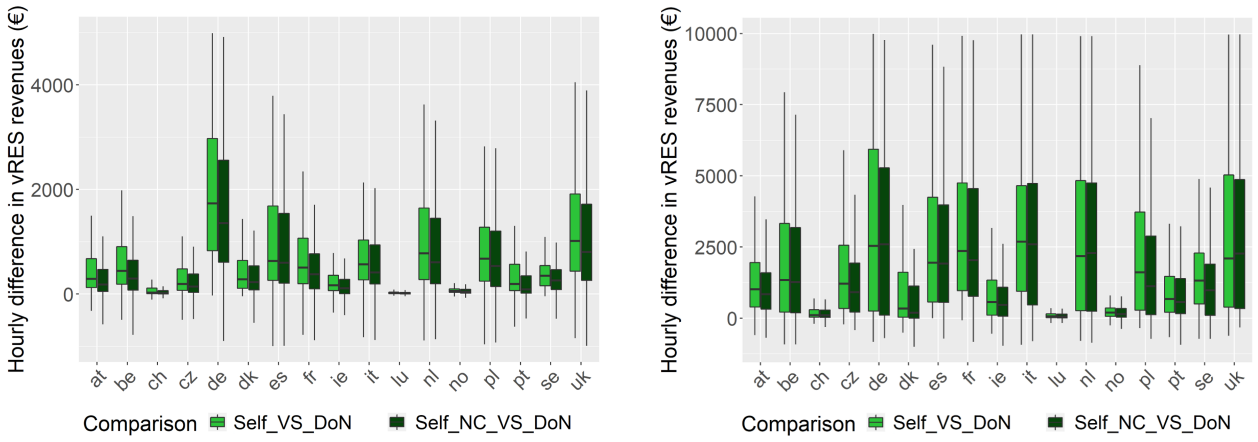

(a) Summer period

(b) Winter period

Figure 4.19: Differences in hourly balancing revenues for vRES actors with the different bidding behavior

For both types of BSP-TSO communication, the *Self-balancing* behavior yields benefits over the majority of time steps. Consequently, we believe that it should be an attractive option for vRES units.

However, the variant without BSP-TSO communication brings additional risk for the acceptance ratio of self-balancing orders. Indeed, while all self-balancing orders are entirely accepted with BSP-TSO communication, it is not the case for the variant without since they can "compete" with the TSO balancing needs (as they cover the same imbalance). The number and quantities of self-balancing orders not entirely accepted are indicated in Table 4.4, with a distinction between upward (sell) and downward (buy) orders. This is an important distinction since both are not formulated at the same price, which defines the clearing price of their area because these orders are marginal. As a reminder, upward self-balancing orders are formulated at 0 €/MWh, while downward self-balancing orders are formulated at 10,000 €/MWh which can lead to extreme RR prices. In our simulations, the rejected downward orders are all from market areas in the south of Italy: this is a consequence of the large amount of solar capacity installed in this region, and of its relatively low interconnection state. As represented in the power system map of Figure 4.3, this region is only connected to other European areas through the ITn (Italy north) market area, and can be isolated if the ITcn-ITn transmission is saturated.

Period	**Upward (number)**	**Upward (total volume)**	**Downward (number)**	**Downward (total volume)**
Summer	71	199,234	2	1,041
Winter	32	74,996	12	12,667

Table 4.4: Number and total quantity (in MW) of self-balancing orders not entirely accepted for the *Self-balancing* scenario without BSP-TSO communication

If we now focus on systemic impacts, Figure 4.20 plots the boxplots of TSO balancing costs for all 2050 scenarios. Two main observations can be made when comparing the *Do-nothing* scenario with both *Self-balancing* scenarios:

- With BSP-TSO communication, the variability of TSO balancing costs is greatly reduced (light green boxes). This observation is consistent across all areas and in both summer and winter: the interquartile[11] is reduced in every area, on average by 58%. Balancing costs are also much more centered around 0 with the *Self-balancing* behavior, as shown by the dotted lines representing the average hourly values.

- Without BSP-TSO communication, the variability of balancing costs is still rather high (dark green boxes). In addition, average balancing costs are higher for both seasons, driven by occasional high RR clearing prices induced by the marginal self-balancing orders previously presented.

(a) Summer (b) Winter

Figure 4.20: Balancing costs for both vRES bidding behaviors

In terms of social welfare, the difference between behaviors is less pronounced. This is represented in Figure 4.21, which aggregates both periods as they lead to the same conclusions. The scenario without BSP-TSO communication is not included in the social welfare analysis: since it artificially generates a larger volume of orders because of the overcompensation of balancing needs, it cannot be easily compared to the other scenarios. The overall social welfare with the *Self-balancing* behavior with BSP-TSO communication is slightly reduced compared to the *Do-nothing* behavior. A moderate welfare transfer from TSOs to BSPs is also found.

[11] The interquartile corresponds to the difference between quantiles 0.25 and 0.75 (i.e. the size of the colored box of each boxplot on the graph).

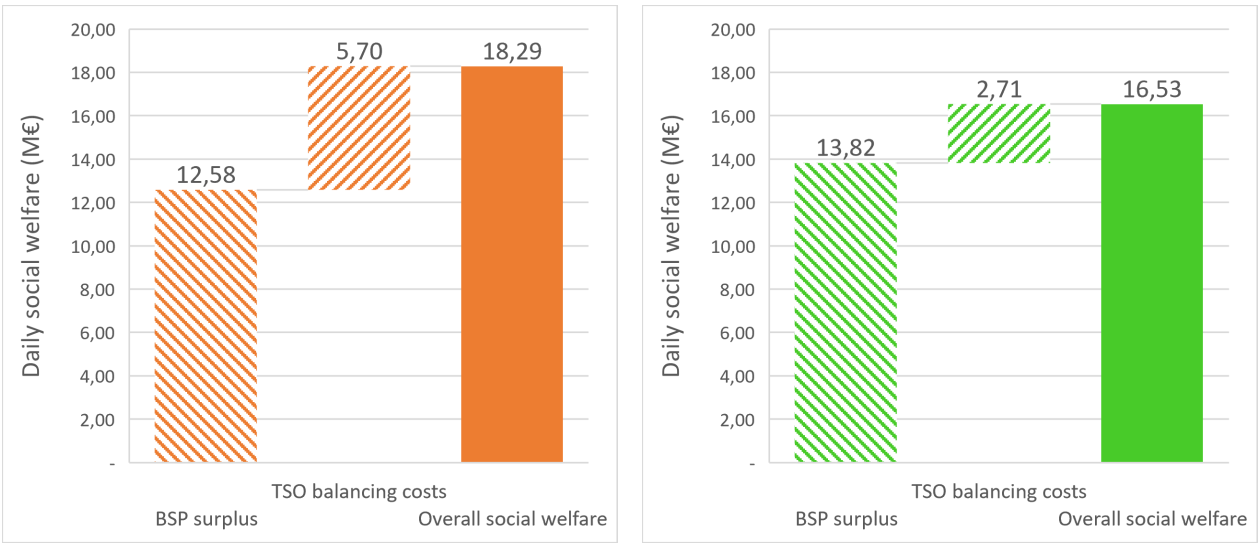

(a) *Do-nothing* behavior

(b) *Self-balancing* behavior

Figure 4.21: Daily social welfare over both summer and winter

Finally, the last important result is the imbalances in each area *after* the RR market, represented in Figure 4.22. In the *Do-nothing* scenario and the *Self-balancing* scenario with BSP-TSO communication, areas are almost always balanced after the market, to the point where their imbalances are almost indistinguishable on the graph. Meanwhile, the *Self-balancing* behavior without BSP-TSO communication displays significant post-RR market imbalances. A critical impact of the absence of communication is consequently the overcompensation of balancing needs: imbalance volumes are carried out (in the opposite direction) to closer-to-real-time balancing processes, that usually offer a significantly lower pool of reserves. This is a major security of supply concern.

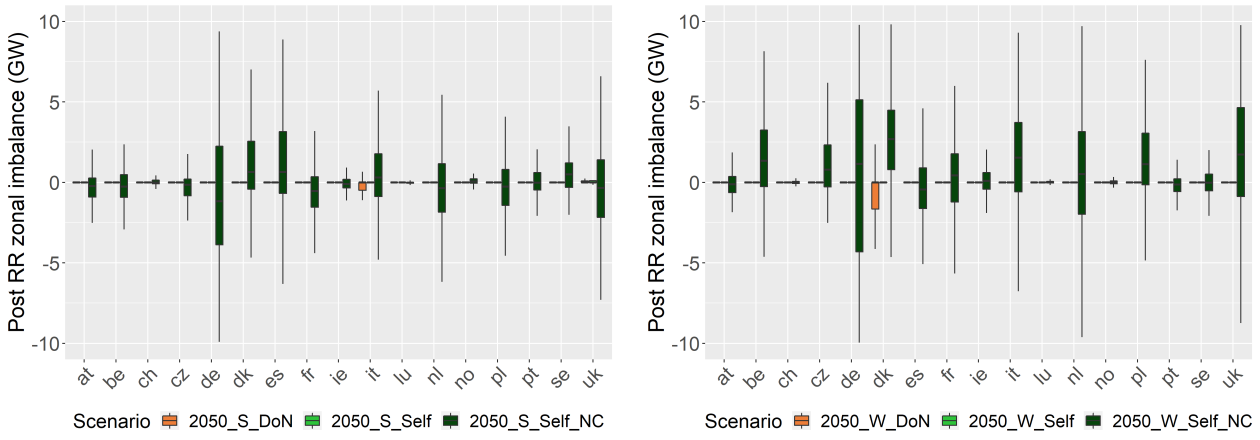

(a) Summer period

(b) *Self-balancing* behavior

Figure 4.22: Local imbalances after the RR market

Regulatory discussion of the *Self-balancing* behavior

Overall, the *Self-balancing* behavior of vRES actors in balancing energy markets has contrasted results.

It should increase their revenues and help in the balancing management of the system (reduction of TSO balancing needs and of the variability of their balancing costs), but we found that it also induces a slight loss in overall welfare. Nonetheless, permitting this behavior can be a good incentive to facilitate the integration of vRES, by allowing them to mitigate the financial impact of their imbalances.

However, our results show that it can also be very detrimental if not managed properly, both in terms of costs and security of supply. Consequently, if this behavior is permitted, we believe that it should be framed by an important regulatory evolution: the communication processes between BSPs and TSOs should be adapted. Proactive TSOs need to know if self-balancing orders are formulated in their area, to avoid taking into account this volume in their RR market demand. Hence, we propose that self-balancing orders should be clearly identified when BSPs transmit their orders to their respective TSOs.

The price of self-balancing orders is also a topic of discussion, both in terms of security of supply and economic efficiency. It was set to guarantee acceptance by the RR market in this first study. BSPs could instead try to price their orders according to forecasts of closer-to-real-time alternatives (other balancing markets and eventually the imbalance settlement process), much like the TSO bidding strategies investigated in Chapter 3. In that regard, the economic efficiency of BSP pricing must be investigated in future studies, as their access to information about RR market alternatives is much more limited than that of a TSO. As demonstrated before, a poor pricing method can lead to higher balancing costs, and to imbalances in real time in the case of BSPs.

4.5 Conclusion

One of the main objectives of the European balancing energy markets is to facilitate the large integration of variable Renewable Energy Sources (vRES) in the power system, which is a projected step of decarbonization. Indeed, these new markets were designed to mitigate the expected increase in balancing needs induced by the uncertainty of vRES power generation. To our knowledge, the existing literature does not examine the performance of balancing energy markets at the 2050 horizon, nor does it assess their role in compensating for the expected increase in balancing needs. This performance can be linked with the new opportunities for market actors created by the design of these markets. Since they can match Balancing Services Provider (BSP) orders together, RR and mFRR balancing energy markets can act as close-to-real-time dispatch optimization tools, similar to intraday markets. Notably, vRES actors can use them to correct imbalances induced by their variability, through self-balancing market orders. This potential behavior is all the more relevant when looking at long-term scenarios, given the large installed capacities of solar and wind plants. It could have significant impacts on market inputs and outputs, especially since it interacts with the balancing needs formulation process of proactive TSOs.

In this chapter, we quantified the long-term impact of the energy transition on the RR balancing energy markets, comparing scenarios at the 2030 and 2050 horizons with the electricity market model ATLAS. The two input datasets used are constructed based on scenarios from (RTE, 2022) that represent projected national trajectories. We simulated 3 consecutive days of electricity markets in two different seasons (summer and winter) and for both time horizons. Each day includes a day-ahead market, an intraday market and 24 RR balancing markets. Two types of vRES bidding behaviors are compared for each scenario of the 2050 horizon: with the *Do-nothing* behavior, vREs follow their forecast evolution and are settled according to a

simplified model of the French imbalance settlement process; with the *Self-balancing* behavior, vRES actors submit self-balancing orders on the RR market to try to balance their forecast evolution. In addition, two different levels of communication between BSPs and TSOs are considered. The key findings of this case study can then be classified into two categories.

First, we assessed how the power system evolution between both time horizons affects the performance of the RR market, without considering the vRES behaviors:

- As expected, absolute balancing needs increase significantly, being multiplied by a factor of 2 to 4.5 between our 2030 and 2050 scenarios. This is accentuated in areas that possess large capacities of vRES (Germany, Spain, France, Italy, the Netherlands and the United Kingdom notably). This increase is partially compensated by the increased netting of balancing needs between areas, which is amplified by investments in transmission lines between the two time horizons. Eventually, the netting reduces balancing needs by 30% to 50% in 2050 scenarios. In addition, the volume of BSP orders also compensates for this increase in balancing needs. It rises by a factor of 1.5 to 2 between both time horizons, with significant increases in volumes provided by new flexibilities (mainly vRES, demand-response, power-to-gas and storage units). It is important to note that, in these simulations, BSPs offered their entire available capacities on the RR market. Consequently, they illustrate an ideal situation, that can only be reached if the aforementioned new flexilibities are correctly incentivized to participate in balancing markets.

- The observations previously made translate into market outputs, as all TSO balancing needs were completely accepted by the RR market, in all scenarios. In terms of security of supply, these results tend to indicate that RR balancing markets can fulfill their role as they compensate for the increased balancing needs, under the assumption of significant participation of new flexibilities in balancing processes. The impact on average TSO balancing costs is harder to quantify, as it seems to depend on multiple components (notably on the season, and the associated availability of vRES generation). However, their variance is substantially accentuated at the 2050 horizon, particularly in areas with large vRES installed capacities. In contrast, the overall social welfare is significantly increased between 2030 and 2050, in all scenarios. Two components drive this augmentation: the increase in TSO demands, and the role of balancing energy markets as economic redispatch tools (extending that of day-ahead and intraday markets).

In a second step, the two possible vRES behaviors are analyzed at the 2050 horizon and lead to the following results:

- The *Self-balancing* behavior is profitable on average for vRES actors, for all scenarios. This implies that we can expect it to be used by actors in the future, assuming that the benefits outweigh the costs of entering the market (IT and workers dedicated to managing the creation and activation of RR orders).

- When BSPs and TSOs communicate about self-balancing orders, this behavior leads to substantial reductions in both balancing need volumes and variability of TSO balancing costs on the RR market. When looking at the overall social welfare of the RR market, however, this behavior does induce slight losses, and mainly results in a welfare transfer between TSOs and vRES actors.

- When BSPs and TSOs are not communicating, the *Self-balancing* behavior can lead to significant disturbances. Indeed, in this case, the forecast evolution of vRES actors is compensated twice on the RR market (both by BSPs and TSOs), canceling the benefits in balancing needs and costs previously observed. In addition, the overcompensation of imbalances leads to additional balancing needs in closer-to-real-time processes, which could threaten the security of supply.

In light of these results, we argue that if the self-balancing behavior is permitted, it should be framed by an important regulatory evolution: self-balancing orders should be noticed by BSPs to their TSO, to avoid the negative effects previously observed. The price of these orders is also a topic of discussion, and would require additional studies.

As this work is the first approach to quantify the long-term performance of common balancing energy markets, it could be improved by several future research avenues. First, we note that all results are naturally tied with the hypotheses of both the input datasets and the modeling choices. A single scenario of the European power system evolution is considered for both time horizons. Hence, this work should be complemented with simulation based on other power system projections, especially at the 2050 horizon. In addition, multiple days were simulated across different seasons to capture diverse market situations, but we could not ensure that they included extreme events (for instance weather events leading to large forecast evolutions, or unavailability of generation units). The performance of balancing markets under these extreme events should then be studied in future work.
We also believe that the study of the self-balancing behavior should be extended. It was only applied to vRES actors in this chapter, but it can theoretically be used by any BRP that is imbalanced before balancing energy markets. Moreover, it can also be studied in mFRR markets. We expect that the resulting dynamics would resemble those presented in this chapter, but the smaller reserve pool in mFRR markets (given their closer-to-real-time execution) could accentuate the security of supply risks without BSP-TSO communication. The self-balancing behavior was also studied with a dual imbalance price mechanism, and it could be relevant to evaluate if it is still profitable for imbalanced actors under a single imbalance price. To conclude, we would like to point out that if BRPs are able to rebalance themselves on RR and mFRR markets, it could be relevant to question the ongoing trend of reducing the intraday gate closure time. Indeed, keeping a reasonable gate closure time would allow for better system management by TSOs (Petitet et al., 2019), while actors could perform supervised self-balancing activations in balancing energy markets.

4.A Appendix A - Detailed description of input datasets

	Thermal				Hydraulic		Storage			Wind	Solar	Other non dispatchable
Area	Gas	Oil	Coal	Nuclear	ROR	Reservoir	Electric Vehicle	PHS	Batteries	-	-	-
AT	4365	168	0	0	7800	6300	54	3159	0	4478	3054	388
BE	8839	158	541	0	100	0	104	1395	0	8864	11004	320
CH	660	0	0	2565	3800	8200	55	3989	0	255	5500	555
CZ	2450	14	4981	4055	1000	1100	90	0	0	960	3936	513
DE	40541	841	18530	0	4200	2900	493	7811	0	103199	91300	4337
DK	1192	842	1611	0	0	0	0	0	0	9548	5294	93
ES	28481	0	0	3041	7100	10100	419	8465	0	48550	45704	1050
FR	11538	990	0	59400	7400	8400	624	3800	470	38401	35100	1403
IE	2202	324	78	0	400	0	44	292	0	9500	400	112
IT	51477	866	0	0	6900	10100	265	9391	0	19600	52001	2452
LU	100	0	0	0	0	0	0	1310	0	428	560	44
NL	14903	0	3381	486	0	0	140	0	0	21057	27150	216
NO	270	0	0	0	0	34471	41	1115	0	7764	1500	67
PL	11401	0	19598	0	600	400	0	1495	0	13799	7737	1417
PT	3619	0	0	0	1300	6700	123	3554	0	9591	9717	781
SE	1655	660	0	6835	0	14319	114	0	0	20258	4347	3099
UK	45326	724	3984	9281	1900	0	219	2744	0	42673	17155	3622

Table 4.5: Installed capacities in MW by generation type - 2030 horizon

Remarks:

- The gas subtype of thermal units aggregates CCGT, OCGT and conventional gas units.
- Run of River (ROR) hydraulic generation output varies considerably throughout the year in each area, following local inflows. The value indicated in the table corresponds to the maximum power output. The same remark can be made for electric vehicles (since the number of units connected to the network varies at each hour).
- The “Other non dispatchable" category includes geothermal, waste, and biomass units.

	Thermal				Hydraulic		Storage			Wind	Solar	Other non dispatchable
Area	Gas	Oil	Coal	Nuclear	ROR	Reservoir	Electric Vehicle	PHS	Batteries	-	-	-
AT	6750	0	0	0	4458	3917	829	5149	0	23300	55200	359
BE	10520	0	0	0	83	0	1122	1395	1281	50700	39900	115
CH	890	0	0	0	3402	8152	0	3989	1903	2200	12800	555
CZ	8030	0	0	2054	287	1100	817	1126	5009	28600	31300	799
DE	73656	0	0	0	2723	2900	9004	9754	0	272000	196600	681
DK	490	0	0	0	0	0	697	0	0	53100	6700	430
ES	13850	0	0	0	1896	10100	4055	9261	20426	99300	172800	1351
FR	2860	0	0	38620	7004	8409	11750	7180	190	87600	90000	699
IE	1886	0	0	0	217	0	736	292	1203	25300	7200	63
IT	19832	0	0	0	4032	10100	6772	7088	22684	73500	326300	2564
LU	30	0	0	0	24	0	0	1310	0	1600	1900	38
NL	9230	0	0	0	17	0	1845	0	4481	108400	116300	216
NO	270	0	0	0	0	34946	872	1115	0	7764	2100	18
PL	22940	0	0	4500	179	400	0	1495	481	98100	42000	1439
PT	780	0	0	0	563	6700	975	3578	1864	24600	26800	862
SE	90	0	0	0	0	14319	1318	0	0	62300	9000	2864
UK	27280	0	0	15920	799	0	7244	4004	47	132300	70000	5820

Table 4.6: Installed capacities in MW by generation type - 2050 horizon

4.B Appendix B - Impacts on exports-imports and transmission lines usage

As seen in Section 4.4.1.1, the volumes of balancing needs netted between areas increased in 2050 scenarios. Consequently, we expect an intensification of exchanges between them. This appendix quantifies these changes with the help of two indicators.

The first indicator studied is the export-import balance of flexibility, for all areas. It represents how much a given area (i.e. a given TSO) relies on local reserves to compensate for its imbalances, and how much it imports or exports to other areas. It is computed according to Equation 4.7:

$$\forall t,\ \forall z \in Z,\quad \begin{cases} FlexBal_{z,t} = \sum\limits_{o \in O_{z,t}^{BSP}} (-\sigma_o * q_o^{acc}) - bn_{z,t} & if\ bn_{z,t} > 0 \\ FlexBal_{z,t} = bn_{z,t} - \sum\limits_{o \in O_{z,t}^{BSP}} (-\sigma_o * q_o^{acc}) & if\ bn_{z,t} < 0 \end{cases} \tag{4.7}$$

With $bn_{z,t}$ the balancing needs in area z at time t, and $O_{z,t}^{BSP}$ the set of BSP orders of area z at time t.

It is notably interesting to separate both balancing directions as, on average, an area can be importing flexibility in a given direction but exporting in the other.

Boxplots indicating the exports-imports balance in each area are plotted in Figures 4.23 (summer period) and 4.24 (winter period). Positive values indicate an export of flexibility, while negative values indicate an import.

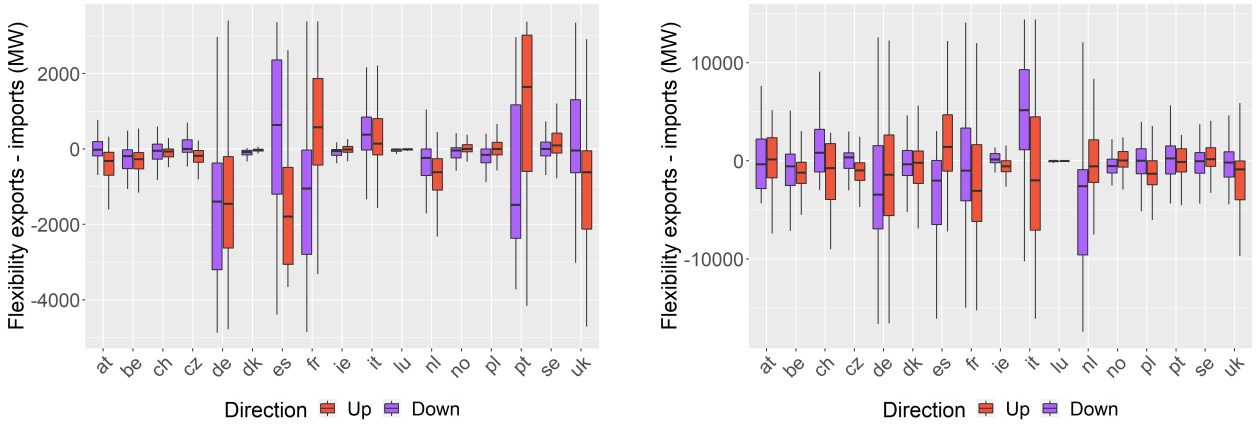

(a) 2030 (b) 2050

Figure 4.23: Exports imports flexibility - Summer period

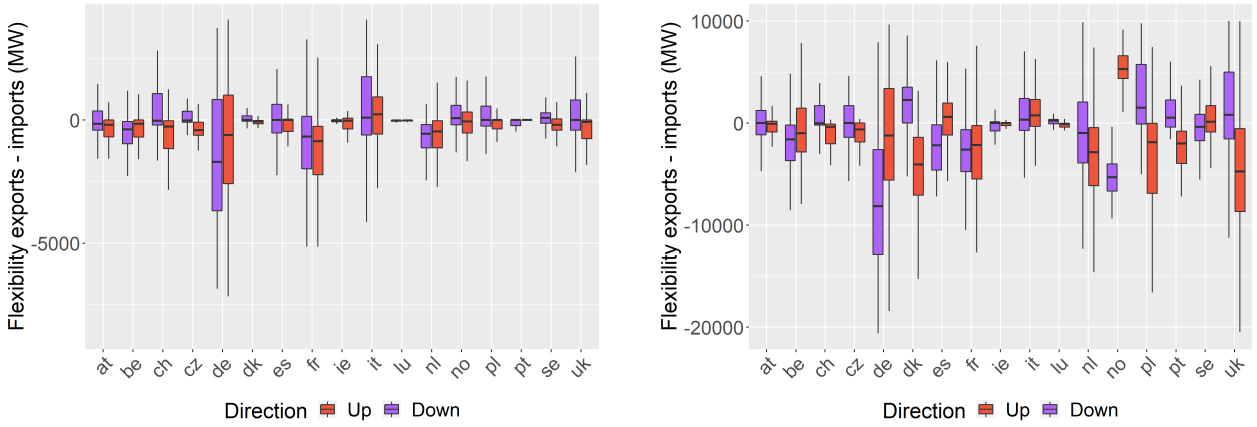

(a) 2030

(b) 2050

Figure 4.24: Exports imports flexibility - Winter period

The general amplitude of exports and imports of flexibility is much greater in 2050 scenarios. Once again, this is accentuated in areas with large wind capacities (Germany, Spain, France, the Netherlands, Poland and the United Kingdom). Notably, Germany is the area importing the most downward flexibility on average in 2030, and this tendency is confirmed in 2050 with a much greater amplitude. This importing state not only reflects the local installed capacities of both vRES units and flexibilities, but also the interconnection degree of this area: being very well interconnected, it can rely on flexibilities from other areas.

We can also observe seasonal influences linked with the share of wind and solar power installed. Italy, which has by far the largest capacities of solar power, has a larger amplitude in summer while Germany experiences this in winter, especially in the downward direction. We can also observe shifts between the two time horizons in certain areas: for instance, during the summer period in France, the area is exporting upward flexibility and importing downward flexibility in 2030 (Figure 4.23a); in 2050, it is now importing upward flexibility and neutral (slightly exporting) downward flexibility (Figure 4.23b).

These last results, along with (i) the increased netting between areas and (ii) the increase in BSP-BSP order matches (Section 4.4.1), point towards the intensified use of transmission lines between areas. This is confirmed by Figures 4.25 and 4.26, which plot the average usage ratio of the Available Transmission Capacity (ATC) on each cross-border transmission line in our power system. The ATC represents the capacity available for the RR market on a transmission line in a given direction, taking into account the maximum capacity of the line and flows resulting from previous markets. The usage ratio is then defined in Equation 4.8.

$$\forall mb \in MB, \quad r_{mb}^{RR} = 1/n * \sum_{t} \frac{|Flow_{mb,t}^{RR}|}{ATC_{mb,\delta_t^f,t}} \tag{4.8}$$

With:

- n the total number of RR market time steps in our simulation period, i.e. $3 * 96$ for each scenario.
- MB the set of all transmission lines (market borders).
- $Flow_{mb,t}^{RR}$ is the flow generated by the RR market on market border mb at time t.

- $ATC_{mb,\delta_t^f,t}$ is the ATC on market border mb in the direction δ_t^f, at time t. δ_t^f designate the same direction as $Flow_{mb,t}^{RR}$.

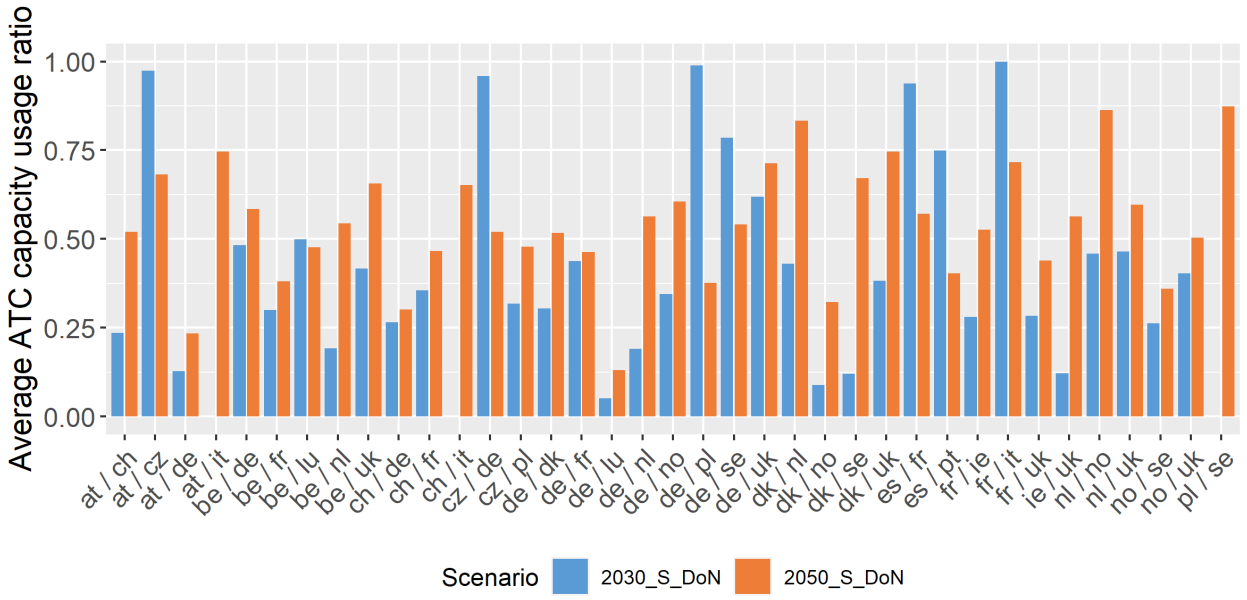

Figure 4.25: Usage ratio of cross-border transmission lines ATC - Summer period

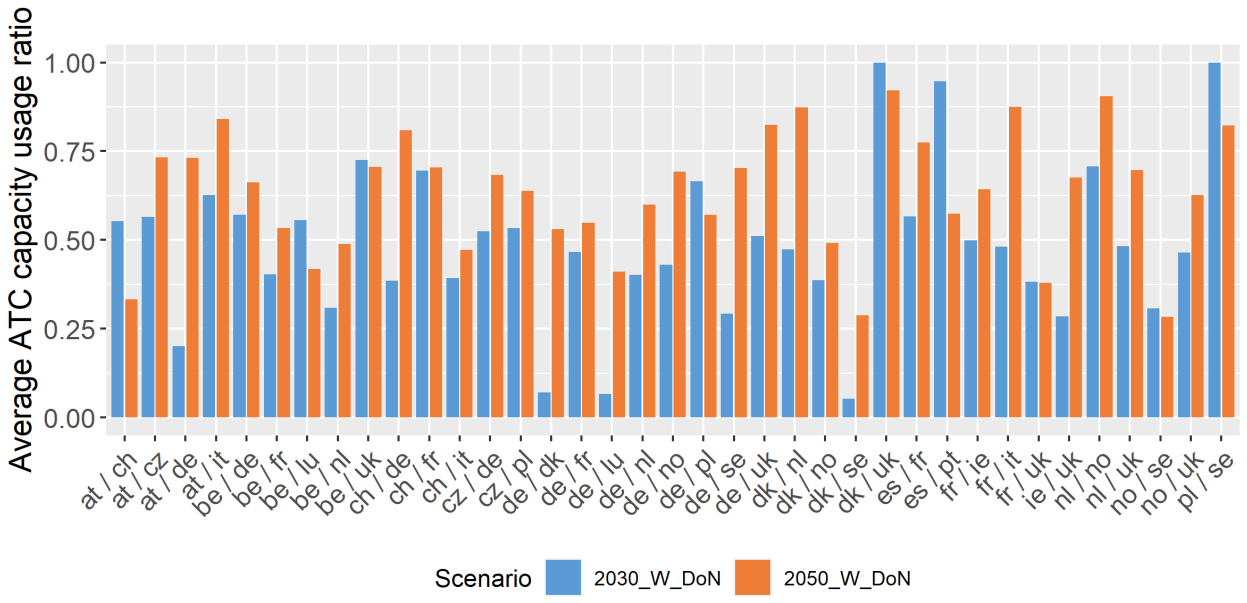

Figure 4.26: Usage ratio of cross-border transmission lines ATC - Winter period

Not only are the transmission capacities enhanced between both time horizons (see Section 4.3.2), but almost all of them see an increase in their usage ratio at the 2050 horizon. On average across all areas, the ATC usage ratio is increased by 14.4% in the summer period and by 14.8% in the winter period. This

emphasizes the importance of exchanges between areas in future balancing processes and investments in cross-border transmission lines.

Chapter 5

General conclusion

Contents

5.1 Summary and main contributions

The balancing stage of the European power system is currently undergoing two significant evolutions. First, its organization is transitioning from a diverse and heterogeneous state, in which balancing was designed and operated locally by the different Transmission System Operators (TSOs), to cross-border common energy markets. In addition, the ever-needed decarbonization requires a profound power system transformation, notably by installing large capacities of variable Renewable Energy Sources. Both aspects will reshape the supply and demand sides of balancing processes, bringing new challenges and opportunities in the notoriously complex short-term power system management. It then becomes important to consider the following questions: **What are the impacts of the ongoing liberalization and decarbonization on the short-term management of the supply-demand balance?**

These concepts are further detailed in the general introduction (**Chapter 1**), which also provides an overview of the historical local balancing processes and of the design of the new European balancing energy markets.

This thesis focuses on two main types of balancing products: Replacement Reserve (RR) and manual Frequency Restoration Reserve (mFRR). It then approaches the general research question from three separate but complementary angles.

Chapter 2 focuses on the supply side, and more specifically on the interaction between the physical limitations of thermal generation units (referred to as operating constraints) and the order standardization imposed by common energy markets. Indeed, historical balancing processes were constructed to match the

specific features of their local power system, using adapted balancing products to partially mitigate the aforementioned operating constraints. As an example, the French historical balancing process, called "Mécanisme d'ajustement", does not impose any requirement on the shape of reserves submitted by Balancing Services Providers (BSPs). In contrast, the design chosen for cross-border common markets imposes a standard shape for balancing reserve market orders, which can conflict with operating constraints and eventually limit the volume offered by BSPs. In this chapter, we define a list of operating constraints of thermal units, relevant to the time frame of balancing markets. We then conduct a literature review of electricity market models used to simulate balancing markets, aiming to identify their integration of operating constraints. It reveals that most models only consider a subset of the list previously defined, which could impact their results. Consequently, the main research question addressed by this chapter is: *How do the operating constraints of thermal units impact balancing market performances, especially on indicators discussed in previous studies, and is their representation in electricity market models relevant?*

To address this question, a modeling approach for the formulation of BSP balancing energy orders is proposed and developed in the electricity market model ATLAS. This method notably integrates the list of relevant thermal operating constraints, using the order complexity tools permitted by the design of balancing markets (order divisibility and coupling links). This method is applied in a case study, in which sequential electricity markets (day-ahead to RR markets) are simulated at the European scale for several days covering different power systems situations and with six scenarios. The six scenarios analyze the impact of each advanced operating constraint taken individually, and of their joint consideration, in RR market inputs and outputs.

Results first show that integrating operating constraints in the BSP order formulation induces a significant decrease in RR market liquidity. This effect varies according to the local power system composition, as the impact of each advanced operating constraint is specific to the type of thermal units: minimum time ON and minimum time OFF constraints have a significant impact on power systems predominantly composed of CCGT units (e.g. Germany), while the minimum stable power duration constraint is most relevant for power systems with large installed capacities of nuclear assets (e.g. France). When looking at market outputs, the observed liquidity drop leads to (i) an increase in TSO balancing, (ii) a decrease in overall social welfare, and (iii) a potential impact on the security of supply, through an increase in the volume of TSO unsupplied needs.

Overall, this first part of the thesis demonstrates that the combination of the order standardization process of common energy markets and the physical limitations of generation units has significant impacts on market performances. The solution provided by RR markets to integrate these operating constraints in the bidding process is to create complex orders (indivisibility or coupling links). These solutions, taken into account in our model, prove insufficient: for instance, the flexibility potential of nuclear units is not captured by the RR market. This chapter also advocates for the integration of operating constraints in balancing market models. Not taking this effect into account could distort market results and possibly lead to an overestimation of market performances, which could in turn affect the accuracy of regulatory proposals.

Chapter 3 studies the demand side of balancing energy markets, by focusing on the order formulation process of TSOs. As indicated in the general introduction, this aspect sets balancing markets apart from usual wholesale markets, as TSOs were not market actors in the former. Consequently, there is a significant gap in the academic literature on TSO bidding strategies: to our knowledge, this topic has only been approached by a single article, (Håberg and Doorman, 2017) in 2017. Since then, we found no further research on this, and all subsequent articles modeling balancing energy markets consider the TSO demand to be price-inelastic.

However, the RR market has been operational since 2020, and recent market reports published by ENTSO-E[1] suggest that the vast majority of TSO demands are actually formulated as price-elastic. Hence, this chapter challenges the price-inelastic assumption of TSOs in light of this information, which leads to the second research question of this thesis: *How can we improve TSOs' bidding methods on balancing energy markets? And what are the impacts of such methods on market outcomes and balancing costs?*
First, this chapter proposes an empirical analysis of the RR market which complements the initial information displayed in the aforementioned market reports. Using publicly available data of the French TSO RTE, this analysis highlights the price elasticity of TSO and demonstrates that demand curves are already formulated in practice, emphasizing the value of studying TSO bidding strategies. Consequently, this section of the thesis builds on the initial work of (Håberg and Doorman, 2017), addressing complicating issues noted by the authors and providing a practical case study that evaluates the impact of price-elastic strategies on balancing market inputs and outputs. In sequential balancing processes, TSOs can perform arbitrages between the RR market and closer-to-real-time processes to extract opportunity costs, used to define their price elasticity. The different types of alternatives to the RR market are analyzed and discussed based on their relevance.
Then, a framework for the TSO order formulation process is proposed. It notably separates the cost estimation function from a new function that introduces volume uncertainty in the bidding process. Finally, we conducted a case study with the ATLAS model, aiming to compare the performance of the proposed bidding method with volume uncertainty to both the usual price inelastic formulation and the initial bidding method proposed in (Håberg and Doorman, 2017). Two different types of RR alternatives are considered. Results indicate that the proposed bidding method can yield significant TSO balancing cost reductions. They also show that an inaccurate opportunity cost estimation function can substantially affect the performance of price elastic methods. Consequently, it raises questions about the regulatory aspects of TSO bidding strategies, to avoid market distortions either (i) wanted (e.g., the prioritization of local balancing processes over common markets) or (ii) unwanted (because of an inaccurate bidding strategy).

Finally, **Chapter 4** focuses on the impact of decarbonization on common balancing energy markets. The large-scale integration of vRES capacities in the European system is expected to increase balancing needs. Meanwhile, these new markets are designed to partially alleviate this challenge, first by increasing the pool of available reserves (thanks to their cross-border aspect), and also by facilitating the participation of new types of flexibilities in balancing markets with a more transparent process. Consequently, assessing their performance with future power system compositions is important. Although the existing literature studies many long-term aspects of European power system balancing processes (notably inertia requirements, frequency control, or reserve procurement requirements), it is rather scarce when we focus on balancing energy markets. Notably, to our knowledge, no analysis of these markets has been conducted at the 2050 horizon.
In addition, as discussed in the general introduction, RR and mFRR markets can also act as close-to-real-time dispatch optimization tools, since their design allows to match BSP offers together. Imbalanced BSPs could then bet on these markets to balance themselves, by submitting their imbalance as RR of mFRR market orders (a behavior that we call self-balancing). This should apply in particular to vRES actors at the 2050 horizon, as they will face significant imbalances because of the variability of their power output. To our knowledge, self-balancing behavior in RR and mFRR markets is currently not studied in the literature.
Both literature gaps presented previously lead to the last research questions of this thesis: *What is the impact of the evolution induced by decarbonization on the European power system on both inputs and outputs of balancing energy markets? And what are the possible consequences of the self-balancing behavior of vRES*

[1] ENTSO-E is the association of European TSOs.

actors at the 2050 horizon?

These questions are investigated through a case study using the ATLAS model with two different time horizons, 2030 and 2050. Input datasets are based on RTE's publication *Energy pathways to 2050* (RTE, 2022), and represent European power systems based on national projections of installed capacities. For each time horizon, multiple days of sequential electricity markets (day-ahead, intraday and RR) are simulated in both winter and summer seasons, to capture the seasonal differences of vRES. Results confirm the expected increase in TSO balancing needs, notably in areas with large vRES installed capacities. However, it is partially compensated by (i) the increase in netting between areas, and (ii) the enhanced volume of BSP offers, driven by new flexible assets (vRES, storage or power-to-gas technologies), under the assumption that they offer their entire available capacity on balancing markets. We also observe a significant increase in the variability of TSO balancing costs.

Finally, the self-balancing behavior of vRES actors is simulated at the 2050 horizon. Results show that, with an imbalance settlement price that incites actors to be balanced, the revenues of vRES actors increase when they formulate "at all costs" self-balancing orders. Meanwhile, TSO balancing needs are significantly reduced since vRES actors internalize their imbalance, leading to a lower variability of TSO balancing costs. The overall social welfare is almost unchanged (albeit slightly reduced), as this behavior mainly induces a welfare transfer between TSOs and vRES BSPs. However, we argue that, if permitted, these self-balancing orders should be framed by regulatory evolutions. Notably, the communication between self-balancing BSPs and proactive TSOs must be improved, to avoid an overcompensation of imbalances.

5.2 General remarks and regulatory implications

Overall, this dissertation discusses several key aspects of the future of short-term balancing processes in Europe and raises several regulatory questions.

It illustrates how the new common balancing energy markets could improve the balancing efficiency, notably thanks to their cross-border aspect. Our analyses indicate that they should be adapted to the long-term evolution and decarbonization of the European power system. The underlying assumption is that of significant participation of new flexibilities in balancing markets, which implies sending the right incentives to BSPs. The design of the new markets partially contributes to this, as demonstrated in Chapter 4 through their ability to match BSP orders together. In general, if balancing markets can provide enhanced options to BSPs to limit the financial impact of imbalances, it should encourage their participation in balancing processes. However, design adaptations should still be considered, in light of our proposal of BSP-TSO communication for self-balancing orders. The sequential aspect of balancing markets can also contribute to improvements in market performances. Chapter 3 showed how TSOs can leverage it to activate balancing reserves more optimally, integrating arbitrages in bidding strategies. Nonetheless, these new opportunities provided by the design of European balancing markets should be further evaluated from a regulatory point of view, as inappropriate usage could negatively impact market performance and the security of supply.

This work also demonstrates the sheer complexity of balancing markets, and their deep interactions with the physical features of power systems, which are rarely studied in the literature. They should not be considered as mere extensions of usual wholesale markets, because of their extreme proximity to real time as well as their crucial role as a last tool in maintaining the supply-demand balance. In that regard, this thesis

contributes to the improvement of the modeling of European balancing energy markets, by (i) describing with precision their actual design and (ii) developing a market model as close as possible to this design. This modeling notably captures the actual process and the different steps of RR and mFRR markets, and their precise requirements or complex order tools, which are almost never considered in models found in the literature. When applied in balancing market simulations, it reveals additional regulatory implications.

First, the standardization of market orders can limit the pool of available flexibilities. This is notably highlighted through the example of nuclear units in Chapter 2, which are almost entirely prohibited from participating in RR markets by their operating constraints. This limitation of market liquidity is bound to be even stronger on shorter reserve types (e.g. mFRR or aFRR), as they impose heavier requirements on market orders. In that sense, it raises questions on a topic regularly evoked in the literature: the benefits of reducing the duration of balancing products. In light of our findings, we argue that maintaining longer balancing products is beneficial for the overall system flexibility in the short- to mid-term. In the long-term, assuming a power system mostly comprised of flexible units, longer balancing products may not be required anymore.

In addition, if modeling the different steps of balancing energy markets–especially bidding processes–is difficult from a theoretical and academic point of view, it could also be a challenging process for actual market actors. In the literature, BSPs are usually assumed to participate in all available markets, which may not hold in practice. This is illustrated by the lack of French BSP offers observed empirically on the RR market (Chapter 3): our analysis shows that the RR market was the most profitable solution, yet most actors did not participate in it. Indeed, participating in several interrelated markets occurring multiple times within an hour, with little downtime between them, is difficult. As an example, one can consider the timeline of a single hour or RR, mFRR and aFRR markets (see Figure 3.6 in Chapter 3), and picture the different decision stages faced by a BSP. This actor must ensure that its units are always able to respond to every market activation, while respecting all their technical requirements. Because of the intricacy of these technical aspects, participating in interrelated markets also induces hidden costs, mainly through required IT developments and the need for workers to manage interaction with markets. While this should not be a blocking factor for large market actors, it could deter smaller actors from entering balancing markets: this challenges the usual assumption of common balancing markets facilitating the integration of small-scale actors. Consequently, we should not forget the human aspect when proposing regulatory evolutions: a behavior deemed theoretically optimal for a rational actor may not be followed in practice, because of the complexity described above.

To conclude, this thesis underlines the growing importance of balancing processes through the analysis conducted in Chapter 4. In a power system shaped by decarbonization, the volumes of energy exchanged in close-to-real-time processes will be significantly increased. This makes the definition of an effective design all the more meaningful.

5.3 Future research avenues

The different works performed during the thesis open multiple research avenues, that could deepen the understanding of market actor behavior and balancing energy market determinants, eventually leading to further improvements in balancing processes efficiency.

Direct extensions and improvements of our studies

During this thesis, the behavior of BSPs was only approached in two instances. First, with the 50% capacity withholding modeled in Chapter 3, extracted from an empirical analysis and required to model the FrBM alternative. Second, in Chapter 4, with the self-balancing behavior of vRES actors. In all other cases, BSPs were assumed to act in pure and perfect competition, meaning that they would bid their entire available capacity at their true cost. We believe that this assumption should be challenged. For instance, the notion of arbitrage between sequential markets studied for TSOs in Chapter 3 can be applied to BSPs as well. If we take the example of a generation unit that is able to participate in both RR and mFRR markets, it could prioritize offering on the market with the highest expected revenues. While the literature already studies arbitrages between markets, to our knowledge, the arbitrage between different balancing energy markets is yet to be addressed. Studying the bidding process of BSPs is all the more relevant if we take into account the power system evolution associated with decarbonization. For instance, the share of storage units is expected to increase significantly in the following decades. As one of the main sources of new flexibilities, these units are bound to be important actors in balancing processes. However, their behavior integrates different intricacies compared to that of conventional thermal units: while the former could rely on tangible parameters, such as fuel costs, to estimate its true costs, the variable cost of storage units cannot be estimated in the same way. Finally, the learning behavior of BSPs should also be studied, notably with reinforcement learning. This topic is already partially covered by (Poplavskaya et al., 2020) and (Poplavskaya et al., 2021), but we can still identify novel aspects highlighted by this thesis: the interaction between BSP learning and TSO bidding methods, or the arbitrages between sequential balancing energy markets previously evoked.

While Chapter 2 covers in detail the modeling of thermal generation units within balancing energy markets, it does not extensively study the constraints applied to other types of units. This should be a topic of interest, as the chapter showed the impact of accurate unit constraint modeling on market performance. We previously mentioned that the behavior of storage units is a topic of interest for future research. Their physical limits are also noteworthy of considerations, such as the aging of batteries caused by a strong participation in balancing processes, the management of small reservoir sizes or the specific features of electric vehicles (variable connected capacities, required load to cover for displacement). Both aspects could conflict with order standardization, and require using order complexity tools similar to the proposed modeling of thermal units.

Regarding the TSO bidding strategies studied in Chapter 3, future work could integrate notions of risk aversion in the formulation process, as results showed that bidding strategies with volume uncertainty could occasionally lead to important balancing costs. We also restricted the analysis to individual alternatives to the RR market, but we believe that an optimal bidding strategy should consider the set of all possible RR alternatives in its calculation.

The analysis of RR market long-term performance proposed in Chapter 4 could be extended in several ways. First, improving the modeling of BSP behavior, as discussed above, should modify the supply curves. The overall assessment of RR markets at the 2050 horizon should also be conducted on additional scenarios of European power system development, and by selecting specific situations of high stress on the supply-demand balance.

Future research on balancing market design

In addition to the direct improvements and extensions of our studies, the thesis also opens broader research

avenues.

To tackle the liquidity loss generated by the order standardization of common markets, other options for integrating balancing processes at the European scale could be considered. For instance, a common balancing mechanism constructed on the basis of the French process could be a relevant consideration. For BSPs, it should partially alleviate the intricacy of the bidding process, as it is much less constraining. It would also have the benefit of integrating a more detailed network representation, by considering internal transmission lines. Apart from the order standardization aspect, the various features of this new design could still follow the choices made for common markets (e.g. marginal pricing). The proximity to real-time of such a mechanism, and the length of its delivery period could progressively be reduced according to the integration of more flexible assets in the power system. The main challenge of this approach should be its computational complexity.

A cross-analysis comparing the efficiency of the TSO bidding strategies developed in Chapter 3 and of the BRPs self-balancing behavior from Chapter 4 should provide relevant elements to estimate the benefits or costs induced by the internalization of imbalances within BRPs, compared to a centralized approach managed by TSOs. First, this could settle the question of allowing self-balancing or not. In addition, it could also provide new information to the ongoing discussion about the balancing Gate Closure Time (GCT): if a centralized approach yields significant cost reduction, then it would be optimal to keep a longer GCT, allowing for better management by the TSO while permitting supervised balancing behaviors of BRPs in balancing processes.

Finally, our findings identified significant increases in social welfare at the 2050 horizon, especially for reserve providers. The resulting benefits for market actors should then be considered in long-term power system assessments, as they could influence the optimal composition of the power system.

Chapter 6

Résumé en français

Le système électrique est un des piliers des sociétés modernes, alimentant des infrastructures et services vitaux et fournissant un accès instantané à l'énergie aux consommateurs. Cette importance ne va que s'intensifier dans les prochaines décennies: la part de l'électricité dans la consommation mondiale d'énergie, actuellement plus de 20%, devrait atteindre 50% d'ici 2050 (IEA, 2021). Seulement, l'électricité est un vecteur énergétique particulier, car c'est le seul qui nécessite une conversion vers un autre vecteur pour être stocké. Si l'on prend également en compte la diversité des technologies installées, la variabilité des consommations et des sources de production renouvelables, ou encore les contraintes de réseau, la gestion de l'approvisionnement en électricité se présente comme une tâche particulièrement complexe. A ce titre, la section d'équilibrage a un rôle crucial: en tant que dernier phase avant le temps réel, elle doit garantir que l'équilibre entre production et consommation est assuré à tout instant. La gestion de l'équilibrage en Europe subit actuellement deux évolutions importantes. Tout d'abord, son organisation passe progressivement d'un état diversifié et hétérogène, dans lequel il était conçu et géré localement par les différents gestionnaires de réseaux de transport (GRT), vers des marchés communs et internationaux d'activation. Cette transformation est représentée en Figure 6.1:

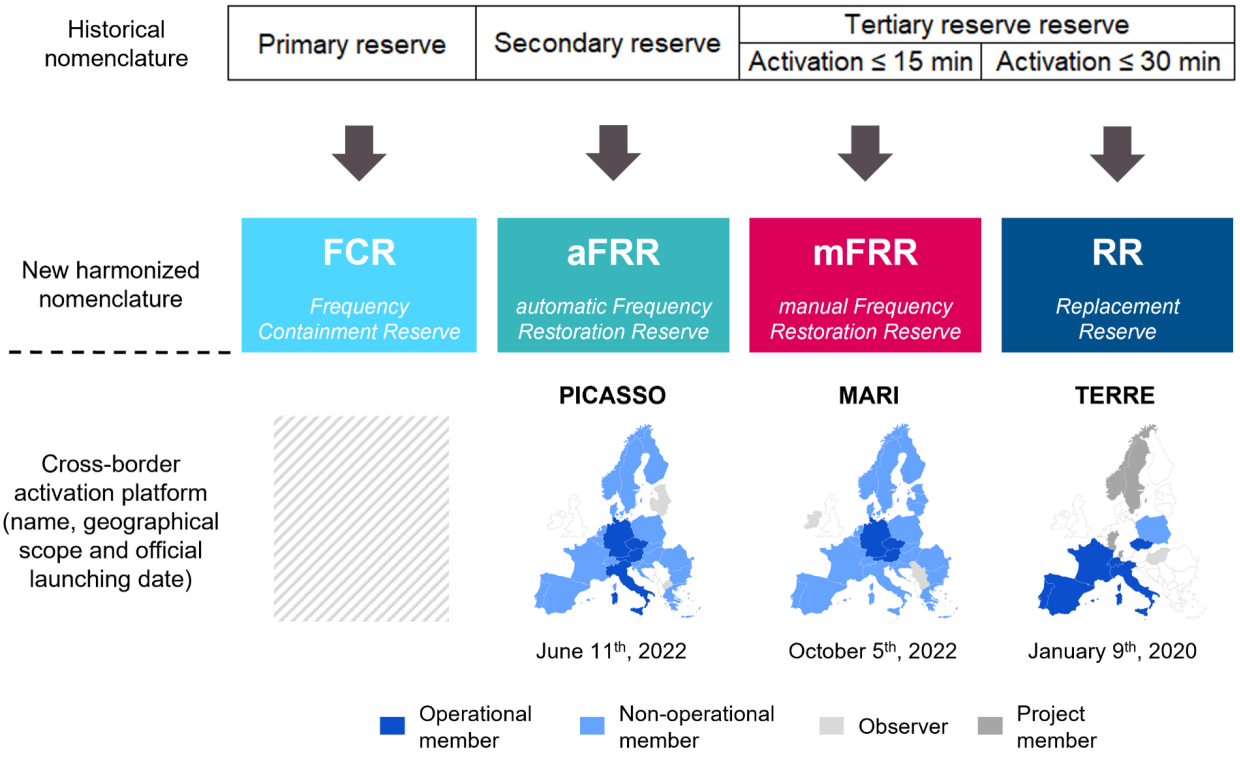

Figure 6.1: Illustration de la libéralisation progressive de l'équilibrage Européen

En outre, la décarbonisation, qui devient de plus en plus urgente chaque jour, exige une transformation profonde du système électrique, notamment par l'installation de larges capacités de sources d'Energie Renouvelable variables (ENRv). La variabilité de ces moyens associée à des prévisions par nature imparfaite ont une conséquence importante: les besoins d'équilibrage des GRTs devraient augmenter de manière significative (Holttinen et al., 2011, Heggarty et al., 2019).

Ces deux aspects vont remodeler l'offre et la demande au sein des processus d'équilibrage, apportant de nouveaux défis et de nouvelles opportunités dans la gestion du système électrique à court terme. Ces éléments conduisent à la question générale à laquelle cette thèse répondra: **Quels sont les impacts de la libéralisation et de la décarbonisation sur la gestion à court terme de l'équilibre offre-demande en Europe ?**

Cette thèse se concentre sur deux principaux types de produits d'équilibrage : la Réserve de Remplacement (RR) et la Réserve manuelle de Restauration de Fréquence (mFRR). Elle aborde ensuite la question de recherche générale sous trois angles distincts mais complémentaires.

Le **chapitre 2** se concentre sur l'offre de réserves au sein des nouveaux marchés d'équilibrage européens, et plus spécifiquement sur l'interaction entre les limitations physiques des unités de production thermique (appelées contraintes opérationnelles) et la standardisation des ordres imposée par ces marchés. En effet, les processus d'équilibrage historiques étaient construits pour correspondre aux caractéristiques spécifiques de leur système électrique local, en utilisant des produits d'équilibrage adaptés pour atténuer partiellement les contraintes opérationnelles mentionnées précédemment. Par exemple, le processus d'équilibrage historique français, appelé "Mécanisme d'ajustement", n'impose aucune exigence sur la forme des réserves soumises

par les Entités d'Ajustement (EDA). En revanche, le design choisi pour les marchés communs d'équilibrage impose une forme standard pour les ordres de marché de réserve d'équilibrage (Figure 6.2), ce qui peut entrer en conflit avec les contraintes opérationnelles et finalement limiter le volume offert par les EDA.

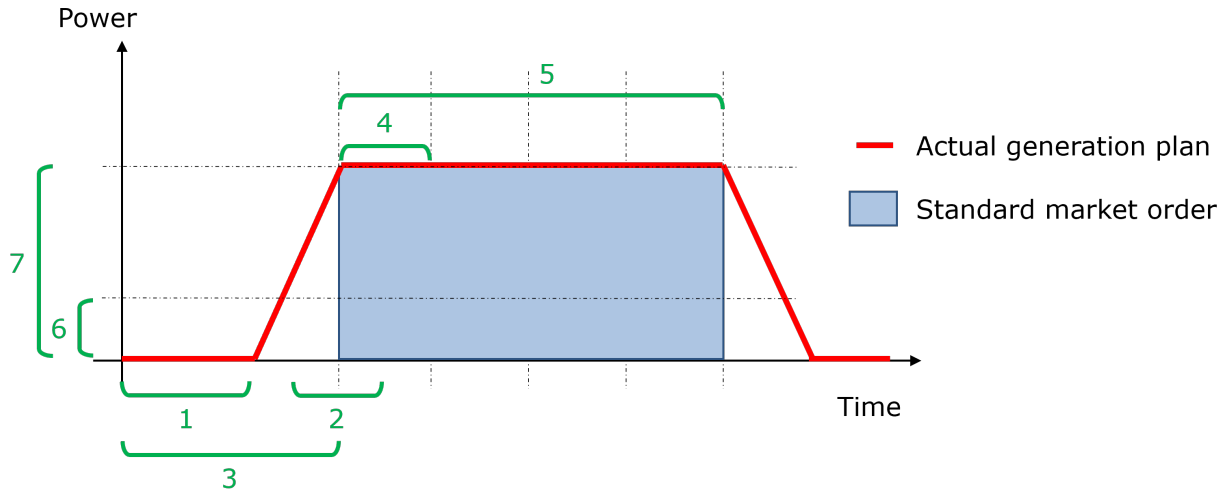

Figure 6.2: Offre d'équilibrage standardisée

Dans ce chapitre, nous définissons une liste de contraintes opérationnelles des unités thermiques, pertinentes compte tenu de la pour la fenêtre temporelle des marchés d'équilibrage. Il est composée des contraintes suivantes: **Puissance maximale**, **Puissance minimale**, **Gradient maximal**, **Durée minimale de marche**, **Durée minimale arrêté**, **Temps de démarrage**, **Temps d'arrêt**, **Temps de palier** et **Délai de préparation**. Nous procédons ensuite à une revue de la littérature des modèles de marché de l'électricité utilisés pour simuler les marchés d'équilibrage, dans le but d'identifier leur degré d'intégration des contraintes opérationnelles. Il apparaît que la plupart des modèles ne prennent en compte qu'un sous-ensemble de la liste précédemment définie, ce qui pourrait avoir un impact sur leurs résultats. Par conséquent, la principale question de recherche abordée par ce chapitre est la suivante : *Comment les contraintes opérationnelles des unités thermiques impactent-elles les performances des marchés d'équilibrage, en particulier sur les indicateurs discutés dans la littérature académique, et leur représentation dans les modèles de marché de l'électricité est-elle pertinente ?*

Pour répondre à cette question, nous proposons une approche de modélisation pour la formulation d'énergie d'équilibrage des EDA sous forme d'ordres de marché standards. Cette méthode est développée dans le modèle de marché de l'électricité ATLAS. Elle intègre notamment la liste des contraintes opérationnelles thermiques pertinentes, en utilisant les outils de complexité des ordres permis par le design des marchés d'équilibrage (divisibilité des ordres et liens de couplage). Cette méthode est appliquée dans une étude de cas, dans laquelle nous simulons une séquence de marchés de l'électricité (marché j-1 et marchés RR) à l'échelle européenne, sur plusieurs jours couvrant différentes situations du système électrique, et selon six scénarios. Les cinq premiers scénarios intègrent progressivement chaque contrainte opérationnelle, puis le dernier propose leur intégration commune, pour permettre une étude poussée de chacune et de leur ensemble sur les entrants et les sortants des marchés RR.

Scénario / Contraintes opérationnelles	Minimum constraints	Basecase (BS)	BS + MinTimeOn/Off	BS + Startup/Shutdown	BS + MinStablePower	All constraints
Puissance maximale/ Puissance minimale	✓	✓	✓	✓	✓	✓
Gradient maximal	✗	✓	✓	✓	✓	✓
Durée minimale de marche / Durée minimale d'arrêt	✗	✗	✓	✗	✗	✓
Temps de démarrage / Temps d'arrêt	✗	✗	✗	✓	✗	✓
Temps de palier	✗	✗	✗	✗	✓	✓

Table 6.1: Chapitre I - Scénarios

Les résultats montrent d'abord que l'intégration des contraintes opérationnelles dans la formulation des ordres des EDA induit une diminution significative de la liquidité du marché RR. Cet effet varie en fonction de la composition du système électrique local, car l'impact de chaque contrainte opérationnelle diffère selon type d'unités thermiques : les contraintes de durée minimale de marche et de durée minimale arrêté ont un impact significatif sur les systèmes électriques composés principalement d'unités CCGT (par exemple l'Allemagne), tandis que la contrainte de temps de palier est particulièrement pertinente pour les systèmes électriques majoritairement composés de centrales nucléaires (comme la France).

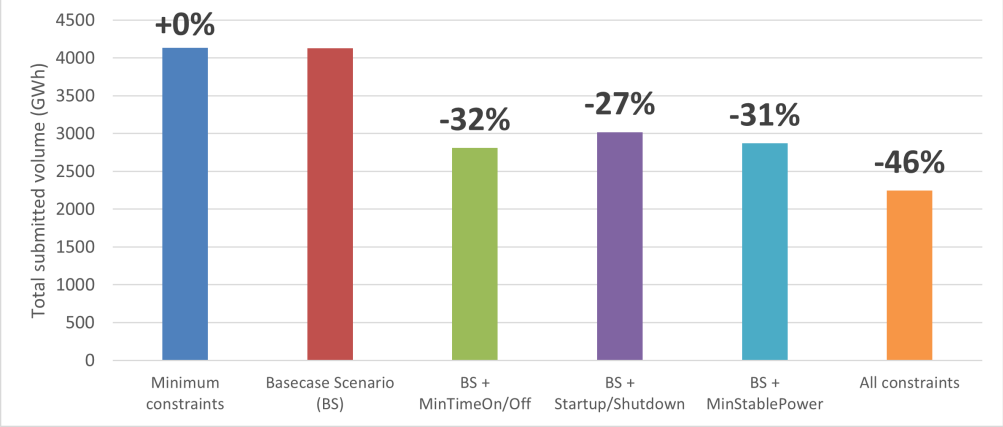

Figure 6.3: Impact sur la liquidité de marché

Si l'on se concentre sur les sorties des marché RR, la baisse de liquidité observée conduit à (i) une augmentation de l'équilibrage des GRT, (ii) une diminution du bien-être social global, et (iii) un impact potentiel sur la sécurité d'approvisionnement, causé par l'augmentation du volume des besoins d'équilibrage non satisfaits. La Figure 6.4 illustre l'évolution des coûts d'équilibrage par rapport au scénario *Basecase*, qui est considéré comme le scénario de base.

Dans l'ensemble, cette première partie de la thèse démontre que la combinaison du processus de standardisation des ordres de marché et des contraintes opérationnelles des unités de production a des impacts significatifs sur les performances des marchés. La solution fournie par les marchés de RR pour intégrer ces contraintes opérationnelles dans le processus de formulation est de créer des ordres complexes (indivisibilité ou liens de couplage). Ces solutions, prises en compte dans notre modèle, s'avèrent insuffisantes : par

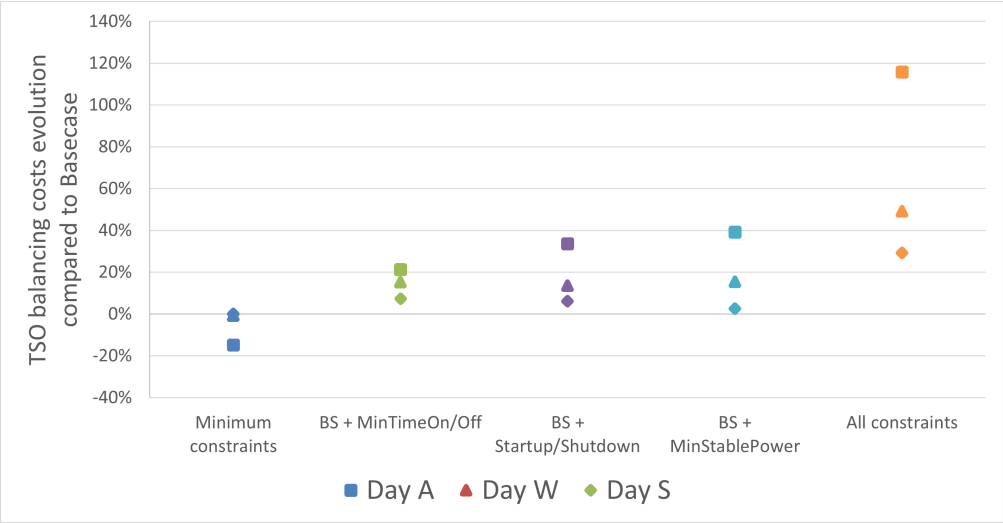

Figure 6.4: Evolution des coûts d'équilibrage par rapport au scénario *Basecase*

exemple, le potentiel de flexibilité des unités nucléaires ne peut pas être offert sur le marché de RR. Ce chapitre démontre également la nécessité de la prise en compte des contraintes opération dans les modèles de simulation des marchés d'équilibrage, afin d'éviter des surestimations potentielles des performances de marché ou des propositions régulatoires imprécises.

Le **Chapitre 3** étudie cette dois la demande sur les marchés d'équilibrage, en se concentrant sur le processus de formulation des besoins d'équilibrage des GRTs. Les marchés d'équilibrage se différencient des marchés de gros (J-1 et infrajournaliers) sur cet aspect, car les GRTs n'étaient pas des acteurs du marché sur ces derniers. Par conséquent, la littérature académique sur les stratégies de formulation d'offres des GRTs présente un manque significatif : à notre connaissance, ce sujet n'a été abordé que dans un seul article, (Håberg and Doorman, 2017) en 2017. Depuis, nous n'avons pas trouvé d'autres recherches sur ce sujet, et tous les articles ultérieurs modélisant les marchés de l'énergie d'équilibrage considèrent que la demande du GRT est inélastique par rapport aux prix. Cependant, le marché RR est opérationnel depuis 2020, et les récents rapports de marché publiés par ENTSO-E suggèrent que la grande majorité des demandes GRTs sont en fait formulées avec une élasticité-prix. Par conséquent, ce chapitre remet en question l'hypothèse d'élasticité des prix des GRT à la lumière de ces nouvelles informations, ce qui conduit à la deuxième question de recherche de cette thèse : *Comment pouvons-nous améliorer les stratégies de formulation d'offres des GRT sur les marchés d'équilibrage communs ? Et quels sont les impacts de ces stratégies sur les résultats de marché et les coûts d'équilibrage ?*

Tout d'abord, ce chapitre propose une analyse empirique du marché de RR conduite sur 2021 et 2022, qui complète les informations initiales présentées dans les rapports de marché susmentionnés. En utilisant les données publiées par le GRT français RTE, cette analyse empirique met en évidence l'élasticité-prix du GRT (voir Figure 6.5) et démontre que les courbes de demande sont déjà formulées sur les marchés de RR, soulignant l'intérêt d'étudier les stratégies GRT.

En conséquence, cette partie de la thèse s'appuie et complète les travaux initiaux de (Håberg and Doorman,

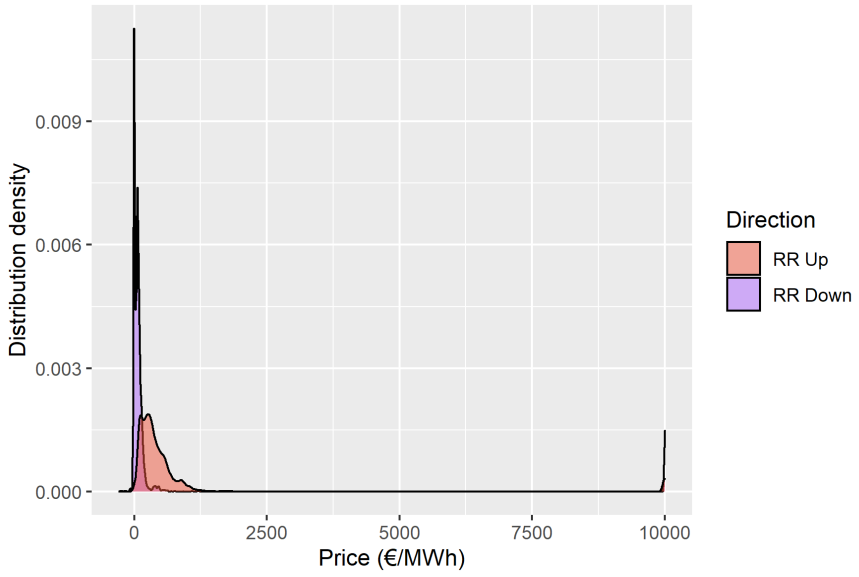

Figure 6.5: Distribution des prix d'offres du GRT français sur le marché de RR entre 2021 et 2022

2017), tout d'abord en abordant les problèmes et pistes de recherche soulignées par les auteurs, puis en proposant une étude de cas qui évalue l'impact des stratégies d'élasticité des prix sur les entrants et les sortants du marché d'activation de RR. Comme les processus d'équilibrage sont devenus séquentiels avec la mise en place des marchés communs, les GRT peuvent effectuer des arbitrages entre le marché RR et les processus plus proches du temps réel pour extraire des coûts d'opportunité, utilisés ensuite pour définir leur élasticité-prix. Les différents types d'alternatives au marché de RR sont analysés et discutés en fonction de leur pertinence. Nous mettons en évidence l'existence d'alternatives supplémentaires, non envisagées dans (Håberg and Doorman, 2017): les processus locaux, qui sont encore exploités en parallèle des marchés communs dans certains pays.

Ensuite, une nouvelle méthode pour la formulation des besoins d'équilibrage GRTs est proposée. Elle sépare notamment la fonction d'estimation des coûts d'opportunités d'une nouvelle fonction qui introduit l'incertitude sur le volume de besoin dans le processus de formulation. Cette incertitude est prise en compte via des distributions des fonctions d'erreurs de prévision du besoin. Cette nouvelle méthode permet également de se baser sur plusieurs types d'alternatives au marché RR, sans présupposer de la capacité du GRT à prédire avec précision la courbe d'offre de l'alternative.

Enfin, cette nouvelle méthodologie a été appliquée dans une étude de cas avec le modèle ATLAS, visant à comparer ses performances avec celles de l'habituelle formulation inélastique au prix, et également à la stratégie de formulation initialement proposée dans (Håberg and Doorman, 2017). Deux types différents d'alternatives au marché de RR sont pris en compte dans le cas d'étude: le processus local d'équilibrage français et le marché de mFRR, plus proche du temps réel. Les résultats montrent que la stratégie proposée peut entraîner des réductions significatives des coûts d'équilibrage du GRT: le Tableau 6.2 illustre cet aspect, en comparant les coûts journaliers de trois scénarios. Le premier correspond à la stratégie inélastique au prix, le deuxième à la stratégie élastique proposée par (Håberg and Doorman, 2017), et le troisième à notre proposition intégrant l'incertitude sur le volume des besoins.

Scénario	Coûts du marché de RR	Coûts du processus local	Coûts totaux
Inel_local	331.2	105.4	436.6
FrBMalt_basic	305.9	100.8	406.7
FrBMalt_vol	54.4	203.2	257.6

Table 6.2: Coûts d'équilibrage GRTs (in milliers d'€) pour les scénarios basés sur l'alternative du processus local français

Ils soulignent également l'importance de la précision de la fonction d'estimation des coûts d'opportunité: une estimation peut affecter de manière substantielle la performance des méthodes élastiques au prix. Par conséquent, ces résultats soulèvent des questions sur les aspects réglementaires des stratégies de formulation d'offres des GRT. Il serait nécessaire de les étudier de façon plus approfondie afin d'éviter des distorsions du marché (i) voulues (par exemple, en favorisant les processus d'équilibrage locaux par rapport aux marchés d'équilibrage communs), ou même (ii) non souhaitées (en raison d'une stratégie imprécise, telle que celle employée pour l'alternative mFRR dans notre cas d'étude).

Enfin, **Chapitre 4** combine les approches sur l'offre et la demande, en se concentrant sur l'impact de la décarbonation sur les marchés d'activation de réserve européens à horizon 2050.

L'intégration massive des Énergies Renouvelables variables (ENRv) sur le réseau européen devrait accroître significativement les besoins d'équilibrage GRTs. Cependant, les nouveaux marchés d'équilibrage sont conçus pour partiellement atténuer cette problématique, tout d'abord en augmentant le volume de réserves disponibles (grâce à la mutualisation à l'échelle internationale), mais également en facilitant la participation de nouveaux types de flexibilités dans les marchés d'équilibrage grâce à un processus plus transparent. Par conséquent, il est important d'évaluer la performance de ces marchés dans des configurations long-terme du système électrique européen. Bien que la littérature existante étudie de nombreux aspects long-terme des processus d'équilibrage en Europe (notamment le dimensionnement des besoins futurs en inertie, le contrôle de la fréquence ou les besoins de contractualisation de réserves), elle est très clairsemée lorsque l'on se concentre sur les marchés d'activation de réserves. En particulier, à notre connaissance, aucune analyse de ces marchés n'a été réalisée à l'horizon 2050.

En outre, le design des marchés de RR et de mFRR font émerger de nouvelles opportunités pour les acteurs d'équilibage. En effet, en plus de leur rôle habituels de fournisseur de réserves à destination des GRTs, ces marchés peuvent également remplir le rôle d'optimisation de la production en proche temps réel, car ils permettent d'activer simultanément des offres d'EDA de sens opposés. Les responsables d'équilibres dont le périmètre est déséquilibré pourraient alors parier sur ces marchés pour s'équilibrer d'eux-mêmes, en soumettant leur déséquilibre sous forme d'ordres de marché RR ou mFRR (un comportement que nous appelons "auto-équilibrage"). Ceci est particulièrement pertinent pour les acteurs ENRv à l'horizon 2050, car ils seront confrontés à des déséquilibres importants en raison de la variabilité de leur production. À notre connaissance, le comportement d'auto-équilibrage sur les marchés RR et mFRR n'est actuellement pas étudié dans la littérature.

Les deux manques dans la littérature présentés précédemment nous conduisent à l'identification des dernières questions de recherche de cette thèse : *Quel est l'impact de l'évolution induite par la décarbonisation du système électrique européen sur les entrants et les sortants des marchés communs d'activation de réserves ? Et quelles sont les conséquences possibles du comportement d'auto-équilibrage des acteurs ENRv à l'horizon 2050 ?*

Ces questions sont examinées via une étude de cas utilisant le modèle ATLAS à deux horizons différents, 2030 et 2050. Les données d'entrée sont basées sur le rapport *Futurs énergétiques 2050*, publié par RTE (RTE, 2022), et représentent le système électrique européen sur la base des projections nationales de capacités installées. Pour chaque horizon temporel, une séquence complète de marchés de l'électricité (J-1, infrajournaliers et marchés d'activation de RR) est simulée sur plusieurs jours d'hiver et d'été, afin de capturer les évolutions saisonnières de production des ENRv.

Les résultats confirment l'augmentation attendue des besoins d'équilibrage GRT, notamment dans les pays possédant d'importantes capacités installées d'ENRv (Figure 6.6). On peut notamment souligner le cas de l'Allemagne, qui dans nos jeux de données possède de loin le plus grand nombre de groupes éoliens. De fait, c'est dans ce pays que les besoins d'équilibrage les plus importants sont constatés. Cependant, cette augmentation est partiellement compensée par deux aspects. D'une part, par l'augmentation des échanges entre zones, en particulier via l'effet de "netting" qui correspond à la compensation des déséquilibres d'une zone par une autre zone ayant un déséquilibre dans le sens inverse.

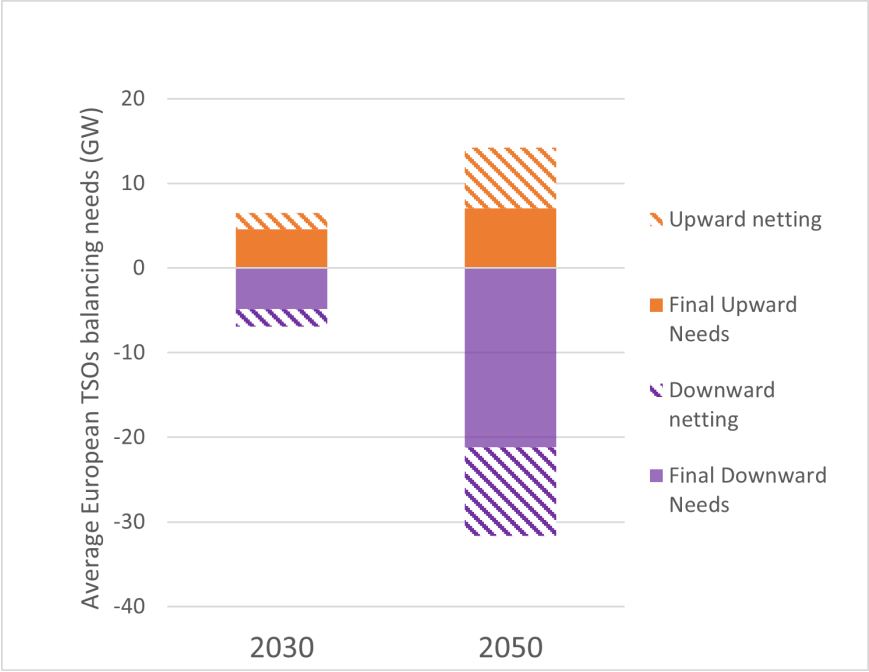

Figure 6.6: Besoins moyens d'équilibrage GRTs à l'échelle de l'Europe (les section hachurées correspondent aux réductions engendrées par le netting)

Le deuxième aspect atténuant l'amplification des besoins GRTs est l'augmentation du volume des offres des EDAs (Figure 6.7), alimentée par l'importante intégration des nouvelles sources de flexibilité (les ENRv, mais aussi les groupes de stockage ou les technologies de conversion de l'électricité en hydrogène). Cet aspect

est néanmoins conditionné par une hypothèse structurante: dans nos simulations, ces nouvelles technologies offrent la totalité de leur capacité disponible sur les marchés d'équilibrage, un comportement qui n'est pas garanti car sujet à de nombreux facteurs (incitations, investissement des producteurs pour participer aux marchés d'activation de réserves, etc.). En effet, si tous les besoins GRTs sont fournis par les marchés dans nos simulations, une analyse complémentaire révèle qu'en l'absence d'offres des nouvelles technologies, des manques de réserves sont constatés dans 5% des pas de temps (ce qui est considérable).

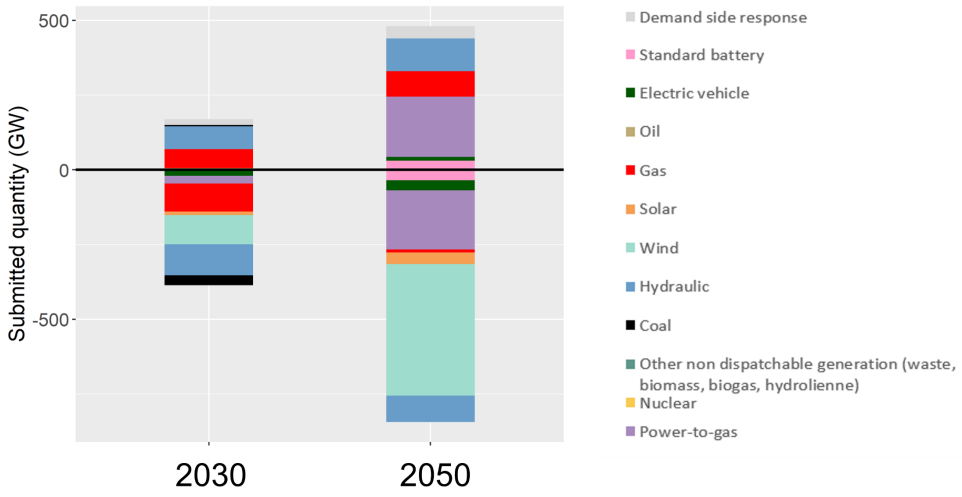

Figure 6.7: Moyenne horaire des volumes offerts par les EDAs en Europe, avec une distinction selon le type de technologie

Nous observons également une augmentation significative de la variabilité des coûts d'équilibrage des GRTs. Au niveau de chaque pays, ces observations sont d'autant plus fortes que les capacités installées d'ENRv sont importantes, en particulier pour les groupes éoliens.

Enfin, le deuxième volet de contributions de ce dernier chapitre est lié à la question du comportement d'auto-équilibrage des acteurs de ENRv, qui est simulé à l'horizon 2050 et comparé avec les scénarios 2050 préalablement présentés. Les résultats montrent que, si l'on fait l'hypothèse d'un prix de règlement des écarts qui incite les acteurs à s'équilibrer (tel que celui utilisé actuellement en France), les acteurs ENRv voient leurs revenus augmenter lorsqu'ils pratiquent l'auto-équilibrage, en formulant leur déséquilibre sur le marché de RR "à tout prix". Avec ce comportement, les besoins d'équilibrage des GRTs sont considérablement réduits, puisque les acteurs ENRv internalisent leur déséquilibre. Ceci engendre également une diminution importante dans la variabilité des coûts d'équilibrage GRTs mise en lumière précédemment. En revanche, le bien-être social global n'est pas augmenté, est est même légèrement réduit. Ce comportement induit principalement un transfert de bien-être social entre les GRTs et les acteurs ENRv. Dans l'ensemble, autoriser ce comportement pourrait inciter les acteurs à participer aux marchés communs d'équilibrage, ce qui irait dans le sens de l'enjeu soulevé précédemment sur l'importance de la participation des nouvelles technologies aux processus d'équilibrage.

Cependant, nous pensons que, s'ils sont autorisés, ces comportements d'auto-équilibrage devraient être encadrés par des évolutions réglementaires. En particulier, la communication entre les EDAs concernées et les

GRT proactifs doit être améliorée, afin d'éviter une surcompensation des déséquilibres. En effet, un dernier jeu de simulations démontre les effets négatifs importants de ce comportement ENRv s'il n'est pas accompagné d'une bonne communication EDA-GRT. D'une part, les gains constatés sur les besoins et coûts d'équilibrage sont complètement annulés, et d'autre part des problèmes notables de sécurité d'approvisionnement sont constantes. En effet, la non-communication conduit à compenser deux fois le même déséquilibre, puisque les EDAs et les GRTs font simultanément la même demande sur les marchés de RR. En conséquence, les déséquilibres locaux ne sont presque pas réduits en sortie du marché de RR , mais sont principalement inversés dans l'autre direction. Nous proposons donc que les offres d'auto-équilibrage sur les marchés de RR et de mFRR soit correctement référencées, de manière à être interprétées comme telles par les GRTs proactifs afin qu'ils puissent intégrer cette information dans leurs estimations de besoins d'équilibrage.

References

Abbasy, A., van der Veen, R. A., & Hakvoort, R. A. (2009). Effect of integrating regulating power markets of northern europe on total balancing costs. *2009 IEEE Bucharest PowerTech*, 1–7.

Abrell, J., & Kunz, F. (2015). Integrating intermittent renewable wind generation-a stochastic multi-market electricity model for the european electricity market. *Networks and Spatial Economics*, *15*(1), 117–147.

Agathokleous, C., & Ehnberg, J. (2020). A quantitative study on the requirement for additional inertia in the european power system until 2050 and the potential role of wind power. *Energies*, *13*(9), 2309.

Ahlqvist, V., Holmberg, P., & Tangerås, T. P. (2018). *Central-versus self-dispatch in electricity markets*. JSTOR.

Akbari-Dibavar, A., Mohammadi-Ivatloo, B., & Zare, K. (2020). Electricity market pricing: Uniform pricing vs. pay-as-bid pricing. In *Electricity markets* (pp. 19–35). Springer.

Aravena, I., & Papavasiliou, A. (2016). Renewable energy integration in zonal markets. *IEEE Transactions on Power Systems*, *32*(2), 1334–1349.

Auer, H., & Haas, R. (2016). On integrating large shares of variable renewables into the electricity system. *Energy*, *115*, 1592–1601.

Batalla-Bejerano, J., & Trujillo-Baute, E. (2016). Impacts of intermittent renewable generation on electricity system costs. *Energy Policy*, *94*, 411–420.

Battula, S., Tesfatsion, L., & McDermott, T. E. (2020). An ercot test system for market design studies. *Applied Energy*, *275*, 115182.

Bellman, R. (1966). Dynamic programming. *Science*, *153*(3731), 34–37.

Boehnke, F., Botor, B., Kolkmann, S., Kramer, H., Weber, C., Kasmi, G., Girod, M., Brenas, C., Laasri, M., Bortolotti, S., Dussartre, V., Heggarty, T., & Pisano, G. (2022). *Models for market mechanisms simulation taking into account space-time downscaling and novel flexibility technologies* (tech. rep.).

Boiteux, M. (1951). La tarification au coût marginal et les demandes aléatoires. *Cahiers du Séminaire d'économétrie*, 56–69.

Boomsma, T. K., Juul, N., & Fleten, S.-E. (2014). Bidding in sequential electricity markets: The nordic case. *European Journal of Operational Research*, *238*(3), 797–809.

Borne, O., Korte, K., Perez, Y., Petit, M., & Purkus, A. (2018). Barriers to entry in frequency-regulation services markets: Review of the status quo and options for improvements. *Renewable and Sustainable Energy Reviews*, *81*, 605–614.

Botterud, A., Wang, J., Bessa, R., Keko, H., & Miranda, V. (2010). Risk management and optimal bidding for a wind power producer. *IEEE PES General Meeting*, 1–8.

Bottieau, J., Hubert, L., De Grève, Z., Vallée, F., & Toubeau, J.-F. (2019). Very-short-term probabilistic forecasting for a risk-aware participation in the single price imbalance settlement. *IEEE Transactions on Power Systems*, *35*(2), 1218–1230.

Brijs, T., Geth, F., De Jonghe, C., & Belmans, R. (2019). Quantifying electricity storage arbitrage opportunities in short-term electricity markets in the cwe region. *Journal of Energy Storage*, *25*, 100899.

Bublitz, A., Ringler, P., Genoese, M., & Fichtner, W. (2014). Agent-based simulation of the german and french wholesale electricity markets-recent extensions of the powerace model with exemplary applications. *International Conference on Agents and Artificial Intelligence*, *2*, 40–49.

Bunn, D. W., & Kermer, S. O. (2021). Statistical arbitrage and information flow in an electricity balancing market. *The Energy Journal*, *42*(5), 19–40.

Burgholzer, B. (2016). Evaluation of different balancing market designs with the edison+ balancing model. *2016 13th International Conference on the European Energy Market (EEM)*, 1–6.

Bussar, C., Stöcker, P., Cai, Z., Moraes Jr, L., Magnor, D., Wiernes, P., van Bracht, N., Moser, A., & Sauer, D. U. (2016). Large-scale integration of renewable energies and impact on storage demand in a european renewable power system of 2050—sensitivity study. *Journal of Energy Storage*, *6*, 1–10.

Cany, C., Mansilla, C., Mathonnière, G., & Da Costa, P. (2018). Nuclear power supply: Going against the misconceptions. evidence of nuclear flexibility from the french experience. *Energy*, *151*, 289–296.

Caramanis, M. C., Bohn, R. E., & Schweppe, F. C. (1982). Optimal spot pricing: Practice and theory. *IEEE Transactions on Power Apparatus and Systems*, (9), 3234–3245.

Chaves-Ávila, J. P., Hakvoort, R. A., & Ramos, A. (2014). The impact of european balancing rules on wind power economics and on short-term bidding strategies. *Energy Policy*, *68*, 383–393.

Cincotti, S., & Gallo, G. (2012). Gapex: An agent-based framework for power exchange modeling and simulation. *International Conference on Agents and Artificial Intelligence*, *2*, 33–43.

Cogen, F., Little, E., Dussartre, V., & Bustarret, Q. (2024). Atlas: A model of short-term european electricity market processes under uncertainty – balancing modules.

Cogen, F., Roques, F., Dussartre, V., & Little, E. (2023). Towards the use of pricing methods by transmission system operators on electricity balancing markets. *2023 19th International Conference on the European Energy Market (EEM)*, 1–7.

Colmenar-Santos, A., Muñoz-Gómez, A.-M., Rosales-Asensio, E., & López-Rey, Á. (2019). Electric vehicle charging strategy to support renewable energy sources in europe 2050 low-carbon scenario. *Energy*, *183*, 61–74.

Commission, T. E. (2017). *Commission regulation (eu) 2017/2195 of 23 november 2017 establishing a guideline on electricity balancing*. https://eur-lex.europa.eu/legal-content/EN/TXT/?uri=CELEX:02017R2195-20210315

Core Writing Team, H. L., & (eds.), J. R. (2023). *Climate change 2023: Synthesis report: Contribution of working groups i, ii and iii to the sixth assessment report of the intergovernmental panel on climate change*. IPCC.

Dallinger, B., Auer, H., & Lettner, G. (2018). Impact of harmonised common balancing capacity procurement in selected central european electricity balancing markets. *Applied Energy*, *222*, 351–368.

De Jonghe, C., Delarue, E., Belmans, R., & D'haeseleer, W. (2011). Determining optimal electricity technology mix with high level of wind power penetration. *Applied Energy*, *88*(6), 2231–2238.

Doherty, R., Mullane, A., Nolan, G., Burke, D. J., Bryson, A., & O'Malley, M. (2009). An assessment of the impact of wind generation on system frequency control. *IEEE transactions on power systems*, *25*(1), 452–460.

Dukpa, A., Duggal, I., Venkatesh, B., & Chang, L. (2010). Optimal participation and risk mitigation of wind generators in an electricity market. *IET renewable power generation*, *4*(2), 165–175.

ENTSO-E. (2022). *Balancing report 2022*.

ENTSO-E. (2023a). *Mari activation optimization function public description*.

ENTSO-E. (2023b). *Market report 2023*.

ENTSO-E. (2017). *Survey on ancillary services procurement, balancing market design 2016* (tech. rep.). ENTSO-E.

ENTSO-E. (2021). *Survey on ancillary services procurement, balancing market design 2020* (tech. rep.). ENTSO-E.

ENTSO-E. (2023c). *Terre activation optimization function public description - libra platform*.

European commission, quarterly report on european electricity markets (tech. rep.). (2023). European Commission.

Farahmand, H., & Doorman, G. L. (2012). Balancing market integration in the northern european continent. *Applied Energy*, *96*, 316–326.

Fedele, A., Di Benedettto, G., Pascucci, A., Pecoraro, G., Allella, F., & Carlini, E. M. (2020). European electricity market integration: The exchange of manual frequency restoration reserves among terna and the other tsos. *2020 AEIT International Annual Conference (AEIT)*, 1–5.

Fleten, S.-E., & Pettersen, E. (2005). Constructing bidding curves for a price-taking retailer in the norwegian electricity market. *IEEE Transactions on Power Systems*, *20*(2), 701–708.

Frade, P., Shafie-khah, M., Santana, J., & Catalao, J. (2019). Cooperation in ancillary services: Portuguese strategic perspective on replacement reserves. *Energy Strategy Reviews*, *23*, 142–151.

Fraunholz, C., Keles, D., & Fichtner, W. (2021). On the role of electricity storage in capacity remuneration mechanisms. *Energy Policy*, *149*, 112014.

Fraunholz, C., Kraft, E., Keles, D., & Fichtner, W. (2021). Advanced price forecasting in agent-based electricity market simulation. *Applied Energy*, *290*, 116688.

Gebrekiros, Y., & Doorman, G. (2014). Balancing energy market integration in northern europe—modeling and case study. *2014 IEEE PES General Meeting| Conference & Exposition*, 1–5.

Gebrekiros, Y., Doorman, G., Jaehnert, S., & Farahmand, H. (2015). Reserve procurement and transmission capacity reservation in the northern european power market. *International Journal of Electrical Power & Energy Systems*, *67*, 546–559.

Gils, H. C. (2014). Assessment of the theoretical demand response potential in europe. *Energy*, *67*, 1–18.

Girod, M., Donnot, B., Dussartre, V., Terrier, V., Bourmaud, J.-Y., & Perez, Y. (2024). Bid filtering for congestion management in european balancing markets–a reinforcement learning approach. *Applied Energy*, *361*, 122892.

Girod, M., Karangelos, E., Little, E., Terrier, V., Bourmaud, J.-Y., Dussartre, V., Jouini, O., & Perez, Y. (2022). Improving cross-border capacity for near real-time balancing. *2022 18th International Conference on the European Energy Market (EEM)*, 1–6.

Goodarzi, S., Perera, H. N., & Bunn, D. (2019). The impact of renewable energy forecast errors on imbalance volumes and electricity spot prices. *Energy Policy*, *134*, 110827.

Grueger, F., Möhrke, F., Robinius, M., & Stolten, D. (2017). Early power to gas applications: Reducing wind farm forecast errors and providing secondary control reserve. *Applied energy*, *192*, 551–562.

Guo, H., Chen, Q., Shahidehpour, M., Xia, Q., & Kang, C. (2022). Bidding behaviors of gencos under bounded rationality with renewable energy. *Energy*, *250*, 123793.

Håberg, M., & Doorman, G. (2016). Classification of balancing markets based on different activation philosophies: Proactive and reactive designs. *2016 13th International Conference on the European Energy Market (EEM)*, 1–5.

Håberg, M., & Doorman, G. (2017). Proactive planning and activation of manual reserves in sequentially cleared balancing markets. *2017 IEEE Electrical Power and Energy Conference (EPEC)*, 1–6.

Haring, T., Mountouri, D., & Andersson, G. (2012). Ensuring energy-market liquidity through adequate imbalance settlement. *2012 47th International Universities Power Engineering Conference (UPEC)*, 1–6.

Haring, T. W., Kirschen, D. S., & Andersson, G. (2015). Incentive compatible imbalance settlement. *IEEE Transactions on Power Systems*, *30*(6), 3338–3346.

Hary, N. (2018). *Quantitative assessment of electricity market designs: Illustrations of short-term and long-term dynamics* [Doctoral dissertation, Université Paris sciences et lettres].

Heggarty, T., Bourmaud, J.-Y., Girard, R., & Kariniotakis, G. (2019). Multi-temporal assessment of power system flexibility requirement. *Applied Energy*, *238*, 1327–1336.

Heydarian-Forushani, E., Moghaddam, M. P., Sheikh-El-Eslami, M. K., Shafie-khah, M., & Catalão, J. P. (2014). Risk-constrained offering strategy of wind power producers considering intraday demand response exchange. *IEEE Transactions on sustainable energy*, *5*(4), 1036–1047.

Hirst, E. (2001). Real-time balancing operations and markets: Key to competitive wholesale electricity markets. *Edison Electric Institute*.

Hirth, L., & Ziegenhagen, I. (2015). Balancing power and variable renewables: Three links. *Renewable and Sustainable Energy Reviews*, *50*, 1035–1051.

Holttinen, H., Meibom, P., Orths, A., Lange, B., O'Malley, M., Tande, J. O., Estanqueiro, A., Gomez, E., Söder, L., Strbac, G., et al. (2011). Impacts of large amounts of wind power on design and operation of power systems, results of iea collaboration. *Wind Energy*, *14*(2), 179–192.

Holttinen, H., Miettinen, J. J., Couto, A., Algarvio, H., Rodrigues, L., & Estanqueiro, A. (2016). Wind power producers in shorter gate closure markets and balancing markets. *2016 13th International Conference on the European Energy Market (EEM)*, 1–5.

Huber, M., Dimkova, D., & Hamacher, T. (2014). Integration of wind and solar power in europe: Assessment of flexibility requirements. *Energy*, *69*, 236–246.

IEA. (2021). *Net zero by 2050: A roadmap for the global energy sector*. https://www.iea.org/reports/net-zero-by-2050

Jacobsen, H. K., & Schröder, S. T. (2012). Curtailment of renewable generation: Economic optimality and incentives. *Energy Policy*, *49*, 663–675.

Jaehnert, S., & Doorman, G. (2010). Modelling an integrated northern european regulating power market based on a common day-ahead market. *Proc. of IAEE International Conference, Rio de Janeiro*.

Jenkins, J. D., Zhou, Z., Ponciroli, R., Vilim, R. B., Ganda, F., de Sisternes, F., & Botterud, A. (2018). The benefits of nuclear flexibility in power system operations with renewable energy. *Applied energy*, *222*, 872–884.

Joos, M., & Staffell, I. (2018). Short-term integration costs of variable renewable energy: Wind curtailment and balancing in britain and germany. *Renewable and Sustainable Energy Reviews*, *86*, 45–65.

Joskow, P. L., & Schmalensee, R. (1983). Markets for power: An analysis of electric utility deregulation.

Just, S., & Weber, C. (2015). Strategic behavior in the german balancing energy mechanism: Incentives, evidence, costs and solutions. *Journal of Regulatory Economics*, *48*, 218–243.

Kannavou, M., Zampara, M., & Capros, P. (2019). Modelling the eu internal electricity market: The primes-iem model. *Energies*, *12*(15), 2887.

Khodadadi, A., Herre, L., Shinde, P., Eriksson, R., Söder, L., & Amelin, M. (2020). Nordic balancing markets: Overview of market rules. *2020 17th International Conference on the European Energy Market (EEM)*, 1–6.

Kirkerud, J., Nagel, N. O., & Bolkesjø, T. (2021). The role of demand response in the future renewable northern european energy system. *Energy*, *235*, 121336.

Klyve, Ø. S., Klæboe, G., Nygård, M. M., & Marstein, E. S. (2023). Limiting imbalance settlement costs from variable renewable energy sources in the nordics: Internal balancing vs. balancing market participation. *Applied Energy*, *350*, 121696.

Koch, C., & Hirth, L. (2019). Short-term electricity trading for system balancing: An empirical analysis of the role of intraday trading in balancing germany's electricity system. *Renewable and Sustainable Energy Reviews*, *113*, 109275.

Kolkmann, S., Fortin, M., Böcker, B., & Weber, C. (2019, April). *OSMOSE - Methodology for error forecasts at European scale* (tech. rep.). https://ec.europa.eu/research/participants/documents/downloadPublic?documentIds=080166e5c47c7da0&appId=PPGMS

Lauvergne, R., Perez, Y., Françon, M., & De La Cruz, A. T. (2022). Integration of electric vehicles into transmission grids: A case study on generation adequacy in europe in 2040. *Applied Energy*, *326*, 120030.

Little, E., Cogen, F., Bustarret, Q., Dussartre, V., Lâasri, M., Kasmi, G., Girod, M., Bienvenu, F., Fortin, M., & Bourmaud, J.-Y. (2024). Atlas: A model of short-term european electricity market processes under uncertainty.

Lorenz, C. (2017). Balancing reserves within a decabonized european electricity system in 2050—from market developments to model insights. *2017 14th International Conference on the European Energy Market (EEM)*, 1–8.

Lund, P. D., Lindgren, J., Mikkola, J., & Salpakari, J. (2015). Review of energy system flexibility measures to enable high levels of variable renewable electricity. *Renewable and sustainable energy reviews*, *45*, 785–807.

Lux, B., & Pfluger, B. (2020). A supply curve of electricity-based hydrogen in a decarbonized european energy system in 2050. *Applied Energy*, *269*, 115011.

Maenhoudt, M., & Deconinck, G. (2010). Agent-based modelling as a tool for testing electric power market designs. *2010 7th International Conference on the European Energy Market*, 1–5.

Maenhoudt, M., & Deconinck, G. (2013). Strategic offering to maximize day-ahead profit by hedging against an infeasible market clearing result. *IEEE Transactions on Power Systems*, *29*(2), 854–862.

Mansur, E. T. (2008). Measuring welfare in restructured electricity markets. *The Review of Economics and Statistics*, *90*(2), 369–386.

Mansur, E. T., & White, M. (2012). Market organization and efficiency in electricity markets. *unpublished results*.

Marañón-Ledesma, H., & Tomasgard, A. (2019). Analyzing demand response in a dynamic capacity expansion model for the european power market. *Energies*, *12*(15), 2976.

Marneris, I. G., Roumkos, C. G., & Biskas, P. N. (2019). Towards balancing market integration: Conversion process for balancing energy offers of central-dispatch systems. *IEEE Transactions on Power Systems*, *35*(1), 293–303.

Marquet, S. (2018). *Mari: Algorithm design principles* (tech. rep.).

Matsumoto, T., Bunn, D., & Yamada, Y. (2021). Mitigation of the inefficiency in imbalance settlement designs using day-ahead prices. *IEEE Transactions on Power Systems*, *37*(5), 3333–3345.

Meeus, L. (2020). *The evolution of electricity markets in europe*. Edward Elgar Publishing.

Mier, M., & Weissbart, C. (2020). Power markets in transition: Decarbonization, energy efficiency, and short-term demand response. *Energy Economics*, *86*, 104644.

Mileva, A., Johnston, J., Nelson, J. H., & Kammen, D. M. (2016). Power system balancing for deep decarbonization of the electricity sector. *Applied Energy*, *162*, 1001–1009.

Morales-España, G., Gentile, C., & Ramos, A. (2015). Tight mip formulations of the power-based unit commitment problem. *OR spectrum*, *37*(4), 929–950.

Newbery, D., Strbac, G., & Viehoff, I. (2016). The benefits of integrating european electricity markets. *Energy Policy*, *94*, 253–263.

Nordström, H., Söder, L., & Eriksson, R. (2022). Estimating the future need of balancing power based on long-term power system market simulations. *arXiv preprint arXiv:2207.04683*.

Ocker, F., Braun, S., & Will, C. (2016). Design of european balancing power markets. *2016 13th International Conference on the European Energy Market (EEM)*, 1–6.

Ocker, F., & Ehrhart, K.-M. (2017). The "german paradox" in the balancing power markets. *Renewable and Sustainable Energy Reviews*, *67*, 892–898.

Ocker, F., Ehrhart, K.-M., & Ott, M. (2018). Bidding strategies in austrian and german balancing power auctions. *Wiley Interdisciplinary Reviews: Energy and Environment*, *7*(6), e303.

Ortner, A., & Totschnig, G. (2019). The future relevance of electricity balancing markets in europe-a 2030 case study. *Energy Strategy Reviews*, *24*, 111–120.

Pei, W., Du, Y., Deng, W., Sheng, K., Xiao, H., & Qu, H. (2016). Optimal bidding strategy and intramarket mechanism of microgrid aggregator in real-time balancing market. *IEEE Transactions on Industrial Informatics*, *12*(2), 587–596.

Petitet, M. (2016). Effects of risk aversion on investment decisions in electricity generation: What consequences for market design? *2016 13th International Conference on the European Energy Market (EEM)*, 1–5.

Petitet, M., Perrot, M., Mathieu, S., Ernst, D., & Phulpin, Y. (2019). Impact of gate closure time on the efficiency of power systems balancing. *Energy Policy*, *129*, 562–573.

Petrichenko, R., Kozadajevs, J., Petrichenko, L., & Silis, A. (2022). Reserve power estimation according to the baltic power system 2050 development plan. *2022 IEEE 7th International Energy Conference (ENERGYCON)*, 1–6.

Pichoud, M. (2023). *Optimizing distributed flexibility provision in competitive wholesale markets considering local constraints in the distribution grid* [Doctoral dissertation, Université Paris sciences et lettres].

Poncela, M., Purvins, A., & Chondrogiannis, S. (2018). Pan-european analysis on power system flexibility. *Energies*, *11*(7), 1765.

Poncelet, K., Delarue, E., & D'haeseleer, W. (2020). Unit commitment constraints in long-term planning models: Relevance, pitfalls and the role of assumptions on flexibility. *Applied Energy*, *258*, 113843.

Poplavskaya, K. (2021). Balancing and redispatch: The next stepping stones in european electricity market integration: Improving the market design and the efficiency of the procurement of balancing and redispatch services.

Poplavskaya, K., & De Vries, L. (2019). Distributed energy resources and the organized balancing market: A symbiosis yet? case of three european balancing markets. *Energy policy*, *126*, 264–276.

Poplavskaya, K., Lago, J., & De Vries, L. (2020). Effect of market design on strategic bidding behavior: Model-based analysis of european electricity balancing markets. *Applied Energy*, *270*, 115130.

Poplavskaya, K., Lago, J., Strömer, S., & De Vries, L. (2021). Making the most of short-term flexibility in the balancing market: Opportunities and challenges of voluntary bids in the new balancing market design. *Energy Policy*, *158*, 112522.

Quoilin, S., Hidalgo Gonzalez, I., & Zucker, A. (2017). Modelling future eu power systems under high shares of renewables: The dispa-set 2.1 open-source model.

Qussous, R., Harder, N., & Weidlich, A. (2022). Understanding power market dynamics by reflecting market interrelations and flexibility-oriented bidding strategies. *Energies*, *15*(2), 494.

Rancilio, G., Rossi, A., Falabretti, D., Galliani, A., & Merlo, M. (2022). Ancillary services markets in europe: Evolution and regulatory trade-offs. *Renewable and Sustainable Energy Reviews*, *154*, 111850.

Rebours, Y. G., Kirschen, D. S., Trotignon, M., & Rossignol, S. (2007a). A survey of frequency and voltage control ancillary services—part i: Technical features. *IEEE Transactions on power systems*, *22*(1), 350–357.

Rebours, Y. G., Kirschen, D. S., Trotignon, M., & Rossignol, S. (2007b). A survey of frequency and voltage control ancillary services—part ii: Economic features. *IEEE Transactions on power systems*, *22*(1), 358–366.

Reeg, M., Hauser, W., Wassermann, S., Kast, T., Klann, U., Nienhaus, K., Pfenning, U., & Weimer-Jehle, W. (2012). Amiris: An agent-based simulation model for the analysis of different support schemes and their effects on actors involved in the integration of renewable energies into energy markets. *2012 23rd International Workshop on Database and Expert Systems Applications*, 339–344.

Roumkos, C., Biskas, P. N., & Marneris, I. G. (2022). Integration of european electricity balancing markets. *Energies*, *15*(6), 2240.

RTE. (2017). *French electricity balancing roadmap, green paper - short version.* https://www.services-rte.com/files/live/sites/services-rte/files/pdf/Mecanisme%20d%27ajustement/livre_vert_equilibre_od_short_version.pdf

RTE. (2022). *Futurs énergétiques 2050.*

Schill, W.-P., Pahle, M., & Gambardella, C. (2017). Start-up costs of thermal power plants in markets with increasing shares of variable renewable generation. *Nature Energy*, *2*(6), 1–6.

Schneider, I., & Roozbehani, M. (2017). Energy market design for renewable resources: Imbalance settlements and efficiency–robustness tradeoffs. *IEEE Transactions on Power systems*, *33*(4), 3757–3767.

Seck, G. S., Krakowski, V., Assoumou, E., Maizi, N., & Mazauric, V. (2020). Embedding power system's reliability within a long-term energy system optimization model: Linking high renewable energy integration and future grid stability for france by 2050. *Applied Energy*, *257*, 114037.

Shortt, A., Kiviluoma, J., & O'Malley, M. (2012). Accommodating variability in generation planning. *IEEE Transactions on Power Systems*, *28*(1), 158–169.

Silva, A. R., Pousinho, H., & Estanqueiro, A. (2022). A multistage stochastic approach for the optimal bidding of variable renewable energy in the day-ahead, intraday and balancing markets. *Energy*, *258*, 124856.

Sirin, S. M., & Yilmaz, B. N. (2021). The impact of variable renewable energy technologies on electricity markets: An analysis of the turkish balancing market. *Energy Policy*, *151*, 112093.

Teng, F., Aunedi, M., & Strbac, G. (2016). Benefits of flexibility from smart electrified transportation and heating in the future uk electricity system. *Applied energy*, *167*, 420–431.

Tesfatsion, L., & Battula, S. (2020). Analytical scuc/sced optimization formulation for ames v5. 0.

Teufel, F., Miller, M., Genoese, M., & Fichtner, W. (2013). Review of system dynamics models for electricity market simulations.

Tuohy, A., Meibom, P., Denny, E., & O'Malley, M. (2009). Unit commitment for systems with significant wind penetration. *IEEE Transactions on power systems*, *24*(2), 592–601.

Vale, Z., Pinto, T., Praca, I., & Morais, H. (2011). Mascem: Electricity markets simulation with strategic agents. *IEEE Intelligent Systems*, *26*(2), 9–17.

van Hout, M., Koutstaal, P. R., Özdemir, Ö., & Seebregts, A. (2014). *Quantifying flexibility markets*. ECN Petten.

Van den Bergh, K., Bruninx, K., Delarue, E., & D'haeseleer, W. (2014). Lusym: A unit commitment model formulated as a mixed-integer linear program. *KU Leuven, TME Branch Working Paper*, *7*.

Van den Bergh, K., & Delarue, E. (2020). Energy and reserve markets: Interdependency in electricity systems with a high share of renewables. *Electric Power Systems Research*, *189*, 106537.

Van der Veen, R., Abbasy, A., & Hakvoort, R. A. (2010). A qualitative analysis of main cross-border balancing arrangements. *2010 7th International Conference on the European Energy Market*, 1–6.

Van Der Veen, R. A., Abbasy, A., & Hakvoort, R. A. (2012). Agent-based analysis of the impact of the imbalance pricing mechanism on market behavior in electricity balancing markets. *Energy Economics*, *34*(4), 874–881.

van der Veen, R. A., Abbasy, A., & Hakvoort, R. A. (2010). A comparison of imbalance settlement designs and results of germany and the netherlands. *Young Energy Engineers & Economists Seminar (YEEES)*, 1–24.

van der Veen, R. A., & Hakvoort, R. A. (2016). The electricity balancing market: Exploring the design challenge. *Utilities Policy*, *43*, 186–194.

Vandezande, L., Meeus, L., Belmans, R., Saguan, M., & Glachant, J.-M. (2010). Well-functioning balancing markets: A prerequisite for wind power integration. *Energy policy*, *38*(7), 3146–3154.

Vandezande, L., Meeus, L., Belmans, R., Saguan, M., Glachant, J.-M., & Rious, V. (2009). Lacking balancing market harmonisation in europe: Room for trader profits at the expense of economic efficiency? *32nd IAEE International Conference*, 17–pages.

Ventosa, M., Baıllo, A., Ramos, A., & Rivier, M. (2005). Electricity market modeling trends. *Energy policy*, *33*(7), 897–913.

Veselka, T., Boyd, G., Conzelmann, G., Koritarov, V., Macal, C., North, M., Schoepfle, B., Thimmapuram, P., et al. (2002). Simulating the behavior of electricity markets with an agent-based methodology: The electric market complex adaptive systems (emcas) model. *Vancouver, Canada*.

Weber, A., Glachant, J.-M., Rious, V., Saguan, M., Gil, J. B., Puente, E. R., Kitzing, L., Morthorst, P. E., Schröder, S. T., Bourmand, J.-Y., et al. (2012). Optimate–a modeling breakthrough for market design analysis to test massive intermittent generation integration in markets. *9th International Conference on the European Energy Market (EEM 2012)*.

Weidlich, A., & Veit, D. (2008). A critical survey of agent-based wholesale electricity market models. *Energy economics*, *30*(4), 1728–1759.

Xu, Z., Hu, Z., Song, Y., & Wang, J. (2015). Risk-averse optimal bidding strategy for demand-side resource aggregators in day-ahead electricity markets under uncertainty. *IEEE Transactions on Smart Grid*, *8*(1), 96–105.

Xue, Y., Venkatesh, B., & Chang, L. (2008). Bidding wind power in short-term electricity market based on multiple-objective fuzzy optimization. *2008 Canadian Conference on Electrical and Computer Engineering*, 001135–001138.

Zani, A., & Migliavacca, G. (2014). Pan-european balancing market: Benefits for the italian power system. *2014 AEIT Annual Conference-From Research to Industry: The Need for a More Effective Technology Transfer (AEIT)*, 1–6.

Zhang, H., Gao, F., Wu, J., Liu, K., & Liu, X. (2012). Optimal bidding strategies for wind power producers in the day-ahead electricity market. *Energies*, *5*(11), 4804–4823.

Zolotarev, P. (2017). Social welfare of balancing markets. *2017 14th International Conference on the European Energy Market (EEM)*, 1–6.

Appendix A

ATLAS balancing modules

Acknowledgment: This description of the balancing stage in ATLAS was also published on arXiv (Cogen, F., Little, E., Dussartre, V., & Bustarret, Q. (2024). ATLAS: A Model of Short-term European Electricity Market Processes under Uncertainty-Balancing Modules. arXiv preprint arXiv:2402.12859.). Adjustments have been made to the version of this appendix.

A.1 ATLAS Balancing Stage - Introduction and Context

This paper is part of the documentation of the ATLAS electricity market model. It follows and complements (Little et al., 2024) by focusing on modules specifically developed for the balancing section of the electricity market process. Certain steps of the balancing section, such as the Clearing, are done using modules also applied for day-ahead or intraday market simulations that are already explained in the aforementioned article, and therefore not detailed here.

A.1.1 Overview of balancing markets characteristics

The European power system is currently experiencing a significant change in its balancing stage. Historically managed locally by each European Transmission System Operator (TSO) using diverse processes, it is now switching to common balancing markets occurring within the last hour before real-time, and that are structured around 4 different types of reserves:

- Frequency Containment Reserves (FCR) are the fastest amongst them, being automatically activated within a few seconds when an imbalance arises to stop the induced frequency deviation.
- automatic Frequency Restoration Reserves (aFRR) are automatically activated in 30 seconds in order to bring the frequency back to 50 Hz.

- manual Frequency Restoration Reserves (mFRR) take over the role of aFRR in 12.5 minutes, with a manual activation process.
- Finally, Replacement Reserves (RR) are manually activated in 30 minutes to compensate for the activation of all previously described reserves.

Amongst these reserve types, mFRR and RR stand out for being activated manually. They are consequently part of energy markets, respectively traded on the cross-border platforms MARI and TERRE. Both markets include two kinds of actors, Balancing Services Providers (BSPs) that offer reserve energy and TSOs that formulate balancing needs.

A.1.1.1 The RR market

A sequential representation of the RR market operational process is given in Figure A.1, based on public descriptions available in (ENTSO-E, 2023c). It is executed at an hourly frequency, and spans over an effective time frame T_{RR} (meaning the time frame over which the traded reserves are activated) that lasts for 1 hour between t_{RR}^{start} and t_{RR}^{end}. The whole market process is comprised of the following stages:

1. BSPs send their reserve orders to their respective TSOs before their Gate Closure Time (GCT_{RR}^{BSP}), whose value is decided by each TSO for its own area. Consequently, different BSP GCTs exist in Europe, usually comprised between 55 and 50 minutes before t_{RR}^{start}.
2. TSOs can filter out certain BSP marker orders if a strong justification is given, mainly related to internal congestions that may be created by these orders and that cannot be addressed by the RR market process. In addition, they need to compute their balancing needs, convert them into market orders and send them to the TERRE platform before GCT_{RR}^{TSO}, universally set at 40 minutes before t_{RR}^{start}, alongside all BSP orders that were not filtered.
3. The TERRE platform conducts the Clearing stage between GCT_{RR}^{TSO} and t_{RR}^{ex}. In this stage, market orders are activated using a common merit order list and the market clearing price is determined using the marginal pricing method.
4. Clearing results are transmitted back to all actors 30 minutes before t_{RR}^{start}.

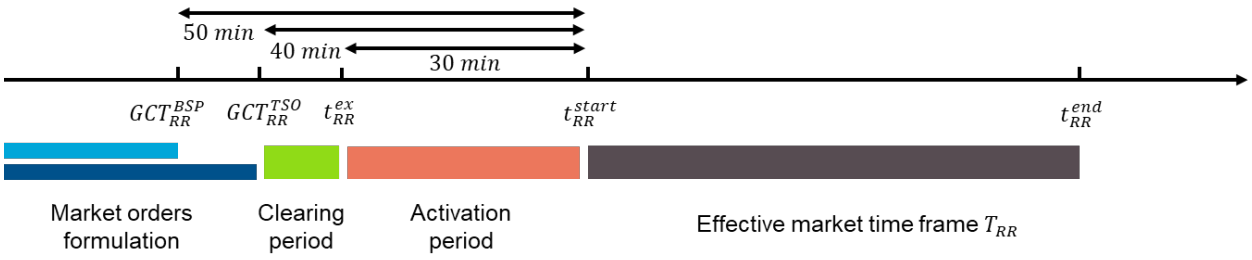

Figure A.1: RR market schematic time frame

A.1.1.2 The mFRR market

Compared to RR markets, mFRR markets add another layer of complexity as they combine two different activation processes, as described in (ENTSO-E, 2023a): "direct" and "scheduled" activations. The direct activation mode is a continuous market, where a pool of BSP orders is always available. A TSO can submit a balancing need to the platform at any time, and it is instantly cleared with a merit order list constituted of BSP orders of the relevant direction (for instance, given an upward balancing need–i.e. a need for additional generation–, only upward BSP orders are considered in the merit order list). In contrast, the scheduled activation mode is basically identical to the RR market process, with different time frames. This activation mode is the only one implemented in ATLAS, as the direct activation mode was deemed to complex to model and it is currently not integrated in it.

The sequential process of the scheduled mFRR market is described in Figure A.2. It is executed at a quarter-hourly frequency, and spans over an effective time frame T_{mFRR} that lasts for 15 minutes between t^{start}_{mFRR} and t^{end}_{mFRR}. The whole process is divided into the same 4 steps as the ones presented in Section A.1.1.1, with the following specific values:

- The BSP Gate Closure Time (GCT^{BSP}_{mFRR}) is set at 25 minutes before t^{start}_{mFRR}.
- The TSO GCT^{TSO}_{mFRR} is set at 10 minutes before t^{start}_{mFRR}.
- The Clearing is conducted on the MARI platform between GCT^{TSO}_{mFRR} and t^{ex}_{mFRR}, and results are transmitted back to all actors at t^{ex}_{mFRR} (7.5 minutes before t^{start}_{mFRR}).

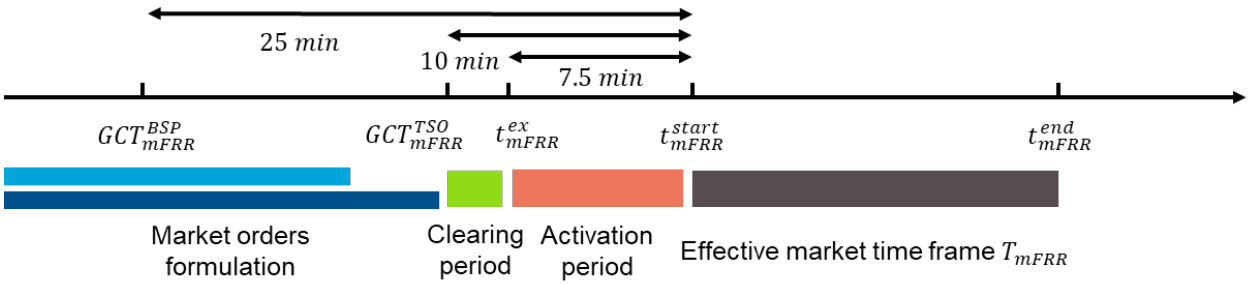

Figure A.2: mFRR market schematic time frame

A.1.2 Balancing stage within ATLAS

The ATLAS model consists of several modules (coded in Python) that can be used in a variety of combinations in order to model the chain of electricity markets from day-ahead to close-to-real time, and the basic structure for the most common market simulation pattern is shown in Figure A.3. All modules of the data preparation, Spot market and Intraday market stages are described in (Little et al., 2024).

Figure A.3 only offers an overview of the balancing stage. In practice, several configurations exist and are modeled in ATLAS:

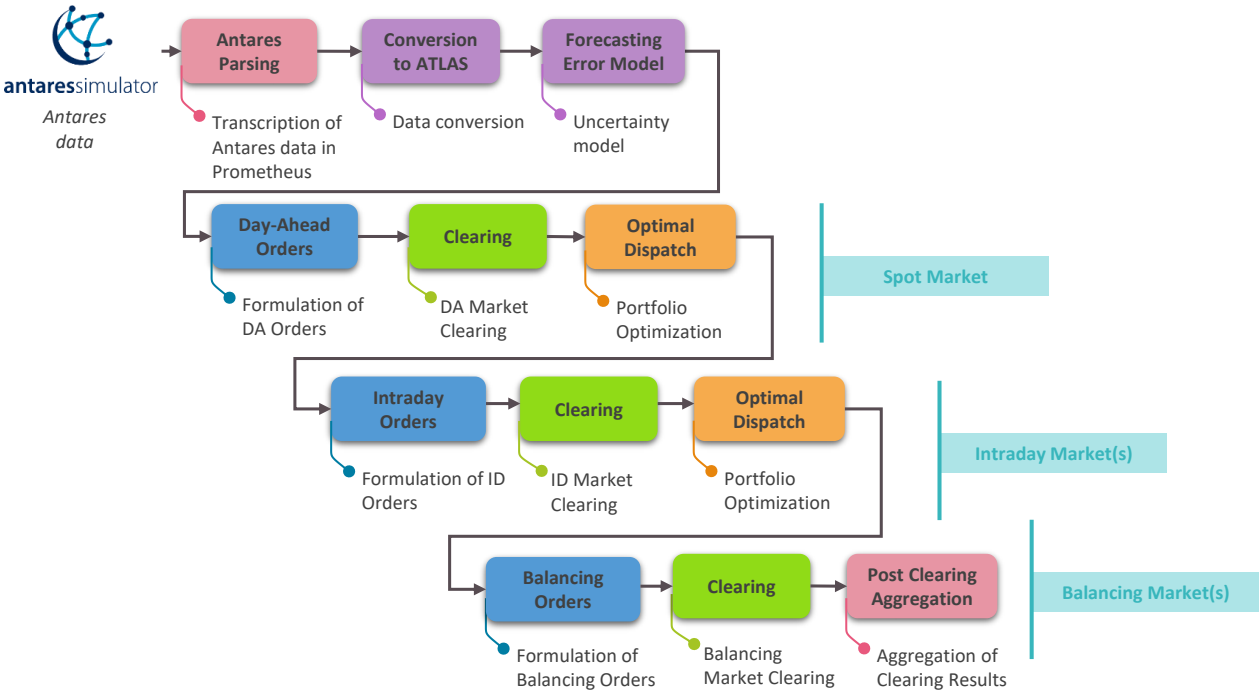

Figure A.3: ATLAS Modules

1. Relying on balancing markets only (depicted in A.4). This figuration is comprised of 4 successive steps. The formulation of BSP orders is described in Section A.2, while the formulation of TSO orders is covered by Section A.4. The Clearing process is described in (Little et al., 2024), and finally Section A.5 of this appendix explains the Post Clearing Aggregation.

Figure A.4: ATLAS - Detailed balancing market

2. Using a local balancing process. In ATLAS, this is modeled by the Balancing Mechanism (described in Section A.5), which is implemented based on the historical French balancing process (Figure A.5). The Balancing Mechanism will serve as the reference for all local balancing processes in ATLAS.

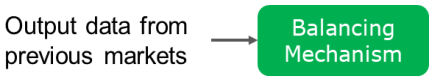

Figure A.5: ATLAS - Balancing Mechanism used alone

3. Using balancing markets followed by a local balancing process, a configuration that integrates all modules previously described (Figure A.6).

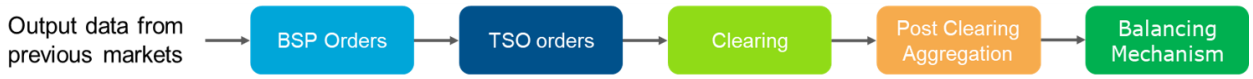

Figure A.6: ATLAS - Detailed balancing market followed by a Balancing Mechanism

In addition, an Imbalance Settlement process can be run after each of the previous configurations. It is described in Section A.6.

A.1.3 Nomenclature

This section describes notations used across all sections of this appendix. Some elements correspond to a specific type, which is indicated in bold and italics:

- ***Parameter*** refers to a parameter, which is indicated by the user before the execution of the module.
- ***Input data*** refers to an element that is extracted from the input dataset.
- ***Variable*** refers to an optimization variable.

Remark: For sets, the notation A_b refers to the subset of A linked with variable b. For instance, Z_{ca} indicates the subset of market areas belonging to the control area ca.

Sets	
Notation	**Description**
CA	Set of all control areas (or control blocks)
Z	Set of all market areas.
PF	Set of all portfolios.
U	Set of all units.
U^{unit_type}	Set of all units of type $unit\_type \in [g, l, th, h, st, w, pv]$. ($g$ = generation, l = flexible load, th = thermal, h = hydraulic, st = storage, w = wind, pv = photovoltaic)
ID_u	Set of all combinatorial indexes for unit $u \in U$
O	Set of all market orders. O^{up} refers to the subset of upward orders and O^{dn} to the subset of downward orders
C^{excl}	Set of all coupling instances of type $Exclusion$
C^{pc}	Set of all coupling instances of type $ParentChildren$
C^{idr}	Set of all coupling instances of type $IdenticalRatio$

Temporal variables

Notation	Description	Units
t_m^{ex}	Execution date of the market $m \in \{RR, mFRR\}$	-
t_m^{start}	Start date of the effective period of the market m	-
t_m^{end}	End date of the effective period of the market m	-
Δt_m	Time step of the market m	min
T_m	Effective time frame of the market m, i.e. $T_m = [t_m^{start}, t_m^{start} + \Delta t_m, \ldots, t_m^{end} - \Delta t_m]$	-
t_{id}^{start}	Start date of the combinatorial index id	-
t_{id}^{end}	End date of the combinatorial index id	-
T_{id}	Time frame of the combinatorial index id, i.e. $T_{id} = [t_{id}^{start}, t_{id}^{start} + \Delta t_m, \ldots, t_{id}^{end} - \Delta t_m]$	-
ΔT_{id}	Length of the combinatorial index id, i.e. $\Delta T_{id} = t_{id}^{end} - t_{id}^{start}$	min

TSO-specific characteristics		
Notation	**Description**	**Units**
$bn_{m,ca,t,t_m^{ex}}$ (short: bn_t)	Balancing needs for market m in control area $ca \in CA$ for time $t \in T_m$, seen from t_m^{ex}. For readability, it is shortened as bn_t	MW
$\sigma^{bn}_{ca,t,t_m^{ex}}$ (short: σ_t^{bn})	Binary parameter indicating the direction of TSO (area ca) balancing needs at time t seen from t_m^{ex}. $\sigma^{bn}_{ca,t,t_m^{ex}} = 1\ if\ bn_{m,ca,t,t_m^{ex}} > 0$, and 0 otherwise. For readability, it is shortened as σ_t^{bn}	-
δ_{ca}^{for}	Binary parameter indicating if TSO associated with control area $ca \in CA$ takes into account forecasts errors in its imbalance needs computation. ***Parameter***	-
δ_{ca}^{elas}	Binary parameter indicating if the demand of TSO associated with control area $ca \in CA$ is formulated as elastic ($\delta_{ca}^{elas} = 1$) or not ($\delta_{ca}^{elas} = 0$). ***Parameter***	-
alt_{ca}	Alternative chosen to compute prices and volumes of the demand of TSO associated with control area $ca \in CA$. Possible values are $\{"mFRRalt", "FrBMalt"\}$. ***Parameter***.	-
V^s	Maximum quantity of each slice of TSO demand formulated on markets. Only relevant if $\delta_{ca}^{elas} = 1$. ***Parameter***	MW
δ_{ca}^{risk}	Binary parameter indicating if the demand of TSO associated with control area $ca \in CA$ is taking into account volume-based risk aversion ($\delta_{ca}^{risk} = 1$) or not ($\delta_{ca}^{risk} = 0$). Only relevant if $\delta_{ca}^{elas} = 1$. ***Parameter***	-

$\epsilon_{ca}^{alt_{ca}}$	List of quantiles of the distribution of the TSO forecast error function of area ca associated with alternative alt_{ca}. Only relevant if $\delta_{ca}^{risk} = 1$. ***Parameter***	-

Zonal-specific characteristics		
Notation	**Description**	**Units**
$q_{m,ca,t}^{\sigma_t^{bn},max}$	Overall quantity for orders in direction opposite to σ_t^{bn} formulated by BSPs included in control area ca on market m, at time t	MW
$(\Delta q)_{z,t}^{bal}$	Commercial (power) balance of area $z \in Z$ at time t, equal to the sum of all power exports minus the sum of all power imports	MW
$\rho_{m,ca}^{FrBMalt}$	Percentage of BSP available capacity in area ca that is not submitted on the market m, and is consequently directly sent to the FrBM market. Only relevant if $\delta_{ca}^{elas} = 1$, with $alt_{ca} =$ "$FrBMalt$". ***Parameter***	-

Global unit characteristics		
Notation	**Description**	**Units**
$P_{u,t,t_m^{ex}}^{plan}$	Power output of unit $u \in U$ at time $t \in T_m$, seen from time t_m^{ex}. ***Input data***	MW
$P_{u,t}^{max}$	Maximum power output of unit $u \in U$ at time $t \in T_m$. ***Input data***	MW
$P_{u,t}^{min}$	Minimum power output of unit $u \in U$ at time $t \in T_m$. ***Input data***	MW
$\Delta P_{u,t}^{max}$	Maximum ramping limit of unit $u \in U$ at time $t \in T_m$. ***Input data***	MW/min
c_u^{VAR}	Variable cost of unit $u \in U$. ***Input data***	€/MWh
c_u^{SU}	Startup cost of unit $u \in U$. ***Input data***	€
$\delta_{u,t}^{turned\_on}$	Binary variable indicating if unit $u \in U^{th}$ is starting at $t \in T_m$	-
$\delta_{u,t}^{turned\_off}$	Binary variable indicating if unit $u \in U^{th}$ is shutting down at $t \in T_m$. ***Variable***	-
d_u^{notice}	Notice delay of unit $u \in U$. ***Input data***	min
$Res_{ut,t_m^{ex}}^{ResType,ResDir}$	Procured reserves of type $ResType \in [FCR, aFRR, mFRR, RR]$ in direction $ResDir \in [up, down]$ on unit u at time t, seen from t_m^{ex}. ***Input data***	-
$Q_{u,id}^{ResDir,max}$	Maximum quantity in direction $ResDir \in [up, down]$ that can be offered on unit u, for the combinatorial index id	MW
$Q_{u,id}^{ResDir,min}$	Minimum quantity in direction $ResDir \in [up, down]$ that can be offered on unit u, for the combinatorial index id	MW

Thermal-specific unit characteristics		
Notation	**Description**	**Units**
d_u^{SU}	Startup duration of unit $u \in U^{th}$. ***Input data***	min
d_u^{SD}	Shutdown duration of unit $u \in U^{th}$. ***Input data***	min
d_u^{minOn}	Minimum time on duration of unit $u \in U^{th}$. ***Input data***	min
d_u^{minOff}	Minimum time off duration of unit $u \in U^{th}$. ***Input data***	min
$d_u^{minStable}$	Minimum stable power duration of unit $u \in U^{th}$. ***Input data***	min
$\delta^{SU}_{u,T_{id},t_m^{ex}}$	Binary variable indicating if orders formulated on the unit u, for the combinatorial index id seen from t_m^{ex} should be treated as startup orders ($\delta^{SU}_{u,T_{id},t_m^{ex}} = 1$) or not ($= 0$)	-
$\delta^{SD}_{u,T_{id},t_m^{ex}}$	Binary variable indicating if the unit u is able to be shutdown at time t seen from t_m^{ex}. If written $\delta^{SD}_{u,T_{id},t_m^{ex}}$, it signifies that the variable concerns the entire set of times in T_{id}.	-
$\sigma^{SU}_{u,T_{id}}$	Binary variable indicating if orders formulated on the combinatorial index id induced ($\sigma^{SU}_{u,T_{id}} = 1$) or canceled ($\sigma^{SU}_{u,T_{id}} = -1$) a startup, or had no impact on startups ($\sigma^{SU}_{u,T_{id}} = 0$) of unit u	-

Hydraulic- and Storage-specific unit characteristics		
Notation	**Description**	**Units**
$E^{stored}_{u,t,t_m^{ex}}$	Stored energy in the reservoir of unit $u \in U^h \cup U^{st}$ at time $t \in T_m$, seen from time t_m^{ex}	MWh
$E^{max}_{u,t}$	Maximum storage level in the reservoir of unit $u \in U^h \cup U^{st}$ at time $t \in T_m$. ***Input data***	MWh
$E^{min}_{u,t}$	Minimum storage level in the reservoir of unit $u \in U^h \cup U^{st}$ at time $t \in T_m$. ***Input data***	MWh
d_u^{tran}	Transition duration between pumping and turbining of unit u of type Pumped Hydraulic Storage (PHS), that are modeled as storage units in ATLAS (i.e. $u \in U^{st}$). ***Input data***	min
$WV_{u,t,E^{stored}_{u,t,t_m^{ex}}}$	Marginal storage value of unit $u \in U^h$ at time t, for stored energy level $E^{stored}_{u,t,t_m^{ex}}$. ***Input data***	€/MWh
h_{DA}^{ex}	Execution hour of the day-ahead market, used to apply energy constraints to Hydraulic and Storage units in the BSP Order Formulation module. ***Parameter***	-

Load-, Photovoltaic- and Wind-specific unit characteristics		
Notation	**Description**	**Units**
P^{for}_{u,t,t^{ex}_m}	Forecast of the maximum power output of unit $u \in \{U^w, U^{pv}, U^l\}$ at time $t \in T_m$. ***Input data***	MW
$Curt_u$	Percentage of curtailed power allowed on unit $u \in \{U^w, U^{pv}\}$. ***Input data***	-

Market order characteristics	
Notation	**Meaning**
p_o	Price of order o
q^{min}_o	Minimum quantity of power offered for order o
q^{max}_o	Maximum quantity of power offered for order o
t^{start}_o	Start date of order
t^{end}_o	End date of order
t^{ex}_o	Execution date of order
d_o	Duration of order
σ_o	Sale/Purchase indicator, $\sigma = 1$ for purchase, -1 for sale
δ^{TSO}_o	Binary variable indicating if order o is from a TSO ($\delta^{TSO}_o = 1$) or not.
q^{acc}_o	Amount of power accepted by the Clearing stage for order o
δ^{acc}_o	Binary variable indicating if order o is activated by the Clearing stage ($\delta^{acc}_o = 1$ if $q^{acc}_o > 0$)

Other notations		
Notation	**Description**	**Units**
$VoLL$	Value of loss load. ***Parameter***	€/MWh
p^{spill}	Spillage penalty. ***Parameter***	€/MWh
$p^{redispatch}$	Redispatch penalty. ***Parameter***	€/MWh
$E^{VoLL}_{ca,t}$	Loss load energy in control area ca at time t. ***Variable***	MWh
$E^{spill}_{ca,t}$	Spillage power in control area ca at time t. ***Variable***	MW

A.2 ATLAS Balancing Stage - BSP Orders

A.3 Overview of the module

The objective of this module is to formulate BSP balancing energy market orders, for RR or mFRR markets. Submitted market orders are required to display all information indicated in Table A.18. In ATLAS, the formulation of balancing market orders is done with a unit-based hypothesis. This is justified by the extremely short full activation time of balancing markets (at most 30 minutes for RR orders), combined with their high frequency. Under these constraints, running a portfolio optimization process to determine the unit dispatch after each market would be unfeasible for BSPs.

In addition, this module does not include any optimization problem, even for the modeling of operating constraints. This is a deliberate choice: we observed that using an optimization problem for each unit of our input dataset, and for each balancing market simulated, led to significant computation time, mainly because of the high frequency of said markets. Consequently, the computation of the available capacity for each unit is performed through a non-optimization algorithm.

This section first introduces the concept of combinatorial orders that will be used to integrate detailed operating constraints in the formulation algorithm of thermal units (Section A.3.2). The complete order formulation is then presented in Section A.3.3, which includes the calculation of upward and downward available power, and the definition of both the quantity and price of market orders. Finally, Section A.3.4 presents the coupling links used in the module and the different situations they cover.

A.3.1 Nomenclature and inputs

This section describes notations used in the BSP order formulation module. Some elements correspond to a specific type, which is indicated in bold and italics:

- ***Parameter*** refers to a parameter, which is indicated by the user before the execution of the module.
- ***Input data*** refers to an element that is extracted from the input dataset.
- ***Variable*** refers to an optimization variable.

Remark: For sets, the notation A_b refers to the subset of A linked with variable b. For instance, Z_{ca} indicates the subset of market areas belonging to the control area ca.

Sets	
Notation	**Description**
CA	Set of all control areas (or control blocks)
Z	Set of all market areas.

PF	Set of all portfolios.
U	Set of all units.
U^{unit_type}	Set of all units of type $unit\_type \in [g, l, th, h, st, w, pv]$. ($g$ = generation, l = flexible load, th = thermal, h = hydraulic, st = storage, w = wind, pv = photovoltaic)
ID_u	Set of all combinatorial indexes for unit $u \in U$
O	Set of all market orders. O^{up} refers to the subset of upward orders and O^{dn} to the subset of downward orders
C^{excl}	Set of all coupling instances of type $Exclusion$
C^{pc}	Set of all coupling instances of type $ParentChildren$
C^{idr}	Set of all coupling instances of type $IdenticalRatio$

Temporal variables		
Notation	**Description**	**Units**
t_m^{ex}	Execution date of the market $m \in \{RR, mFRR\}$	-
t_m^{start}	Start date of the effective period of the market m	-
t_m^{end}	End date of the effective period of the market m	-
Δt_m	Time step of the market m	min
T_m	Effective time frame of the market m, i.e. $T_m = [t_m^{start}, t_m^{start} + \Delta t_m, \ldots, t_m^{end} - \Delta t_m]$	-
t_{id}^{start}	Start date of the combinatorial index id	-
t_{id}^{end}	End date of the combinatorial index id	-
T_{id}	Time frame of the combinatorial index id, i.e. $T_{id} = [t_{id}^{start}, t_{id}^{start} + \Delta t_m, \ldots, t_{id}^{end} - \Delta t_m]$	-
ΔT_{id}	Length of the combinatorial index id, i.e. $\Delta T_{id} = t_{id}^{end} - t_{id}^{start}$	min

Zonal-specific characteristics		
Notation	**Description**	**Units**
$q_{m,ca,t}^{\sigma_t^{bn},max}$	Overall quantity for orders in direction opposite to σ_t^{bn} formulated by BSPs included in control area ca on market m, at time t	MW
$(\Delta q)_{z,t}^{bal}$	Commercial (power) balance of area $z \in Z$ at time t, equal to the sum of all power exports minus the sum of all power imports	MW

$\rho_{m,ca}^{FrBMalt}$	Percentage of BSP available capacity in area ca that is not submitted on the market m, and is consequently directly sent to the FrBM market. Only relevant if $\delta_{ca}^{elas} = 1$, with $alt_{ca} =$ "$FrBMalt$". ***Parameter***	-

Global unit characteristics		
Notation	**Description**	**Units**
$P_{u,t,t_m^{ex}}^{plan}$	Power output of unit $u \in U$ at time $t \in T_m$, seen from time t_m^{ex}. ***Input data***	MW
$P_{u,t}^{max}$	Maximum power output of unit $u \in U$ at time $t \in T_m$. ***Input data***	MW
$P_{u,t}^{min}$	Minimum power output of unit $u \in U$ at time $t \in T_m$. ***Input data***	MW
$\Delta P_{u,t}^{max}$	Maximum ramping limit of unit $u \in U$ at time $t \in T_m$. ***Input data***	MW/min
c_u^{var}	Variable cost of unit $u \in U$. ***Input data***	€/MWh
c_u^{SU}	Startup cost of unit $u \in U$. ***Input data***	€
$\delta_{u,t}^{turned\_on}$	Binary variable indicating if unit $u \in U^{th}$ is starting at $t \in T_m$	-
$\delta_{u,t}^{turned\_off}$	Binary variable indicating if unit $u \in U^{th}$ is shutting down at $t \in T_m$. ***Variable***	-
d_u^{notice}	Notice delay of unit $u \in U$. ***Input data***	min
$R_{ut,t_m^{ex}}^{m^R,\sigma^R}$	Procured reserves of type $m^R \in [FCR, aFRR, mFRR, RR]$ in direction $\sigma^R \in [up, dn]$ on unit u at time t, seen from t_m^{ex}. ***Input data***	-
$Q_{u,id}^{\sigma^R,max}$	Maximum quantity in direction $\sigma^R \in [up, dn]$ that can be offered on unit u, for the combinatorial index id	-
$Q_{u,id}^{\sigma^R,min}$	Minimum quantity in direction $\sigma^R \in [up, dn]$ that can be offered on unit u, for the combinatorial index id	-

Thermal-specific unit characteristics		
Notation	**Description**	**Units**
d_u^{SU}	Startup duration of unit $u \in U^{th}$. ***Input data***	min
d_u^{SD}	Shutdown duration of unit $u \in U^{th}$. ***Input data***	min
d_u^{minOn}	Minimum time on duration of unit $u \in U^{th}$. ***Input data***	min
d_u^{minOff}	Minimum time off duration of unit $u \in U^{th}$. ***Input data***	min
$d_u^{minStable}$	Minimum stable power duration of unit $u \in U^{th}$. ***Input data***	min

$\delta^{SU}_{u,T_{id},t^{ex}_m}$	Binary variable indicating if orders formulated on the unit u, for the combinatorial index id seen from t^{ex}_m should be treated as startup orders ($\delta^{SU}_{u,T_{id},t^{ex}_m} = 1$) or not ($= 0$)	-
$\delta^{SD}_{u,T_{id},t^{ex}_m}$	Binary variable indicating if the unit u is able to be shutdown at time t seen from t^{ex}_m. If written $\delta^{SD}_{u,T_{id},t^{ex}_m}$, it signifies that the variable concerns the entire set of times in T_{id}.	-
$\sigma^{SU}_{u,T_{id}}$	Binary variable indicating if orders formulated on the combinatorial index id induced ($\sigma^{SU}_{u,T_{id}} = 1$) or canceled ($\sigma^{SU}_{u,T_{id}} = -1$) a startup, or had no impact on startups ($\sigma^{SU}_{u,T_{id}} = 0$) of unit u	-

Hydraulic- and Storage-specific unit characteristics		
Notation	**Description**	**Units**
$E^{stored}_{u,t,t^{ex}_m}$	Stored energy in the reservoir of unit $u \in U^h \cup U^{st}$ at time $t \in T_m$, seen from time t^{ex}_m	MWh
$E^{max}_{u,t}$	Maximum storage level in the reservoir of unit $u \in U^h \cup U^{st}$ at time $t \in T_m$. ***Input data***	MWh
$E^{min}_{u,t}$	Minimum storage level in the reservoir of unit $u \in U^h \cup U^{st}$ at time $t \in T_m$. ***Input data***	MWh
d^{tran}_u	Transition duration between pumping and turbining of unit u of type Pumped Hydraulic Storage (PHS), that are modeled as storage units in ATLAS (i.e. $u \in U^{st}$). ***Input data***	min
$WV_{u,t,E^{stored}_{u,t,t^{ex}_m}}$	Marginal storage value of unit $u \in U^h$ at time t, for stored energy level $E^{stored}_{u,t,t^{ex}_m}$. ***Input data***	€/MWh
h^{ex}_{DA}	Execution hour of the day-ahead market, used to apply energy constraints to Hydraulic and Storage units. ***Parameter***	-

Load-, Photovoltaic- and Wind-specific unit characteristics		
Notation	**Description**	**Units**
P^{for}_{u,t,t^{ex}_m}	Forecast of the maximum power output of unit $u \in \{U^w, U^{pv}, U^l\}$ at time $t \in T_m$. ***Input data***	MW
$Curt_u$	Percentage of curtailed power allowed on unit $u \in \{U^w, U^{pv}\}$. ***Input data***	-

Market order characteristics	
Notation	**Meaning**

p_o	Price of order o
q_o^{min}	Minimum quantity of power offered for order o
q_o^{max}	Maximum quantity of power offered for order o
t_o^{start}	Start date of order
t_o^{end}	End date of order
t_o^{ex}	Execution date of order
σ_o	Sale/Purchase indicator, $\sigma = -1$ for purchase, 1 for sale
δ_o^{TSO}	Binary variable indicating if order o is from a TSO ($\delta_o^{TSO} = 1$) or not.
q_o^{acc}	Amount of power accepted by the Clearing stage for order o
δ_o^{acc}	Binary variable indicating if order o is activated by the Clearing stage ($\delta_o^{acc} = 1$ if $q_o^{acc} > 0$)

Other notations		
Notation	**Description**	**Units**
p^{spill}	Spillage penalty. ***Parameter***	€/MWh
$p^{redispatch}$	Redispatch penalty. ***Parameter***	€/MWh
$E_{ca,t}^{spill}$	Spillage power in control area ca at time t. ***Variable***	MW

A.3.2 Concepts of combinatorial orders and indexes

A.3.2.1 Context and objective

On balancing markets, BSPs may have to formulate orders over several time steps in order to respect operating constraints. This principle is illustrated in Figure A.7, in the case where a generation group is constrained by a stable power duration constraint (see details about this constraint in Section A.3.3.1.2).

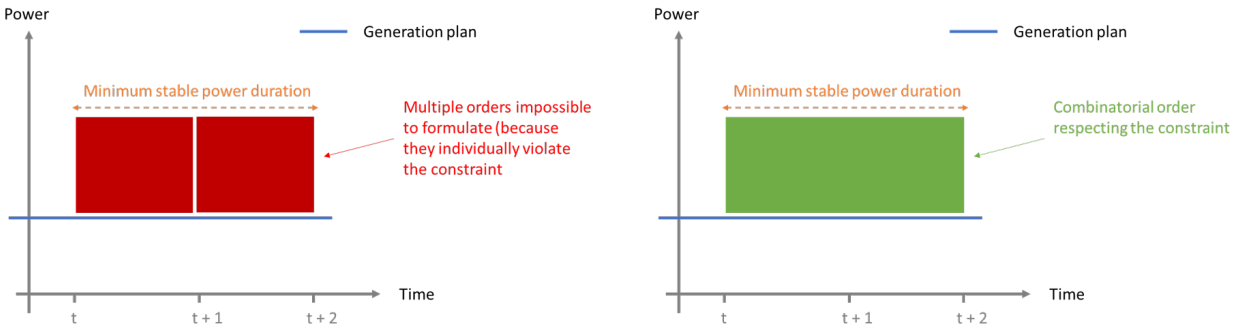

Figure A.7: Example of operating constraint inducing an order over multiple time steps

The objective of combinatorial orders is to represent this behavior and the resulting orders. To do so, the module considers subsets of successive time steps and tries to formulate feasible orders on them, linked with various coupling instances (see Section A.3.4 for more information on coupling instances). These subsets of time steps are called combinatorial indexes. Except in very specific cases, all orders from the same combinatorial index share identical price and volume, to eventually represent a single order on the entire index.

The behavior of the BSP Order Formulation module regarding combinatorial orders is defined by a boolean parameter. If it is set to True, the module will formulate combinatorial orders. Otherwise, it will only compute the available capacity on individual time steps, which usually leads to lower submitted volumes as it has less leeway to account for operating constraints.

A.3.2.2 Method used to identify combinatorial indexes

In order to formulate every combinatorial order possible on a given balancing time frame, the module determines all possible combinations of indexes $id \in ID$ composed of successive time steps over which the studied unit u has available power (either upward or downward). A first approximation of the available power is done by considering the maximum or the minimum power (see Section A.3.3.1.1) and the previously procured reserves (see Section A.3.3.1.1). Upward (ID_{up}) and downward (ID_{dn}) combinatorial indexes are then computed based on this first estimation of available power, using the following method:

- Identification of all time steps within the balancing time frame, for which there is available power.

- Determination of all combinations of successive time steps within those previously identified.

Figure A.8 illustrates this method on an example of a balancing time frame of 4 time steps (by only looking at upward orders).

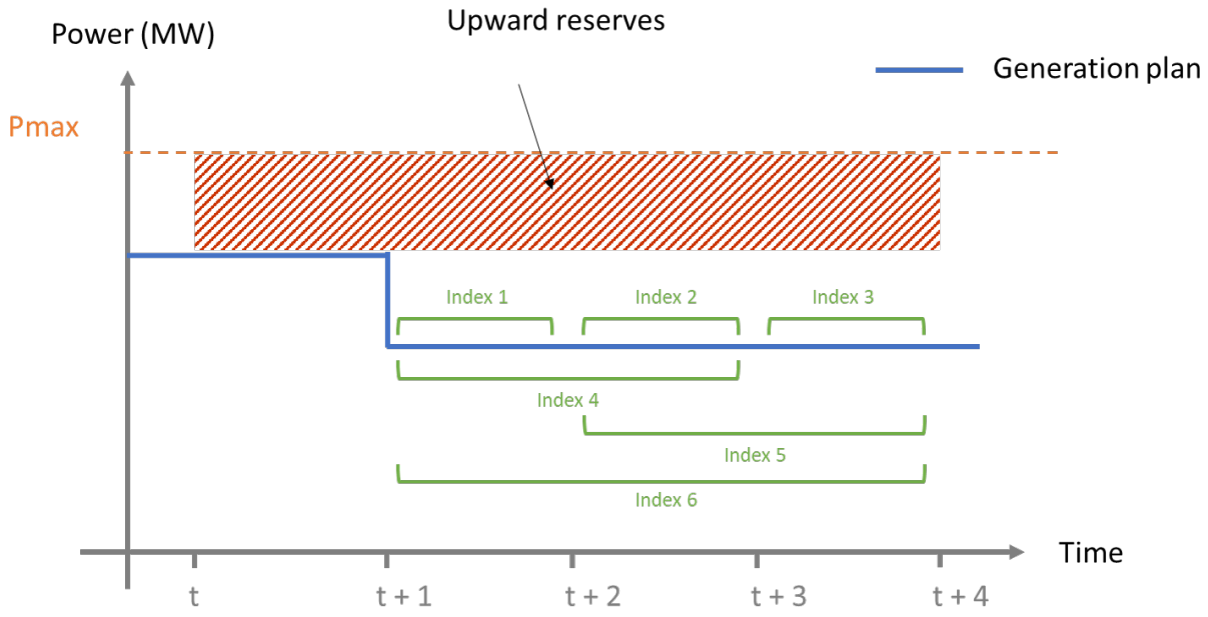

Figure A.8: Combinatorial indexes determination for upward orders

In this example, the maximum power value and previously procured upward reserves constraints imply that there is no power available in the first time period. For the following 3 periods, 6 combinatorial indexes exist and are represented in green.

A third type of combinatorial index can be created by the module. It is specific to thermal units and aims at identifying available indexes for shutdown orders, which are a specific kind of downward orders that force the equipment to stop[1]. The identification of time steps over which a shutdown order is feasible differs from that of downward orders. Indeed, the minimum power constraint doesn't have the same effect on shutdown orders. The requirements for a period to be part of a shutdown combinatorial index are the following:

- The unit must be thermal, hence $u \in U^{th}$. Other types of units are not concerned by shutdown orders and simply formulate downward orders.
- The unit must produce at least its minimum power over the entire period. In some situations, the power output of the unit may be between 0 and its minimum power, which means that it is in a starting or shutdown state. It is then considered unable to formulate shutdown orders.

[1]For thermal units, shutdown orders are separated from usual downward orders. For a given time step, a classic downward order and a shutdown order can be formulated simultaneously, and later be linked by an *Exclusion* coupling as detailed in Section A.3.4.2.3. Other types of units are not concerned by shutdown orders as they are assumed to be able to turn their power output to 0 at will

- The unit must not have any procured reserve (upward or downward) during this period.

Operating constraints are then successively applied on each combinatorial index, following the process described in Section A.3.3, to check the feasibility of orders and to determine their characteristics.

A.3.3 Orders formulation

The BSP order formulation process uses a unit-based method: each unit in the input dataset is studied individually to identify available upward and downward capacities. The outcome of this process is the creation of market orders, that should indicate all the characteristics displayed in Table A.18, except for δ_o^{acc} and q_o^{acc} which are filled by the Clearing stage.

If we take any BSP order formulated on market m for time t, some properties can already be filled (Equation A.1): its start date is equal to t, its end date is equal to $t + \Delta t_m$, its execution date corresponds to the execution date of the market t_m^{ex}, its binary variable tagging a TSO order is set to 0.

$$\forall o \in O^{BSP}, \begin{cases} t_o^{start} = t \\ t_o^{end} = t + \Delta t_m \\ t_o^{ex} = t_m^{ex} \\ \delta_o^{TSO} = 0 \end{cases} \tag{A.1}$$

To compute any remaining property, the formulation of the market order takes place in two steps. First, the module determines q_o^{max} and q_o^{min} values based on the available power at time t_o^{start} (t_o^{end} is always assumed to be equal to $t_o^{start} + \Delta t_m$), computed according to generation plans and operating constraints applied to units. This module doesn't currently integrate a notion of strategic behavior for the volume of orders, which means that every unit is supposed to offer its entire available power on balancing markets. Then, the order price is computed based on variable and fixed costs. Other properties are easier to fill and do not require specific calculations.

A.3.3.1 Determination of the available power for upward and downward orders

For each time $t \in T$, the module follows a series of steps to precise the available power range for both upward reserves (this range is comprised between upper bound $Q_{u,t,t_m^{ex}}^{up,min}$ and lower bound $Q_{u,t,t_m^{ex}}^{up,max}$) and downward reserves (ranging between $Q_{u,t,t_m^{ex}}^{dn,min}$ and $Q_{u,t,t_m^{ex}}^{dn,max}$), taking into account operating constraints and previously planned power output of the studied equipment. A first set of general constraints are applied regardless of the unit type. They are detailed in Section A.3.3.1.1. Specific constraints are then applied to certain types of unit (Section A.3.3.1.2 for thermal units, Section A.3.3.1.3 for hydraulic and storage units). For wind, photovoltaic and flexible units, no specific constraints are required[2].

[2]In particular, it is assumed that the maximum ramping limit of these types of units is infinite.

In principle, the upper bounds of both upward $Q^{up,max}_{u,t,t^{ex}_m}$ and downward $Q^{dn,max}_{u,t,t^{ex}_m}$ available power are updated at each following step. In contrast, the lower bounds $Q^{up,min}_{u,t,t^{ex}_m}$ and $Q^{dn,min}_{u,t,t^{ex}_m}$ are updated only when necessary, as only specific cases may impose restrictions on the lower bound. In the equations of this document, the update is denoted by the symbol $\leftarrow$, as the calculation of the updated values usually includes the previous value.

A.3.3.1.1 General constraints

Maximum power and minimum power

A first estimation of $Q^{up,max}_{u,t,t^{ex}_m}$ (resp. $Q^{dn,max}_{u,t,t^{ex}_m}$) is computed based on the maximum power (resp. minimum power) of the unit and the last generation plan available. This is straightforward for units whose power output is not associated with forecasts (Equations A.2a and A.2b):

$$\forall u \in U^{th} \cup U^{h} \cup U^{st},\ \forall t \in T_m,$$
$$Q^{up,max}_{u,t,t^{ex}_m} \leftarrow P^{max}_{u,t} - P^{plan}_{u,t,t^{ex}_m} \tag{A.2a}$$
$$Q^{dn,max}_{u,t,t^{ex}_m} \leftarrow P^{plan}_{u,t,t^{ex}_m} - P^{min}_{u,t} \tag{A.2b}$$

For wind, photovoltaic and flexible load units, the maximum power output evolves according to forecasts. Consequently, the latest maximum power forecast available at t^{ex}_m is taken as a reference. The minimum power of flexible load is assumed to always be 0, which leads to Equations A.3a and A.3b. For wind and photovoltaic units, the minimum power depends on the curtailment ratio $Curt_u$ authorized on each unit (Equations A.4a and A.4b):

$$\forall u \in U^{l},\ \forall t \in T_m,$$
$$Q^{up,max}_{u,t,t^{ex}_m} \leftarrow P^{for}_{u,t,t^{ex}_m} - P^{plan}_{u,t,t^{ex}_m} \tag{A.3a}$$
$$Q^{dn,max}_{u,t,t^{ex}_m} \leftarrow P^{plan}_{u,t,t^{ex}_m} \tag{A.3b}$$

$$\forall u \in U^{w} \cup U^{pv},\ \forall t \in T_m,$$
$$Q^{up,max}_{u,t,t^{ex}_m} \leftarrow P^{for}_{u,t,t^{ex}_m} - P^{plan}_{u,t,t^{ex}_m} \tag{A.4a}$$
$$Q^{dn,max}_{u,t,t^{ex}_m} \leftarrow P^{plan}_{u,t,t^{ex}_m} - P^{for}_{u,t,t^{ex}_m} * Curt_u \tag{A.4b}$$

Previously procured reserves

Previously procured upward (resp. downward) reserves are subtracted from $Q^{up,max}_{u,t,t^{ex}_m}$ (resp. $Q^{dn,max}_{u,t,t^{ex}_m}$). Procured reserves of the same type of the studied market are not taken into account in this step, as they

obviously can be part of the activation market.

$$\forall u \in U,\ \forall t \in T_m,$$

$$Q^{up,max}_{u,t,t^{ex}_m} \leftarrow Q^{up,max}_{u,t,t^{ex}_m} - \sum_{m^R \neq m} R^{m^R,up}_{u,t,t^{ex}_m} \tag{A.5a}$$

$$Q^{dn,max}_{u,t,t^{ex}_m} \leftarrow Q^{dn,max}_{u,t,t^{ex}_m} - \sum_{m^R \neq m} R^{m^R,dn}_{u,t,t^{ex}_m} \tag{A.5b}$$

Notice delay

The last step before determining combinatorial indexes is to check if certain time steps of the balancing time frame are *de facto* unavailable for the unit because of the notice delay constraint d^{notice}_u. This constraint imposes a set time before the unit can modify its power output, and it may conflict with the duration between the end of the Clearing stage and the real-time:

$$\forall u \in U,\ \ \forall t \in T_m,\ \forall \sigma^R \in \{up, dn\},$$

$$\textbf{if } (t^{start}_{id} - t^{ex}_m < d^{notice}_u) \textbf{ then } \begin{cases} Q^{\sigma^R,max}_{u,t,t^{ex}_m} \leftarrow 0 \\ Q^{\sigma^R,min}_{u,t,t^{ex}_m} =\leftarrow 0 \end{cases} \tag{A.6}$$

A.3.3.1.2 Thermal-specific constraints

This section details all specific constraints applied to thermal units. In particular, if the user chooses the option to formulate combinatorial orders, they are defined at this stage for thermal units (Section A.3.3.1.2). Constraints applied to thermal units include:

- Maximum ramping.
- Startup and shutdown duration.
- Minimum time ON and minimum time OFF.
- Minimum stable power duration.

Determination of combinatorial indexes

Combinatorial indexes are then determined for every other type of unit, by following the method described in section A.3.2.2. If the user chooses not to generate combinatorial orders, using the associated parameter, then these indexes are each made of exactly one time period (for instance, such a set of indexes for a RR market could be $[t_1]$, $[t_2]$, $[t_3]$ and $[t_4]$). Once indexes are defined, the module studies each one individually. From now on, all following steps are done a certain combinatorial index $id \in ID_u$ whose time frame is T_{id}. The notation T_{id} will be used in place of t for some variable to indicate that it applies for any time $t \in T_{id}$.

Maximum ramping constraint

The maximum ramping constraint is verified for both upward and downward orders:

- Between $t_{id}^{start} - \Delta t_m$ and t_{id}^{start}.
- Between t_{id}^{end} and $t_{id}^{end} + \Delta t_m$

Note: to simplify notations, $t \pm n * \Delta t_m$ will be noted $t \pm n$.

This constraint is written as in Equation A.7:

$$\begin{aligned}
&\forall u \in U^{th},\ \forall T_{id}, \\
Q^{up,max}_{u,T_{id},t_m^{ex}} \leftarrow min(&Q^{up,max}_{u,T_{id},t_m^{ex}}, \\
&\Delta P^{max}_{u,t_{id}^{start}} * \Delta t_m - (P^{plan}_{u,t_{id}^{start},t_m^{ex}} - P^{plan}_{u,t_{id}^{start}-1,t_m^{ex}}), \\
&\Delta P^{max}_{u,t_{id}^{end}} * \Delta t_m - (P^{plan}_{u,t_{id}^{end}+1,t_m^{ex}} - P^{plan}_{u,t_{id}^{end},t_m^{ex}})) \qquad \text{(A.7a)} \\
Q^{dn,max}_{u,T_{id},t_m^{ex}} \leftarrow min(&Q^{dn,max}_{u,T_{id},t_m^{ex}}, \\
&\Delta P^{max}_{u,t_{id}^{start}} * \Delta t_m - (P^{plan}_{u,t_{id}^{start}-1,t_m^{ex}} - P^{plan}_{u,t_{id}^{start},t_m^{ex}}), \\
&\Delta P^{max}_{u,t_{id}^{end}} * \Delta t_m - (P^{plan}_{u,t_{id}^{end},t_m^{ex}} - P^{plan}_{u,t_{id}^{end}+1,t_m^{ex}})) \qquad \text{(A.7b)}
\end{aligned}$$

In this module, we make the hypothesis that ramping constraints are not taken into account when starting or stopping a thermal unit. Thus, it can be shutdown from any power between its minimum and maximum power, and in a similar way start to any power in this interval.

Since combinatorial orders from the same index have similar $Q^{\sigma^R,max}$ and $Q^{\sigma^R,min}$, and generation plans in the input market are assumed to always be feasible, it is not necessary to check ramping constraints between time steps within combinatorial indexes.

Startup of a thermal unit

Seen from a time t_m^{ex}, a thermal unit $u \in U^{th}$ whose power output is 0 for every time step of a combinatorial index needs to start to provide upward reserves. This is expressed by $\forall t \in T_{id},\quad P^{plan}_{u,t,t_m^{ex}} = 0$, and is a prerequisite check before applying any equation of this section. Other types of units are considered to be able to start at will.

Several cases can emerge, depending on the power output that is planned before and after the combinatorial index. In some cases, startup orders can conflict with minimum time OFF, minimum time ON and startup duration constraints and these will be checked if relevant. On top of this, depending on the case, formulating an upward order can induce or cancel a startup, and in these situations the upward order is divided into two parts to properly take into account any additional or reduced costs generated. This is tracked by the variables $\delta^{SU}_{u,T_{id},t_m^{ex}}$ and $\sigma^{SU}_{u,T_{id}}$, initialized as follows when the startup of unit u is checked:

$$\begin{aligned}
&\forall u \in U^{th},\ \forall T_{id}, \\
&\textbf{if } (P^{plan}_{u,t,t_m^{ex}} = 0) \textbf{ then } \begin{cases} \delta^{SU}_{u,T_{id},t_m^{ex}} \leftarrow 1 \\ \sigma^{SU}_{u,T_{id}} \leftarrow 0 \end{cases} \qquad \text{(A.8)}
\end{aligned}$$

- Case 1): The unit is ON at times $t_{id}^{start}-1$ and $t_{id}^{end}+1$. Here, an upward order isn't a startup, it is rather canceling a shutdown. This is a case where two orders need to be created, to properly distribute these cost savings. These orders can be formulated if the maximum ramping constraint is not violated between times $t_{id}^{start}-1$ and $t_{id}^{end}+1$. This principle is illustrated in a simple example, in Figure A.9, with an index of 1 time period, for which the maximum ramping constraint is violated and the order cannot be formulated.

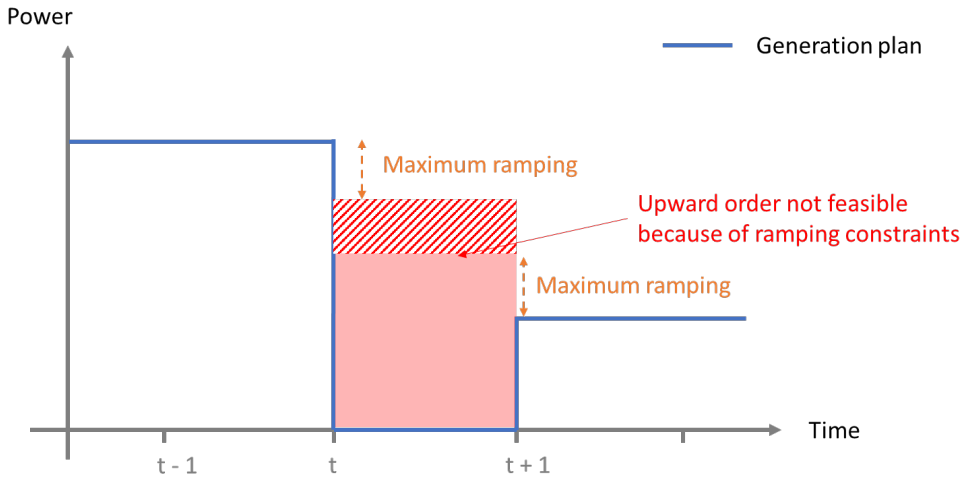

Figure A.9: Example of a startup order infeasible because of maximum ramping constraints

Respecting maximum ramping constraints both before and after the combinatorial index imposes bounds to the order, which means updating values of both Q^{max} and Q^{min}. If formulating orders would always violate said constraints (the striped red area in Figure A.9, then they cannot be formulated. This is verified by Equation A.9c. There is no need to check for minimum time ON / OFF or startup duration constraints, since there will be no actual startup.

$\forall u \in U^{th}, \quad \forall t \in T_{id}, \quad$ **if** $(P^{plan}_{u,t_{id}^{start}-1,t_m^{ex}} > 0 \ \& \ P^{plan}_{u,t_{id}^{end}+1,t_m^{ex}} > 0)$ **then**

$$\begin{cases} \textbf{if } (P^{plan}_{u,t_{id}^{end}+1,t_m^{ex}} \geq P^{plan}_{u,t_{id}^{start}-1,t_m^{ex}}), \ \textbf{then} & \begin{cases} Q^{up,min}_{u,T_{id},t_m^{ex}} \leftarrow max(P^{min}_{u,t_{id}^{start}}, P^{plan}_{u,t_{id}^{end}+1,t_m^{ex}} - \Delta P^{max}_{u,t_{id}^{start}} * \Delta t_m) \\ Q^{up,max}_{u,T_{id},t_m^{ex}} \leftarrow min(P^{max}_{u,t_{id}^{start}}, P^{plan}_{u,t_{id}^{start}-1,t_m^{ex}} - \Delta P^{max}_{u,t_{id}^{start}} * \Delta t_m) \\ \sigma^{SU}_{u,T_{id}} \leftarrow -1 \end{cases} & \text{(A.9a)} \\ \textbf{if } (P^{plan}_{u,t_{id}^{end}+1,t_m^{ex}} < P^{plan}_{u,t_{id}^{start}-1,t_m^{ex}}) \ \textbf{then} & \begin{cases} Q^{up,min}_{u,T_{id},t_m^{ex}} \leftarrow max(P^{min}_{u,t_{id}^{start}}, P^{plan}_{u,t_{id}^{start}-1,t_m^{ex}} - \Delta P^{max}_{u,t_{id}^{start}} * \Delta t_m) \\ Q^{up,max}_{u,T_{id},t_m^{ex}} \leftarrow min(P^{max}_{u,t_{id}^{start}}, P^{plan}_{u,t_{id}^{end}+1,t_m^{ex}} - \Delta P^{max}_{u,t_{id}^{start}} * \Delta t_m) \\ \sigma^{SU}_{u,T_{id}} \leftarrow -1 \end{cases} & \text{(A.9b)} \\ \textbf{if } (|P^{plan}_{u,t_{id}^{end}+1,t_m^{ex}} - P^{plan}_{u,t_{id}^{start}-1,t_m^{ex}}| > 2 * \Delta P^{max}_{u,t_{id}^{start}} * 60) \ \textbf{then} & \begin{cases} Q^{up,min}_{u,T_{id},t_m^{ex}} \leftarrow 0 \\ Q^{up,max}_{u,T_{id},t_m^{ex}} \leftarrow 0 \\ \delta^{SU}_{u,T_{id},t_m^{ex}} \leftarrow 0 \end{cases} & \text{(A.9c)} \end{cases}$$

- Case 2): The unit is ON at time $t_{id}^{start}-1$, and OFF at $t_{id}^{end}+1$. No startup costs are induced in this case, as the unit was already running during the previous time step. The upward order is feasible if the minimum time OFF constraint is respected after $t_{id}^{end}+1$, and its Q^{max} and Q^{min} values are bounded because of maximum ramping constraints related with $P^{plan}_{u,t_{id}^{start}-1,t_m^{ex}}$.

$\forall u \in U^{th},\ \forall t \in T_{id},\quad$ **if** $(P^{plan}_{u,t_{id}^{start}-1,t_m^{ex}} > 0\ \&\ P^{plan}_{u,t_{id}^{end}+1,t_m^{ex}} = 0)$ **then**

$$\begin{cases} \textbf{if } (\exists\ t' \in \{t_{id}^{end}, \dots, t_{id}^{end}+d_u^{minOff}\}\ |\ P^{plan}_{u,t',t_m^{ex}} > 0) \textbf{ then} & \begin{cases} Q^{up,min}_{u,t,t_m^{ex}} \leftarrow 0 \\ Q^{up,max}_{u,t,t_m^{ex}} \leftarrow 0 \\ \delta^{SU}_{u,T_{id},t_m^{ex}} \leftarrow 0 \end{cases} \\ \textbf{else}, & \begin{cases} Q^{up,min}_{u,T_{id},t_m^{ex}} \leftarrow max(P^{min}_{u,t_{id}^{start}}, P^{plan}_{u,t_{id}^{start}-1,t_m^{ex}}) \\ Q^{up,max}_{u,T_{id},t_m^{ex}} \leftarrow min(P^{max}_{u,t_{id}^{start}}, P^{plan}_{u,t_{id}^{start}-1,t_m^{ex}} + \Delta P^{max}_{u,t_{id}^{start}} * \Delta t_m) \\ \delta^{SU}_{u,T_{id},t_m^{ex}} \leftarrow 0 \end{cases} \end{cases} \tag{A.10}$$

- Case 3): The unit is OFF at time $t_{id}^{start}-1$, and ON at $t_{id}^{end}+1$. In that situation, there is indeed a startup but it does not induce startup costs (because it is only advancing the startup planned later). The upward order is feasible if the unit has time to start between t_m^{ex} and t_{id}^{start}, and if the minimum time OFF constraint is respected before t_{id}^{start}.

$\forall u \in U^{th},\ \forall t \in T_{id},\quad$ **if** $(P^{plan}_{u,t_{id}^{start}-1,t_m^{ex}} = 0\ \&\ P^{plan}_{u,t_{id}^{end}+1,t_m^{ex}} > 0)$ **then**

$$\begin{cases} \textbf{if } (t_{id}^{start} - t_m^{ex} < d_u^{SU}) \textbf{ then} & \begin{cases} Q^{up,min}_{u,t,t_m^{ex}} \leftarrow 0 \\ Q^{up,max}_{u,t,t_m^{ex}} \leftarrow 0 \\ \delta^{SU}_{u,T_{id},t_m^{ex}} \leftarrow 0 \end{cases} & \text{(A.11a)} \\ \textbf{elif } (\exists\ t' \in \{t_{id}^{start} - d_u^{minOff}, \dots, t_{id}^{start}-1\}\ |\ P^{plan}_{u,t',t_m^{ex}} > 0) \textbf{ then} & \begin{cases} Q^{up,min}_{u,t,t_m^{ex}} \leftarrow 0 \\ Q^{up,max}_{u,t,t_m^{ex}} \leftarrow 0 \\ \delta^{SU}_{u,T_{id},t_m^{ex}} \leftarrow 0 \end{cases} & \text{(A.11b)} \\ \textbf{else}, & \begin{cases} Q^{up,min}_{u,t,t_m^{ex}} \leftarrow max(P^{min}_{u,t_{id}^{start}}, P^{plan}_{u,t_{id}^{end}+1,t_m^{ex}}) \\ Q^{up,max}_{u,t,t_m^{ex}} \leftarrow min(P^{max}_{u,t_{id}^{start}}, P^{plan}_{u,t_{id}^{end}+1,t_m^{ex}} + \Delta P^{max}_{u,t_{id}^{start}} * \Delta t_m) \\ \delta^{SU}_{u,T_{id},t_m^{ex}} \leftarrow 0 \end{cases} & \text{(A.11c)} \end{cases}$$

- Case 4): The unit is within a startup already planned, at any time within T_{id}. This state is a possible outcome of day-ahead and intraday markets and is defined by a power output between 0 and the minimum power of the unit (meaning that the unit is currently ramping up to its minimum power). No balancing order can be formulated in that case:

$$\forall u \in U^{th},\ \forall T_{id},$$

$$\textbf{if } (\exists t \in T_{id}\ |\ 0 < P^{plan}_{u,t,t_m^{ex}} < P^{min}_{u,t}) \textbf{ then} \quad \begin{cases} Q^{up,min}_{u,T_{id},t_m^{ex}} \leftarrow 0 \\ Q^{up,max}_{u,T_{id},t_m^{ex}} \leftarrow 0 \\ \delta^{SU}_{u,T_{id},t_m^{ex}} \leftarrow 0 \end{cases} \tag{A.12}$$

- Case 5): The unit is OFF at both $t_{id}^{start}-1$ and $t_{id}^{end}+1$. This is the most basic case of startup, and the only one that actually induces startup costs. An upward order can be formulated if the following conditions are respected:
  - Startup duration between t_m^{ex} and t_{id}^{start} (Equation A.13a).
  - Minimum time OFF before t_{id}^{start} (Equation A.13b) and after t_{id}^{end} (Equation A.13c).
  - Minimum time ON during T_{id} (Equation A.13d).

  Which can be expressed as:

$$\forall u \in U^{th},\ \forall t \in T_{id}, \quad \textbf{if } (P^{plan}_{u,t_{id}^{start}-1,t_m^{ex}} = 0 \quad \& \ P^{plan}_{u,t_{id}^{end}+1,t_m^{ex}} = 0) \textbf{ then}$$

$$\begin{cases}
\textbf{if } (t_{id}^{start} - t_m^{ex} < d_u^{SU}) \textbf{ then} & \begin{cases} Q^{up,min}_{u,T_{id},t_m^{ex}} \leftarrow 0 \\ Q^{up,max}_{u,T_{id},t_m^{ex}} \leftarrow 0 \\ \delta^{SU}_{u,T_{id},t_m^{ex}} \leftarrow 0 \end{cases} & \text{(A.13a)} \\
\textbf{elif } (\exists\ t' \in \{t_{id}^{start} - d_u^{minOff}, \dots, t_{id}^{start}-1\} \mid P^{plan}_{u,t',t_m^{ex}} > 0) \textbf{ then} & \begin{cases} Q^{up,min}_{u,T_{id},t_m^{ex}} \leftarrow 0 \\ Q^{up,max}_{u,T_{id},t_m^{ex}} \leftarrow 0 \\ \delta^{SU}_{u,T_{id},t_m^{ex}} \leftarrow 0 \end{cases} & \text{(A.13b)} \\
\textbf{elif } (\exists\ t' \in \{t_{id}^{end}, \dots, t_{id}^{end} + d_u^{minOff}\} \mid P^{plan}_{u,t',t_m^{ex}} > 0) \textbf{ then} & \begin{cases} Q^{up,min}_{u,T_{id},t_m^{ex}} \leftarrow 0 \\ Q^{up,max}_{u,T_{id},t_m^{ex}} \leftarrow 0 \\ \delta^{SU}_{u,T_{id},t_m^{ex}} \leftarrow 0 \end{cases} & \text{(A.13c)} \\
\textbf{elif } (\Delta T_{id} \geq d_u^{minOn}) \textbf{ then} & \begin{cases} Q^{up,min}_{u,T_{id},t_m^{ex}} \leftarrow 0 \\ Q^{up,max}_{u,T_{id},t_m^{ex}} \leftarrow 0 \\ \delta^{SU}_{u,T_{id},t_m^{ex}} \leftarrow 0 \end{cases} & \text{(A.13d)} \\
\textbf{else } \sigma^{SU}_{u,T_{id}} \leftarrow 1 & & \text{(A.13e)}
\end{cases}$$

Shutdown of a thermal unit

The following constraints are applied to verify if a shutdown order is feasible for thermal units. First, a thermal unit is only concerned by shutdown orders over a shutdown combinatorial index $id \in ID^{shut}$ if it is ON on every time period of id, meaning that these checks are only done if $\forall t \in T_{id}, \quad P^{plan}_{u,t,t_m^{ex}} > P^{min}_{u,t,t_m^{ex}}$.

Similarly to startup orders, variables $\delta^{SD}_{u,T_{id},t_m^{ex}}$ and $\sigma^{SU}_{u,T_{id}}$ are respectively used to indicate if the shutdown order is feasible, and if it generates or cancels startup costs, and are initialized as follows:

$$\forall u \in U^{th},\ \forall t \in T_{id},$$
$$\textbf{if } (P^{plan}_{u,t,t_m^{ex}} \geq P^{min}_{u,t,t_m^{ex}}) \textbf{ then} \quad \begin{cases} \delta^{SD}_{u,T_{id},t_m^{ex}} \leftarrow 1 \\ \sigma^{SU}_{u,T_{id}} \leftarrow 0 \end{cases} \tag{A.14}$$

First, if the unit has any amount of procured reserves (either upward or downward) during at least one time step $t \in T_{id}$, then it cannot be shutdown on id as it would no longer be able to provide said reserves

(Equation A.15).

$$\forall u \in U^{th},\ \forall t \in T_m,\ \forall m^R,\ \forall\ \sigma^R \in \{up, dn\}$$
$$\textbf{if}\ (R^{m^R,\sigma^R}_{u,t,t^{ex}_m} > 0)\quad \textbf{then}\quad \delta^{SD}_{u,t} \leftarrow 0 \tag{A.15}$$

Then, if the notice delay constraint checked in section A.3.3.1.1 was not respected, the shutdown order is not feasible (Equation A.16):

$$\forall u \in U^{th},\ \forall t \in T_{id},$$
$$\textbf{if}\ (t^{start}_{id} - t^{ex}_{id} < d^{notice}_u)\ \textbf{then}\quad \delta^{SD}_{u,T_{id},t^{ex}_m} \leftarrow 0 \tag{A.16}$$

Once these first checks are complete, several cases emerge:

- Case 1): The unit is OFF at times $t^{start}_{id} - 1$ and $t^{end}_{id} + 1$. In this case, the shutdown order is always feasible, and in practice it cancels a startup:

$$\forall u \in U^{th},\ \forall t \in T_{id},$$
$$\textbf{if}\ (P^{plan}_{u,t^{start}_{id}-1,t^{ex}_m} = 0\ \&\ P^{plan}_{u,t^{end}_{id}+1,t^{ex}_m} = 0)\ \textbf{then}\quad \sigma^{SU}_{u,T_{id}} \leftarrow -1 \tag{A.17}$$

- Case 2): The unit is OFF at time $t^{start}_{id} - 1$ and ON at $t^{end}_{id} + 1$. The shutdown order can be formulated if the minimum time ON is respected after t^{end}_{id}, Q^{max} is not modified and no additional startup is created by the order.

$$\forall u \in U^{th},\ \forall t \in T_{id},\quad \textbf{if}\ (P^{plan}_{u,t^{start}_{id}-1,t^{ex}_m} = 0\ \&\ P^{plan}_{u,t^{end}_{id}+1,t^{ex}_m} > 0)\ \textbf{then}$$
$$\textbf{if}\ (\exists\, t' \in \{t^{end}_{id}, \ldots, t^{end}_{id} + d^{minOn}_u\}\ |\ P^{plan}_{u,t',t^{ex}_m} = 0)\ \textbf{then}\quad \delta^{SD}_{u,T_{id},t^{ex}_m} \leftarrow 0 \tag{A.18}$$

- Case 3): The unit is ON at $t^{start}_{id} - 1$ and OFF at $t^{end}_{id} + 1$. Here, the shutdown order can be formulated if the minimum time ON is respected before t^{start}_{id}. If it is verified, the shutdown order can be formulated and no additional startup is generated.

$$\forall u \in U^{th},\ \forall t \in T_{id},\quad \textbf{if}\ (P^{plan}_{u,t^{start}_{id}-1,t^{ex}_m} > 0\ \&\ P^{plan}_{u,t^{end}_{id}+1,t^{ex}_m} = 0)\ \textbf{then}$$
$$\textbf{if}\ (\exists\, t' \in \{t^{start}_{id} - d^{minOn}_u, t^{start}_{id}\}\ |\ P^{plan}_{u,t',t^{ex}_m} = 0)\ \textbf{then}$$
$$\delta^{SD}_{u,T_{id},t^{ex}_m} \leftarrow 0 \tag{A.19}$$

- Case 4): The unit is starting during T_{id}. Same situation as for case 4 of startup orders (see Section A.3.3.1.2), no order is permitted on T_{id}.

$$\forall u \in U^{th},\ \forall t \in T_{id},$$
$$\textbf{if}\ (\exists\, t' \in T_{id}\ |\ 0 < P^{plan}_{u,t',t^{ex}_m} < P^{min}_{u,t'})\ \textbf{then}\quad \delta^{SD}_{u,T_{id},t^{ex}_m} \leftarrow 0 \tag{A.20}$$

- Case 5): The unit is ON at $t^{start}_{id} - 1$ and at $t^{end}_{id} + 1$. A shutdown order can be formulated if the following conditions are satisfied:

– The startup duration is less than a time step, to make sure that it can restart in time at the end of the order activation.

$$\forall u \in U^{th},\ \forall t \in T_{id},$$
$$\textbf{if } (P^{plan}_{u,t_{id}^{start}-1,t_m^{ex}} > 0 \ \&\ P^{plan}_{u,t_{id}^{end}+1,t_m^{ex}} > 0 \ \&\ d_u^{SU} > \Delta t_m) \textbf{ then } \quad \delta^{SD}_{u,T_{id},t_m^{ex}} \leftarrow 0 \tag{A.21}$$

– The minimum time OFF is not violated during the order:

$$\forall u \in U^{th},\ \forall t \in T_{id},$$
$$\textbf{if } (P^{plan}_{u,t_{id}^{start}-1,t_m^{ex}} > 0 \ \&\ P^{plan}_{u,t_{id}^{end}+1,t_m^{ex}} > 0 \ \&\ d_u^{minOff} > \Delta T_{id}) \textbf{ then } \quad \delta^{SD}_{u,T_{id},t_m^{ex}} \leftarrow 0 \tag{A.22}$$

– The minimum time ON is respected before t_{id}^{start} and after t_{id}^{end}:

$$\forall u \in U^{th},\ \forall t \in T_{id}, \quad \textbf{if } (P^{plan}_{u,t_{id}^{start}-1,t_m^{ex}} > 0 \ \&\ P^{plan}_{u,t_{id}^{end}+1,t_m^{ex}} > 0) \textbf{ then}$$

$$\begin{cases} \textbf{if } (\exists\, t' \in \{t_{id}^{start} - 1 - d_u^{minOn}, \dots, t_{id}^{start} - 1\} \mid P^{plan}_{u,t',t_m^{ex}} = 0) \textbf{ then } \quad \delta^{SD}_{u,T_{id},t_m^{ex}} \leftarrow 0 & \text{(A.23a)} \\ \textbf{elif } (\exists\, t' \in \{t_{id}^{end}, \dots, t_{id}^{end} + d_u^{minOn}\} \mid P^{plan}_{u,t',t_m^{ex}} = 0) \textbf{ then } \quad \delta^{SD}_{u,T_{id},t_m^{ex}} \leftarrow 0 & \text{(A.23b)} \end{cases}$$

If all requirements are met, the shutdown order is feasible on index id and it induces a startup cost:

$$\textbf{if } (\delta^{SD}_{u,T_{id},t_m^{ex}} = 1) \textbf{ then } \quad \sigma^{SU}_{u,T_{id}} \leftarrow 1 \tag{A.24}$$

Minimum stable power duration constraint

The minimum stable power duration constraint forces units to keep a constant power output for a certain duration before being able to modify it. In the current version of ATLAS, it is only applied to thermal units. When trying to formulate orders on unit $u \in U_{th}$ on the combinatorial index $id \in ID_u$, the module checks if these orders cannot generate violations of this constraint before, during, and after id.

The first step is to check if $d_u^{minStable} > \Delta t_m$, to make sure that this constraint is relevant for the studied market. If it is, the module proceeds to a series of checks for available power in upward and downward directions:

- Stable power level before the index:

$$\forall u \in U^{th},\ \forall t \in T_{id},$$
$$\textbf{if } (\exists t \in \{t_{id}^{start} - 1 - d_u^{minStable}, \dots, t_{id}^{start} - 1\} \mid P^{plan}_{u,t,t_m^{ex}} \neq P^{plan}_{u,t_{id}^{start}-1,t_m^{ex}}) \textbf{ then } \quad \begin{cases} Q^{up,max}_{u,T_{id},t_m^{ex}} \leftarrow 0 \\ Q^{dn,max}_{u,T_{id},t_m^{ex}} \leftarrow 0 \\ \delta^{SD}_{u,T_{id},t_m^{ex}} \leftarrow 0 \end{cases} \tag{A.25}$$

- Stable power level after the index:

$$\forall u \in U^{th},\ \forall t \in T_{id},$$

$$\textbf{if } (\exists\, t \in \{t_{id}^{end}+1, \ldots, t_{id}^{end}+1+d_u^{minStable}\} \mid P^{plan}_{u,t,t_m^{ex}} \neq P^{plan}_{u,t_{id}^{end}+1,t_m^{ex}}) \textbf{ then } \begin{cases} Q^{up,max}_{u,T_{id},t_m^{ex}} \leftarrow 0 \\ Q^{dn,max}_{u,T_{id},t_m^{ex}} \leftarrow 0 \\ \delta^{SD}_{u,T_{id},t_m^{ex}} \leftarrow 0 \end{cases} \tag{A.26}$$

If the previous conditions are verified, but the duration of the index is shorter than the minimum stable power duration, the offer can still be formulated as an extension of a previous or later stable power level (similar to cases 1 and 2 of both startup or shutdown orders). This principle is illustrated in Figure A.10, in which the possibility of formulating an order between t and t+1 while having a minimum stable power duration of 2 time steps is looked at. The only feasible order is indicated in green. Such an order is necessarily indivisible, and its Q^{max} is also imposed, and this means that if it conflicts with other constraints, the order cannot be formulated.

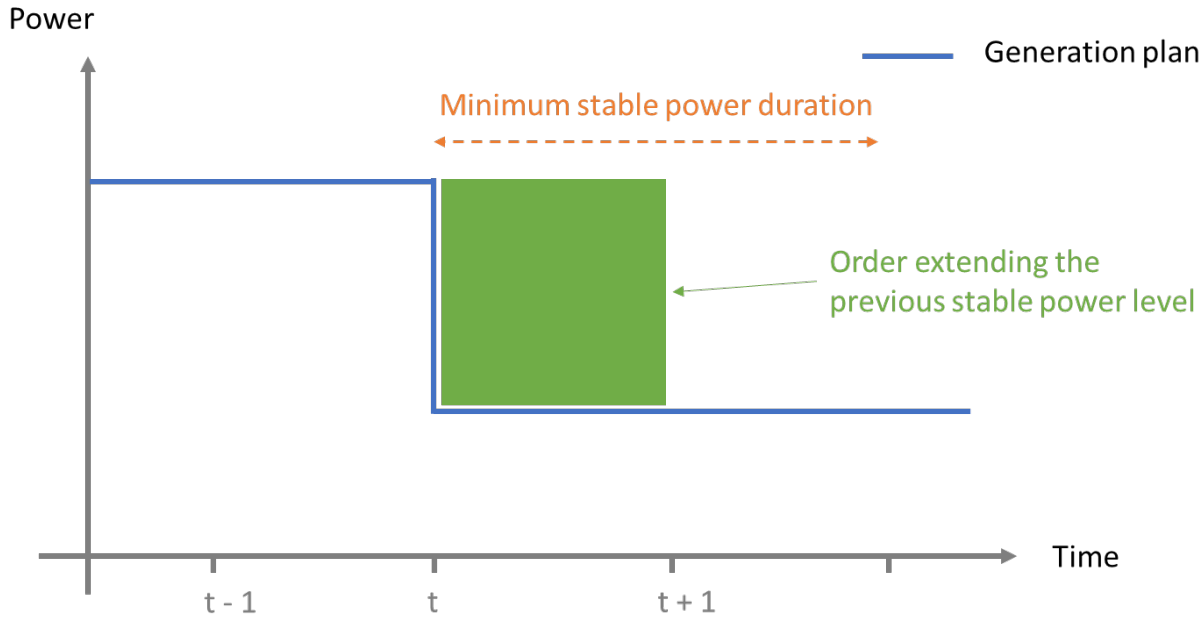

Figure A.10: Minimum stable power extension example

Once again, several cases emerge, depending on how the stable power level extension is done (before or after, and upward or downward). In all cases, it leads to indivisible orders:

- If the unit is within a ramp, no order can be formulated:

$$\forall u \in U^{th},\ \forall T_{id},$$

$$\textbf{if } (P^{plan}_{u,t_{id}^{start}-1,t_m^{ex}} \neq P^{plan}_{u,t_{id}^{start},t_m^{ex}} \ \&\ P^{plan}_{u,t_{id}^{end},t_m^{ex}} \neq P^{plan}_{u,t_{id}^{end}+1,t_m^{ex}}) \textbf{ then } \begin{cases} Q^{up,max}_{u,T_{id},t_m^{ex}} \leftarrow 0 \\ Q^{dn,max}_{u,T_{id},t_m^{ex}} \leftarrow 0 \end{cases} \tag{A.27}$$

- If $P^{plan}_{u,t^{start}_{id}-1,t^{ex}_m} > P^{plan}_{u,t^{start}_{id},t^{ex}_m}$, then the previous stable power level can be extended only by an upward order:

$$\forall u \in U^{th},\ \forall T_{id},$$
$$\textbf{if } (P^{plan}_{u,t^{start}_{id}-1,t^{ex}_m} > P^{plan}_{u,t^{start}_{id},t^{ex}_m}) \textbf{ then } \begin{cases} Q^{up,max}_{u,T_{id},t^{ex}_m} \leftarrow P^{plan}_{u,t^{start}_{id}-1,t^{ex}_m} - P^{plan}_{u,t^{start}_{id},t^{ex}_m} \\ Q^{up,min}_{u,T_{id},t^{ex}_m} \leftarrow Q^{up,max}_{u,T_{id},t^{ex}_m} \\ Q^{dn,max}_{u,T_{id},t^{ex}_m} \leftarrow 0 \\ Q^{dn,min}_{u,T_{id},t^{ex}_m} \leftarrow 0 \end{cases} \tag{A.28}$$

- If $P^{plan}_{u,t^{start}_{id}-1,t^{ex}_m} < P^{plan}_{u,t^{start}_{id},t^{ex}_m}$, then the previous stable power level can be extended only by a downward order:

$$\forall u \in U^{th},\ \forall T_{id},$$
$$\textbf{if } (P^{plan}_{u,t^{start}_{id}-1,t^{ex}_m} < P^{plan}_{u,t^{start}_{id},t^{ex}_m}) \textbf{ then } \begin{cases} Q^{up,max}_{u,T_{id},t^{ex}_m} \leftarrow 0 \\ Q^{up,min}_{u,T_{id},t^{ex}_m} \leftarrow 0 \\ Q^{dn,max}_{u,T_{id},t^{ex}_m} \leftarrow P^{plan}_{u,t^{start}_{id},t^{ex}_m} - P^{plan}_{u,t^{start}_{id}-1,t^{ex}_m} \\ Q^{dn,min}_{u,T_{id},t^{ex}_m} \leftarrow Q^{dn,max}_{u,T_{id},t^{ex}_m} \end{cases} \tag{A.29}$$

- If $P^{plan}_{u,t^{end}_{id},t^{ex}_m} < P^{plan}_{u,t^{end}_{id}+1,t^{ex}_m}$, then the next stable power level can be extended only by an upward order:

$$\forall u \in U^{th},\ \forall T_{id},$$
$$\textbf{if } (P^{plan}_{u,t^{end}_{id},t^{ex}_m} < P^{plan}_{u,t^{end}_{id}+1,t^{ex}_m}) \textbf{ then } \begin{cases} Q^{up,max}_{u,T_{id},t^{ex}_m} \leftarrow P^{plan}_{u,t^{end}_{id}+1,t^{ex}_m} - P^{plan}_{u,t^{end}_{id},t^{ex}_m} \\ Q^{up,min}_{u,T_{id},t^{ex}_m} \leftarrow Q^{up,max}_{u,T_{id},t^{ex}_m} \\ Q^{dn,max}_{u,T_{id},t^{ex}_m} \leftarrow 0 \\ Q^{dn,min}_{u,T_{id},t^{ex}_m} \leftarrow 0 \end{cases} \tag{A.30}$$

- If $P^{plan}_{u,t^{end}_{id},t^{ex}_m} > P^{plan}_{u,t^{end}_{id}+1,t^{ex}_m}$, then the next stable power level can be extended only by a downward order:

$$\forall u \in U^{th},\ \forall T_{id},$$
$$\textbf{if } (P^{plan}_{u,t^{end}_{id},t^{ex}_m} > P^{plan}_{u,t^{end}_{id}+1,t^{ex}_m}) \textbf{ then } \begin{cases} Q^{up,max}_{u,T_{id},t^{ex}_m} \leftarrow 0 \\ Q^{up,min}_{u,T_{id},t^{ex}_m} \leftarrow 0 \\ Q^{dn,max}_{u,T_{id},t^{ex}_m} \leftarrow P^{plan}_{u,t^{end}_{id},t^{ex}_m} - P^{plan}_{u,t^{end}_{id}+1,t^{ex}_m} \\ Q^{dn,min}_{u,T_{id},t^{ex}_m} \leftarrow Q^{dn,max}_{u,T_{id},t^{ex}_m} \end{cases} \tag{A.31}$$

A.3.3.1.3 Hydraulic- and Storage-specific constraints

Specific constraints applied to hydraulic and storage units include:

- Maximum ramping, although it is usually set to infinite for this kind of unit.
- Maximum and minimum storage level.
- For pumped hydraulic storage units, the transition duration between pumping and turbining states.

In contrast with thermal units, there is no combinatorial index to be considered, and each time step of the market time frame is considered individually.

Maximum ramping constraint

The maximum ramping constraint is verified for both upward and downward orders for hydraulic and storage units, when the maximum ramping ΔP^{max} is not equal to 0 (which indicates an infinite ramping limit by convention):

$$\forall u \in U^h \cup U^{st},\ \forall t \in T_m,$$

$$\begin{aligned} Q^{up,max}_{u,t,t^{ex}_m} \leftarrow min(&Q^{up,max}_{u,t,t^{ex}_m}, \\ &\Delta P^{max}_{u,t} * \Delta t_m - (P^{plan}_{u,t,t^{ex}_m} - P^{plan}_{u,t-1,t^{ex}_m}), \\ &\Delta P^{max}_{u,t^{end}_{id}} * \Delta t_m - (P^{plan}_{u,t+1,t^{ex}_m} - P^{plan}_{u,t,t^{ex}_m})) \end{aligned} \tag{A.32a}$$

$$\begin{aligned} Q^{dn,max}_{u,t,t^{ex}_m} \leftarrow min(&Q^{dn,max}_{u,t,t^{ex}_m}, \\ &\Delta P^{max}_{u,t} * \Delta t_m - (P^{plan}_{u,t-1,t^{ex}_m} - P^{plan}_{u,t,t^{ex}_m}), \\ &\Delta P^{max}_{u,t} * \Delta t_m - (P^{plan}_{u,t,t^{ex}_m} - P^{plan}_{u,t+1,t^{ex}_m})) \end{aligned} \tag{A.32b}$$

Maximum and minimal storage level

These constraints ensure that the activation of reserves (and the stored energy evolution resulting from it) does not violate the maximum and minimum storage levels of hydraulic and storage units. Any stored energy evolution resulting from activations in balancing markets is modifying not only storage levels within T_m, but also all subsequent time steps until the operational time frame of the next day-ahead market[3]. 2 different situations arise, depending on the comparison between t^{ex}_m and the hour h^{ex}_{DA} at which the daily day-ahead market is executed:

- If the current balancing market is occurring after h^{ex}_{DA}, it means that storage levels are already largely planned for the following day. In that situation, balancing orders are constrained not to violate reservoir level limits on the following day, and the associated time frame $T_{storage}$ is given in Equation A.33.

$$\textbf{if } (hour(t^{ex}_m) > h^{ex}_{DA}) \textbf{ then } \quad T_{storage} = \{t^{start}_m,\ t^{start}_m + \Delta t_m,\ \ldots,\ t^{end}_{DA+1}\} \tag{A.33}$$

  Where t^{end}_{DA+1} corresponds to the end of the following day, and the function $hour(date)$ simply returns the hour of $date$.

- If the current balancing market is occurring before h^{ex}_{DA}, then the storage time frame lasts until the end of the current day (t^{end}_{DA}):

$$\textbf{if } (hour(t^{ex}_m) < h^{ex}_{DA}) \textbf{ then } \quad T_{storage} = \{t^{start}_m,\ t^{start}_m + \Delta t_m,\ \ldots,\ t^{end}_{DA}\} \tag{A.34}$$

[3]The day-ahead market is here taken as the reference, where the main part of power outputs is decided, and consequently where the main decisions shaping the storage levels of hydraulic and storage units are taken.

Once the storage time frame is defined, $Q^{up,max}$ and $Q^{dn,max}$ are updated, potentially reduced if they would induce a violation of E^{max}_{u,t,t^{ex}_m} or E^{min}_{u,t,t^{ex}_m} for any time t in this time frame:

$$\forall u \in U^h \cup U^{st},\ \ \forall t \in T_m,\ \ \forall t_{st} \in T_{storage},$$

$$Q^{up,max}_{u,t,t^{ex}_m} \leftarrow \min\left(Q^{up,max}_{u,t,t^{ex}_m}, \frac{\min\limits_{t' \in T_m}\left(E^{stored}_{u,t',t^{ex}_m}\right) - E^{min}_{u,t_{st},t^{ex}_m}}{\Delta T_m/60}\right) \tag{A.35a}$$

$$Q^{dn,max}_{u,t,t^{ex}_m} \leftarrow \min\left(Q^{dn,max}_{u,t,t^{ex}_m}, \frac{E^{max}_{u,t_{st},t^{ex}_m} - \max\limits_{t' \in T_m}\left(E^{stored}_{u,t',t^{ex}_m}\right)}{\Delta T_m/60}\right) \tag{A.35b}$$

Finally, if the constraint is limiting Q^{max}, then it means that orders of each time $t \in T_m$ should be linked by an *Exclusion* coupling with all orders of other time steps of T_m. If not, simultaneous activations across different time steps may lead to a violation of said constraint (see section A.3.4.1.2 for more details about the *Exclusion* coupling type).

Pumping / turbining transition duration constraint

This constraint is only applied to PHS units, that are modeled as storage equipments in ATLAS. It represents the duration required for the unit to switch from a pumping mode (when the unit is consuming energy) to a turbining mode (when the unit is producing energy), or conversely. During this transition phase, the power output of the unit must be equal to 0. By hypothesis, we assume that this duration is symmetrical in both directions (from pumping to turbining, or from turbining to pumping).

Because of the limited number of time steps in the current design of balancing markets (at most 4, for the RR market), it is basically impossible for a unit to switch between modes within the time frame of these markets. To keep a reasonable complexity, the module only considers that, if the transition constraint is active and applied to a unit, then it cannot switch mode. Formally, this means:

$$\forall u \in U^{phs},\ \ \forall t \in T_m,\ \ \textbf{if}\ (d^{trans}_u > \Delta t_m)\ \textbf{then}$$
$$\begin{cases} \textbf{if}\ (P^{plan}_{u,t,t^{ex}_m} < 0)\ \textbf{then} \quad Q^{up,max}_{u,t,t^{ex}_m} \leftarrow \min(Q^{up,max}_{u,t,t^{ex}_m},\ |P^{plan}_{u,t,t^{ex}_m}|) \\ \textbf{if}\ (P^{plan}_{u,t,t^{ex}_m} > 0)\ \textbf{then} \quad Q^{dn,max}_{u,t,t^{ex}_m} \leftarrow \min(Q^{dn,max}_{u,t,t^{ex}_m},\ |P^{plan}_{u,t,t^{ex}_m}|) \end{cases} \tag{A.36a}$$

A.3.3.2 Setting q^{max}_o and q^{min}_o for all orders o

For any unit $u \in U$, once the available power has been computed following all steps in section A.3.3.1, market orders o are created. No strategic behavior is modeled regarding the amount of reserve offered on the balancing markets, meaning that each unit offers all the energy available.

In a general fashion, the following criteria are applied to determine if an upward (resp. downward) order should be formulated for any $t \in T_m$: the upper bound of the upward (resp. downward) available power has to be strictly positive ($Q^{\bullet,max}_{u,t,t^{ex}_m} > 0$) and, and it has to be greater than the lower bound ($Q^{\bullet,max}_{u,t,t^{ex}_m} > Q^{\bullet,min}_{u,t,t^{ex}_m}$).

The general case is described in Section A.3.3.2.1. Once again, specific unit types require to be treated separately from the others:

- For thermal units, a specific treatment is required to take into account the different combinatorial indexes as well as possible startup and shutdown orders (Section A.3.3.2.2).
- For hydraulic units, the convention of both day-ahead and intraday markets is taken into account (see Little et al., 2024, Section 4.2.4). The range $[0, P_u^{max}]$ is divided into 7 fragments, each one priced according to a spread around the water value $WV_{u,t,E^{stored}_{u,t,t^{ex}_m}}$ to avoid an all or nothing effect (Section A.3.3.2.3).

A.3.3.2.1 General case

For all storage, wind, photovoltaic and flexible load units, the characteristics q^{max} and q^{min} of an upward order o_t^{up} are directly given by the available upward power (Equation A.37). The same principle is applied for downward orders (Equation A.38)

$$\forall u \in U^{st} \cup U^{w} \cup U^{pv} \cup U^{l},\ \ \forall t \in T_m,\ \ \forall o_t^{up} \in O_{up}, \quad \begin{cases} \sigma_{o_t^{up}} = -1 \\ q^{min}_{o_t^{up}} = Q^{up,min}_{u,t,t^{ex}_m} \\ q^{max}_{o_t^{up}} = Q^{up,max}_{u,t,t^{ex}_m} \end{cases} \tag{A.37}$$

$$\forall u \in U^{st} \cup U^{w} \cup U^{pv} \cup U^{l},\ \ \forall t \in T_m,\ \ \forall o_t^{dn} \in O_{dn}, \quad \begin{cases} \sigma_{o_t^{dn}} = 1 \\ q^{min}_{o_t^{dn}} = Q^{dn,min}_{u,t,t^{ex}_m} \\ q^{max}_{o_t^{dn}} = Q^{dn,max}_{u,t,t^{ex}_m} \end{cases} \tag{A.38}$$

A.3.3.2.2 Thermal units specific case

For a given thermal unit $u \in U^{th}$, and for each combinatorial index $id \in ID_u$, all market orders o_t are created for every time $t \in T_{id}$, when possible. Compared to the general case, two specific types of orders can be formulated for thermal units:

- If the tracking variable $\delta^{SU}_{u,T_{id},t^{ex}_m} = 1$, then the upward orders on index id will all be startup orders.
- If the tracking variable $\delta^{SD}_{u,T_{id},t^{ex}_m} = 1$, then shutdown orders will be formulated in addition to usual downward orders.

The characteristics q_o^{max} and q_o^{min} of every order o can be deduced from $Q^{\sigma^R,max}_{u,T_{id},t^{ex}_m}$ and $Q^{\sigma^R,max}_{u,T_{id},t^{ex}_m}$. The relation is straightforward for downward orders $o_{id}^{dn} \in O^{dn}$ (Equation A.40), and for upward orders $o_{id}^{up} \in O^{up}$ that do not induce or cancel a startup (Equation A.39):

$$\forall t \in T_{id}, \quad \textbf{if } (\delta^{SU}_{u,T_{id},t^{ex}_m} = 0) \textbf{ then } \quad \begin{cases} \sigma_{o_t^{up}} = -1 \\ q^{min}_{o_t^{up}} = Q^{up,min}_{u,T_{id},t^{ex}_m} \\ q^{max}_{o_t^{up}} = Q^{up,max}_{u,T_{id},t^{ex}_m} \end{cases} \tag{A.39}$$

$$\forall t \in T_{id}, \quad \begin{cases} \sigma_{o_t^{dn}} = 1 \\ q_{o_t^{dn}}^{min} = Q_{u,T_{id},t_m^{ex}}^{dn,min} \\ q_{o_t^{dn}}^{max} = Q_{u,T_{id},t_m^{ex}}^{dn,max} \end{cases} \tag{A.40}$$

For upward orders, if a startup generating is required after verifying all constraints ($\delta_{u,T_{id},t_m^{ex}}^{SU} = 1$), two orders are actually formulated for each time step to have a proper representation of startup costs:

- An indivisible order o_{id}^{s1} between 0 and minimum power. For this first order, $q_{o_{id}^{s1}}^{min}$ and $q_{o_{id}^{s1}}^{max}$ are equal and correspond to the minimum power.

$$\forall u \in U^{th}, \ \forall t \in T_{id}, \quad \textbf{if } (\delta_{u,T_{id},t_m^{ex}}^{SU} = 1) \textbf{ then } \quad \begin{cases} \sigma_{o_t^{s1}} = -1 \\ q_{o_t^{s1}}^{min} = P_{u,t_{id}^{start}}^{min} \\ q_{o_t^{s1}}^{max} = P_{u,t_{id}^{start}}^{min} \end{cases} \tag{A.41}$$

- A divisible order o_{id}^{s2} that covers the entire power range between minimum power and maximum power. As a reminder, it is assumed that the unit can start anywhere in this range, without considering ramping constraints. Consequently, $q_{o_{id}^{s2}}^{min}$ and $q_{o_{id}^{s2}}^{max}$ are set as followed:

$$\forall u \in U^{th}, \ \forall t \in T_{id}, \quad \textbf{if } (\delta_{u,T_{id},t_m^{ex}}^{SU} = 1) \textbf{ then } \quad \begin{cases} \sigma_{o_t^{s2}} = -1 \\ q_{o_t^{s2}}^{min} = 0 \\ q_{o_t^{s2}}^{max} = P_{u,t_{id}^{start}}^{max} - P_{u,t_{id}^{start}}^{min} \end{cases} \tag{A.42}$$

Both startup orders are linked with a *Parent Children*, o_{id}^{s1} being the parent and o_{id}^{s2} being the child (more information in A.3.4.2.1).

Finally, all feasible shutdown orders $o_{id}^{shut} \in O^{shut}$ are formulated as indivisible orders:

$$\forall u \in U^{th}, \ \forall t \in T_{id}, \quad \textbf{if } (\delta_{u,T_{id},t_m^{ex}}^{SD} = 1) \textbf{ then } \quad \begin{cases} \sigma_{o_{id}^{shut}} = 1 \\ q_{o_{id}^{shut}}^{min} = P_{u,t,t_m^{ex}}^{plan} \\ q_{o_{id}^{shut}}^{max} = P_{u,t,t_m^{ex}}^{plan} \end{cases} \tag{A.43}$$

Downward orders and shutdown orders formulated over overlapping combinatorial index are linked with an *Exclusion* to avoid simultaneous activations (see Section A.3.4.2.3).

A.3.3.2.3 Hydraulic units specific case

For hydraulic units, the available upward power and the available downward power are divided into fragments to keep a relevant level of consistency with both day-ahead and intraday market results. In these markets, the entire range between 0 and the maximum power of each unit $u \in U^h$ was divided into 7 fragments, each one leading to an individual market order.

In balancing markets, the same fragment division is kept. The last generation plan of the unit is used to identify where it stands in this division, and to deduce the subsequent upward and downward volumes that should be formulated. This computation is illustrated in Figures A.11a and A.11b in a general case, for a given time t.

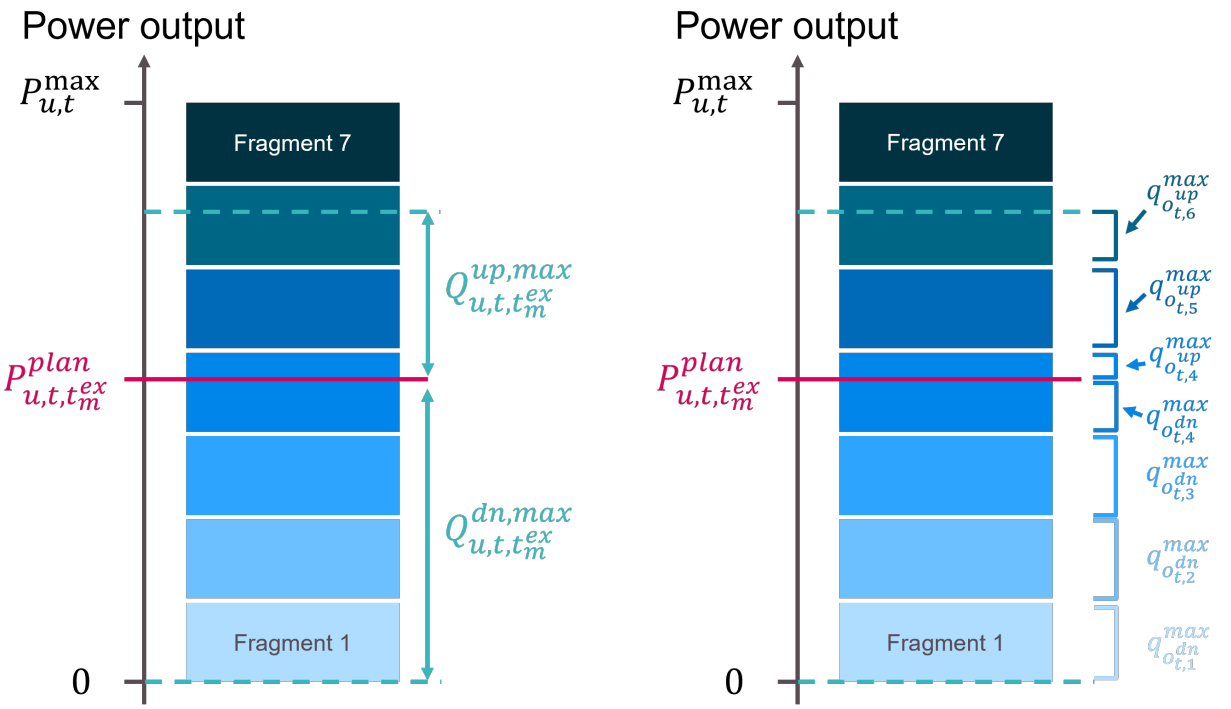

(a) Identification of the power output state

(b) Computation of q^{max}_{o}

Figure A.11: Example of the computation of orders volume for hydraulic units

In this example, the previously calculated available upward power does not allow the unit to reach its maximum power $P^{max}_{u,t}$, resulting in 3 upward orders of respective maximum quantities $q^{max}_{o^{up}_{t,i}}$, where i is the fragment number associated with the order.

The minimum quantity $q^{min}_{o^{\bullet}_{t,\bullet}}$ of all of these orders is set to 0.

A.3.3.3 Order price determination

The price of the order $o^{\bullet}_{u}$ is determined based on the type of unit u, and the order direction $\bullet$.

A.3.3.3.1 Thermal units

For a thermal unit $u \in U^{th}$, 2 cases are possible depending on the value of the variable $\delta^{SU}_{u,T_{id},t^{ex}_m}$ tracking a startup order:

- If the order is not part of a startup, then its price is computed as a combination of its variable costs c_u^{var} and startup costs c_u^{SU} (Equation A.44). Remark: a non startup order can still induce startup costs.

$$\begin{aligned} &\forall u \in U^{th},\ \ \forall o_{u,id} \in O^{up} \cup O^{dn} \cup O^{shut}, \\ &\textbf{if } (\delta^{SU}_{u,T_{id},t_m^{ex}} = 0) \textbf{ then } \quad p_{o_{u,id}} = c_u^{var} + \sigma^{SU}_{u,T_{id}} * \frac{c_u^{SU}}{Q^{max}_{u,T_{id},t_m^{ex}} * \Delta T_{id}} \end{aligned} \tag{A.44}$$

- If the order creates a startup, then it is separated into 2 parts as explained in Section A.3.3.1.2. The price of the first order o_{id}^{s1}, which corresponds to the start of the unit from 0 to its minimum power, includes the startup cost and is calculated in Equation A.45:

$$\begin{aligned} &\forall u \in U^{th},\ \forall T_{id}, \\ &\textbf{if } (\delta^{SU}_{u,T_{id},t_m^{ex}} = 1) \textbf{ then } \quad p_{o^{s1}_{u,id}} = c_u^{var} + \sigma^{SU}_{u,T_{id}} * \frac{c_u^{SU}}{q^{max}_{o^{s1}_{u,id}} * \Delta T_{id}/60} \end{aligned} \tag{A.45}$$

  Here, startup costs are spread across all startup orders of the combinatorial index id, as is indicated by the division by $\Delta T_{id}/60$.

  The price of the second order o_{id}^{s2} is directly given by the variable cost, as Equation A.46 indicates:

$$\begin{aligned} &\forall u \in U^{th},\ \forall T_{id},\ \ \forall o \in O^{up}, \\ &\textbf{if } (\delta^{SU}_{u,T_{id},t_m^{ex}} = 1) \textbf{ then } \quad p_{o^{s2}_{u,id}} = c_u^{var} \end{aligned} \tag{A.46}$$

A.3.3.3.2 Hydraulic units

For hydraulic units, the price of an order is computed using water value $WV_{u,t,E^{stored}_{u,t,t_m^{ex}}}$, which indicates the value of the current energy stored in the unit reservoir by estimating the opportunity cost of using it later over a certain period. In ATLAS, water values are preemptively computed over an entire year, for each hydraulic unit in the input dataset. This module then performs linear interpolations on both the storage level and the temporal axis to extract the storage marginal value corresponding to the situation at time t, for stored energy $E^{stored}_{u,t,t_m^{ex}}$.

In Section A.3.3.2.3, the available upward and downward power was divided into orders corresponding to power fragments. In the day-ahead and intraday market processes, each fragment is associated with a given spread that is applied to the water value, and that will be noted $Spread_i$, with i the fragment number. The same spreads are used to compute the price of balancing market orders:

$$\forall u \in U^h,\ \ \forall t \in T_m,\ \ \forall o_{t,i} \in O^{up} \cup O^{dn}, \quad p_{o_{t,i}} = WV_{u,t,E^{stored}_{u,t,t_m^{ex}}} + Spread_i \tag{A.47}$$

A.3.3.3.3 Storage units

For storage units, the price of each order is set according to the average of clearing prices of previous electricity markets at the corresponding time t. These markets may include day-ahead, intraday or previous RR markets

(for the order formulation on mFRR markets).

$$\forall u \in U^{st},\ \forall t \in T_m,\ \forall o_u \in O^{up} \cup O^{dn},$$
$$p_{o_{u,t}} = \frac{1}{n_{DA} + n_{ID} + n_{RR}} * \Big(\sum_{1 \leq i \leq n_{DA}} \lambda_{ca,t}^{DA,i} + \sum_{1 \leq j \leq n_{ID}} \lambda_{ca,t}^{ID,j} + \sum_{1 \leq k \leq n_{RR}} \lambda_{ca,t}^{RR,k} \Big) \tag{A.48}$$

Where n_m is the number of markets of type m for which a price is available at t, in the area ca of the unit u.

In further work, we are looking to refine this price estimation, using a method similar to the one used in intraday processes (Little et al., 2024).

A.3.3.3.4 Wind, photovoltaic and flexible load units

Finally, for wind, photovoltaic and flexible load units, the price of both upward and downward orders is directly given by the variable cost associated with each unit (Equation A.49).

$$\forall u \in U^{w} \cup U^{pv} \cup U^{l},\ t \in T_m,\ \forall o_{u,t} \in O^{up} \cup O^{dn},$$
$$p_{o_{u,t}} = c_u^{var} \tag{A.49}$$

For wind and photovoltaic units, variable costs are usually set to 0, although the user can choose to set a different value at will. This can be used to represent specific market incentives for instance. For flexible load units, variable costs are often set exogenously. For example, power-to-gas units usually take as a reference the price of the gas market.

A.3.4 Coupling links between orders

Once all their characteristics are determined by previous steps, market orders are formulated by creating instances of the Order class. However, one last phase is required to complete the balancing market orders formulation. As the aforementioned characteristics are not sufficient to accurately translate operating constraints in market orders, coupling links must be created between them in many cases. The types of coupling available in ATLAS are described in Section A.3.4.1, and Section A.3.4.2 explains how they are used in the module.

A.3.4.1 Types of coupling

This module uses 3 different types of coupling instances, which are explained hereafter.

A.3.4.1.1 *Identical ratio*

If several orders are coupled by *Identical ratio*, it will force the Clearing stage to activate them with the same acceptance ratio. This ratio is calculated based on $q_{o_i}^{max}$ and $q_{o_i}^{min}$ of each order o_i, and is shown in equation

A.50 in a simplified example with 2 orders:

$$\forall c^{idr} \in C^{idr},\ \forall \{o_1, o_2\} \in c^{idr},\quad \frac{q^{acc}_{o_1} - q^{min}_{o_1}}{q^{max}_{o_1} - q^{min}_{o_1}} = \frac{q^{acc}_{o_2} - q^{min}_{o_2}}{q^{max}_{o_2} - q^{min}_{o_2}} \tag{A.50}$$

A.3.4.1.2 *Exclusion*

If several orders are linked by an *Exclusion* coupling, the Clearing will only be able to activate at most one of these orders (even if it is partially accepted). If we note $\delta^{acc}_{o_i}$ the boolean indicating if an order o_i is accepted by the Clearing (meaning that $\delta^{acc}_{o_i} = 1\ if\ q^{acc}_{o_i} > 0$ and $\delta^{acc}_{o_i} = 0\ if\ q^{acc}_{o_i} = 0$), equation A.51 gives an example of this coupling link for two orders:

$$\forall c^{excl} \in C^{excl},\ \forall \{o_1, o_2\} \in c^{excl},\quad \delta^{acc}_{o_1} + \delta^{acc}_{o_2} \leq 1 \tag{A.51}$$

A.3.4.1.3 *Parent Children*

A coupling of type *Parent Children* contains a list of orders $\{o_1, ..., o_N\}$. The first order o_1 is the parent by convention, and the rest are the children. This coupling type forces the Clearing to activate (at least partially) the parent order if at least one child is activated, which is described by equation A.52:

$$\forall c^{pc} \in C^{pc},\ \forall \{o_1, ..., o_N\} \in c^{pc},\quad \delta^{acc}_{o_1} \geq \min(1, \sum_{n=2}^{N} \delta^{acc}_{o_n}) \tag{A.52}$$

A.3.4.2 Creation of coupling links

A.3.4.2.1 *Parent Children* coupling between both parts of a startup order

The two orders o^{s1} and o^{s2} that form a startup are linked with a *Parent Children* coupling instance in the following way: the indivisible order o^{s1} between 0 and the minimum power of the unit is the parent order, and the other is the child (Equation A.53).

$$\forall u \in U^{th},\ \forall T_{id} \mid \delta^{SU}_{u,T_{id},t^{ex}_m} = 1,\ \forall t \in T_{id},\quad \exists\, c^{pc} \in C^{pc} \mid \{o^{s1}_{u,t}, o^{s2}_{u,t}\} \in c^{pc} \tag{A.53}$$

Consequently, the Clearing has to activate the bottom order (entirely, because of its indivisibility–$q^{min}_{o^{s1}_{u,t}} = q^{max}_{o^{s1}_{u,t}}$) in order to activate the top one.

A.3.4.2.2 *Identical Ratio* coupling between orders of the same combinatorial index

For thermal units, all orders from the same combinatorial index *id* are linked with an *Identical Ratio* coupling, to represent the fact that they are meant to be a single order over several time steps (Equation A.54). The only exception is the bottom part o^{s1} of startup orders. Since all bottom parts are indivisible, there is no

need for an additional coupling between them as they are all fully activated, and only top orders o^{s2} are linked (Equation A.55).

$$\forall u \in U^{th},\ \forall T_{id} \mid \delta^{SU}_{u,T_{id},t^{ex}_m} = 0, \quad \exists\, c^{idr} \in C^{idr} \mid \forall o_u \in O_{u,id},\ o_u \in c^{idr} \tag{A.54}$$

$$\forall u \in U^{th},\ \forall T_{id} \mid \delta^{SU}_{u,T_{id},t^{ex}_m} = 1, \quad \exists\, c^{idr} \in C^{idr} \mid \forall o^{s2}_u \in O_{u,id},\ o^{s2}_u \in c^{idr} \tag{A.55}$$

A.3.4.2.3 *Exclusion* between orders of different combinatorial indexes formulated on the same time period

The order formulation on thermal units can create several market orders of the same direction in the same time period that belong to different combinatorial indexes. These orders are meant to provide flexibility regarding operating constraints, but should never be activated together by the Clearing. This is enforced by creating *Exclusion* couplings between them (Equation A.56), while excluding startup orders linked with a *Parent Children* coupling.

$$\forall u \in U^{th},\ t \in T_m, \quad \begin{cases} \exists\, c^{excl}_{up} \in C^{excl} \mid \left(\forall o_{u,t} \in O_{u,t} \mid (\sigma_{o_{u,t}} = -1)\ \&\ (o_{u,t} \notin c^{pc}),\ o_{u,t} \in c^{excl}_{up} \right) \\ \exists\, c^{excl}_{dn} \in C^{excl} \mid \left(\forall o_{u,t} \in O_{u,t} \mid (\sigma_{o_{u,t}} = 1)\ \&\ (o_{u,t} \notin c^{pc}),\ o_{u,t} \in c^{excl}_{dn} \right) \end{cases} \tag{A.56}$$

Remark: this does not concern orders of opposite directions. If their price is set correctly, it should prevent the Clearing from activating them simultaneously.

A.3.4.2.4 *Exclusion* between consecutive orders of opposite directions

The maximum ramping constraints may be violated if the Clearing activates consecutive orders of opposite directions (see Figure A.12). Indeed, this module tries to maximize the quantity offered by each unit, it can frequently correspond to the quantity directly feasible by its maximum ramping constraints.

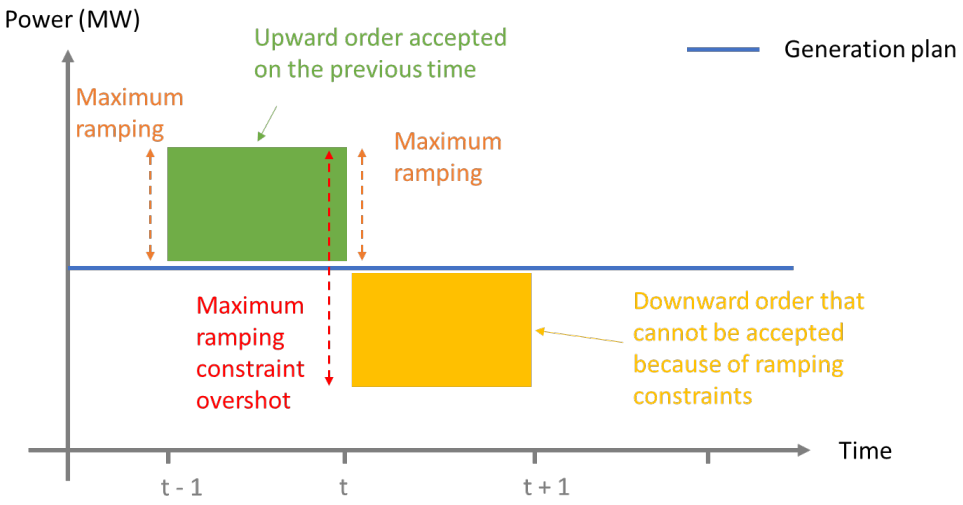

Figure A.12: Consecutive opposite orders violating gradient constraints

Consequently, an *Exclusion* coupling is created between the first order of a combinatorial index (so at t_{id}^{start}) and every order of the opposite direction formulated on the previous time period (at $t_{id}^{start} - 1$). The same operation is done for the last order (at t_{id}^{end}) and orders of the next time period ($t_{id}^{end} + 1$).

$$\forall u \in U^{th},\ \forall T_{id},\quad \begin{cases} \forall o_u \in O_u \mid \left((t_{o_u}^{start} = t_{id}^{start} - 1)\ \&\ (\sigma_{o_u} \neq \sigma_{o_{u,id}^{start}}) \right), & \exists\, c^{excl} \in C^{excl} \mid \{o_{u,id}^{start}, o_u\} \in c^{excl} \\ \forall o_u \in O_u \mid \left((t_{o_u}^{start} = t_{id}^{end} + 1)\ \&\ (\sigma_{o_u} \neq \sigma_{o_{u,id}^{end}}) \right), & \exists\, c^{excl} \in C^{excl} \mid \{o_{u,id}^{end}, o_u\} \in c^{excl} \end{cases} \tag{A.57}$$

Where $o_{u,id}^{start}$ is the order in id with the start date equal to the first date of id ($t_{o_{u,id}^{start}}^{start} = t_{id}^{start}$), and $o_{u,id}^{end}$ the corresponding order for the last date of id ($t_{o_{u,id}^{end}}^{start} = t_{id}^{end}$).

A.3.4.2.5 Orders completely exclusive

Certain orders are considered to be completely exclusive, which means that they need to be exclusive to all other orders of the same direction, regardless of the time period. These orders are those for which:

- A storage capacity constraint is limiting the quantity offered. Since the orders of the combinatorial index are formulated so that the constraint is respected on this index exactly, and not on other time periods of the balancing time frame, it would conflict with another activation (in the same direction) within the balancing time frame.
- The minimum stable power duration constraint is active. For a given index, the unit power must remain unchanged to be sure that the constraint is respected.

Eventually, *Exclusion* coupling instances are created between every order completely exclusive and all other orders of the same direction.

A.4 ATLAS Balancing Stage - TSO Orders

A.4.1 Overview

The objective of this module is to formulate TSO balancing energy market orders, for RR or mFRR markets. Submitted market orders are required to display all information indicated in Table A.27. The general process described in this chapter is repeated for each individual TSO in the power system, and consists of two main steps: the computation of the balancing need in the control area *ca* of the studied TSO (Section A.4.2), followed by the computation of orders prices and volumes depending on the volume of need previously computed and on the bidding strategy parameter chosen for the TSO (Section A.4.3). The bidding step is designed to be flexible in multiple aspects.

This module and the bidding strategies previously presented can be used for formulating both RR or mFRR market orders, depending on the parameters chosen by the user. Note that if the simulated market is mFRR, the alternative chosen should logically not be the mFRR market (but the aFRR market is still a relevant alternative).

Finally, as the process is the same for every TSO, it is assumed in all following sections that a specific TSO is chosen, along with its control area $ca \in CA$. This control area may include several market areas $z \in Z_{ca}$.

A.4.1.1 Nomenclature

The following notations are used in this chapter. Some elements correspond to a specific type, which is indicated in bold and italics:

- ***Parameter*** refers to a parameter, which is indicated by the user before the execution of the module.
- ***Input data*** refers to an element that is extracted from the input dataset.
- ***Variable*** refers to an optimization variable.

Remark: For sets, the notation A_b refers to the subset of A linked with variable b. For instance, Z_{ca} indicates the subset of market areas belonging to the control area ca.

Sets and global market notations	
Notation	**Description**
CA	Set of all control areas (or control blocks)
Z	Set of all market areas. Z_{ca} indicates all market areas within control area $ca \in CA$
PF	Set of all portfolios. PF_z indicates all portfolios in market area $z \in Z$
U	Set of all units. U_z indicates units in market area $z \in Z$, and U_{pf} indicates units in portfolio $pf \in PF$

U^{unit_type}	Set of all units of type $unit\_type \in [g, l, th, h, st, w, pv]$. ($g$ = generation, l = flexible load, th = thermal, h = hydraulic, st = storage, w = wind, pv = photovoltaic)
O	Set of all market orders
O^{up}	Set of all upward market orders
O^{dn}	Set of all downward market orders
C^{excl}	Set of all coupling instances of type $Exclusion$
m	Type of market simulation, amongst $\{RR,\ mFRR\}$

Temporal variables		
Notation	**Description**	**Units**
t_m^{ex}	Execution date of the market $m \in \{RR, mFRR\}$. ***Parameter***	-
t_m^{start}	Start date of the effective period of the market m. ***Parameter***	-
t_m^{end}	End date of the effective period of the market m. ***Parameter***	-
Δt_m	Time step of the market m. ***Parameter***	min
T_m	Effective time frame of the market m, i.e. $T_m = [t_m^{start}, t_m^{start} + \Delta t_m, \ldots, t_m^{end} - \Delta t_m]$	-

TSO-specific characteristics		
Notation	**Description**	**Units**
$bn_{m,ca,t,t_m^{ex}}$ (short: bn_t)	Balancing needs for market m in control area $ca \in CA$ for time $t \in T_m$, seen from t_m^{ex}. For readability, it is shortened as bn_t	MW
$\sigma^{bn}_{ca,t,t_m^{ex}}$ (short: σ_t^{bn})	Binary parameter indicating the direction of TSO (of area ca) balancing needs at time t seen from t_m^{ex}. $\sigma^{bn}_{ca,t,t_m^{ex}} = up\ if\ bn_{m,ca,t,t_m^{ex}} > 0$, and $\sigma^{bn}_{ca,t,t_m^{ex}} = dn$ otherwise. For readability, it is shortened as σ_t^{bn}	-
δ_{ca}^{for}	Binary parameter indicating if TSO associated with control area $ca \in CA$ takes into account forecasts errors in its imbalance needs computation. ***Parameter***	-
δ_{ca}^{elas}	Binary parameter indicating if the demand of TSO associated with control area $ca \in CA$ is formulated as elastic ($\delta_{ca}^{elas} = 1$) or not ($\delta_{ca}^{elas} = 0$). ***Parameter***	-
alt_{ca}	Alternative chosen to compute prices and volumes of the demand of TSO associated with control area $ca \in CA$. Possible values are $\{"mFRRalt", "FrBMalt"\}$. ***Parameter***.	-

V^s	Maximum quantity of each slice of TSO demand formulated on markets. Only relevant if $\delta_{ca}^{elas} = 1$. ***Parameter***	MW
δ_{ca}^{vol}	Binary parameter indicating if the demand of TSO associated with control area $ca \in CA$ is taking into account volume uncertainty ($\delta_{ca}^{vol} = 1$) or not ($\delta_{ca}^{vol} = 0$). Only relevant if $\delta_{ca}^{elas} = 1$. ***Parameter***	-
$\epsilon_{ca}^{alt_{ca}}$	List of quantiles of the distribution of the TSO forecast error function of area ca associated with alternative alt_{ca}. Only relevant if $\delta_{ca}^{vol} = 1$. ***Parameter***	-

Zonal-specific characteristics		
Notation	**Description**	**Units**
$q_{m,ca,t}^{\sigma_t^{bn},max}$	Overall quantity for orders in direction opposite to σ_t^{bn} formulated by BSPs included in control area ca on market m, at time t	MW
$(\Delta q)_{z,t}^{bal}$	Commercial (power) balance of area $z \in Z$ at time t, equal to the sum of all power exports minus the sum of all power imports	MW
$\rho_{m,ca}^{FrBMalt}$	Percentage of BSP available capacity in area ca that is not submitted on the market m, and is consequently directly sent to the FrBM market. Only relevant if $\delta_{ca}^{elas} = 1$, with $alt_{ca} =$ "$FrBMalt$". ***Parameter***	-

Global unit characteristics		
Notation	**Description**	**Units**
$P_{u,t,t_m^{ex}}^{plan}$	Power output of unit $u \in U$ at time $t \in T_m$, seen from time t_m^{ex}	MW
$P_{u,t}^{max}$	Maximum power output of unit $u \in U$ at time $t \in T_m$	MW
$P_{u,t}^{min}$	Minimum power output of unit $u \in U$ at time $t \in T_m$	MW
$R_{ut,t_m^{ex}}^{m^R,\sigma^R}$	Procured reserves of type $m^R \in [FCR, aFRR, mFRR, RR]$ in direction $\sigma^R \in [up, dn]$ on unit u at time t, seen from t_m^{ex}	-

Hydraulic- and Storage-specific unit characteristics		
Notation	**Description**	**Units**
$E_{u,t,t_m^{ex}}^{stored}$	Stored energy in the reservoir of unit $u \in U^h \cup U^{st}$ at time $t \in T_m$, seen from time t_m^{ex}	MWh
$E_{u,t}^{max}$	Maximum storage level in the reservoir of unit $u \in U^h \cup U^{st}$ at time $t \in T_m$	MWh

$E^{min}_{u,t}$	Minimum storage level in the reservoir of unit $u \in U^h \cup U^{st}$ at time $t \in T_m$	MWh
d^{tran}_u	Transition duration between pumping and turbining of unit u of type Pumped Hydraulic Storage (PHS), that are modeled as storage units in ATLAS (i.e. $u \in U^{st}$)	min
$WV_{u,t,E^{stored}_{u,t,t^{ex}_m}}$	Marginal storage value of unit $u \in U^h$ at time t, for stored energy level $E^{stored}_{u,t,t^{ex}_m}$	€/MWh

Load-, Photovoltaic- and Wind-specific unit characteristics		
Notation	**Description**	**Units**
P^{for}_{u,t,t^{ex}_m}	Forecast of the maximum power output of unit $u \in \{U^w, U^{pv}, U^l\}$ at time $t \in T_m$	MW
$Curt_u$	Percentage of curtailed power allowed on unit $u \in \{U^w, U^{pv}\}$	-

Market order characteristics	
Notation	**Meaning**
p_o	Price of order o
q^{min}_o	Minimum quantity of power offered for order o
q^{max}_o	Maximum quantity of power offered for order o
t^{start}_o	Start date of order
t^{end}_o	End date of order
t^{ex}_o	Execution date of order
σ_o	Sale/Purchase indicator, $\sigma = -1$ for purchase, 1 for sale
δ^{TSO}_o	Binary variable indicating if order o is from a TSO ($\delta^{TSO}_o = 1$) or not.
δ^{acc}_o	Binary variable indicating if order o is activated by the Clearing stage ($\delta^{acc}_o = 1$ if $q^{acc}_o > 0$)

Other notations		
Notation	**Description**	**Units**
$VoLL$	Value of loss load	€/MWh
$E^{VoLL}_{ca,t}$	Loss load energy in control area ca at time t	MWh
$E^{spill}_{ca,t}$	Spillage power in control area ca at time t	MW

A.4.2 TSO balancing needs computation

The module studies independently each TSO in the power system extracted from the input marker, and aims at formulating its balancing market orders. To do so, the first step is to compute its balancing needs bn_t for every time t in the entire effective time frame T_m of the market m, seen from t_m^{ex}. They correspond to the forecasted imbalance in its control area $ca \in CA$ (that may be composed of several market areas), computed based on the planned power output of all generation and consumption units in ca. This calculation is not trivial for several reasons:

- A specific restriction exists for balancing markets: in a nominal state, the volume of TSO needs submitted to the market in a given direction σ_t^{bn} cannot exceed $q_{m,ca,t}^{\sigma_t^{bn},max}$ the sum of reserves offered by BSPs in ca in the opposite direction to σ_t^{bn}. This models the actual RR market rule stating that a TSO cannot submit a larger volume of needs than what market orders in its area could compensate for[4]. In practice, TSOs can ask for a specific exemption to this rule for a given time step if the security of supply or their network is compromised, which has to be justified thoroughly (this feature is not implemented in ATLAS). The estimation of $q_{m,ca,t}^{\sigma_t^{bn},max}$ is done in Section A.4.2.1.
- The type of power output that should be taken into account when computing TSO needs is not straightforward. It challenges the role of TSOs in these new balancing markets, by questioning the integration of forecasts in the computation process. This issue is discussed in Section A.4.2.2

A.4.2.1 Computation of the overall volume submitted by BSPs in each control area

For time step $t \in T_m$, the overall volume of power offered by BSPs $q_{m,ca,t}^{\sigma_t^{bn},max}$ is computed for depending on σ_t^{bn}, the direction of TSO balancing needs. Only BSP orders in the opposite direction are taken into account (BSP shutdown orders explained in Section A.3.3.1.2 are included in the dn direction). Coupling links need to be considered in the calculation. Indeed, multiple orders of the same time step ($t_o^{start} = t$, that is noted o_t in the equation below) linked with an *Exclusion* coupling should not be simultaneously participating in the overall volume. In that situation, only the order with the largest q_o^{max} is included in the computation:

$$\forall u \in U_{ca},\ \forall c \in C^{excl},\ \forall t \in T^m,$$
$$q_{m,ca,t}^{\sigma_t^{bn},max} = \sum_{o_t \in O_u \,|\, (\sigma_{o_t} \neq \sigma_t^{bn})\ \&\ (o_t \notin c)} q_{o_t}^{max} + \max_{o_t \in c \,|\, (\sigma_{o_t} \neq \sigma_t^{bn})} q_{o_t}^{max} \tag{A.58}$$

A.4.2.2 Imbalance computation

As hinted at before, the balancing needs computation depends on the role of TSOs in balancing markets. The main question revolves around whether TSOs or Balancing Responsible Parties (BRPs)[5] should take into account imbalances that arise because of forecasts errors or even because of unexpected shutdown of

[4]This is indicated in the document https://eepublicdownloads.entsoe.eu/clean-documents/events/2018/terre/20180319_TERRE_Stakeholders_presentation.pdf

[5]BRPs possess a portfolio of generation and consumption units and face financial penalties if their portfolio is imbalanced compared to the energy they sold/bought on markets

units. To be as flexible as possible, both options exist in ATLAS for a given ca, depending on the parameter δ_{ca}^{for}.

$$\forall ca \in CA, \ \forall t \in T_m,$$

$$if \ \delta_{ca}^{for} = 1, \quad bn_t = \sum_{u \in U^l} |P_{u,t,t_m^{ex}}^{for}| - (\sum_{u \in U^{th} \cup U^h \cup U^{st}} P_{u,t,t_m^{ex}}^{plan} + \sum_{u \in U^w \cup U^{pv}} P_{u,t,t_m^{ex}}^{for}) + \sum_{z \in Z_{ca}} (\Delta q)_{z,t}^{bal} \tag{A.59}$$

$$if \ \delta_{ca}^{for} = 0, \quad bn_t = \sum_{u \in U^l} |P_{u,t,t_m^{ex}}^{plan}| - \sum_{u \in U^g} P_{u,t,t_m^{ex}}^{plan} + \sum_{z \in Z_{ca}} (\Delta q)_{z,t}^{bal} \tag{A.60}$$

Where $(\Delta q)_{z,t}^{bal}$ is the power balance of area z at time t, meaning the sum of all exports minus the sum of all imports. Absolute values of power outputs and power forecasts of load units are considered in the computation, since by convention in ATLAS a negative power output corresponds to a consumption.

Finally, balancing needs are capped by the overall volume submitted by BSPs, which was just computed before:

$$if \ bn_t < 0, \quad bn_t \leftarrow \min(bn_t, \ q_{m,ca,t}^{dn,max}) \tag{A.61}$$

$$if \ bn_t > 0, \quad bn_t \leftarrow \min(bn_t, \ q_{m,ca,t}^{up,max}) \tag{A.62}$$

A.4.3 Bidding strategies

Once overall balancing needs are defined, they are translated into market orders depending on the set of bidding strategy parameters chosen for the TSO of control area ca, which are illustrated in the diagram of Figure A.13. The current section details all bidding strategies available in ATLAS, including the final characteristics of all market orders formulated (Table A.27. Filling most characteristics is straightforward, as all orders o formulated by a TSO at time t share the following attributes:

$$\forall o \in O_{TSO}, \ \forall t \in T_m, \quad \begin{cases} t_o^{ex} = t_m^{ex} \\ t_o^{start} = t \\ t_o^{end} = t + \Delta t_m \\ q_o^{min} = 0 \\ \delta_o^{TSO} = 1 \end{cases} \tag{A.63}$$

The q^{min} is set to 0 as the regulation of balancing markets requires TSO orders to be entirely divisible. The only characteristics that need to be determined by the bidding strategies are then the maximum quantity p_o, the price p_o and the order direction σ_o.

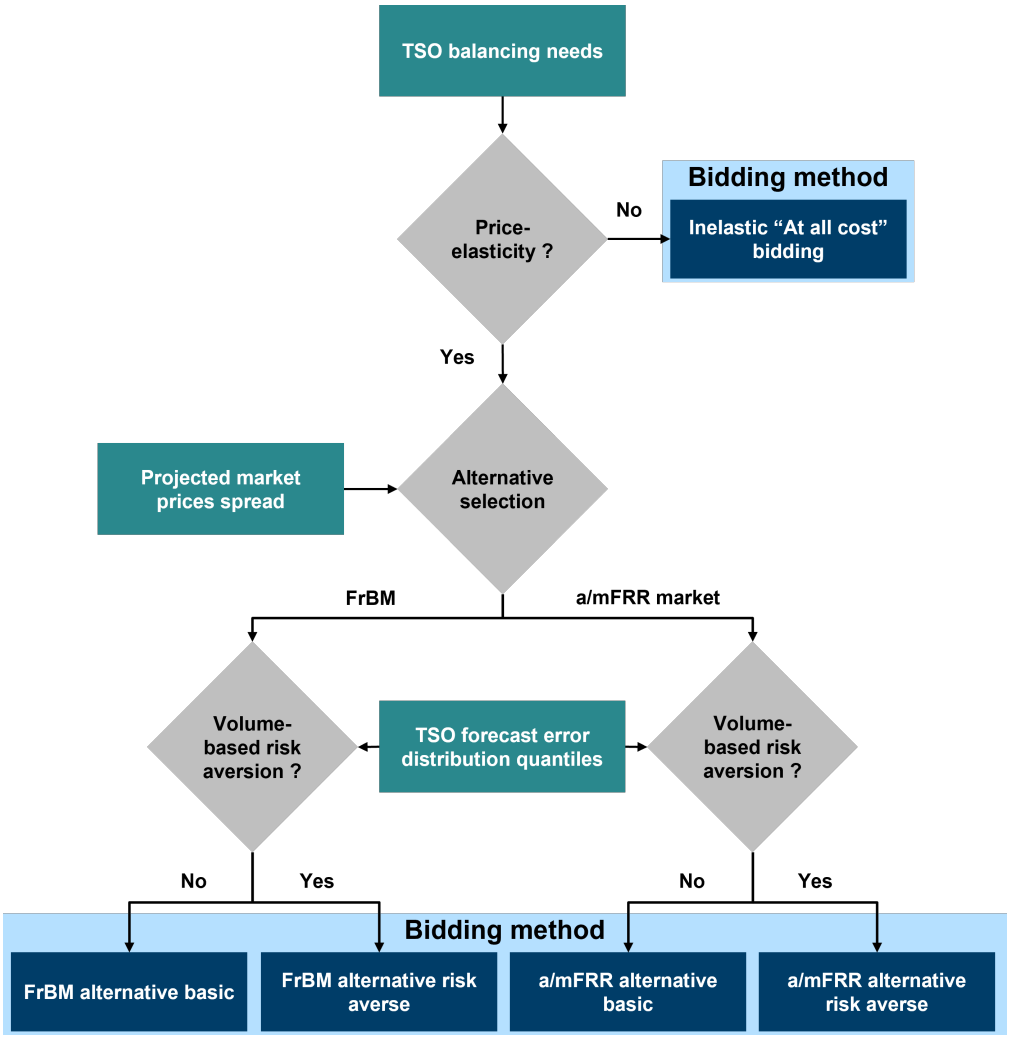

Figure A.13: TSO Orders Formulation Strategies Framework

A.4.3.1 Price-inelastic bidding strategy

With the inelastic bidding strategy, the TSO is willing to accept any price for its entire balancing needs to be fulfilled by the market. Consequently, this strategy leads to the formulation of a single market order o, whose quantity, price and direction are described in Equation A.64. Notably, the quantity corresponds to the entire balancing need of the given TSO, and the price to the maximum (resp. minimum) price authorized by

the market for upward (resp. downward) balancing needs:

$$\forall ca \in CA, \ \forall t \in T_m, \ if \ \delta_{ca}^{elas} = 0,$$

$$if \ bn_t > 0, \quad \begin{cases} q_o^{max} = bn_t \\ p_o = 10,000 \\ \sigma_o = -1 \end{cases} \tag{A.64}$$

$$if \ bn_t < 0, \quad \begin{cases} q_o^{max} = bn_t \\ p_o = -10,000 \\ \sigma_o = 1 \end{cases} \tag{A.65}$$

Notably, it is required for all TSO orders to be completely divisible (q^{min} is always set to 0). This will be consistent across all other types of bidding strategies.

A.4.3.2 Elastic bidding strategies

A.4.3.2.1 Key concepts

In ATLAS, price-elastic bidding strategies result in the creation of bidding curves for TSO balancing needs. In terms of market orders at a given time t, it implies the creation of a finite set of orders $o_i, \quad \forall i \in 1, \ldots, n$ where n is the number of slices into which the balancing needs are divided. All orders share the same general characteristics described at the beginning of Section A.4.3, and each order o_i has its specific quantity-price-direction characteristics that we will note $q_{t,i}$, $p_{t,i}$ and $\sigma_{t,i}$.

The price-elastic bidding process depends on two main parameters:

- The type of alternative that is used as a reference to estimate opportunity costs, from which are derived the price of TSO market orders. That alternative can either be a closer-to-real-time market (such as the mFRR market when formulating orders on the RR market), or the local balancing process in the TSO area. These two categories of alternatives have their own specific features, that are detailed in Section A.4.3.2.2.
- The integration of volume uncertainty in the bidding process, which can influence both the quantities and prices of TSO market orders. It is detailed in Section A.4.3.2.3.

A.4.3.2.2 Alternative types and their features

Local balancing process

With this alternative selection, the TSO considers that its local balancing process is a viable alternative to the simulated market. In other words, the TSO assumes that it can rely on its local process after the balancing market, and uses this assumption to compute the prices of its market orders. In ATLAS, the local

balancing process is modeled by the Balancing Mechanism module, detailed in Section A.5. It is based on the historical French Balancing Mechanism process, and will consequently be referred to as FrBM.

A key hypothesis is required when considering this type of alternative. Since the TSO uses an estimate of its local balancing process costs, it has to predict that a certain volume of power (either upward or downward, depending on its needs) will be available on the BM. This prediction is made before the clearing of balancing markets, for a BM that occurs after said balancing markets, which means that the TSO has to predict the power that is either not submitted to the market or not activated on it. The prediction process currently used in ATLAS revolves around the parameter $\rho_{m,ca}^{FrBMalt}$ which indicates the percentage of available capacity that is not submitted on the balancing market m by BSPs, and goes directly on the FrBM. This process then consists of the following steps, according to the unit type:

- For thermic units, a random draw is performed for each subset of fuel types in the area of the TSO, selecting units that are only submitting capacity to the FrBM to reach $\rho_{m,ca}^{FrBMalt}$ with a tolerance band of 10%. For instance, if an area has both CCGT and nuclear assets with $\rho_{m,ca}^{FrBMalt} = 50\%$, then each type of fuel is looked at individually. Units belonging to the CCGT group are randomly selected so that their combined capacity is within the range [40%, 60%] of the total CCGT capacity in the area. The same selection is applied to nuclear units. Performing the selection by fuel type allows to avoid randomly selecting all units of a certain type, which could have an important impact on cost estimations.
- Hydraulic and storage units are usually modeled by a single asset for each zone in ATLAS. Consequently, it is assumed that the percentage $\rho_{m,ca}^{FrBMalt}$ of the available capacity of each unit is available on the FrBM.

The calibration of the capacity percentage parameter then plays a key role. An empirical analysis carried out on data published by RTE over 2022 was used for this calibration, leading to the following estimation (using a conservative approach that tends to favor the volume submitted on balancing markets): 50% of the available upward (resp. downward) power is not formulated on the RR market, and is always available on the French local balancing process.

We are looking to refine this estimation in the future. First, the empirical study only provides aggregated data, and in particular does not distinguish unit types. It is consequently difficult to evaluate if the volume not submitted to the RR market is mostly associated with a specific type, or spread homogeneously (the latter is chosen as a basis in ATLAS). In addition, the study was only conducted in the French area for data availability reasons, and this estimator could be very different in other areas. Nonetheless, as this is the only value at our disposal, it is consequently applied to all areas in ATLAS.

Once the determination of available units on the projected FrBM is done, simulations of the alternative using the Balancing Mechanism module are performed. The cost $C^{FrBMalt}(q)$ of balancing a given volume of TSO needs q is a direct output of the simulation process.

Alternative market process

A TSO can consider that a closer-to-real-time market is an alternative to its current studied market m, as illustrated by the timeline in Figure A.14. While the aFRR market could be a relevant alternative to both

RR and mFRR markets, it is currently not implemented in ATLAS. This means that the alternative market process currently works in a single configuration: $m = RR$, and $alt_{ca} = mFRRalt$. However, the following description is sufficiently generic that it could be applied in the case $alt_{ca} = aFRRalt$, should the aFRR market be implemented in ATLAS in the future.

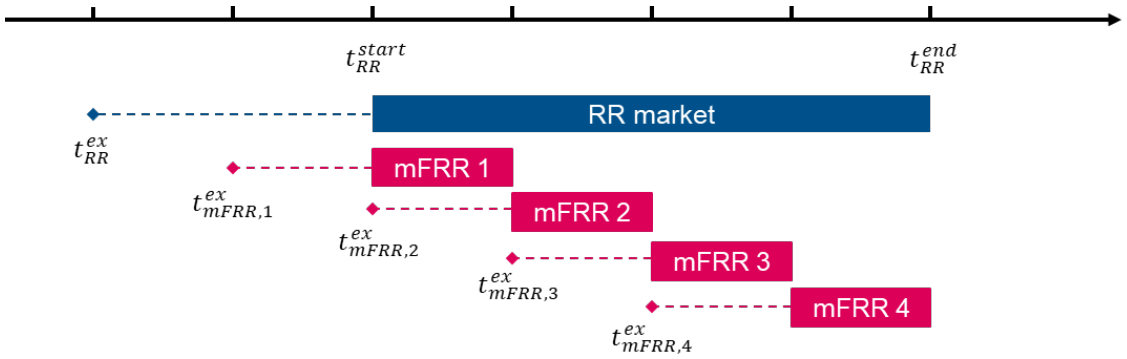

Figure A.14: Schematic representation of RR and mFRR markets overlays used in the mFRR alternative pricing

In contrast with the FrBM alternative, there is no need for an assumption of available units. The alternative market is not simulated, as a simulation of future balancing markets would require the TSO to make a significant number of assumptions about the state of the power system, especially given that balancing markets include multiple European areas. We considered that it was not a realistic approach. Instead, the projected market prices are estimated based on fixed input data.

Several options are possible for this estimation. The first one would be to use historical data of the alternative. However, actual mFRR markets have only been operational for a year[6]. Based on past experiences with the operational RR market, it seems that a year is not enough time to reach a stable state for the market, as both BSPs and TSOs are still progressively entering it and experimenting with it. Another basis could be to preemptively simulate mFRR markets in ATLAS and gather the output clearing prices. However, this would require large numbers of simulations of mFRR markets to generate sufficient data, and this option was currently ruled out for computational time reasons.

Consequently, the data we chose to use for the estimation of mFRR prices was extrapolated from the historical FrBM over 6 years, between 2018 and 2023[7]. First, offers made by units that could have participated in mFRR markets were extracted. These offers were then used to generate a table giving the projected ratio between the day-ahead market price and the mFRR price, both for upward and downward regulations, for several ranges of imbalance to compensate A.29.

[6]The Go-Live of the MARI platform was announced by ENTSO-E the 2022/10/05, c.f. https://www.entsoe.eu/news/2022/10/06/go-live-of-mari-the-european-implementation-project-for-the-creation-of-the-european-manual-frequency-restoration-reserves-mfrr-platform

[7]This data is public and was downloaded from the RTE services website https://www.services-rte.com/en/home.html, categorizedinMarket/BalancingEnergy/Prices

Imbalance volumes ranges (MW)	Ratio^{dn}	Ratio^{up}
0 - 300	0.81	1.28
300 - 600	0.76	1.33
600 - 900	0.73	1.36
900 - 1200	0.7	1.37
1200 - 1500	0.7	1.38
1500 - ∞	0.59	1.47

Table A.29: Price ratio in France between day-ahead and mFRR prices over 2018-2023

Eventually, the price estimation $\tilde{\lambda}^{\sigma^R}_{mFRR}$ of the mFRR for an imbalance q in the direction $\sigma^R \in \{up, dn\}$ is given by:

$$\tilde{\lambda}^{\sigma^R}_{mFRR}(q) = \lambda_{DA} * Ratio^{\sigma^R}(q) \tag{A.66}$$

Where λ_{DA} is the day-ahead price endogenously obtained within the ATLAS simulation process[8].

This leads to the following cost estimation for the mFRR market alternative for a given imbalance quantity q, where σ^R is here given by the direction of q ($\sigma^R = 1$ if $q >= 0$, and $\sigma^R = -1$ otherwise):

$$C^{mFRRalt}(q) = \sigma_q * q * \tilde{\lambda}^{\sigma^R}_{mFRR}(q) \tag{A.67}$$

A.4.3.2.3 Volume uncertainty integration

Pro-active TSOs try to estimate this volume at the execution date of the studied market, and it can consequently be under- or over-estimated. These forecast errors would then induce subsequent balancing needs that should be resolved with the alternative.

Two degrees relative to volume uncertainty can be chosen in ATLAS: a basic approach that considers estimated balancing needs to be exact (Section A.4.3.2.3), and another that takes into account volume-based uncertainties previously described (Section A.4.3.2.3).

Basic formulation

With the basic formulation, the division of TSO balancing needs into slices follows a process based on the parameter V^s, which indicates the maximum quantity of each order wanted by the user. When possible, the quantity q_{o_i} of order i will be equal to V^s. However, it is required to modify this quantity in some cases, mainly to improve computational performances. For instance, the simulation of the FrBM alternative is performed over the complete time frame T_m, comprised of several time steps. For that reason, the size of certain slices is reduced to harmonize as much as possible the different time steps. This example is illustrated in Figure A.15, which indicates the balancing needs division over two consecutive time steps for $V^s = 100MW$.

[8]In ATLAS, balancing markets are assumed to be simulated following at least a day-ahead market, and not entirely alone.

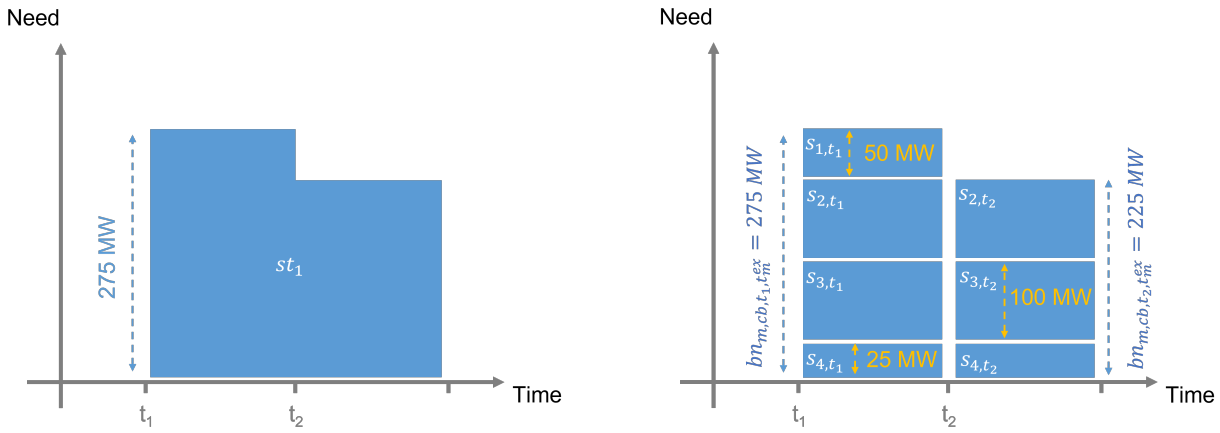

(a) Total TSO need

(b) Division into slices

Figure A.15: Deterministic Pricing Slicing Process Illustration

The two first slices of need reach the maximum quantity V_s. To divide the entire balancing needs of both time steps, the quantities of the two top slices are set at a lower value, respectively 25 MW and 50 MW in the example.

It is relevant to note that balancing needs can be positive for some time steps of a given time frame T_m, and negative for others. If this situation arises, the division is performed separately for positive and negative needs. The division process is formally described in Algorithm 8 for time steps with positive needs, and in Algorithm 9 for time steps with negative needs. In these algorithms, V_i is the relative quantity of slice i[9].

[9]For all time steps t for which slice i is reached, $q_{t,i}$ is set to the absolute value of V_i in the algorithm, and σ_{o_i} is set in accordance to the sign of V_i.

Algorithm 8 Basic elastic formulation slice division process (positive balancing needs)

Initialization of the set of time steps

$T_{div} \leftarrow t \in T_m \mid bn_t > 0$

Initialization of the first slice $i = 1$

$V_1 \leftarrow \min(V^s, \max_{t \in T_{div}} bn_t)$

Recursion

for $i > 1$ **do**

  while $\sum_{1 \leq j < i} (V_j) < \max_{t \in T_{div}} bn_t$ **do**

    $V_i \leftarrow \min(V^s, \min_{t \in T_{div}} (bn_t - \sum_{1 \leq j < i} (V_j)))$ ▷ Compute the maximum size of V_i

    for $t \in T_{div}$ **do**

      $q_{t,i} \leftarrow |V_i|$ ▷ Extract the order quantity for relevant time steps

      $\sigma_{t,i} \leftarrow -1$ ▷ Set the order direction

      if $bn_t - \sum_{1 \leq j \leq i} (V_j) = 0$ **then** ▷ Remove now "empty" time steps from T_{div}

        $T_{div} \leftarrow T_{div} - \{t\}$

      end if

    end for

    $i \leftarrow i + 1$

  end while

end for

Algorithm 9 Basic elastic formulation slice division process (negative balancing needs)

Initialization of the set of time steps

$T_{div} \leftarrow t \in T_m \mid bn_t < 0$

Initialization of the first slice $i = 1$

$V_1 \leftarrow \max(-V^s, \max_{t \in T_{div}} bn_t)$

Recursion

for $i > 1$ **do**

  while $\sum_{1 \leq j < i} (V_j) > \min_{t \in T_{div}} bn_t$ **do**

    $V_i \leftarrow \max(-V^s, \max_{t \in T_{div}} (bn_t - \sum_{1 \leq j < i} (V_j)))$ ▷ Compute the maximum size of V_i

    for $t \in T_{div}$ **do**

      $q_{t,i} \leftarrow |V_i|$ ▷ Extract the order quantity for relevant time steps

      $\sigma_{t,i} \leftarrow 1$ ▷ Set the order direction

      if $bn_t - \sum_{1 \leq j \leq i} (V_j) = 0$ **then** ▷ Remove now "empty" time steps from T_{div}

        $T_{div} \leftarrow T_{div} - \{t\}$

      end if

    end for

    $i \leftarrow i + 1$

  end while

end for

Eventually, the price of each slice i is computed according to the cost of the complete stack of needs $\sum_{1 \leq j \leq i} (V_j)$ using the selected alternative alt, as Equation A.68 indicates:

$$\forall t \in T_m, \ \forall i \in \{1, \dots, n\}, \quad p_{t,i} = \frac{C^{alt}(\sum_{1 \leq j \leq i} (q_{t,j}))}{\sum_{1 \leq j \leq i} (q_{t,j})} \tag{A.68}$$

With $C^{alt}(q)$ the cost estimation of balancing quantity q using the alternative alt, as explained in Section A.4.3.2.2.

Volume uncertainty formulation

Readers note: The description of this formulation is extracted from Chapter 3, Section 3.4.2.3.

The general idea of this method is to create a bidding curve in which the size of each slice i is directly defined by the distribution quantiles, and its price integrates the costs of under- or over-estimation of needs in addition to the cost of the stack $St_{t,i}$. Our proposed method is then comprised of the following steps:

1. Determining the distribution of the error made by the TSO when forecasting its balancing needs between two different dates: the execution date of the RR market, and the execution date of its chosen

alternative. This can be performed by using either real or simulated data, but it requires a large volume of forecasts in any case.

2. Using quantiles of this distribution to compute the size of each slice and the associated probability of occurrence. This step is illustrated in Figure A.16, using an arbitrary normal distribution. Quantiles ϵ_i of probability $\alpha_i \in [0.1, \dots, 0.9]$ are displayed, bounded by extreme quantiles ϵ_0 of probability $\alpha_0 = 0.01$ and ϵ_n of probability $\alpha_n = 0.99$ that will be used as references for outer bounds. In this example, we arbitrarily choose $n = 10$ for clarity purposes, meaning that 9 quantiles are considered outside of the extremes. However, the following method can function for any value of n.

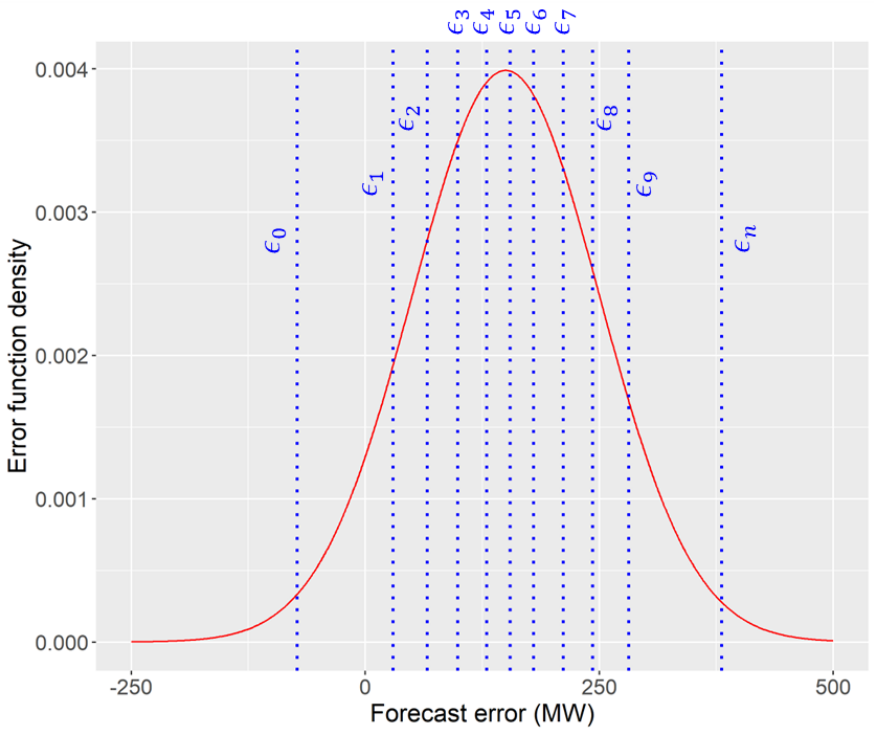

Figure A.16: TSO forecast error distribution example (for readability concerns, we will note $i \in [1, \dots, 9]$)

The quantile i indicates that the real forecast error ϵ made by the TSO has a probability α_i of being below the associated quantity ϵ_i, and a probability $(1 - \alpha_i)$ of being above this value:

$$\forall i \in [0, \dots, n], \quad P[\epsilon \leq \epsilon_i] = \alpha_i \tag{A.69}$$

Information carried by quantiles can then be translated into the quantity of each slice of need submitted to the RR market. If we look at a given forecasted balancing need in the upward direction ($bn_t > 0$), then $bn_t + \epsilon_i$ should give the imbalance that is likely to be reached with an α_i probability. However, depending on the values of bn_t and ϵ_i, this calculated imbalance volume can be in the opposite direction as bn_t. This makes sense from a practical point of view: if the forecasted imbalance is low (and/or if the margin of error is high), then there is a decent chance that the actual balancing need is eventually in the opposite direction. But it also introduces another layer of complexity when determining the volume of each slice, as it leads to 3 different cases:

- If $bn_t > 0$ and $bn_t + \epsilon_1 \geq 0$, then we are in the simple case where the balancing need submitted is always positive, even when taking into account the possible forecast errors. In that situation, the first slice of need ranges from 0 up until $bn_t + \epsilon_1$. The quantity of every subsequent slice of need i is equal to the quantity between the two successive quantiles ϵ_{i-1} and ϵ_i.

$$\forall t \in T_{RR},\ \ if\ (bn_t > 0)\ \&\ (bn_t + \epsilon_1 \geq 0),$$
$$\begin{cases} q_{t,1} = bn_t + \epsilon_1 \\ q_{t,i} = \epsilon_i - \epsilon_{i-1}, \quad \forall i \in [2, \dots, n-1] \end{cases} \tag{A.70}$$

- If $bn_t < 0$ and $bn_t + \epsilon_{n-1} \leq 0$, then this is the mirror case of the first one, with submitted needs being always negative.

$$\forall t \in T_{RR},\ \ if\ (bn_t < 0)\ \&\ (bn_t + \epsilon_{n-1} \leq 0),$$
$$\begin{cases} q_{t,i} = \epsilon_i - \epsilon_{i+1}, \quad \forall i \in [1, \dots, n-2] \\ q_{t,n-1} = bn_t + \epsilon_{n-1} \end{cases} \tag{A.71}$$

- If $bn_t > 0$ and $bn_t + \epsilon_1 < 0$, or if $bn_t < 0$ and $bn_t + \epsilon_{n-1} > 0$, then some need slices submitted should be negative and other should be positive. It is then important to identify where submitted balancing needs shift from being negative to being positive when browsing through values of i, and between which consecutive slices it happens. Let's note these consecutive slices i_{s1} and i_{s2}, such that:

$$\begin{cases} \nexists\ i \in]i_{s1}, i_{s2}[\\ bn_t + \epsilon_{i_{s1}} < 0\ \ \&\ \ bn_t + \epsilon_{i_{s2}} > 0 \end{cases} \tag{A.72}$$

  As Equation A.73 describes, for slices lower than i_{s1}, submitted balancing needs are always negative. For slices higher than i_{s2}, submitted balancing needs are always positive. Finally, slices i_{s1} and i_{s2} are dealt with in specific cases:

$$\forall t \in T_{RR},\ \ if\ \big(\ (bn_t > 0)\ \&\ (bn_t + \epsilon_1 < 0)\big)\ |\ \big(\ (bn_t < 0)\ \&\ (bn_t + \epsilon_{n-1} > 0)\big),$$
$$\begin{cases} q_{t,i} = \epsilon_i - \epsilon_{i+1}, \quad \forall i \in [1, \dots, i_{s1} - 1] \\ q_{t,i_{s1}} = \epsilon_{i_{s1}} \\ q_{t,i_{s2}} = \epsilon_{i_{s2}} \\ q_{t,i} = \epsilon_i - \epsilon_{i-1}, \quad \forall i \in [i_{s2} + 1, \dots, n-1] \end{cases} \tag{A.73}$$

3. Computing the price of each slice i, taking into account both the opportunity cost of the associated stack of needs $St_{t,i} = \sum_{1 \leq j \leq i} q_{t,i}$, and the potential costs of over-/under-estimation of balancing needs. If we still look at upward balancing needs bn_t for the sake of the explanation, the following reasoning is applied:

   - Opportunity costs associated with the volume of this stack of needs are directly given by the cost estimation function, and are equal to $C^{alt,up}(St_{t,i})$.
   - In addition, there is a α_i chance that the actual imbalance volume is lower than $St_{t,i}$, meaning that the TSO will have to compensate in the downward direction with its alternative if the market

activates it. To be precise, the formula giving the expected cost of overestimation compensation $C^{alt,over}$ would be:

$$C^{alt,over}(St_{t,i}) = \int_0^{\epsilon_i} (\alpha_i - \alpha_\epsilon) * C^{alt,down}(\epsilon_i - \epsilon) d\epsilon \tag{A.74}$$

Where α_ϵ is the probability of error ϵ. As this integral cannot be theoretically solved without any more information on the cost function C^{alt}, an approximation is used here and the associated costs are estimated at:

$$C^{alt,over}(St_{t,i}) = \sum_{0 \leq j < i} (\alpha_{j+1} - \alpha_j) * C^{alt,down}(\epsilon_{j+1} - \epsilon_j) \tag{A.75}$$

- On the other hand, there is a $(1 - \alpha_i)$ chance that the actual imbalance volume is higher than $St_{t,i}$, meaning that the TSO would have to ask for additional upward power with its alternative. Similar to overestimation costs, underestimation costs are approximated at:

$$C^{alt,under}(St_{t,i}) = \sum_{i < j \leq n-1} (\alpha_j - \alpha_{j-1}) * C^{alt,up}(\epsilon_j - \epsilon_{j-1}) \tag{A.76}$$

By gathering all parts together, the price of slice i can be written in Equation A.77:

$$\begin{aligned} & \forall t \in T_{RR}, \ \ \forall i \in [1, \ldots, n-1], \\ p_{t,i} = \frac{1}{St_{t,i}} * \Bigg[& C^{alt,up}(St_{t,i}) + \\ & \sum_{0 \leq j < i} (\alpha_{j+1} - \alpha_j) * \ C^{alt,down}(\epsilon_{j+1} - \epsilon_j) + \\ & \sum_{i < j \leq n-1} (\alpha_j - \alpha_{j-1}) * C^{alt,up}(\epsilon_j - \epsilon_{j-1}) \Bigg] \end{aligned} \tag{A.77}$$

With

$$St_{t,i} = \begin{cases} \sum\limits_{1 \leq j \leq i} q_{t,i} & if \ \ bn_t > 0 \\ \sum\limits_{i \leq j \leq n-1} q_{t,i} & if \ \ bn_t < 0 \end{cases} \tag{A.78}$$

A.5 ATLAS Balancing Stage - Balancing Mechanism

A.5.1 Overview of the actual Balancing Mechanism process

The Balancing Mechanism module in ATLAS aims at emulating the eponymous historical balancing process used by the French TSO RTE, which we will call FrBM (for French Balancing Mechanism). The FrBM has been operational since the beginning of the 21^{th} century, and is now partially being replaced by common European balancing markets. Indeed, its role is to activate the so-called "tertiary reserves"–which mainly correspond to the combination of mFRR and RR reserve types in the new European nomenclature– to correct observed or forecasted supply-demand imbalances in the French control area. Currently, it is still being run after (i.e. closer to real-time than) the European RR market: it serves as a backup option for the French TSO, and is used to resolve any remaining imbalance still existing after the RR market. In its historical configuration, the time frame T_{FrBM} of the Balancing Mechanism is illustrated in Figure A.17.

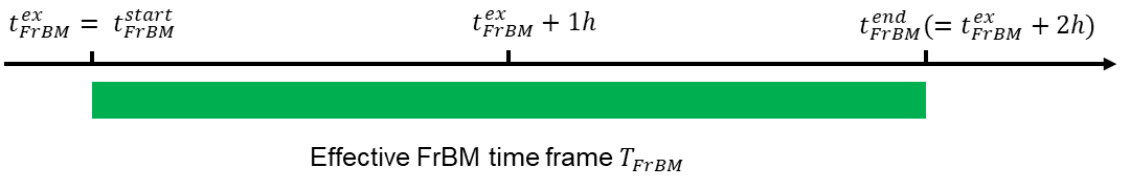

Figure A.17: Historical time frame of the French Balancing Mechanism

The execution date t^{ex}_{FrBM} also corresponds to the beginning t^{start}_{FrBM} of the effective period T_{FrBM} (called "neutralization leadtime") that lasts until t^{end}_{FrBM}, during which no unit in the French area is allowed to change its planned generation or consumption program for any time until t^{end}_{FrBM}. Note that said units are still able to make offers on markets whose effective time frame is after t^{end}_{FrBM}. For instance, if we take $t^{ex}_{FrBM} = 10h$ and $t^{end}_{FrBM} = 12h$, a unit at $t = 11h$ is not allowed to plan a change to its power output for any time until 12h, but can plan a change for time steps after 12h. Historically, the FrBM was run at an hourly frequency, with a maximum neutralization leadtime of 2 hours. The new sequence, in which the FrBM is sequentially executed after the RR market, is represented in Figure A.18. The operational time frame of the FrBM begins after the clearing stage of the last RR market, at t^{ex}_{RR}. Both sequences and time frames are possible in ATLAS, depending on the type of market simulated.

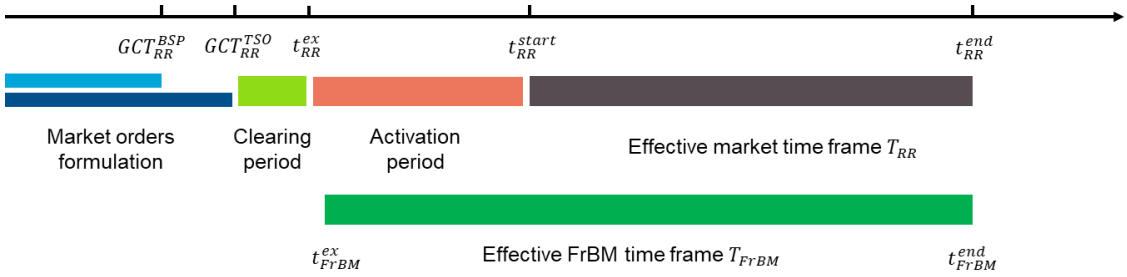

Figure A.18: Current time frame of the French Balancing Mechanism, following the RR market

Each BSP connected to the French transport network (the part of the power grid operated by the French

TSO) is required to submit its entire available capacity in both directions (upward and downward) to the FrBM through reserve orders[10]. These orders are described as "specific" and "implicit", as opposed to the "standard" and "explicit" market orders that can be found on RR or mFRR markets for instance (see Sections A.1.1.1 and A.1.1.2). Indeed, on the FrBM, BSP orders indicate the price at which they should be activated (set by BSPs themselves) but do not specify any maximum or minimum quantity, nor any activation duration. BSPs instead send to the TSO the generation or consumption plans of each of their units, as well as all their technical and operational constraints, leaving to the TSO the role of computing feasible power ranges. In ATLAS, BSPs are currently assumed to have no strategic behavior on the FrBM, and the price of their orders corresponds exactly to their production cost (i.e. their variable cost, plus eventual startup costs if the associated unit is offline).

The resulting problem from the TSO point of view consists in two steps: computing its balancing need, and activating BSP orders to resolve it at minimal cost. The implementation of both steps in ATLAS is described respectively in Sections A.5.3 and A.5.4. Finally, the remuneration scheme of the FrBM is "pay-as-bid", meaning that all activated BSPs are then remunerated at the price of their order multiplied by the activated quantity.

The rest of this document presents the implementation and key methods of the Balancing Mechanism developed in ATLAS. Any information hereafter does not describe the real FrBM process, but rather the model that emulates it, along with is necessary simplifications and approximations.

A.5.2 Nomenclature and inputs

This section describes all notations used in the module. Some elements correspond to a specific type, which is indicated in bold and italics:

- ***Parameter*** refers to a parameter, which is indicated by the user before the execution of the module.
- ***Input data*** refers to an element that is extracted from the input dataset.
- ***Variable*** refers to an optimization variable.

Remark: For sets, the notation A_b refers to the subset of A linked with variable b. For instance, Z_{ca} indicates the subset of market areas belonging to the control area ca.

Sets and global market notations	
Notation	**Description**
CA	Set of all control areas (or control blocks)
Z	Set of all market areas
U	Set of all units

[10] Currently, in ATLAS the distinction between a connection to the transport or the distribution network is not implemented. By default, every unit is required to submit its entire capacity for the Balancing Mechanism of its TSO. We are looking to refine this assumption in future work. This approximation is nonetheless justified for thermal and hydraulic units.

U^{unit_type}	Set of all units of type $unit\_type \in [g, l, th, h, st, w, pv]$. ($g$ = generation, l = flexible load, th = thermal, h = hydraulic, st = storage, w = wind, pv = photovoltaic)

Temporal variables		
Notation	**Description**	**Units**
t_{BM}^{ex}	Execution date of the Balancing Mechanism. ***Parameter***	-
t_{BM}^{start}	Start date of the effective period of the Balancing Mechanism. ***Parameter***	-
t_{BM}^{end}	End date of the effective period of the Balancing Mechanism. ***Parameter***	-
Δt_{BM}	Time step of the Balancing Mechanism. ***Parameter***	min
T_{BM}	Effective time frame of the Balancing Mechanism, i.e. $T_{BM} = [t_{BM}^{start}, t_{BM}^{start} + \Delta t_{BM}, \ldots, t_{BM}^{end} - \Delta t_{BM}]$	-

Zonal- and TSO-specific characteristics		
Notation	**Description**	**Units**
$bn_{BM,ca,t,t_{BM}^{ex}}$ (short: bn_t)	Balancing needs for in control area $ca \in CA$ for time $t \in T_{BM}$, seen from t_{BM}^{ex}. For readability, it is shortened as bn_t. ***Input data***	MW
$(\Delta q)_{z,t}^{bal}$	Commercial (power) balance of area $z \in Z$ at time t, equal to the sum of all power exports minus the sum of all power imports. ***Input data***	MW

Global unit characteristics		
Notation	**Description**	**Units**
$P_{u,t,t_m^{ex}}^{plan}$	Power output of unit $u \in U$ at time $t \in T_m$, seen from time t_m^{ex}. ***Input data***	MW
$P_{u,t}^{act}$	Power activated by the Balancing Mechanism on unit $u \in U$ at time $t \in T_m$. ***Variable***	MW
$P_{u,t,t_m^{ex}}^{final}$	Final power output of the unit u at time $t \in T_m$, seen from t_m^{ex}. It corresponds to the sum of $P_{u,t,t_m^{ex}}^{plan}$ and $P_{u,t}^{act}$.	MW
$P_{u,t}^{max}$	Maximum power output of unit $u \in U$ at time $t \in T_m$. ***Input data***	MW
$P_{u,t}^{min}$	Minimum power output of unit $u \in U$ at time $t \in T_m$. ***Input data***	MW
$p_{u,t}$	Activation price of unit u at time t. ***Input data***	€

$R^{m^R,\sigma^R}_{ut,t^{ex}_m}$	Procured reserves of type $m^R \in [FCR, aFRR, mFRR, RR]$ in direction $\sigma^R \in [up, down]$ on unit u at time t, seen from t^{ex}_m. ***Input data***	-

Hydraulic- and Storage-specific unit characteristics		
Notation	**Description**	**Units**
$E^{stored}_{u,t,t^{ex}_m}$	Stored energy in the reservoir of unit $u \in U^h \cup U^{st}$ at time $t \in T_m$, seen from time t^{ex}_m ***Variable***	MWh
$E^{max}_{u,t}$	Maximum storage level in the reservoir of unit $u \in U^h \cup U^{st}$ at time $t \in T_m$ ***Input data***	MWh
$E^{min}_{u,t}$	Minimum storage level in the reservoir of unit $u \in U^h \cup U^{st}$ at time $t \in T_m$ ***Input data***	MWh
d^{tran}_u	Transition duration between pumping and turbining of unit u of type Pumped Hydraulic Storage (PHS), that are modeled as storage units in ATLAS (i.e. $u \in U^{st}$) ***Input data***	min
$WV_{u,t,E^{stored}_{u,t,t^{ex}_m}}$	Marginal storage value of unit $u \in U^h$ at time t, for stored energy level $E^{stored}_{u,t,t^{ex}_m}$ ***Input data***	€/MWh
η^c_u	Charge efficiency of unit $u \in U^{st}$ ***Input data***	-
η^d_u	Discharge efficiency of unit $u \in U^{st}$ ***Input data***	-

Load-, Photovoltaic- and Wind-specific unit characteristics		
Notation	**Description**	**Units**
P^{for}_{u,t,t^{ex}_m}	Forecast of the maximum power output of unit $u \in \{U^w, U^{pv}, U^l\}$ at time $t \in T_m$. ***Input data***	MW

Other notations		
Notation	**Description**	**Units**
$VoLL$	Value of loss load.***Parameter***	€/MWh
p^{spill}	Spillage penalty. ***Parameter***	€/MWh
$p^{redispatch}$	Redispatch penalty. ***Parameter***	€/MWh
$E^{VoLL}_{ca,t}$	Loss load energy in control area ca at time t. ***Variable***	MWh
$E^{spill}_{ca,t}$	Spilled energy in control area ca at time t. ***Variable***	MW

A.5.3 TSO balancing needs computation

From now on, we place ourselves at the scale of a control area ca associated with a given TSO, and we look at a Balancing Mechanism process executed at t^{ex}_{BM}, on the operating time frame $T_{BM} = [t^{start}_{BM}; t^{end}_{BM}]$.

The balancing needs computation for this TSO is directly given by Equation A.79, and corresponds to the difference between the sum of consumption plans of all load units in ca (taken in absolute value by convention, see Section A.4.2.2) and the sum of all power output from generation units in ca, with an additional term indicating the commercial power balance of the control area:

$$\forall ca \in CA,\ \forall t \in T_{BM},$$
$$bn_t = \sum_{u \in U^l} |P^{plan}_{u,t,t^{ex}_{BM}}| - \sum_{u \in U^g} P^{plan}_{u,t,t^{ex}_{BM}} + \sum_{z \in Z_{ca}} (\Delta q)^{bal}_{z,t} \tag{A.79}$$

As a reminder, the commercial power balance $(\Delta q)^{bal}_{z,t}$ corresponds to the sum of all exports minus the sum of all imports of market area z.

A.5.4 Reserve activation problem formulation

The reserve activation process takes as inputs the following information, for a given TSO associated with its control area ca, and for an operating time frame T_{BM}:

- The volume of balancing needs $bn_t,\ \ \forall t \in T_{BM}$.
- The activation price $p_{u,t}$ for each unit in its control area, in both upward and downward directions (usually symmetrical, except when startup costs are taken into account).
- Generation / consumption plans $P^{plan}_{u,t,t^{ex}_{BM}}$, and operational constraints of each unit u in its control area.

Because of the specific features of reserve orders on the BM previously mentioned, the reserve activation problem that is solved by the TSO is effectively a unit commitment problem made at the scale of the control area. In that sense, it is extremely close to the optimization problem used in both Day-Ahead Orders and Portfolio Optimization modules, described in Little et al., 2024, especially regarding the application of operational constraints that bound the power output of units. A similar optimization problem to the optimal dispatch presented in Little et al., 2024 is consequently used in the BM, and this section will directly refer to this article when a section of the problem is identical.

A.5.4.1 Redefinition of global objective function and of main control variables

The main optimization variable used in the original problem used in the day-ahead market is the power output of each unit u, noted $P_{u,t}$ at time t. For the BM, a generation or consumption plan already exists for each unit, and the quantity to optimize is then the evolution of power output compared to this planning. This quantity will be noted $P^{act}_{u,t}$, standing for activated power. The final power output $P^{final}_{u,t,t^{ex}_{BM}}$ resulting

from the BM process eventually corresponds to the sum of the planned generation or consumption and the activated power:

$$\forall t \in T_{BM}, \ \forall u \in U, \quad P^{final}_{u,t,t^{ex}_{BM}} = P^{plan}_{u,t,t^{ex}_{BM}} + P^{act}_{u,t} \tag{A.80}$$

$P^{act}_{u,t}$ is not directly bounded and can be both positive or negative. Every physical bound consecutive of operating constraints are applied and verified on $P^{final}_{u,t,t^{ex}_{BM}}$, as this represents the actual power output. $P^{act}_{u,t}$ is however the control variable included in the objective function π_{BM} that performs a cost minimization, described in Equation A.81.

$$\begin{aligned}\pi_{BM}(P^{act}_{u,t}, E^{VoLL}_{ca,t}, E^{spill}_{ca,t}) = \min\Bigg[& \sum_{t\in T_{BM}} \sum_{u\in U_{ca}} P^{act}_{u,t} * p_{u,t} * \frac{\Delta t_{BM}}{60} \\ & + \sum_{t\in T_{BM}} E^{VoLL}_{ca,t} * VoLL + \sum_{t\in T_{BM}} E^{spill}_{ca,t} * 26,000 \\ & + \sum_{t\in T_{BM}} |P^{act}_{u,t}| * p^{redispatch} \Bigg]\end{aligned} \tag{A.81}$$

Where:

- $E^{VoLL}_{ca,t}$ is the unsupplied energy and corresponds to the part of the unflexible load that cannot be provided for a given time $t \in T_{BM}$ in the control area ca. Its associated cost is the $VoLL$, standing for Value of Loss Load. This value is a parameter that can be chosen by the user, and is by default set at 26,000 €/MWh.

- $E^{spill}_{ca,t}$ represents the spilled energy, which is the surplus of energy that cannot be consumed in the control area ca at time t. Notably, this variable does not include curtailment of renewable energy sources: it represents the situation where generation units in ca are technically not able to decrease their generation anymore. A spillage penalty is associated with it, and is set at 26,000 €/MWh. Note that this was decided for optimization purposes (cf. the following paragraph), and it does not represent the actual spillage cost p^{spill}, which is a parameter set by the user.

- Finally, the last term of the objective function is added to prevent the Balancing Mechanism from performing economic redispatch. Indeed, its sole purpose is to resolve the balancing needs, and not to reschedule generation plans if it finds an optimal solution to its unit commitments that differs from the input situation. This concretely means that it should avoid as much as possible counter-activations, i.e. activations of power that are not in the direction that contributes to solving balancing needs. Counter-activations cannot completely be prohibited, as this could lead to solver unfeasibility. To penalize counter-activations, the absolute value of activated power is added to the objective function, and penalized by the coefficient $p^{redispatch}$ whose value is set by the user[11].

[11]This value has to be chosen carefully because of its interaction with p^{spill} and $VoLL$. For the redispatch penalty to be effective, it should outweigh any order price $p_{u,t}$ submitted by BSPs. However, if it is chosen too high (higher than p^{spill} and $VoLL$), the optimization will actually prioritize unsupplied energy or spilled energy to meet the balancing needs, even if it is able to activate power instead. It is recommended to choose a value in the range [5,000; 10,000]

A.5.4.2 Main supply-demand balance constraint

The main constraint that enforces the balance between supply and demand is described in Equation A.82:

$$\forall t \in T_{BM}, \quad \sum_{u \in U_{ca}} P^{act}_{u,t,t^{ex}_{BM}} + E^{VoLL}_{ca,t} * \frac{60}{\Delta t_{BM}} - E^{spill}_{ca,t} * \frac{60}{\Delta t_{BM}} = bn_t \tag{A.82}$$

Conversions from energy to power are required for unsupplied energy and spilled energy, explaining the coefficient $\frac{60}{\Delta t_{BM}}$.

A.5.4.3 Bounds of unsupplied energy and spilled energy

Both $E^{VoLL}_{ca,t}$ and $E^{spill}_{ca,t}$ are defined as positive, but are not bounded by an upper limit:

$$\forall t \in T_{BM}, \quad E^{VoLL}_{ca,t} \geq 0 \tag{A.83}$$

$$\forall t \in T_{BM}, \quad E^{spill}_{ca,t} \geq 0 \tag{A.84}$$

A.5.4.4 Notice delay constraint

The notice delay constraint is associated with the unit characteristic d^{notice}_u, and represents the preparation period required for unit u to respond to any request of power output modification, i.e. the delay between the reception of this request and the beginning of the ramping state. This constraint is not included in the core optimization problem that was constructed for the day-ahead market, as it does not appear to be relevant for the time frame of this market. However, it is definitely impactful when looking at balancing processes, and is added to the optimization problem with the following constraint:

$$\forall t \in T_{BM}, \ \forall u \in U, \ if \ t - t^{ex}_{BM} < d^{notice}_u, \quad P^{act}_{u,t} = 0 \tag{A.85}$$

A.5.4.5 Applying operating constraints to generation and consumption units

The Optimal Dispatch function described in Chapter 3 of Little et al., 2024 is also the basis upon which most generation and consumption units are modeled in the Balancing Mechanism:

- For thermal units, the entire modeling method is applied to $P^{final}_{u,t}$ (Section 3.2), notably all constraints from 3.2.2 to 3.2.39.
- For wind and photovoltaic units, constraints 3.3.1 and 3.3.2 of Section 3.3 are applied to $P^{final}_{u,t}$.
- For non dispatchable generation and load, constraints 3.4.1 of Section 3.4 are applied to $P^{final}_{u,t}$.

- For flexible load units, constraints 3.5.1 and 3.5.2 of Section 3.5 are applied to $P_{u,t}^{final}$.
- For hydraulic units, constraints 3.6.1 and 3.6.2 of Section 3.6 are applied to $P_{u,t}^{final}$.

The constraints applied to storage units differ from the description of the Optimal dispatch in Little et al., 2024:

- The optimization done to identify the time steps when it is preferable to buy or sell is not performed. The activated power is separated into positive and negative components (Equation A.86), and both are subject to the following constraints:

$$P_{u,t,t_{BM}^{ex}}^{act} = \sigma_{u,t}^{sell} * P_{u,t}^{sell} - (1 - \sigma_{u,t}^{sell}) * P_{u,t}^{buy} \tag{A.86}$$

$$0 \leq P_{u,t}^{sell} \leq \sigma_{u,t}^{sell} * (P_{u,t}^{max} - P_{u,t,t_{BM}^{ex}}^{for}) \tag{A.87}$$

$$(1 - \sigma_{u,t}^{sell}) * (P_{u,t}^{min} - P_{u,t,t_{BM}^{ex}}^{for}) \leq P_{u,t}^{buy} \leq 0 \tag{A.88}$$

$$P_{u,t,t_{BM}^{ex}}^{for} + P_{u,t}^{sell} \leq P_{u,t}^{max} * \frac{\Delta t}{60} \tag{A.89}$$

$$P_{u,t,t_{BM}^{ex}}^{for} - P_{u,t}^{buy} \geq P_{u,t}^{min} * \frac{\Delta t}{60} \tag{A.90}$$

$$E_{u,t}^{stored} \leq E_{u,t}^{max} \tag{A.91}$$

$$E_{u,t}^{stored} \geq E_{u,t}^{min} \tag{A.92}$$

The storage level is tracked by Equation A.93:

$$\forall t \in T_{BM}, \quad E_{u,t}^{stored} = E_{u,t-1}^{stored} + P_{u,t}^{buy} * \eta_u^c - \frac{P_{u,t}^{sell}}{\eta_u^d} - \delta_u^{EV} * E_{u,t^{start}-1,t}^{disp} \tag{A.93}$$

- An additional constraint is applied to Pumped Hydraulic Storage (PHS) units u_{PHS} in the Balancing Mechanism. It is related to the transition duration between pumping and turbining d^{tran}, which forces the unit to stay at a null power output for at least d^{tran} before switching from a positive to negative power output (or conversely, at it is assumed to be symmetrical in ATLAS). However, this constraint is currently approximated in the Balancing Mechanism, given that the Δt_{BM} used in the model is usually not below 15 minutes. In practice, it is sufficient to prevent a PHS unit with a $d^{tran} \geq \Delta t_{BM}$ from switching mode during a BM time frame, which is implemented in Equations A.95 (restriction to turbining mode) and A.96 (restriction to pumping mode). Equation A.94 describes the case where a transition is already planned within the BM time frame. In that situation, the power output is supposed to be unchangeable to avoid any unfeasibility.

$$\forall u \in U^{PHS}, \ if \ d_u^{tran} \geq \Delta t_{BM},$$

$$if \ (\min_{t \in T_{BM}} P_{u,t,t_{BM}^{ex}}^{plan} < 0) \ \& \ (\max_{t \in T_{BM}} P_{u,t,t_{BM}^{ex}}^{plan} > 0), \quad P_{u,t}^{acc} = 0 \quad \forall t \in T_{BM} \tag{A.94}$$

$$if \ (\min_{t \in T_{BM}} P_{u,t,t_{BM}^{ex}}^{plan} \geq 0) \ \& \ (\max_{t \in T_{BM}} P_{u,t,t_{BM}^{ex}}^{plan} \geq 0), \quad P_{u,t}^{acc} \geq 0 \quad \forall t \in T_{BM} \tag{A.95}$$

$$if \ (\min_{t \in T_{BM}} P_{u,t,t_{BM}^{ex}}^{plan} \leq 0) \ \& \ (\max_{t \in T_{BM}} P_{u,t,t_{BM}^{ex}}^{plan} \leq 0), \quad P_{u,t}^{acc} \leq 0 \quad \forall t \in T_{BM} \tag{A.96}$$

A.5.4.6 Previously procured reserves

All manual reserves (RR or mFRR) previously procured are considered available on the Balancing Mechanism. On the other hand, previously procured automatic reserves (FCR and aFRR) cannot be activated in this process. This is implemented in the optimization by constraining the power output by Equations A.97 and A.98:

$$\forall u \in U, \quad \forall t \in T_{BM},$$

$$P^{plan}_{u,t,t^{ex}_{BM}} + P^{acc}_{u,t} \leq P^{max}_{u,t} - (R^{aFRR,up}_{u,t} + R^{FCR,up}_{u,t}) \tag{A.97}$$

$$P^{plan}_{u,t,t^{ex}_{BM}} + P^{acc}_{u,t} \geq P^{min}_{u,t} + (R^{aFRR,dn}_{u,t} + R^{FCR,dn}_{u,t}) \tag{A.98}$$

A.5.5 Balancing Mechanism outputs

Following variables and quantities are extracted for all time $t \in T_{BM}$ at the end of the Balancing Mechanism:

- The overall and final power output of each unit $P^{final}_{u,t,t^{ex}_{BM}}$, for each unit $u \in U$.
- Both the unsupplied energy $E^{VoLL}_{ca,t}$ and the spilled energy $E^{spill}_{ca,t}$.
- Total balancing costs $c^{BM}_{ca,t}$, defined in Equation A.99, consisting of the final value of the objective function from which are subtracted two terms. First, the entire term corresponding to economic redispatch, as it was only introduced to control the behavior of the optimization and does not represent a physical quantity. Second, the quantity $E^{spill}_{ca,t} * (26,000 - p^{spill})$. p^{spill} is a parameter chosen by the user and represents the actual spillage cost. The last subtraction then corrects the spillage cost from the value required for optimization reliability (equal to $26,000$) to the actual spillage value.

$$\forall t \in T_{BM}, \quad c^{BM}_{ca,t} = \pi_{BM}(P^{act}_{u,t}, E^{VoLL}_{ca,t}, E^{spill}_{ca,t}) - \sum_{u \in U_{ca}} |P^{act}_{u,t}| * p^{redispatch} - E^{spill}_{ca,t} * (26,000 - p^{spill}) \tag{A.99}$$

A.6 ATLAS Balancing Stage - Imbalance Settlement

In ATLAS, the Imbalance Settlement module aims to remunerate or invoice Balancing Responsible Parties (BRPs) according to their imbalance, both in volume and direction. Its design is flexible, in the sense that both the settlement period T_{ISP} and the resolution Δt_{ISP} are indicated by the user. However, the Imbalance Settlement Price (ISP) currently implemented is based on the French ISP, detailed in the General Introduction of the manuscript (Section 1.2.3).

Section A.6.1 details the nomenclature and variables, and Section A.6.2 details the practical implementation.

A.6.1 Nomenclature

As for other sections of the appendix, some elements correspond to a specific type, which is indicated in bold and italics:

- ***Parameter*** refers to a parameter, which is indicated by the user before the execution of the module.
- ***Input data*** refers to an element that is extracted from the input dataset.
- ***Variable*** refers to an optimization variable.

For sets, the notation A_b refers to the subset of A linked with variable b. For instance, Z_{ca} indicates the subset of market areas belonging to the control area ca.

Sets and global market notations	
Notation	**Description**
CA	Set of all control areas (or control blocks)
U	Set of all units

Temporal variables		
Notation	**Description**	**Units**
t_{ISP}^{ex}	Execution date of the Imbalance Settlement. ***Parameter***	-
t_{ISP}^{start}	Start date of the effective period of the Imbalance Settlement. ***Parameter***	-
t_{ISP}^{end}	End date of the effective period of the Imbalance Settlement. ***Parameter***	-
Δt_{ISP}	Time step of the Imbalance Settlement. ***Parameter***	min

T_{ISP}	Effective time frame of the Imbalance Settlement, i.e. $T_{ISP} = [t_{ISP}^{start}, t_{ISP}^{start} + \Delta t_{ISP}, \ldots, t_{ISP}^{end} - \Delta t_{ISP}]$	-

Zonal- and TSO-specific characteristics		
Notation	**Description**	**Units**
$(\Delta Q)_{ca,t}$	Imbalance in area ca at time t ***Input data***	MW
$\lambda_{ca,t}^{w,\bullet}$	Volume-weighted average price of balancing reserves activation in direction $\bullet \in \{up, down\}$, in area ca at time t	€/MWh
$\sigma_{\lambda_{ca,t}^{w,\bullet}}$	Boolean indicating the sign of $\lambda_{ca,t}^{w,\bullet}$	-
k	Coefficient used in the French ISP computation, set to 0.05 by default. ***Parameter***	-
$\lambda_{ca,t}^{m}$	Clearing price of market m in area ca at time t	€/MWh
$c_{ca,t}^{BM}$	Balancing Mechanism costs in area ca at time t	€

BRP and unit characteristics		
Notation	**Description**	**Units**
$(\Delta Q)_{BRP,t}$	Power imbalance of the BRP at time t. ***Input data***	MW
$P_{u,t}^{act}$	Power activated by the Balancing Mechanism on unit $u \in U$ at time $t \in T_m$. ***Input data***	MW
$c_{BRP,t}^{ISP}$	Imbalance settlement costs of BRP at time t	€

Other notations		
Notation	**Description**	**Units**
$VoLL$	Value of loss load.***Parameter***	€/MWh
p^{spill}	Spillage penalty. ***Parameter***	€/MWh
$p^{redispatch}$	Redispatch penalty. ***Parameter***	€/MWh
$E_{ca,t}^{VoLL}$	Loss load energy in control area ca at time t. ***Variable***	MWh
$E_{ca,t}^{spill}$	Spilled energy in control area ca at time t. ***Variable***	MW

A.6.2 Implementation

An illustrative time frame of the imbalance settlement process is represented in Figure A.19. The settlement is executed ex-post, after the last balancing process.

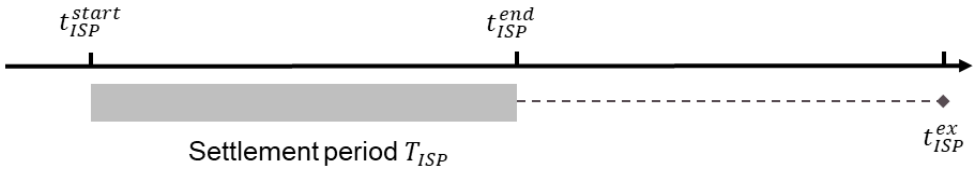

Figure A.19: ATLAS - Imbalance settlement process time frame

The computation of the French ISP, used as a reference in the is module, is summarized in Table A.42. As a dual imbalance price, BRPs are settled differently according to the direction of their imbalance.

	Direction of overall imbalance $\Delta Q_{ca,t}$ in ca at t	
BRP imbalance direction at t	**Upward**	**Downward**
Positive	$\lambda_{ca,t}^{w,up} * (1 - \sigma_{\lambda_{ca,t}^{w,up}} * k)$	$\lambda_{ca,t}^{w,down} * (1 - \sigma_{\lambda_{ca,t}^{w,down}} * k)$
Negative	$\lambda_{ca,t}^{w,up} * (1 + \sigma_{\lambda_{ca,t}^{w,up}} * k)$	$\lambda_{ca,t}^{w,down} * (1 + \sigma_{\lambda_{ca,t}^{w,down}} * k)$

Table A.42: French imbalance settlement price computation

Where:

- ca is the control area belonging to a TSO.
- $t \in T_{ISP}$ is any time in the settlement period.
- $\lambda_t^{w,\bullet}$ is the volume-weighted average price of balancing activations in direction $\bullet$ at time t. These activations include primary, secondary and tertiary reserves, meaning that the weighted price takes into account activations performed by the FrBM and by all common balancing energy markets.
- $\sigma_{\lambda_t^{w,\bullet}}$ indicates the sign of the weighted price ($= 1$ for a positive or null price, and $= -1$ for a negative price), and ensures that the ISP sends the same incentive to BRPs regardless of the sign of $\lambda_t^{w,\bullet}$.
- k is a coefficient defined ex-ante that aims to balance income and expenditure of the energy component of the balancing-imbalances account, based on historical data. This coefficient is occasionally updated, and has been set at 0.05 since 2019.

In ATLAS, the Imbalance Settlement module consists of two steps.

Computation of the volume-weighted average prices

First, in every control area ca belonging to a TSO, the volume-weighted average prices $\lambda_t^{w,\bullet}$ are calculated in both directions, according to Equation A.100. This computation takes into account (i) RR and mFRR markets and (ii) the Balancing Mechanism.

$$\forall ca \in CA, \quad \forall t \in T_{ISP},$$
$$\lambda_{ca,t}^{w,\bullet} = \frac{\sum_{m \in \{RR,mFRR\}} (\delta_{m,ca,t}^{\bullet} * E_{m,ca,t}^{acc} * \lambda_{ca,t}^{m}) + \delta_{BM,ca,t}^{\bullet} * c_{ca,t}^{BM}}{\sum_{m \in \{RR,mFRR\}} (\delta_{m,ca,t}^{\bullet} * E_{m,ca,t}^{acc}) + \delta_{BM,ca,t}^{\bullet} * E_{BM,ca,t}^{acc}} \tag{A.100}$$

With:

- $\delta^{\bullet}_{m,ca,t}$ a boolean indicating if the balancing needs in control area ca were in direction $\bullet \in \{up, down\}$ on market m at time t.
- $\delta^{\bullet}_{BM,ca,t}$ a boolean indicating if the balancing needs in control area ca were in direction $\bullet \in \{up, down\}$ on the Balancing Mechanism at time t.
- $E^{acc}_{m,ca,t}$ is the total volume of TSO needs accepted on market m at time t, in control area ca. Formally, this volume can be written as the sum of all accepted quantities on market m, converted in energy:

$$E^{acc}_{m,ca,t} = \sum_{o \in O^{BSP}_{m,ca,t}} q^{acc}_{o} * \frac{\Delta t_{ISP}}{60} \tag{A.101}$$

- $E^{acc}_{BM,ca,t}$ is the total volume of TSO needs compensated by the Balancing Mechanism at time t, in control area ca. Formally, it is computed in Equation A.102, where $P^{act}_{u,t}$ is the power activated on unit u at time t by the Balancing Mechanism:

$$E^{acc}_{BM,ca,t} = \sum_{u \in U_{ca}} (|P^{act}_{u,t}| * \frac{\Delta t_{ISP}}{60}) \tag{A.102}$$

- $\lambda^{m}_{ca,t}$ is the clearing price of market m at time t, in control area ca.
- $c^{BM}_{ca,t}$ is the total balancing costs resulting from the Balancing Mechanism at time t, in control area ca. It corresponds to the value calculated as an output of the Balancing Mechanism, in Equation A.99 (see Section A.5.5).

Settlement of all BRPs

Once the weighted prices computation is performed, the imbalance $\Delta Q_{BRP,t}$ of each BRP at time t is settled depending on its direction, leading to the costs $c^{ISP}_{BRP,t}$ (counted positively for payments, and negatively for revenues). Equation A.103 details the computation of $\Delta Q_{BRP,t}$, which is equal to the difference between (i) the real-time power, from which Balancing Mechanism activations are substracted and (ii) the sum of all market commitments. Equation A.104 details the imbalance settlement costs computation in the case $\Delta Q_{BRP,t} > 0$, while Equation A.105 represents the case $\Delta Q_{BRP,t} < 0$:

$$\forall BRP \in ca,\ \forall t \in T_{ISP},\quad \Delta Q_{BRP,t} = \sum_{u \in U_{BRP}} \left[P^{final}_{u,t} - P^{act}_{u,t} - \sum_{o \in O_{m,u} \,|\, m \in DA,ID,RR,mFRR} \sigma_o * q^{acc}_{o} \right] \tag{A.103}$$

$$\forall BRP \in ca,\ \forall t \in T_{ISP},\ if\ \Delta Q_{BRP,t} > 0$$

$$\begin{cases} c^{ISP}_{BRP,t} = \lambda^{w,up}_{ca,t} * (1 - \sigma_{\lambda^{w,up}_{ca,t}} * k) * \Delta Q_{BRP,t} * \frac{\Delta t_{ISP}}{60} & if\ \Delta Q_{ca,t} > 0 \\ c^{ISP}_{BRP,t} = \lambda^{w,down}_{ca,t} * (1 - \sigma_{\lambda^{w,down}_{ca,t}} * k) * \Delta Q_{BRP,t} * \frac{\Delta t_{ISP}}{60} & if\ \Delta Q_{ca,t} < 0 \end{cases} \tag{A.104}$$

$$\forall BRP \in ca,\ \forall t \in T_{ISP},\ \ if\ \Delta Q_{BRP,t} < 0$$

$$\begin{cases} c^{ISP}_{BRP,t} = \lambda^{w,up}_{ca,t} * (1 + \sigma_{\lambda^{w,up}_{ca,t}} * k) * \Delta Q_{BRP,t} * \frac{\Delta t_{ISP}}{60} & if\ \Delta Q_{ca,t} > 0 \\ c^{ISP}_{BRP,t} = \lambda^{w,down}_{ca,t} * (1 + \sigma_{\lambda^{w,down}_{ca,t}} * k) * \Delta Q_{BRP,t} * \frac{\Delta t_{ISP}}{60} & if\ \Delta Q_{ca,t} < 0 \end{cases} \tag{A.105}$$

RÉSUMÉ

Le système électrique européen est actuellement en pleine mutation, et en particulier l'équilibrage court-terme. En effet, l'organisation de ce dernier est en transition depuis des processus locaux, à la maille de chaque pays, vers des marchés communs harmonisés. De plus, la décarbonation va modifier les caractéristiques de l'équilibrage court-terme. Cette thèse évalue l'impact de ces deux changements sur l'offre d'activation de réserves et la demande d'équilibrage en Europe. Dans un premier temps, elle montre l'influence des contraintes opérationnelles des groupes de production sur la courbe d'offre des marchés d'équilibrage. La courbe de demande est ensuite étudiée, sous l'angle des stratégies de formulation de demande par les gestionnaires de réseaux de transport. Finalement, une étude à horizon 2050 évalue la capacité de ces nouveaux marchés à résorber les augmentations en besoin d'équilibrage causés par l'intégration massive de sources de production renouvelables et variables.

MOTS CLÉS

Marchés d'électricité européens, Equilibrage, Décarbonation, Modélisation agent, Optimisation

ABSTRACT

The European power system is currently undergoing significant changes, particularly in short-term balancing. Indeed, the organization of the latter is transitioning from local processes at the level of each country to harmonized common markets. Additionally, decarbonization will alter the characteristics of short-term balancing. This thesis assesses the impact of these two changes on the activation of reserves and the balancing needs in Europe. In a first part, it demonstrates the influence of operating constraints of generation units on the supply curve of balancing markets. The demand curve is then examined from the perspective of bidding strategies by transmission system operators. Finally, a study looking ahead to 2050 evaluates the capacity of these new markets to accommodate for increases in balancing needs caused by the large-scale integration of variable renewable energy sources.

KEYWORDS

European electricity markets, Balancing, Decarbonization, Agent-based model, Optimization